THE EFFECT OF CRATOXYLUM COCHINCHINENSE LOUR (CCL) ON GLOBAL mRNA GENE EXPRESSION IN HepG2 LIVER CANCER CELLS

NG YUN KWAN

MASTER OF MEDICAL SCIENCES

FACULTY OF MEDICINE AND HEALTH SCIENCES
UNIVERSITI TUNKU ABDUL RAHMAN
MAY 2017

THE EFFECT OF CRATOXYLUM COCHINCHINENSE LOUR (CCL) ON GLOBAL mRNA GENE EXPRESSION IN HepG2 LIVER CANCER CELLS

BY

NG YUN KWAN

A dissertation submitted to the Department of Pre-Clinical Sciences,
Faculty of Medicine and Health Sciences,
Universiti Tunku Abdul Rahman,
in partial fulfillment of the requirements for the degree of
Master of Medical Sciences
MAY 2017

ABSTRACT

THE EFFECT OF CRATOXYLUM COCHINCHINENSE LOUR (CCL) ON GLOBAL mRNA GENE EXPRESSION IN HepG2 LIVER CANCER CELL

Ng Yun Kwan

Cratoxylum cochinchinense Lour (CCL) has been widely used in many Asian countries over the years for curing various diseases, including cancer. Many studies have been done regarding the phytochemical characteristics isolated from the leaves, stems, roots, barks, and twigs of this plant. However, no details have yet been reported regarding the regulatory effect of these phytochemicals on the cancer signalling pathways so as to support its use as an anticancer agent. Hence, this study was carried out to determine the regulatory effects of CCL on the global gene expression in HepG2 liver cells. A sequential solvent extraction method was used to extract the crude extracts from the barks, stems and exudate of CCL, which were further tested for their cytotoxicity on the HepG2 cancer cells by tetrazolium-based MTT assay. The solvents used in the sequential extraction method included petroleum ether (PE), ethyl acetate (EA) and methanol (MeOH). Results indicated that the bark-PE extract exhibited the most cytotoxic effect towards the cells and was chosen for the microarray gene expression analysis. The gene expression data were not only compared between the bark-PE extract-treated samples and untreated samples, but also compared among different time-points, ranging from 0, 6, 12, 18, 24, to 48 hours. The microarray data summarized that the bark-PE extract showed a significant regulatory effect on focal adhesion, adherens junction, natural killer cell

cytotoxicity, cytokine- cytokine receptor interaction, chemokine signalling, B-cell receptor, apoptosis, WNT signalling, Notch, JAK-STAT and mTOR pathways. Its inhibitory effect was also observed in ErbB, TGF-β, cell cycle, Toll-like, RIG-like, Nod-like signalling, T-cell receptor, VEGF, MAPK, P53, Hedgehog pathway. Genes highly expressed in hepatocellular carcinoma (HCC) that were observed to be down-regulated in this study include *IL8, IL11, IL6R, CCL20, LIF, ACVR1, SOS1, BCAR1, VASP, ZYX, CD22, SLUG, IRAK2, FOSL1, WNT11, PIM1, JAG1, WEE1, HES1, AREG, EREG, DDIT4, IDI, FST, JUND, LCK, RICTOR, PI3KCA, EGFR, PARD3* and *JUN*, while genes expressed low in HCC that were observed to be up-regulated significantly, include *MKK6, RBL1, TRAIL, and TNSRSF19*. These preliminary results suggest that the Bark-PE extract of CCL possess a significant potential in regulating the multiple dysfunctional signalling pathways in HCC. However, downregulated *P38* of MAPK pathway and upregulated *SKP2* of cell cycle may have crosstalk-effect and hold back their inhibitory effects. The finding of this study is significant since it indicates CCL has the inhibitory effect on the HepG2 cancer cells. This provides the scientific proof for interested communities to exploit further on its potential application clinically. The richness of diterpenes and sesquiterpenes was noted in bark-PE extract. This indicates that they are likely the potent inhibitors of liver cancer. The study also paves the way for future studies in CCL, including, but not limited to, identification of active compounds of CCL as potent anti-HCC agent, expansion of the experiment with a broader range of cancer cell lines and clinical study using CCL on HCC subjects.

ACKNOWLEDGEMENT

My gratitude goes to the people who have shown me much support in various ways throughout my study and research. I would like to give my first note of appreciation to Associate Prof Dr Thaw Zin for his supervisory effort to oversee the successful end of this study.

I am incredibly fortunate to have had Prof Dr Lim Yang Mooi as one of the advisors and mentors too. It is her expertise and guidance, without which this research would not come through or be finished in this orderly manner. My gratitude also goes to Associate Prof Dr Yang Zao for his selfless guidance in using TCM for cancer treatment.

I am also deeply indebted to many friends and acquaintances who have lent their unreserved assistance and expertise to this work. Among those who must be singled out are Ms. Le Tian Xin, who guided me through the rudiments of herb extraction, cell culture, DNA & RNA& protein extraction; and my many laboratory friends, with special thanks to the Dr. Wong Teck Yew, Ms. Tan Ping Wey, Ms. Nurul Amira bt Buslima, Dr Lim Kian Lam, Ms. Erica Choong, Mr. Kaliswaran a/l Pannirselvam, Ms. Esther Ho, Mr. Ho Yu Siong, Ms. Lee Mei Wei, Ms. Wong Tze Hann, without whom I may not be able to finish this study in this smooth pace.

I must also extend my appreciation to all my suppliers, especially so to Mr Lai Jiun Yee of Qiagen Malaysia for his selfless sharing in PCR assay and to

Ms Teng Loong Hung of Research Instrument Sdn Bhd for her patient guidance in microarray assays.

APPROVAL SHEET

This dissertation entitled "**THE EFFECT OF CRATOXYLUM COCHINCHINENSE LOUR (CCL) ON GLOBAL mRNA GENE EXPRESSION IN HepG2 LIVER CANCER CELLS**" was prepared by NG YUN KWAN and submitted as partial fulfillment of the requirements for the degree of Master of Medical Sciences at Universiti Tunku Abdul Rahman.

Approved by:

_____

(Associate Prof. Dr. Thaw Zin)
Date:……..
Supervisor
Department of Pre-clinical Sciences
Faculty of Medicine and Health Sciences
Universiti Tunku Abdul Rahman

_____

(Prof. Dr. LIM YANG MOOI)
Date:……..
Co-supervisor
Department of Pre-clinical Sciences
Faculty of Medicine and Health Sciences
Universiti Tunku Abdul Rahman

_____

(Associate Prof. Dr. Yang Zao)
Date:……..
Co-supervisor
Department of Pre-clinical Sciences
Faculty of Medicine and Health Sciences
Universiti Tunku Abdul Rahman

FACULTY OF MEDICINE AND HEATLH SCIENCES

UNIVERSITI TUNKU ABDUL RAHMAN

Date: _____

SUBMISSION OF DISSERTATION

It is hereby certified that ***NG YUN KWAN*** (ID No: ***13UMM08526***) has completed this dissertation entitled "**THE EFFECT OF CRATOXYLUM COCHINCHINENSE LOUR (CCL) ON GLOBAL mRNA GENE EXPRESSION IN HepG2 LIVER CANCER CELLS**" under the supervision of Associate Prof Dr Thaw Zin (Supervisor) from the Department of Pre-clinical Sciences, Faculty of Medicine and Health Sciences, and Prof Dr Lim Yang Mooi (Co-Supervisor) from the Department of Pre-clinical Sciences, Faculty of Medicine and Health Sciences, and Associate Prof Dr Yang Zao (Co-Supervisor) from the Department of Chinese Medicine, Faculty of Medicine and Health Sciences.

I understand that University will upload softcopy of my dissertation in pdf format into UTAR Institutional Repository, which may be made accessible to UTAR community and public.

Yours truly,

_____
(*NG YUN KWAN*)

DECLARATION

I hereby declare that the dissertation is based on my original work except for quotations and citations which have been duly acknowledged. I also declare that it has not been previously or concurrently submitted for any other degree at UTAR or other institutions.

Name: _____
(NG YUN KWAN)

Date: _____

TABLE OF CONTENTS

LIST OF TABLES

LIST OF FIGURES

LIST OF PLATES

LIST OF ABBREVIATIONS

AFB1	Aflatoxin B1
AJ	Adherens junction
AML	Acute myeloid leukaemia
APS	Ammonium Persulfate
AP1	Activator Protein 1
ASEAN	Association of South-East Asia Nations
BCR	B cell receptor
BSA	Bovine Serum Albumin
CCL	*Cratoxylum cochinchinense* Lour.
CDC25	Cell division cycle 25
DAVID	the Database for Annotation, Visualization and Integrated Discovery
DC	dendritic cells
DDIT4	DNA-damage-inducible transcript 4
DMSO	Dimethyl sulfoxide
EA	Ethyl acetate
EC	Expression Console
ECM	Extracellular Matrix
EGFR	Epidermal Growth Factor Receptor
EMT	Epithelial-to-mesenchymal transition
ErbB	Erythroblastic Leukaemia Viral Oncogene Homolog
ERK	Extracellular Signal-Regulated Kinases
FA	Focal adhesion
FASL	Fas ligand

GADD45	DNA damage-inducible gene 45
GC	Gas Chromatography
GLI	Glioma-associated oncogene homologue
GO	Gene ontology
GPCR	G protein-coupled receptors
GSP	Gene-Specific Primers
HBV	Hepatitis B virus
HCC	Hepatocellular carcinoma
HCV	Hepatitis C virus
HPV	Human papillomaviruses
HRP	Horseradish Peroxidase
HTA	Human transcriptome array
IL-6	Interleukin 6
IFN-α	Interferon-α
JAK-STAT	Janus associated kinase-signal transducer and activator of transcription
JNK	c-Jun NH2-terminal kinases
KEGG	Kyoto Encyclopaedia of Genes and Genomes
LC	Liquid Chromatography
LPS	lipopolysaccharide
MAPK	Mitogen Activated Protein Kinase
MeOH	Methanol
MGF	Mangiferin
MHC	major histocompatibility complex
MM	Mismatch

MS	Mass spectrum
MTT	(3-(4, 5-dimethylthiazolyl-2)-2, 5-diphenyltetrazolium bromide
NF-κB	nuclear factor kappaB
NLR	NOD-like receptors
NK	Natural killer
NMR	Nuclear Magnetic Resonance
NO	Nitric oxide
NSCLC	Non–small cell lung carcinoma
PAI-1	Plasminogen activator inhibitor type-1
PAMP	Pathogen-Associated Molecular Pattern
PBS	Phosphate buffer saline
PE	Petroleum Ether
PI3K	Phosphatidylinositol 3-kinase
PDGF	Platelet-Derived Growth Factor
PDGFR	Platelet-Derived Growth Factor Receptor
PGN	Peptidoglycan
PM	Perfect Match
PRL	Prolactin
PRR	Pattern Recognition Receptors
PTEN	Phosphatase and Tensin Homolog
PVDF	Poly-Vinylidene-Difluoride
qRT-PCR	Quantitative real-time PCR
RLR	RIG-I like receptor
RNA	Ribonucleic Acid

ROS	Reactive OxygenSpecies
RPMI	Roswell Park Memorial Institute Media
RTK	Receptor Tyrosine Kinase
SCF	Stem cell factor
SDS	Sodium Dodecyl Sulphate
Smo	Smoothened
TAC	Transcriptome Analysis Console
T-ALL	T-cell acute lymphoblastic leukaemia
TCM	Traditional Chinese Medicine
TNFα	Tumour Necrosis Factor α
TNM	TNM Classification of Malignant Tumours
TGF-β	Transforming growth factor-
TIC	Tumour-Initiating Cell
TLR	Toll-like receptors
TRAIL	TNF-related apoptosis inducing ligand
µPA	Urokinase Plasminogen Activator
µPAR	Urokinase Plasminogen Activator Receptor
VEGF	Vascular Endothelial Growth Factor
VEGFR	Vascular Endothelial Growth Factor Receptor
WHO	World Health Organisation

CHAPTER 1

INTRODUCTION

Based on the GLOBACON 2008 for Southeast Asia, the fatality (overall ratio of mortality/incidence) of liver cancer at the level of 0.93 reflects the low survival rate of the liver cancer patients. It also indicates the complexity and limited treatment options for liver cancer patients(Kimman et al., 2012).Moreover, majority of patients with HCC are complicated with other advanced diseases, including liver cirrhosis, hepatic dysfunction. These complications limit the treatment options available to them and cut them off from treatments such as liver transplantation, surgical resection, or regional therapy (Thomas and Abbruzzese, 2005).

However, most of the anti-neoplastic drugs used in chemotherapy in conventional treatment nowadays have exhibited different level of cell toxicity to not just neoplastic cells, but also to normal healthy cells. Their adverse effects are observed in a lot of organs, especially lung, liver, kidney, and nervous system. Abnormal liver functions are noted during the treatment (Ramadori and Cameron, 2010). These side effects limit the use of chemotherapeutic agents. Patient survival or quality of life is not significantly improved despite the high efficacy in treating specific or target malignant cells (Cheng et al., 2009).

Like other cancers, growth of liver cancer cell is a complicated multi-step process in which cells experience profound metabolic and behavioural changes (Barrett, 1993). This carcinogenesis is induced by a lot of genetic and epigenetic changes that disrupt various pathways, which control biological function of cells, including proliferation, apoptosis, differentiation, and senescence. This results in excessive proliferation of cancer cells and subsequent evasion from surveillance by the immune system, and ultimate invasion of distant tissues (Hanahan and Weinberg, 2011).

With the poor overall efficacy and abundance of side effects of the existing medicines, pharmaceutical industries have been aggressively looking for alternative medicines for better prognosis. A better and affordable drug is needed to replace or complement the current cancer treatment. Naturally, medicinal plants in Asia, such as China and India, have become the choice of preference due to its long history of being used as folk medicine as well as in the hospitals. Its beneficial values and effects have been proven for more than 2000 years. In search for better medicines for cancer treatment, effort has been put into screen through tremendous amount of plant extracts against human cancer cell lines over the last thirty years. This results in successful commercialized drugs for cancer treatment. They are obtained from these natural sources and further modified structurally or synthesized as new compounds (Dhiman and Chawla, 2005).

Cratoxylum cochinchinense Lour (CCL) is one of the plants widely available in Southeast Asia and various parts of this plant have been broadly studied. Its xanthones and derivatives isolated from barks, stems, twigs, fruits, roots, and resins are anti-cancer and anti-oxidant (Ho et al., 2002; Tang et al., 2004a; Akao et al., 2008; Ren et al., 2011). It has been widely used as folk medicine in South East Asia for curing various diseases, including fever, cough, diarrhoea, eczema, ulcer, itches, etc. while Chinese physicians have used it for the treatment of liver diseases, including liver cancer. However, this claim is not scientifically proven.

Medical communities have been putting effort to isolate lead compounds out of these natural sources and generate structural analogues with greater pharmacological effects and less adverse effects. However, this effort needs to complement with other disciplines in order to produce the potential drug in a more effective approach. The successful sequencing of the entire human genome has made the identification of genetic mutations causing cancers possible. With the wide application of microarray technology and the advent of next-generation sequencing technologies or RNA sequencing techniques have transformed the landscape of transcriptomics study in samples, especially cancer. Hundreds of oncogenes and tumour suppressor genes on various pathways have been identified. With the strong computational bioinformatics technology, such as DAVID Bioinformatics Resources 6.7 of National Institute of Allergy and Infectious Diseases (NIAID) (https://david.ncifcrf.gov/), more oncogenes and tumour suppressor genes could be identified and their roles could be better understood.

With this advent of genomics, transcriptomics, proteomics and metabonomics, the discovery and production of potent compounds for cancer treatment can be viewed from the perspective of system biology. However, this new perspective needs multi-disciplinary approach, combining knowledge from biology, chemistry, and bio-informatics as well as other disciplines so that interpretation of its multivariate statistics derived is more integrative as a whole. With this perspective in mind, the design of this study lines up various assays, including cytotoxicity assay, metabonomic analysis, microarray, PCR, western blot and bio-informatics. This approach is also in line with the philosophy of traditional Chinese medicine (TCM) that considers human body as a system with which drug system interacts (Luo et al., 2011).

To evaluate of cytotoxicity of extracts of CCL against HepG2 cells, this study used MTT method and subsequently, metabonomic analysis to find out the possible metabolites present in the extract of CCL. It is also the first attempt using microarray technology to elucidate the possible inhibitory effect of CCL on various cancer pathways and identify the genes that are regulated by CCL. Further verification of the result of the microarray experiment using RT-PCR and western blot was also included for this study.

It is expected that this study is able to ascertain the inhibitory effect of CCL on cancer pathways, including focal adhesion, adherens junction, natural killer cell cytotoxicity, cytokine-cytokine receptor interaction, chemokine signalling, B-cell receptor, apoptosis, WNT signalling, Notch signalling, JAK-STAT signalling , mTOR signalling, ErbB signalling, TGF-β signalling, cell

cycle, Toll-like signalling, RIG-like signalling, Nod-like signalling, T-cell receptor, VEGF signalling, MAPK signalling, P53signalling, Hedgehog signalling pathway. These pathways have been widely implicated in various cancers. Through this study, highly regulated oncogenes, tumour suppressor genes and metabolites of CCL are identified. The findings will substantiate the claimed effect of CCL on liver cancer and be used for future study, including isolation of active compounds potentially used for molecular target-based therapeutic treatment for liver cancer.

CHAPTER 2

LITERATURE REVIEW

2.1 Cancer

2.1.1 Burden of Cancer

Cancer has become major public health problem worldwide. It has become primary cause of deaths. Statistics show that the number of deaths caused by cancer is going to surpass the number of death caused by heart-related diseases. It contributes 7.018 million of deaths or 6.53% of total deaths worldwide. However, the low and middle-income countries contribute higher number of total deaths at 4.952 million deaths or constitute lower percentage of total deaths at 5.37%, while higher income countries have contributed 2.066 million deaths or constitute higher percentage of the total death at 17.35%. It is not just a burden on the more developed countries in term of percentage, but also great pressure in less developed countries in term of number. Over the years, the burden has shifted more to less developed countries, which currently account for about 57% of cases and 65% of cancer deaths worldwide (Torre et al., 2015).

According to GLOBOCAN 2012, 14.1 million new cancer cases and 8.2 million cancer-related deaths were occurred in 2012, compared with 12.7 million and 7.6 million, respectively, in 2008. Statistics also reported that 32.6 million people (over the age of 15 years) worldwide live with cancer diagnosed in the previous five years. The most common organs diagnosed with cancers were lung (1.8 million, 13.0% of the total), breast (1.7 million, 11.9%), and colorectum (1.4

million, 9.7%). However, the most common causes of cancer death were lung cancer (1.6 million, 19.4% of the total), liver cancer (0.8 million, 9.1%), and stomach cancer (0.7 million, 8.8%). Projections predict that there would have 19.3 million new cancer cases per year by 2025(Ferlay et al., 2013).

Based on the analysis from GLOBOCAN 2008 for Southeast Asia region, there were 724,699 new cancer cases and 500,439 deaths in the region. Of all new cases, 46% were in males and 54% in females. The three most common cancers among men were lung cancer, liver cancer, and colorectal cancer while breast cancer, cervical cancer and colorectal cancer were for woman. The most common fatal cancer in Southeast Asia for males and females in combination was lung cancer (98,143 cases and 85,772 deaths). The second most common was liver cancer (74,777 cases and 69,115 deaths), followed by colorectal cancer (68,811 cases and 44,280 deaths) (Kimman et al., 2012).

2.1.2 Risk Factors of Cancers

It is difficult to know exactly why one person develops cancer and another does not. Research has identified numerous factors that increase an individual's risk for developing cancer. However, not all factors have the same impact on cancer risk.

The important human carcinogens include alcohol, asbestos, aflatoxins and ultraviolet light. Chronic infections associated with viruses, including hepatitis viruses (HBV, HCV), human papilloma viruses (HPV) and *Helicobacter pylori* play significant roles in the development of cancer. Lifestyle

factors, including diet, physical activity, and alcohol consumption, also play their roles in the development of cancer. Among all the risk factors, tobacco use is the risk factor with the biggest impact (30-35%), followed by obesity and overweight (20%), infection with one of several microorganisms (close to 20%), poor dietary habits (5%) and lack of physical activity (5%) (American Association for Cancer Research, 2015).

2.2 Liver Cancer

2.2.1 Burden of Liver Cancer

Hepatocellular carcinoma (HCC) is the most common liver malignancy in adults worldwide. Approximately 90% of primary liver cancer is HCC and it is much more common in men than in women. Statistically, it is the second leading cause of cancer death for men worldwide and in less developed countries, while the sixth leading cause of cancer death among men in more developed countries. According to GLOBOCAN 2012, 782,500 liver cancer cases and 745,500 deaths occurred worldwide in 2012, with China alone taking up half of the total number of cases and deaths. High liver cancer rates were also observed in South-East Asia as well as Northern and Western Africa.

Liver cancer is the second most common cancer in Southeast Asia and the second leading cause of cancer death. The highest incidence and mortality rates per 100,000 were found in Laos (33.8 and 32.3), Thailand (29.7 and 25.4) and Vietnam (29.3 and 29.2), and the lowest in Brunei (5.2 and 5.4), Malaysia (5.7 and 5.4) and Indonesia (6.7 and 6.6). Their incidence and mortality rates

are more than 2 times higher in males than in females with a poor survival rate, as reflected by almost equal mortality and incidence rates (Kimman et al., 2012).

2.2.2 Risk Factors of Liver Cancer

The global prevalence and mortality resulting from HCC is directly related to underlying risk factors for primary liver cancer. HBV and HCV statistically are the most commonly implicated risk factors for HCC, with HBV responsible for the 54 % of new HCC cases worldwide while HCV take up 31 % of the HCC case. Statistics also show that hepatitis B virus (HBV) and hepatitis C virus (HCV) account for an estimated 32% of infection-related cancer cases, mostly liver cancer, in less developed countries and 19% in more developed countries. The continual inflammations caused by HBV and HCV-associated infection lead to chronic hepatitis and cirrhosis, which are regarded as pre-neoplastic conditions before the formation of HCC(Berasain et al., 2011).

Epidemiological studies show that HBV infection is more prevalent in East Asian and sub-Saharan African populations which are due to unavailability of vaccination, sanitary medical practices, and proper environmental management strategies. Transmission of HBV among these populations is mainly going through vertical transmission (maternal to fetal approach) while the transmission of HCV is mainly through the horizontal approach due to a later exposure to infected body fluids (Hiotis et al., 2012).

Consumption of food contaminated with aflatoxins is another risk factor for the development of HCC. There are approximately 20 related fungal

metabolites in aflatoxins. Among all, aflatoxins B1, B2, G1, and G2 are well studied. Aflatoxin B1 (AFB1) is the most potent chemical liver carcinogen known. Aflatoxins B2 and G2 are the dihydro derivatives of the parent compounds B1 and G1. AFB1 is easily found in agricultural products, including rice, peanuts, cereals, dried fruits, oil seeds and barley. These are the important crops in developing countries, including Southeast Asia and Sub-Saharan Africa. AFB1 is mainly produced by *Aspergillus flavus* and *Aspergillus parasiticus*, which normally grow in humid and dry climates. Crops are exposed to these fungi, during the harvesting and storage, which in turn leads to their proliferation. Cytochrome-P450 enzymes of liver cell metabolize AFB1 to reactive intermediate AFB1-8, 9-epoxide (AFBO) which, in turn, binds to liver cell and causes DNA adducts which subsequently interact with the guanine bases of liver cell DNA and lead to genetic mutation of P53tumour suppressor gene. This mutation causes DNA strand breakage, DNA base damage and oxidative damage leading to cancer. AFB1 induces typical G:C to T:A transversions at the third base in codon 249 of P53 (Staib et al., 2003; Hamid et al., 2013).

However, studies show that the risk from the synergistic effect of having chronic HBV infection and aflatoxin is up to 30 times greater than the risk in individuals exposed to aflatoxin only (Williams et al., 2004). It is believed that increased hepatocyte necrosis caused by chronic HBV infection and AFB1-induced mutations increases the likelihood of the subsequent proliferation of cells with these mutations (Kew, 2003). Aflatoxin also appears to have a synergistic effect on HCV-associated HCC (Liu and Wu, 2010).

Chronic alcohol consumption and smoking are also the risk factors for the development of HCC. Studies show that heavy drinkers have 10-35% chance of developing alcoholic steatohepatitis, 10-20% chance of developing cirrhosis, in which close to 10% of them will progress to HCC. Liver is a major organ for the metabolism and more than 40 tobacco-related active compounds, including known carcinogens such as polycyclic aromatic hydrocarbons, nitrosamines, and aromatic amines are processed in the liver. Nicotine upregulates the CYP2E1 activity, which leads to ROS generation and lipid peroxidation and contributes to the development of HCC (Purohit et al., 2013).

2.2.3 Conventional Treatment Methods for Liver Cancer

The current available conventional treatment options for HCC patients include resection, liver transplant, ablation, embolization, radiotherapy, and chemotherapy. The possible side effects of each treatment option are taken into consideration, along with overall health of patients. Different treatment options offer different chances of curing the disease, extending life, or relieving symptoms. Resection or liver transplant provides better prognosis. When surgery is not available, due to poor health or reduced liver functions, ablation and embolization approaches are used to destroy liver tumours without removing them. However, for most of the patients who are in advanced stage of diseases, these treatment options are not viable. Systemic treatment is deemed as necessary, although chemotherapy being considered ineffective in the treatment of liver cancer (Bruix et al., 2001).

2.3 Targeted Therapy

The chemical agents used in the traditional cancer chemotherapy were designed to block cell division in cancer cells. However, this kind of broad spectrum cytotoxic agents affects the healthy cells too. The low specificity of agents has caused a lot of intolerable side-effects to the patients. Researches have shifted towards targeting specific metabolic pathways, which regulate tumourigenesis to stop cancer growth while inducing less toxic to the normal cells. With the advance of bioinformatic technology with higher computational capability, the anti-cancer drug development has shifted to more pragmatic and rational target-based approach. The strategy has brought clinical benefits to patients with certain tumour types, including leukaemia, breast, colorectal and lung cancers (Weinstein and Joe, 2006; Robert and Der, 2007).

Tumour formation and progression is a complicated process. It involves the malfunction or alteration of certain genes, which cause the deviation of normal pathways which involve various biological functions, including proliferation, transcription, growth, migration, differentiation and death. Among these pathways, most are implicated by the interaction between growth factors and their receptors. Anticancer drugs have been developed to target specific pathways, disrupt their interaction between receptor and ligand, and inhibit these signalling pathways.

Researches have also shown that any change in the microenvironment around cancer cells helps the spread or metastasis of the cancer cells. Cancer forms a complicate linked structure among cancer cells, including endothelial

cells, stromal cells, immune cells and its ever-changing surrounding environment. With its angiogenesis capability, it develops vasculature in new environment (Barrett, 1993, Hawkins, 1995, Hanahan and Folkman, 1996).

Changes in immune response in the surrounding stroma allow the tumour form new blood vessels and spread to other organs. The prevalence of vascular endothelial growth factors (VEGFs) and its receptors (VEGFRs) on the endothelial cells of the tumour vessels as well as the strong presence of platelet-derived growth factor (PDGF) and its receptors (PDGFRs) on the pericytes that support blood vessel growth may suggest their roles in regulating vasculogenesis and angiogenesis which form blood vessels from pre-existing vessels (Shibuya, 2011). Receptor tyrosine kinase (RTK) binds its ligand and activates the downstream phosphorylation before triggering its subsequent signalling for tumour growth or metastasis. RTK inhibitors are developed to disrupt these pathways and slow the growth of the tumour.

Many cancer pathways have been implicated in HCC, including VEGF/RAS pathway, PI3K/AKT/ mTOR pathway as well as WNT/β-catenin Pathway (Wu and Li, 2012a). By altering the genes in these pathways, cancer cells evade apoptosis and stimulate transcription of genes that promote cell-cycle progression, survival and migration. Overexpression of *RAS* was observed in HCC, leading to the down-regulation of its downstream tumour suppressor *SLUG*. Aberrant activation of phosphatidylinositol-3-kinase (PI3K) has a cascade effect on the downstream effector AKT, which is associated with HCC progression and poor HCC prognosis. Phosphorylation of β-catenin and

inhibition of β-catenin degradation manage to stimulate its downstream target genes in HCC (Liu et al., 2015). Many agents have been designed to disrupt these pathways in order to block proliferation of cancer cell. Sorafenib is one of them.

2.3.1 Targeted Therapy for Liver Cancer - Sorafenib

Sorafenib (BAY43-9006; Nexavar) is a multi-kinase inhibitor drug initially used in the treatment of advanced renal cell carcinoma before approved for the treatment of other cancer, including HCC, non-small cell lung cancer and radioactive iodine resistant advanced thyroid carcinoma (Liu et al., 2015). It is the first multi-kinase inhibitor that functioning as a molecular target drug for HCC treatment. It acts by inhibiting the serine–threonine kinases Raf-1, B-RAF, VEGFR, PDGFR, the cytokine receptor c-KIT oncogene and the receptor tyrosine kinases FLT-3 oncogene (Llovet et al., 2008).

Study has shown that Sorafenib inhibited cell growth in HepG2. Genes implicated in angiogenesis, apoptosis, transcription regulation, signal transduction, protein biosynthesis were significantly upregulated while genes involved in cell cycle control, DNA replication recombination and repair, cell adhesion, metabolism and transport were downregulated after the treatment with Sorafenib (Cervello et al., 2012). However, it comes with side-effects, including diarrhoea, skin eruption, and bone marrow dysfunction (Kaseb, 2013). In a study carried out in Asia Pacific, including China, South Korea and Taiwan in 2009, the overall survival period of Sorafenib-treated group has only improved marginally (6.5 months) compared with placebo's (4.2 months) (Cheng et al.,

2009). These suggest that safer and more integrative approach should be explored for the treatment of HCC patients.

2.4 *In vitro* model of the human liver cancer - HepG2 Cell Line

Human cell lines are broadly used to assess the toxic properties and activities of both novel and well known chemical entities. Cell line based assays are a more affordable or effective way of evaluating the properties, compared with the animal models.

HepG2 (ATCC HB-8065) has been listed on the American Type Culture Collection (ATCC) repository in the USA. It was derived from the liver tissue of a 15-year-old white male with a well-differentiated hepatocellular carcinoma. It has been widely used as an *in vitro* model of the human liver cancer due to its high degree of morphological and functional differentiation *in vitro* as well as the absence of viral infection.

However, the origin of the HepG2 is confusing. Studies show that more than 9000 HepG2 references in the scientific literature published in PubMed from 1979 to March 2009 have referred it as hepatocarcinoma or hepatoma more than 7000 times and as hepatoblastoma less than 500 times (Lopez-Terrada et al., 2009). In the study of RNA-Seq gene expression profiling of HepG2 cell versus hepatocarcinoma, it reflected the fact that HepG2 cells are derived from a hepatocarcinoma (Tyakht et al., 2014).

2.5 Potential of Plant as a Source of Alternative Medicine for Cancer Treatment

During the last few decades, tremendous effort has been put in by various parties, including pharmaceutical companies, research institutions, to develop various novel synthetic chemotherapeutic agents so that cancer could be eradicated or reduced with fewer side effects such as nausea, hair loss, vomit, fatigue and so on, upon patients. However, their effectiveness is still far from satisfactory. One of the main problems in cancer treatment is gradual resistance of cancer cells against treatment. The fatality rate of cancer is rather high compared with other diseases. Therefore, there is a constant demand to develop new, effective, and affordable anticancer drugs.

Plants provide a broad spectrum of sources as a drug for diseases, including cancers. Throughout the history, our ancestor has accumulated a lot of experience about medicinal uses of various plants. The records of their therapeutic uses were passed down in different ways. Some could be traced back to ancient literatures, such as those in Traditional Chinese Medicine (TCM) and Ayurveda. However, most of other folkloric medicine systems are not as well-established as TCM and Ayurveda. For many communities, knowledge of therapeutics uses of plants was passed down from one generation to another generation orally. Not recorded, they are at risk of disappearing from mainstream of treatment. It includes procedure of preparing different parts of plant, procedure of handling herbal material so that it could be consumed safely, way of administering the multiple plants together in water decoction to obtain their synergistic effect as a whole.

Close to 80% of world population residing in third world countries is still using natural resources for primary health care (Gordaliza, 2007). Based on the study on the anti-cancer drugs effectively available to the West and Japan covering a time frame from 1940s to 2010, there are 175 small molecule medicines for cancer treatment and 131 medicines or 74.8% of them are other than synthetic medicine, with 85 or48.6% actually being either natural products or medicines directly derived from these natural products (Newman and Cragg, 2012). In the same study, the significant influence of natural product structures can be observed, especially in the area of anti-infections.

Some of the well-known anticancer drugs include Vincaalkaloids (Vinblastine, Vincristine, Vindesine, and Vinorelbine), Taxus diterpenes (Paclitaxel, Docetaxel), Camptotheca alkaloids, Podophyllotoxin and its derivatives (Topothecan, Irinothecan), derived from the Madagascar periwinkle plant *Catharantus Roses*, the Pacific Yew *Taxus Brevifolia*, and the Chinese tree *Camptotheca Acuminate* and Podophyllum species respectively (Mans et al., 2000). These findings were the effort initiated by National Cancer Institute since 1960. It took 30 years (1960-1990) to develop various types of anticancer drug and bring them into clinical uses (Safarzadeh et al., 2014). This small success in discovering the therapeutic agents for cancer has excited the researchers to put in the effort to identify more potential agents from the plants.

However, there are 250,000 to 300,000 plant species in the world with only 5000 over the plant species studied for their possible medical application. Although high throughput screening technology has managed to reduce the drug

discovery time significantly and accelerated the development of drug, a more rational and pragmatic approach should be considered and adopted, instead of using a random screening approach on the plants. With the long history of TCM and Ayurveda and their documented medical effects on humans, they have provided a very fast-track opportunity in screening through some of the plants effectively. The uses of natural plants based on the TCM theory or Ayurveda have been refined on humans, through centuries of trial and error. This refinement has made the molecular target-based therapeutic treatment possible (Wang et al., 2012).

TCM herbalists tend to use different parts of plants, such as the roots, leaves, barks, stems, flowers and exudates, for boiling. They do not isolate any particular phytochemicals from plants before consumption. They believe in combined synergistic effects of herbs. However, for the purpose of "perceived" drug safety and standardization, pharmaceutical companies prefer single ingredients or compounds. Both, medicinal herbs and their derivative phytocompounds are being increasingly used as complementary treatments for cancer patients. Clinical studies have shown the benefit of using herbal medicines together with conventional therapeutics for cancer treatment, especially in extending the survival, improving quality of life, and boosting the immunological systems (Yin et al., 2013).

2.5.1 Plant - *Cratoxylum cochinchinense* (CCL) Lour

Countries in the Southeast Asia are very rich in biodiversity. However, more efforts are still needed to be poured into the researches on the potential benefits of those known tropical plants as well as those unknown plants. It is believed that these tropical plants could be the useful sources of new anti-cancer agents.

There are about 40 genera and 1200 species in the family of Clusiaceae (Guttieferae) and Cratoxylum is one of the genus belonged to Guttiferae. In total, there are six species in Cratoxylym: *Cratoxylum cochinchinense* Lour (CCL) (Figure 2.1; Plate 2.1), *Cratoxylum sumatranum*, *Cratoxylum maingayi*, *Cratoxylumarborescens*, *Cratoxylum neriifolium*, and *Cratoxylum formosanum* (Li and Li, 1990; Soepadmo and Wong, 1995). Among all, CCL has been broadly studied. Its common name is Yellow Cow Wood. It is called Kayu Arang in Malay or 黄牛木 in Chinese. It could be found in low land and hill forest of equatorial countries, including Malaysia, Indonesia, Philippines, Brunei, Indo-China, and South China, Brunei.

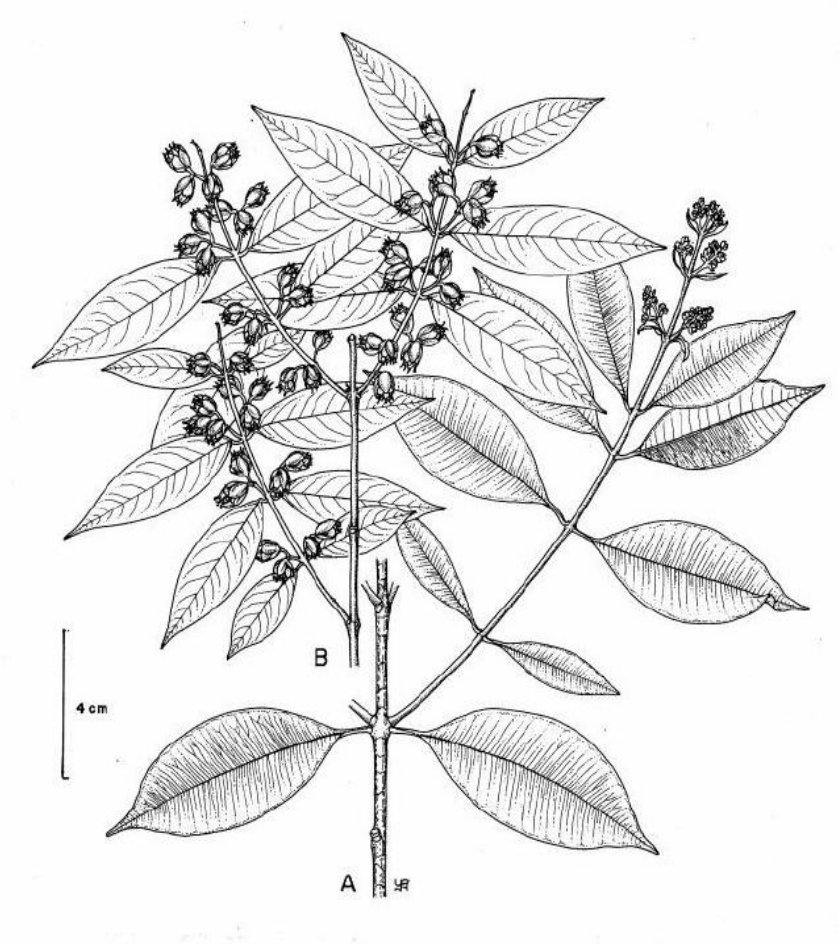

Figure 2.1: Macroscopic morphology of *Cratoxylum cochinchinense* (Soepadmo and Wong, 1995)

Plate 2.1: Photo of full-grown (left) and young (right) *Cratoxylum cochinchinense*

Vietnamese has been using CCL as folk medicine for various illnesses. Its barks, roots and leaves are used for the treatment of fevers, coughs, flatulence, diarrhoea, stomach aches, scabies and eczema, whilst its twigs are used to treat scabies, burns and injuries (Nguyen et al., 2011). In Thailand, it is called ‘‘tuegliang’’ locally and has been used as folk medicine to treat fevers, coughs, diarrhoea, itches, ulcers and abdominal while the decoction of roots and stems of CCL has been used as a diuretic (Laphookhieo et al., 2006; Mahabusarakam et al., 2006). In China, it has been used to detoxify our body and for other treatments, including colds, fever, diarrhoea, jaundice, bruises, carbuncles as well as cancer (Liu, 2003).

Previous investigations on chemical constituents of various parts of CCL have shown its richness in xanthones, triterpenoids, tocotrienols, tocotrienols and flavonoids (Table 2.1).Various xanthones were isolated and identified from hexane extracts of the roots (Laphookhieo et al., 2006), hexane extracts of its stems (Udomchotphruet et al., 2012), ethyl acetate(EA) extract of its barks (Bennett et al., 1993), and EA extract of twigs(Nguyen et al., 2011),dichloromethane extract of its resin and green fruits(Boonnak et al., 2009), and dichloromethane extract of its roots (Mahabusarakam et al., 2006).

Triterpenoids were isolated and identified from the EA extract of its barks (Bennett et al., 1993) and hexane extract of its barks (Nguyen and Harrison, 1999)while tocotrienols were isolated and identified from EA extract of its barks (Bennett et al., 1993). Benzophenones were isolated and identified from ethanol extract of its stems(Yu et al., 2009), while flavonoids were derived from EA extract of leaves (Hoang et al., 2006). Among all, xanthones are the most abundant composition (Nguyen et al., 2011; Table 2.1).

Table 2.1: Summary of various reported chemical compounds detected from different plant parts of CCL

No.	Type	Compound Name	Extraction Solvent Used	Plant Parts	References
1	Xanthone	1,3,5,6-tetrahydroxyxanthone	Ethyl acetate	Bark	(Bennett et al., 1993)
2	Xanthone	celebixanthone	*n*-hexane	Root	(Laphookhieo et al., 2006)
			Dichloromethane	Root	(Mahabusarakam et al., 2006)
3	Xanthone	5-O-methylcelebixanthone	*n*-hexane	Root	(Laphookhieo et al., 2006)
4	Xanthone	α -mangostin	*n*-hexane	Root	(Laphookhieo et al., 2006)
			Combination of *n*-hexane, dichloromethane, methanol	Stem	(Phuwapraisirisan et al., 2006)
			Dichloromethane	Resin & Fruit	(Boonnak et al., 2009)
5	Xanthone	Cratoxylone	Ethyl acetate	Bark	(Bennett et al., 1993)
6	Xanthone	Garcinone D	Ethyl acetate	Bark	(Bennett et al., 1993)
			Dichloromethane	Root	(Mahabusarakam et al., 2006)
7	Xanthone	Dulxis-xanthone B	Combination of *n*-hexane, dichloromethane, methanol	Stem	(Phuwapraisirisan et al., 2006)
8	Xanthone	β-mangostin	*n*-hexane	Root	(Laphookhieo et al., 2006)
			Ethyl acetate	Bark	(Bennett et al., 1993)
			Dichloromethane	Root	(Mahabusarakam et al., 2006)
			Combination of *n*-hexane, dichloromethane, methanol	Stem	(Phuwapraisirisan et al., 2006)
			Ethyl acetate	Twig	(Nguyen et al., 2011)
			Dichloromethane	Resin & Fruit	(Boonnak et al., 2009)
9	Xanthone	Cratoxylumxanthone A	Combination of *n*-hexane, dichloromethane, methanol	Stem	(Phuwapraisirisan et al., 2006)
10	Xanthone	Garcinone B	Dichloromethane	Root	(Mahabusarakam et al., 2006)
11	Xanthone	11-hydoxy-1-isomangostin	Ethyl acetate	Bark	(Bennett et al., 1993)
12	Xanthone	1,3,7-trihydroxy-2,4-di(3-methylbut-2-enyl)xanthone	*n*-hexane	Root	(Laphookhieo et al., 2006)
			Dichloromethane	Root	(Mahabusarakam et al., 2006)
			n-hexane	Bark	(Nguyen and Harrison, 1999)
13	Xanthone	Macluraxanthone	Dichloromethane	Root	(Mahabusarakam et al., 2006)
			Dichloromethane	Resin & Fruit	(Boonnak et al., 2009)
14	Xanthone	7-geranyloxy-1,3-dihyxroxyxanthone	*n*-hexane	Bark	(Nguyen and Harrison, 1999)
			Dichloromethane	Resin & Fruit	(Boonnak et al., 2009)
15	Xanthone	Tovophyllin A	Ethyl acetate	Bark	(Bennett et al., 1993)
16	Xanthone	2-geranyl-1,3,7-trihydroxy-4-(3-methylbut-2-enyl)xanthone	Ethyl acetate	Bark	(Bennett et al., 1993)
17	Xanthone	Cochinchinone A	*n*-hexane	Root	(Laphookhieo et al., 2006)
			Dichloromethane	Root	(Mahabusarakam et al., 2006)
			Ethyl acetate	Twig	(Nguyen et al., 2011)
			Dichloromethane	Resin & Fruit	(Boonnak et al., 2009)
18	Xanthone	Cochinchinone B	Dichloromethane	Root	(Mahabusarakam et al., 2006)

Table 2.1 continued: Summary of various reported chemical compounds detected from different plant parts of CCL

No.	Type	Compound Name	Extraction Solvent Used	Plant Parts	References
19	Xanthone	Cochinchinone C	*n*-hexane	Root	(Laphookhieo et al., 2006)
			Dichloromethane	Root	(Mahabusarakam et al., 2006)
20	Xanthone	Cochinchinone D	Dichloromethane	Root	(Mahabusarakam et al., 2006)
21	Xanthone	3,3a,4,5-tetrahydro-8-10-dihydroxy-3,3-dimethyl-1(3-methyl-2-buten-1-yl)-1,5-Methano-1H,7H-fluro(3,4-d)Xanthone-7,13-dione	Dichloromethane	Root	(Mahabusarakam et al., 2006)
22	Xanthone	5' -demethoxycadensin G	Ethyl acetate	Bark	(Bennett et al., 1993)
23	Xanthone	Cratoxyxanthone	Ethyl acetate	Bark	(Bennett et al., 1993)
24	Triterpenoid	Friedelin	Ethyl acetate	Bark	(Bennett et al., 1993)
25	Triterpenoid	Lupeol	*n*-hexane	Bark	(Nguyen and Harrison, 1999)
26	Triterpenoid	Polypoda-8(26),13,17,21-tetraen-3b-ol	Ethyl acetate	Bark	(Bennett et al., 1993)
27	Triterpenoid	(13E,17E)-polypoda-7,13,17,21-tetraen-3b-01	*n*-hexane	Bark	(Nguyen and Harrison, 1998)
			Ethyl acetate	Twig	(Nguyen et al., 2011)
28	Tocotrienol	d-tocotrienol	Ethyl acetate	Bark	(Bennett et al., 1993)
			Ethyl acetate	Twig	(Nguyen et al., 2011)
29	Tocotrienol	d-tocotrienol dimer	Ethyl acetate	Bark	(Bennett et al., 1993)
30	Tocotrienol	5-(g-tocotrienyl)-g-tocotrienol	Ethyl acetate	Bark	(Bennett et al., 1993)
31	Flavonoid	Tectochrystin	Combination of *n*-hexane, dichloromethane, methanol	Stem	(Phuwapraisirisan et al., 2006)
32	Xanthone	6-Hydroxy-3,7-dimethoxy-8-(3-methylbut-2-enyl)-6',6'-dimethyl-5'-hydroxy-4',5'-dihydropyrano(2',3':1,2) xanthone	Ethanol	Stem	(Jin et al., 2009)
33	Xanthone	6-Hydroxy-3,7-dimethoxy-8-(2-oxo-3-methylbut-3-enyl)-6',6'-dimethyl-5'-hydroxy-4',5'-dihydropyrano(2',3':1,2) xanthone	Ethanol	Stem	(Jin et al., 2009)
34	Xanthone	1,3,7-trihydroxy-2-(2-hydroxy-3-methylbut-3-enyl)-4-(3-methylbut-2-enyl)-xanthone	Ethyl acetate	Twig	(Nguyen et al., 2011)
35	Xanthone	8-hydroxy-1,2,3-trimethoxyxanthone	Ethyl acetate	Twig	(Nguyen et al., 2011)
36	Xanthone	3-O-methylmangostenone D	Ethyl acetate	Twig	(Nguyen et al., 2011)
37	Xanthone	1,6-dihydroxy-5-methoxyxanthone	Ethyl acetate	Twig	(Nguyen et al., 2011)
38	Xanthone	1-hydroxy-5,6-dimethoxyxanthone	Ethyl acetate	Twig	(Nguyen et al., 2011)
39	Xanthone	blancoic acid	Ethyl acetate	Twig	(Nguyen et al., 2011)
40	Xanthone	cochinchinones I–K	Dichloromethane	Resin & Fruit	(Boonnak et al., 2009)
41	Xanthone	Dulxis-Xanthone F	Dichloromethane	Resin & Fruit	(Boonnak et al., 2009)
42	Xanthone	Pruniflorone G	Dichloromethane	Resin & Fruit	(Boonnak et al., 2009)
43	Xanthone	Caged prenylated Xanthone	Dichloromethane	Resin & Fruit	(Boonnak et al., 2009)
44	Xanthone	1,3,7-trihydroxy-2,4-diisoprenylxanthone	Dichloromethane	Resin & Fruit	(Boonnak et al., 2009)
45	Xanthone	Celebixanthone methyl ether	Dichloromethane	Resin & Fruit	(Boonnak et al., 2009)
46	Xanthone	3-geranyloxy-1,7-dihydroxyxanthone	Dichloromethane	Resin & Fruit	(Boonnak et al., 2009)

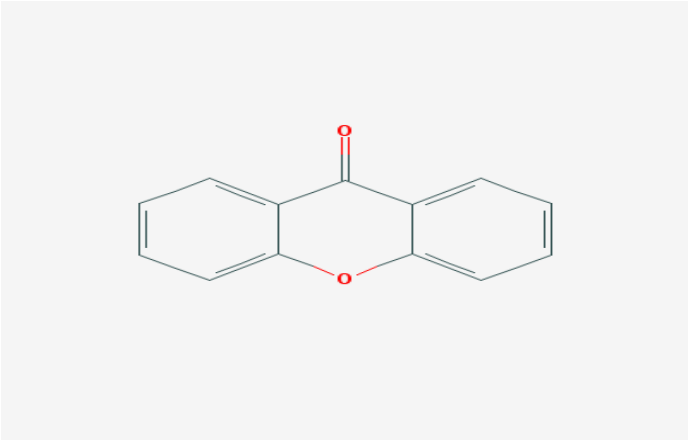

Figure 2.2: Molecular structure of xanthone ($C_{13}H_8O_2$)

Xanthones (Figure 2.2) are compounds which are structurally similar to anthraquinones, and its derivative, mitoxantrone, has been used widely in cancer treatment. It is also good antioxidants. Taiwanese studies using the mangosteen rind, which is in abundance of xanthones, showed that it was cytotoxic to hepatocellular carcinoma, lung cancer, and gastric cancer(Ho et al., 2002). α-Mangostin, a type of prenylated xanthones, found in the extract of its pericarps, has exhibited a cancer preventive effect and an increase of NK cell activity (Akao et al., 2008). Xanthones and α-Mangostin found in this plant have also shown cytotoxicity towards human lung and colon cancers (Ren et al., 2011).

In another experiment using various cell lines, liver cell lines (HFL and HepG2) are most susceptible to extracts of CCL leaves with viability reduced in a concentration- and time-dependent manner. This suggests that CCL might be hepatotoxic. Besides having immunomodulatory, anti-tumour and anti-viral effects, it has shown protective effects against reactive oxygen species (ROS) related damage (Tang et al., 2004b).

In a study done by Ge (2008), ethanol extract of its stems was isolated where26 xanthones and 2 other kinds of compoundswere identified by bioassay-guided fractionation. Studies have shown that some of the xanthones inhibited the growth of various cancer cell lines. This also suggests that xanthones have the antitumour effect (Ge, 2008)**.**

2.5.2 Metabolic Fingerprinting of Plant

Metabonomics is a branch of system biology, using advanced analytical techniques and data-mining systems, to analyse the metabolome of samples. Along with genomics, transcriptomics and proteomics, it has evolved into another important branch of studies since "system biology" was coined. Not only is system biology studying all the components in biological system, but also investigating the interrelationships among these components. It analyses whole constituents at the molecular level, including gene, proteins, to cell and organ level (Auffray et al., 2003).

System biology has been integrative part of TCM. The formula-based medication commonly used in TCM constitutes a drug system including a mixture of numerous compounds. The philosophy of using TCM is system-to-system in nature: a drug system interacting with the human body system. It is different from approach of western medicine which is point to point in nature: single small molecule on a single target (Luo et al., 2011). With thousands of years of clinical practices, it has shown that compound recipe of TCM is far beyond chemistry, rather it is a complex system which has multi-dimensional nonlinear effects on human. This is a collective effect derived from the synergy

of multiple ingredients in a single plant or from a multiple medicinal plant formulation (Dou et al., 2008).

Metabonomics has been extensively used for the quality control of drugs as well as its toxicities. However, the understanding of metabonomics varies. The first level of understanding is target analysis, which targets a subset of metabolites in a sample while the second level is metabolic profiling in which quantitative analysis of known metabolites and establishment of its structures and characteristics. The third level is metabolic fingerprinting in which qualitative or semi-quantitative analysis of all intracellular and extracellular metabolites is conducted while the fourth level is metabonomics which involves comprehensive quantitative and qualitative analysis of all metabolites present in a specific organism (Xia et al., 2009). Due to the technological constraints, some just view metabonomics either as targeted or as global metabolite profiling.

Metabonomics is a science based on biology, analytical chemistry and information science. With advanced analytical instruments, metabonomics could determine and identify a tremendous number of metabolites simultaneously in complex samples. The analytical techniques used in metabonomic studies are primarily nuclear magnetic resonance (NMR) spectroscopy and mass spectrometry (MS). MS has the advantage over NMR due to its higher sensitivity and specificity after ionization. Besides, MS provides rapid detection, selective qualification and quantification, and simultaneous identification and measurement for a variety of metabolites. Chromatographic separation is needed for the separation of the metabolic components before analysis by MS. Gas

chromatography (GC) or liquid chromatography (LC) is widely used for separation. Nevertheless, different separation approaches are used for different types of substances (Lindon et al., 2007; Zhu et al., 2010).

Chromatography-MS-based technologies have been used widely for analysis of endogenous metabolites in complex samples. Volatile oils are one of the main pharmacologically active components of many herb plants and GC-MS based technologies naturally become the preferred choice for analysis. On the other hand, LC/MS based technologies are used for analysis of non-volatile components of the herb plants. It is aided by the utilization of high mass accuracy and information on the tandem mass spectrometry (MS/MS) fragmentation. Multivariate statistics are generated from the analysis and interpreted by other visualization software as well as chemometric and bioinformatic methods (Lindon et al., 2007; Hu and Xu, 2014).

From the perspective of system biology, metabonomics provide links between compound recipe of TCM or herbal medicine and molecular pharmacology. The first generation of chemotherapeutic drugs for cancer treatment were mostly derived from plant secondary metabolites, such as paclitaxel (Taxol), camptothecin (irinotecan, topotecan), and podophyllotoxins (etoposide, teniposide) (Shyur and Yang, 2008). With the help of the metabonomics technology, the potential of using herbs or plants for cancer treatment could be further explored.

2.6 Overview of Gene Expression Technology

Before DNA microarrays started being used in the biological research in the 1990s, traditional genetic research would manipulate individual gene and monitor the effects of this gene in different experimental settings. Using this traditional approach of gathering the data about the genes, researchers might not be able to get an overall picture of how the relative expression of different genes was although tremendous time had to spend on it.

The invention of DNA microarrays has overcome this problem and has allowed large-scale studies of gene expression. This small chip has been embedded with thousands of small spots, containing different fluorescent dyes, which bonded to particular DNA or RNA. Tens of thousands of transcripts are arranged in these arrays of spots. The relative level of the dye could be optically measured and analysed for the expression level of genes. This is particularly useful in the field of biological research since it allows researchers exploring the wide range of gene expression profiles of two or more conditions (treated vs untreated, or disease vs normal) without prejudices. In another word, just one single chip could interpret the whole genome of the organism. This provides better insights into genetic regulation of different diseases. Microarray products have been in the market for quite some time. Most could accommodate 40,000 and above expressed sequences on a chip and measure the entire complement of known transcriptome (Romero et al., 2012). It is suitable for any global gene pattern study, especially for specific diseases or drug treatments.

The core principle behind microarrays is hybridization between two DNA strands. Single stranded labelled probes of known sequence were used to detect the presence of their complements in unknown samples. The higher number of complementary base pairs in a nucleotide sequence is, the tighter non-covalent bonding between the two strands is. Only the strong paired strands remain hybridized after washing process. The total strength of the signal depends upon the amount of target sample binding to the probes present on that spot. The relative quantitation of fluorescence on a microarray can be optically measured and analysed to determine whether there has been higher or lower expression of a particular gene. This subsequently involves using strong algorithms for grouping or clustering those statistically relevant expression data together before any useful info is sorted out for the elucidation of its functional pathways and interaction of the genes.

However, microarray technology has some limitations. The background hybridization has limited the accuracy measurements, especially for those transcripts with low abundance. The detection of genes is also probes-specific. Different probe design may generate different hybridization results. Probe design varies among microarrays. This hybridization specificity depends on the type of microarray used. Some suppliers, such as Affymetrix, Agilent, Nimblegen, use short-oligomer probe set approach while some, especially those for cDNA microarray, may use long-probe approach which involves few hundreds bases in length (Koltai and Weingarten-Baror, 2008). To overcome some of the limitations, different suppliers use different approaches to address the weaknesses of using microarray technology and prolong the lifespan of the

technology. For example, based on available commercial from Affymetrix about its GeneChip Human Transcriptome Array (HTA) 2.0 which was used in this experiment, it claims it measures expression changes at the exon and sub-exon level, taking into account the diversity of transcript isoforms derived from alternative splicing. Ten probes at each unique exonic region provide independent measurements of every transcript isoform from each gene. In addition, HTA contains four unique probes for every known exon-exon junction. On average, 140 probes per gene are measured. HTA, with content from multiple databases, allows analysis of all 15 transcript isoforms independently. It also claims it delivers what RNA sequencing technology missed (http://www.affymetrix.com/fa/media/hta_array_2_0_flyer.pdf).

No doubt, the advent of next-generation sequencing technologies or RNA sequencing techniques has changed the landscape of transcriptomics study of samples. It is a high throughput sequencing technology and allows direct sequencing of transcripts. It does not need the genome annotation for prior probe selection and hybridization bias could be avoided. It allows comparison of gene expression level at any combination of samples, even when genomic sequences are unclear. This makes the whole-genome transcriptome profiling for samples possible. However, the cost of RNA sequencing technique is still relatively high compared with microarray technologies (Zhao et al., 2014).

CHAPTER 3

MATERIAL AND METHODS

3.1 Extraction of *Crytoxylum Cochinchinense* Lour. (CCL)

3.1.1 Collection and Drying of Plant Sample

Cratoxylum Cochinchinense Lour (CCL) plants were collected from the Rawang forest reserve. Different parts of plant samples were collected; these include barks, stems and exudates. Bark and stems were cut into 25-50 mm length with 5-10 mm width or length. There were then dried in room temperature for one month before subjected for solvent extraction.

3.1.2 Extraction and Fractionation of the Crude Extract of CCL

3.1.2.1 Serial Exhaustive Extraction

Serial exhaustive extraction was used to extract wider range of compounds from CCL. It involved successive extraction with solvents of increasing polarity from a non-polar solvent (petroleum ether) to a more polar solvent (methanol). The plant samples (Plate 3.1), including barks, stems and exudates, were macerated separately in a conical flask (Plate 3.2) successively with the solvents of increasing polarity: petroleum ether (PE), ethyl acetate (EA) and methanol (MeOH), over a period of five days for each solvent. The extracts were filtered subsequently and solvents were removed from extracts by using rotary evaporation (Plate 3.3) and freeze-dried. The extracts were stored in capped vials (Plate 3.4 and Plate 3.5) and were weighed. The extracts collected were labelled asbark-PE, bark-EA, bark-MeOH, stem-PE, stem-EA, and stem-

MeOH. The exudate of the plant was soaked in methanol and filtered before subjecting to rotary evaporation. The collected extracts were freeze-dried.

Plate 3.1: Preparation of bark samples for serial exhaustive extraction

Plate 3.2: Soaking of bark samples in solvent

Plate 3.3: Rotary evaporation of solvent

Plate 3.4: Extracts collected: bark-PE (left), bark-EA (center), bark-MeOH (right)

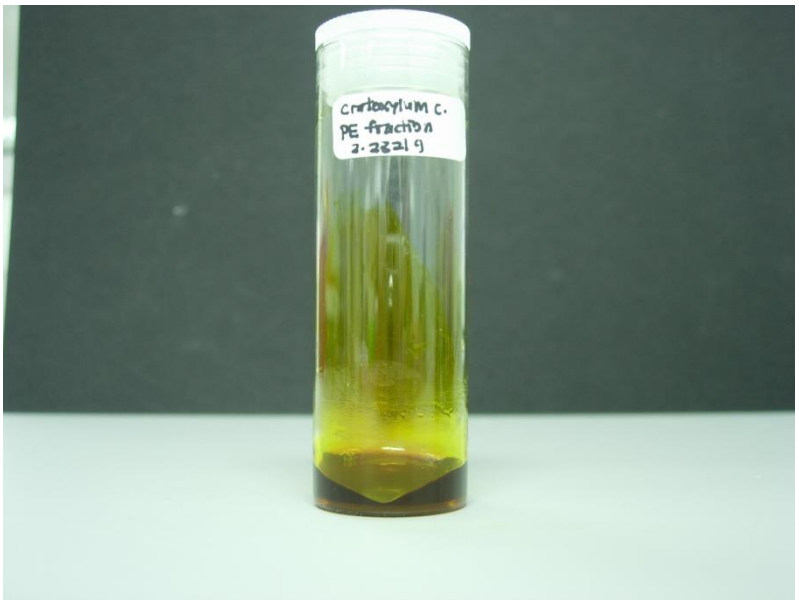

Plate 3.5: Bark-PE extract

3.1.2.2 Aqueous Extraction

The dried plant samples, namely barks and stems, were put separately into steam extractor with 2 L water for 3 hours. Its concentrated extracts were filtered and evaporated before freeze-dried. These aqueous extracts were labelled as bark-boiled and stem-boiled, and then were kept in -20^{o}C for storage.

3.2 Cell Culture

3.2.1 Medium Preparation

The medium used for HepG2 cell maintenance was prepared by dissolving 10.39g of RPMI-1640 powder (Sigma, USA) and 2.0g of sodium bicarbonate with 700-800ml of ultra-pure water and adjusting its pH value to 7.2 before topping up its volume to 1L with ultra-pure water. Then it was filtered using sterilized 0.2 µm cellulose nitrate membrane filter and kept in 4^{o}C before use.

3.2.2 Cell Culture Maintenance

HepG2 were maintained in standard T-75 flask with RPMI complete medium containing 10% of fetal bovine serum (GIBCO, South America) at 37^{o}C in a humidified incubator circulated with 5% of carbon dioxide. Medium was changed when the confluency of the cell in flask reached 80%. Cell number and its viability were determined by trypan blue dye exclusion method by using haemocytometer (Hirschmann Laborgeraete, Germany). A 1:1 ratio of trypan blue (10µl) and cells (10µl) were prepared and put on the haemocytometer. The average number of total viable cells was determined and used for subsequent bioassays.

3.2.3 Cryopreservation of Cell Culture

The cells were checked for its health status, based on the growth, morphology and contamination before cryopreservation. HepG2 cells were transferred into a sterilized centrifuge tube from culture flask and centrifuged at 1500rpm for 5 minutes. The pellet was collected and re-suspended with a mixture of 0.9ml medium with 10% of fetal bovine serum and 0.1ml of dimethyl sulfoxide (DMSO). DMSO acted as a cryoprotectant. It was then transferred into cryopreservation vial and placed in the -80 ^{o}C freezer overnight before transferred to -196^{o}C liquid nitrogen tank.

3.2.4 Thawing of Cell Line

After removed from -80^{O}C freezer, the cells were thawed in 37^{O}C water bath until it was liquefied. The cell was then transferred to a T-75 flask with. The cell culture was cultured with 90% prepared medium supplemented with

10% fetal bovine serum and incubated at 37°C with 5% CO_2 for a day. Fresh prepared medium with 10% of fetal bovine serum was added in the following day.

3.3 Cell Viability Assay

3.3.1 Cell Count Assay

Cells were harvested and cell counting performed using Trypan blue (Sigma-Aldrich, Missouri, US) dye exclusion method by using a haemocytometer (Hirschmann Laboragerate, Germany). 1:1 ratio of Trypan blue and cells were prepared to give a 2-fold dilution of cells. The estimated average number of total viable cells in 1mL was obtained by multiplying this dilution factor above.

3.3.2 Determination of Optimal Cell Concentration

In order to determine the optimum number of HepG2 cells, cells were seeded at different concentrations in the 96-well plates. Approximately $6.5x10^5$ cells/ml of HepG2 were seeded in the wells in triplicate. The cells were serially diluted into $3.25x10^5$, $1.625x10^5$, $0.8125x10^5$, $0.40625x10^5$, $0.203x10^5$, $0.1015x10^5$, $0.5x10^4$, $0.25x10^4$,$0.125x10^4$, $0.625x10^3$ cells/ml respectively. The plated cells were incubated for 4 days, after which MTT assay was carried out and its corresponding absorbance was measured at 570nm by using Tecan Infinite 200 Pro (Tecan, Männedorf, Switzerland). Absorbance versus cell concentration graph was derived and optimum cell concentration in cytotoxicity assay was obtained from the curve of the graph where the exponential phase was.

3.3.3 Evaluation of Cytotoxicity

3.3.3.1 Preparation of Mother Stock for Crude Plant Extracts

The extracts from the serial exhaustive extraction and aqueous extractions, namely bark-PE, bark-EA, bark-MeOH, stem-PE, stem-EA, stem-MeOH, bark-boiled, stem-boiled and exudate were used to prepare the mother stock for this experiment. Twenty mg of each extract was dissolved in 1ml of DMSO, followed by 10 minutes of sonication to ensure full dissolution of extracts. The extracts were kept in 4^{o}C.

3.3.3.2 Preparation of Sub-stocks of Bark Extracts, Stem Extracts, Exudates and Sorafenib for Evaluation of Cytotoxicity

Sub-stocks of extracts from the barks and exudates, namely bark-PE, bark-EA, bark-MeOH, exudates-MeOH, were prepared at the concentration of 100µg/ml from the mother stockof20mg/ml while sub-stocks of other extracts, namely stem-PE, stem-EA, stem-MeOH, stem-boiled, bark-boiled were prepared at the concentration of 200 µg/ml from the mother stock of 20 mg/ml. Mother stock of Sorafenib was prepared by dissolving Sorafenib powder (Bayer, USA) at 10 mg/ml in DMSO.

One hundred µl of each sub-stock, namely bark-PE, bark-EA, bark-MeOH, exudates-MeOH, was added at the concentration of 100 µg/ml into the 96-wells in triplicate. They were then serially diluted to the concentrations of 50, 25, 12.5, 6.25, 3.125, 1.56, 0.78µg/ml in the wells. While 100 µl of other sub-stocks, namely stem-PE, stem-EA, stem-MeOH, stem-boiled, bark-boiled, were added at the concentration of 200 µg/ml to wells in triplicate. They were then

serially diluted to the concentration of 100, 50, 25, 12.5, 6.25, 3.125, 1.56, and 0.78 µg/ml in wells in triplicate. As for the preparation of Sorafenib, 100 µl of sub-stock of Sorafenib at a concentration of 20 µg/ml was added to the wells in triplicate. It was then serially diluted to a concentration of 10, 5, 2.5, 1.25, 0.625, 0.3125, and 0.156 µg/ml in wells in triplicate. Then, $5x10^4$ cells/ml were added into the wells containing the extracts.

Besides the wells with extracts, wells with 100µl of medium only and 100µl of medium with 0.5% of DMSO were prepared in triplicate and served as a control and blank, respectively. The cells were incubated in a CO_2incubator for 24 hours. After that, the cells were treated with extracts and incubated for another 72 hours. MTT was then added into each well with a final concentration of 0.5 mg/ml. The plate was then incubated for another 4 hours until the purple precipitate was visible. Its supernatant was then discarded from each well. 100µl of DMSO was then added into individual well and the plate was then swirled gently by using the low speed shaker in order for the DMSO to dissolve the coloured formazan crystals at room temperature. The absorbance of each well was obtained from the microtiter plate reader Tecan Infinite 200 Pro (Tecan, Männedorf, Switzerland).

3.3.3.3 Determination of IC_{50}

IC_{50} is the concentration of drug required for 50 %inhibition *in vitro*. It is a measurement of the effectiveness of a substance in inhibiting specific biological or biochemical function.

With the concentrations of the extract on the inhibition level of biological function from cytotoxicity assay, the dose-response curve was constructed for each extract, namely bark-PE, bark-EA, bark-MeOH, bark-boiled, stem-PE, stem-EA, stem-MeOH, stem-boiled, exudate, Sorafenib. The value of IC_{50} was derived and further verified by using GraphPad Prism software 5.0 (GraphPad Software Inc., California, US).

3.4 Microarray Gene Expression Analysis

3.4.1 Total RNA Extraction

$4x10^5$of HepG2 cells were seeded in 60.1sqcm culture dish (TPP, Switzerland) with 8ml complete medium in order to get the optimum cell concentration of $5x10^4$ cells/ml which was derived from cell proliferation assay.

After HepG2 cells were seeded for 24hours, the most cytotoxic extract, Bark-PE, was added into the HepG2 cell culture. The IC_{50} concentration of Bark-PE was tested at 20.41µg/ml. The untreated HepG2 cells were incubated with only 0.5% DMSO.

These extract-treated HepG2 cells were then harvested periodically at 0, 6, 12, 18, 24 and 48 hours respectively. Untreated HepG2 cells were also harvested periodically at the similar time points. The harvested cells were subjected total RNA extraction by using total RNA extraction kit (RNeasy Mini Kit, Qiagen) according to manufacturer's instructions.

The purity and integrity of total RNA extracted from the treated and untreated cell at different time points were determined by using Nanodrop UV-Vis Spectrophotometer (Implen, Germany). RNA samples extracted run on a denaturing agarose gel stained with ethidium bromide (EtBr). The 28S rRNA band was approximately twice as intense as the 18S rRNA band. This 2:1 ratio (28S:18S) was a good indication that the RNA was completely intact. These bands were further verified by using Agilent 2100 Bioanalyzer with RNA Labchip Kit.

3.4.2 Target Preparation and Hybridization

GeneChip Human Gene 2.0 ST Array (Affymetrix) was used for this microarray assay. T7 primers (incurring a 3' bias of transcript sensitivity) were used in the cDNA synthesis step for target preparation from the total RNA. An *in vitro* transcription procedure was then carried out to produce biotin-labelled cRNA. In this procedure, second-stranded cDNA template was synthesized and amplified using T7 RNA polymerase. cRNA produced was subsequently purified by removing its enzymes, salts, inorganic phosphates and unincorporated nucleotides. The sense-strand of cDNA was synthesized from this purified cRNA by the reverse transcription using 2^{nd} cycle primers before being hydrolysed. This cDNA was then purified before the procedure of fragmentation and labelling. The fragmented and biotin-labelled ss-cDNA was then mixed with a hybridization cocktail before injected into the GeneChip array, which was then hybridized for 16 hours at 45^{o}C with rotation at 60rpm.

Immediately after hybridization, the hybridized probe arrays underwent an automated washing and staining protocol on the GeneChip" FS450 fluidic station and were then scanned on the GeneChip® Scanner 3000 7G Plus where patterns of hybridization were detected. The hybridization data were collected as light emitted from the fluorescent reporter groups which were already incorporated into the target while being bound to the probe array. Probes that perfectly matched the target generally produced stronger signals than those that had mismatches. Data generated from the scan was then analysed using the Affymetrix GeneChip® Command Console software, v1.1, and the Affymetrix GeneChip® Expression Console software, v 1.1.

3.4.3 Microarray Data Analysis

For each array experiment that was performed using the Affymetrix GeneChip® arrays, six files were generated (*.DAT, *.CEL, *.CHP, *.ARR, *.RPT, *.txt) by the scanner. Affymetrix® Expression Console™ Software was used to perform QC analysis of Gene 2.0 ST Array data. Quality control of chip could be obtained from *.RPT. *.CEL provides cell intensity file that calculates the average intensities for each cell and assigned it to an (x, y) coordinate position. *.ARR contains experimental information. *.CHP contains the analysis output.

Affymetrix GeneChip Human Transcriptome Array (HTA) 2.0, combined with Affymetrix Transcriptome Analysis Console (TAC) software were used for global gene expression analysis for this experiment. Affymetrix GeneChip Human Transcriptome Array Console TAC 2.0 runs a statistical

analysis based on Expression Console (EC) generated CHP to obtain a list of differentially expressed genes and alternative splicing events. The visualization of genes, exons, junctions and transcript isoforms could be obtained. Only those .CEL files and .CHP files satisfied the quality assessment criteria were exported to TAC for further analysis.

3.4.3.1 Quality Control of Arrays

Only those extract-treated samples which fulfilled the quality assessment criteria of microarray assay were selected for further analysis. The quality of microarrays samples was analysed using the functions of RMASketch of Affymetrix Expression Console software (Appendix A-1). The typical values of the pos_vs_neg_auc metric of RMASketch normally fall into the range of 0.8 to 0.9. This AUC value (area under the curve) plots the detection of positive controls against the false detection of negative controls. This metric is a robust measurement for overall data quality. While a value of 1.0 being perfect, a value of 0.5 illustrates no discernible difference between the positive and negative controls. They were further validated by studying the correlation of all the samples. The obvious outliners of triplicate were excluded (Appendix A-2).

3.4.3.2 Grouping of Sample Arrays

The .CEL files and .CHP files of the selected samples were then exported to Affymetrix Transcriptome Analysis Console (TAC) for further analysis. The .CEL files for samples were grouped together based on its type of treated/untreated samples and time points. The.CEL files of individual grouped samples, including sample treated with drug for 6 hours (or extract-treated 6 hrs

sample, and thereafter D6), extract-treated 12 hours sample (D12), extract-treated 18 hours sample (D18), extract-treated 24 hours sample (D24), extract-treated 48 hours sample (D48), untreated 6 hours sample (C6), untreated 12 hours sample (C12), untreated 18 hours sample (C18), untreated 24 hour sample (C24) and untreated 48 hours sample (C48), were then compared with .CEL files of grouped control samples (C0), respectively.

The relative expression fold-change of genes from each grouped sample versus control sample was then derived. This fold change analysis was to measure the change in the expression level of genes by comparing the expression of target genes between two groups of arrays, such as treated sample (D6) versus untreated sample (C6) or D6 versus C0. The data is accessible through GEO Series accession GSE85746 (http://www.ncbi.nlm.nih.gov/geo/query/acc.cgi?acc=GSE85746)

3.4.3.3 Statistical Analysis among Sample Arrays

The statistical data from TAC allows researchers to screen through the *P*-value and level of expression fold change. Only those gene transcripts with *P*-value of less than 0.05 and expression fold change > 2.0 or <-2.0 at any single time point were considered significant (Appendix E). These significant expressed genes were then exported to DAVID Bioinformatics Resources 6.7 of National Institute of Allergy and Infectious Diseases (NIAID) (https://david.ncifcrf.gov/) for functional analysis. Functional annotation cluster analysis of DAVID allows analysing the differentially expressed glycogens from the shortlisted genes from TAC and categorizing them based on gene ontology

(GO) term. These significant genes obtained were then mapped to Kyoto Encyclopaedia of Genes and Genomes (KEGG) pathway and their related well-studied pathways were explicitly indicated.

3.4.4 Gene Selection Guideline for the KEGG Pathway Analysis

The significance of the gene expression was filtered with one-way ANOVA algorithm. *P*-value of less than 0.05 was used to discriminate between differentially expressed genes. Significantly expressed genes, including those with differential expression more than two-fold-changes, were then exported to DAVID Bioinformatics for pathway elucidation analysis.

However, genes which show relatively significant expression between treated samples and untreated samples at their respective time-points were to be included since it indicated the stark difference between expression of treated samples and untreated samples. This selection of these genes was done manually through the screening of genes showing in the Kyoto Encyclopaedia of Genes and Genomes (KEGG) pathways.

3.5 Data Validation and Correlation

3.5.1 Relative Real-time PCR

3.5.1.1 cDNA Synthesis

Total RNA isolated from extractions was used for cDNA synthesis. The Maxima First Strand cDNA Synthesis Kit (Themo Scientific) for RT-qPCR containing oligo(dT)18 and random hexamer primers was used to prime synthesis of first strand cDNA. Five μg of total RNA was mixed with the

Maxima Kit according to manufacturer's instructions. It was then incubated for 10min at 25 ^{o}C, followed by 15 min at 50 ^{o}C. cDNA produced was then used for the qPCR.

3.5.1.2 Preparation for qPCR

QuantiNova SYBR Green PCR kits (Qiagen) was used for qPCR assay. It is composed of Quantinova Yellow template dilution buffer and SYBR Green PCR Master Mix. The dye QuantiNova Yellow template dilution buffer of kit was used for the tracking of the pipette samples in qPCR. When added to the blue SYBR Green PCR Master Mix, the colour changed from blue to green, indicating the successful inclusion of template.

The PCR started with initial heat activation at 95^{o}C for 2minutes to activate the QuantiNova DNA Polymerase. It was followed by 2-steps PCR cycling protocol, which the denaturation step was run at 95^{o}Cfor 5s before a combined annealing and extension step at 60^{o}C for 10s.QuantiNova DNA polymerase remains inactive during low temperature. Within 2 minutes of raising the temperature to 95^{o}C, the Antibody and QuantiNova Guard are denatured and the DNA polymerase is activated and enabled PCR amplification. Gene-specific Primers (GSP) were used based on the shortlisted genes identified in Microarray assays.

3.5.1.3 Construction of Standard Curve of PCR

An exact 5ng/µl of cDNA samples harvested from various time-points at 0, 12, 24, 48 hours, were then diluted to various concentrations at 0.5, 0.05, 0.005 and 0.0005 ng/µl by tenfold serial dilution. The standard curve of each GSP, showing the concentration of GSP versus threshold cycles was then derived. After comparing all the standard curves, the optimum concentration for each GSP was then used for the PCR assay.

3.5.1.4 Normalization of Gene Expression

An exact 2 µl of each cDNA samples were added with 10 µl of SYBR Green and 6 µl of RNase Free water for each GSP. GAPDH was selected as a housekeeping reference gene, while the RNase Free water was used as an internal control for contamination. All of them were prepared in triplicate. The expression of the selected gene was then normalized to GADPH, housekeeping gene.

3.5.2 Western Blot Assay

3.5.2.1 Preparation of Protein and Quantification of Protein

Extract-treated HepG2 cells were harvested at time points of 12, 24, and 48 hours along with untreated HepG2 at time point of 0 hours. RIPA buffer containing protease inhibitor cocktail (Nacalai Tesque, Japan) was then mixed with SDS 1% solution and used to lyse the harvested cells according to manufacturer's instructions (Nacalai Tesque, Japan).

The extracted protein was then quantified using the Thermo Scientific Pierce 660nm Protein Assay. Exact 10 µl of assay standard, extracted protein samples for various time points and blank sample were prepared in triplicate and put into the microplate well. Subsequently, 150 µl of Protein Assay Reagent were added to each well before mixed in a low-speed plate shaker for a minute and incubated at room temperature for 5 minutes. The absorbance of the standards, blank sample, and extracted protein samples were measured at 660 nm using microtiter plate reader Tecan Infinite 200 Pro (Tecan, Männedorf, Switzerland).

A standard curve within the working range of the assay was derived by plotting the average blank-corrected 660nm measurement for each bovine serum albumin (BSA) standard versus its concentration in µg/ml. The protein concentration of the extracted drug-treated samples was then determined.

3.5.2.2Preparation of Western Blot Buffer/Reagents

Western blot buffers and reagents were prepared based on recipes (Appendix B) before the assay.

3.5.2.3 Protein Sample Preparation and Ladder Preparation for SDS-PAGE

Twenty ng of protein samples extracted from untreated cells at 0 hour and extract-treated cell samples at time points of 12 hours, 24 hours, and 48 hours, were prepared in vials and made up to 10 µl with PBS. 10 µl of sample buffer (Thermo Scientific, USA) was then added. This total of 20 µl protein

samples was then denatured at the 90^{o}C for 5 minutes. 1 µl of Chemi-Lumi One Markers Kit (Nacalai Tesque, Japan) was added with 5 µl sample buffer and 4 µl of distilled water. It was then denatured at the 90^{o}C for 4 min. This Chemi ladder was served as detectable protein molecular weight marker on western blotting membrane under chemi-luminescence in gel imager.5 µl of pre-stained standard ladder (Nacalai Tesque, Japan) was used as a detectable protein molecular weight marker for SDS PAGE electrophoresis.

3.5.2.4 Preparation of SDS PAGE Gel

Resolving gel (7.5 %) was poured into the gap between the glass plates in the assembled gel sandwich. Water-saturated *n*-butanol was immediately laid over resolving gel. When polymerization was completed, the overlaid butanol was completely removed. Stacking gel (4 %) was then added on top of the polymerized resolving gel. A 10 wells comb was then inserted into the stacking gel without trapping any bubbles.

After the polymerization of the gels was completed, the comb was removed. The glass plate sandwich was then moved to electrophoresis tank. 1x running buffer was added into the tank so that the wells in the glass plate sandwich were under below buffer surface.

3.5.2.5 Gel Running

An exact 5µl of pre-stained Standards, 10 µl of denatured Chemi ladder and 20 µl denatured protein samples, including untreated protein at 0 hours and extract-treated proteins at time points of 12, 24 and 48hrs, were loaded into the

wells in a pre-determined order. The electrophoresis procedure was run at110V for 80 minutes. After the separation of proteins, the gel was carefully removed from the glass plate sandwich and cut into the right size before being sandwiched by two pieces of filter paper and one piece of Poly-vinylidene-difluoride (PVDF) transfer membrane which was wetted by 100% methanol for 10 minutes prior to the experiment.

The transfer membrane and filter papers were equilibrated with blotting buffer for 15 minutes before the sandwich was then run at 15V at 16 minutes. Once separated proteins were completely transferred onto PVDF membrane, it subsequently was blocked with blocking buffer (Nacalai Tesque, Japan) for 30 minutes and hybridized 1 hour or overnight with the appropriate amount of primary antibody as per manufacturer's instruction (Qiagen, USA). Normally, primary antibody is mixed with the right ratio of washing buffer. The ratio is ranging from 1 µl: 10 ml to 10 µl: 10ml. It was arranged based on the concentrations of primary antibody provided by suppliers.

The blots were then washed for 10 minutes thrice with TBST. The horseradish peroxidase (HRP) conjugated secondary antibody was mixed with the right ratio of washing buffer. The ratio ranged from 1 µl: 10 ml to 10 µl: 10ml. It was arranged based on the concentrations of secondary antibody provided by suppliers. Around 2 µl of HRP conjugated Streptavidin was then added to the 10ml secondary-buffer-washing-buffer. Streptavidin interacted with the biotin of Chemi-Lumi Marker proteins. After one hour of incubation, it was

then followed by the chemiluminescent detection (Nacalai Tesque, Japan) with UVP gel imager (UVP LLC, USA).

3.5.2.6 Stripping Process

After having UVP gel imaging process, the blot membrane was incubated in the stripping buffer for 10 minutes at room temperature for two times before washed with PBS for twice for 10 minutes. Then, it was washed with TBST for twice for 5 minutes before it was kept dry for future use.

3.5.2.7 Hybridization with Primary and Secondary Antibody for Dry Blot Membranes

The dry blot membranes were subsequently blocked with blocking buffer (Nacalai Tesque, Japan) for minimum 30 minutes and hybridized 1 hour or overnight with the appropriate amount of primary antibody as per manufacturer's instruction (Qiagen, USA). Normally, primary antibody is mixed with the right ratio of washing buffer. The ratio is ranging from 1 µl: 10 ml to 10 µl: 10ml. It was arranged based on the concentrations of primary antibody provided by suppliers. The blots were then washed for 10 minutes thrice with TBST. The horseradish peroxidase (HRP) conjugated secondary antibody is mixed with the right ratio of washing buffer. The ratio ranged from 1 µl: 10 ml to 10 µl: 10ml. It was arranged based on the concentrations of secondary antibody provided by suppliers. 2 µl of HRP conjugated Streptavidin was then added to the 10ml secondary-buffer-washing-buffer. Streptavidin interacted with the biotin of Chemi-Lumi Marker proteins.

3.6 Metabolite Analysis

3.6.1 GC-MS Analysis

The extract was dried using vacuum concentrator and then dissolved in a hexane before subjected to GC-MS analysis. GC-MS analysis was performed with a Perkin Elmer Clarus 600 gas chromatography mass spectrometer (GC-MS) equipped with an Elite 5MS fused silica capillary column (30 X 0.25 mm ID X 0.25µm). Helium was used as a carrier gas, constantly set at a flow rate of 1.1 ml/min and the injector split ratio was set to 1:50. An injection volume of 1 µL was used and the solvent cut off time was 5 min. The temperature of the column was programmed to rise from 50ºC, which was held for 2min, to 200ºC at a rate of 10ºC/min and held for 2min. The temperature was then ramped to 250ºC at a rate of 5ºC/min, held for 6min and finally ramped to 280ºC at a rate of 10ºC/min and held for 5min. The total run time was 43min.

The mass spectrometer was operated in electron impact (EI) ionization mode at 70 eV. Elution of solvent, namely PE, was set for the first 5 min. Data acquisition was performed in the full scan mode from mass-to-charge (m/z) of 50 to 600 with a span of scan time from 5 min to 43 min. Chromatogram acquisition and tentative compound identification were performed with TurboMass version 5.4.2.1617 and match against National Institute of Standards and Technology (NIST (2008)) library with match probability cut-off of 650 and above.

CHAPTER 4

RESULTS

4.1 Plant of Interest- *Cratoxylum Cochinchinense* Lour. (CCL)

Cratoxylum Cochinchinense Lour (CCL) was collected from Rawang Forest Reserve, Selangor, Malaysia. Plant identification was authenticated by Mr. Haw Ming Hock, herbalist from Forest Research Institute Malaysia (FRIM). Voucher specimen was prepared and will be deposited at FRIM.

4.2 Extraction of Crude Extract

Serial exhaustive extraction approach was used to sequentially extract various extracts from the barks, stems and exudates of *Cratoxylum Cochinchinense* Lour (CCL). The solvents used for the extraction were petroleum ether (PE), ethyl acetate (EA) and methanol (MeOH) sequentially. Aqueous crude extracts through boiling were collected from the barks and stems.

About 2.2 kg of CCL barks was macerated in solvents sequentially for five days with PE, EA and lastly MeOH. PE, EA, and MeOH extracts of the barks were concentrated using a rotary evaporator, while aqueous extract of barks was concentrated using freeze-dryer. The same procedure was applied to obtain the crude extract from the 9.3 kg of the stem parts of CCL. The weight of raw materials and the yield of extract are listed in Table 4.1.

Table 4.1: The weight of raw materials and their yields

Crude extract	Weight of raw material, g	Yield of extract, g (%)
Bark-PE	2200	2.232 (0.1%)
Bark-EA		84.752 (3.8%)
Bark-MeOH		92.2 (4.14%)
Bark-Boiled	40	1.94 (4.85%)
Stem-PE	930	0.8 (0.086%)
Stem-EA		2.4 (0.26%)
Stem-MeOH		10.2 (1.1%)
Stem-Boiled	60	0.35 (0.6%)
Exudates-MeOH	5.8	0.0267 (4.6%)

4.3 Evaluation of Cytotoxicity

4.3.1 Determination of Optimal Cell Concentration for Bioassay

The optimal cell seeding density was derived from the exponential phase of the standard curve (Figure 4.1). $5x10^4$ cells/ml of HepG2 was used as the initial cell seeding number for subsequent cell cytotoxic assay.

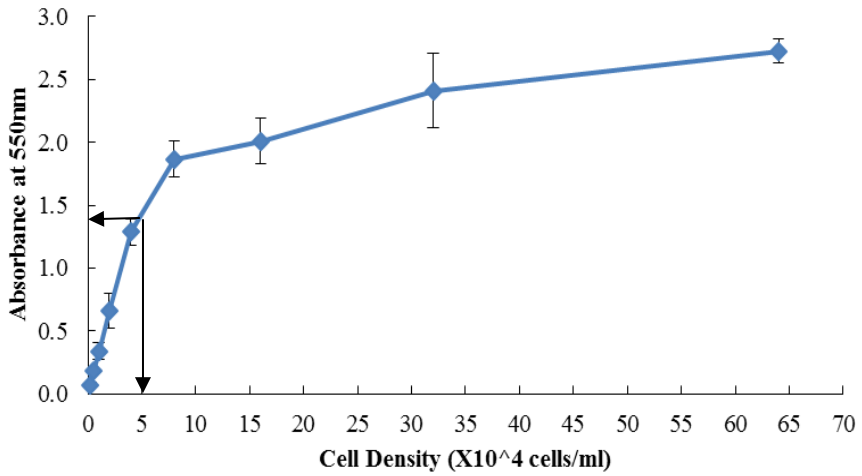

Figure 4.1: Standard curve of HepG2 for optimal cell seeding density in MTT cytotoxicity assay

4.3.2 Determination of Half Maximal Inhibitory (IC_{50}) Concentration of CCL Extracts against HepG2

The optimal cell concentration at $5x10^4$ cells/ml for HepG2 was seeded in each well of 96-well plate before extracts were plated into the wells. Graph of cell viability obtained from each of the serial dilutions of the extract concentration was plotted for each crude extract and standard drug, namely PE extracts, EA extracts, MeOH extracts, aqueous extracts and Sorafenib.

The IC_{50} value of each extract was derived from the corresponding of 50% cell viability in the graph (Figure 4.2). For the extracts of bark, bark-PE extract exhibited the strongest cytotoxicity on the HepG2, followed by bark-EA extract, bark-MeOH extract and lastly aqueous extract. The IC_{50} values obtained were 20.41, 29.56, 35.54 and 44.84 µg/ml, respectively.

Similar observations were seen in the extracts of the stem, in which stem-PE extract showed stronger cytotoxicity towards HepG2 at the IC_{50} value of 83.93 µg/ml, followed by stem-EA extract obtained IC_{50} value of91.52 µg/ml. However, IC_{50}value of the stem MeOH extract and aqueous extract were unable to be derived from the plot due to its relatively low cytotoxicity, with IC_{50} greater than 100 µg/ml.

Methanol exudates (IC_{50}: 20.12µg/ml) showed slightly stronger cytotoxicity towards HepG2 compared with bark PE extract while Sorafenib exhibited an even sharper decrease in cell viability with increasing concentration. The IC_{50} values of all extracts are listed in Table 4.2.

Table 4.2: IC_{50} values of standard drug Sorafenib, the extracts of barks, stems, and exudates of CCL against HepG2 cancer cell

Crude extract	**IC_{50} (µg/ml)**
Sorafenib	3.19
Exudates	20.12
Bark PE	20.41
Bark EA	29.56
Bark MeOH	35.54
Bark Boiled	44.84
Stem PE	83.93
Stem EA	91.52
Stem MeOH	>100
Stem Boiled	>100

(A)

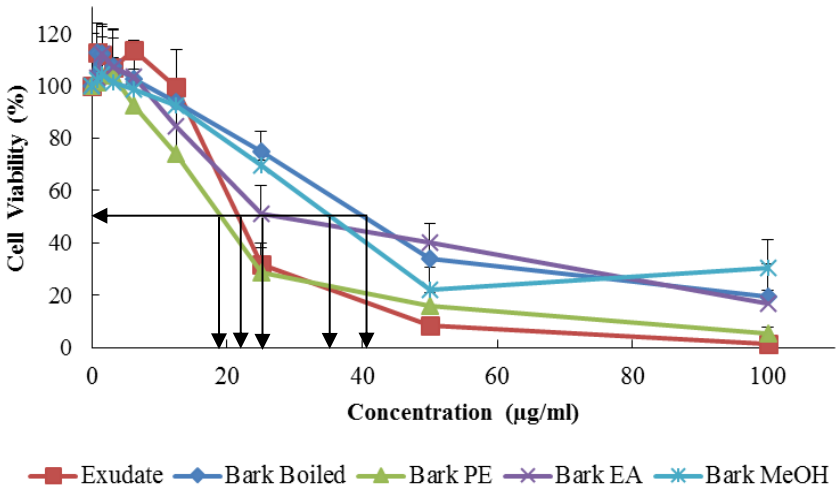

(B)

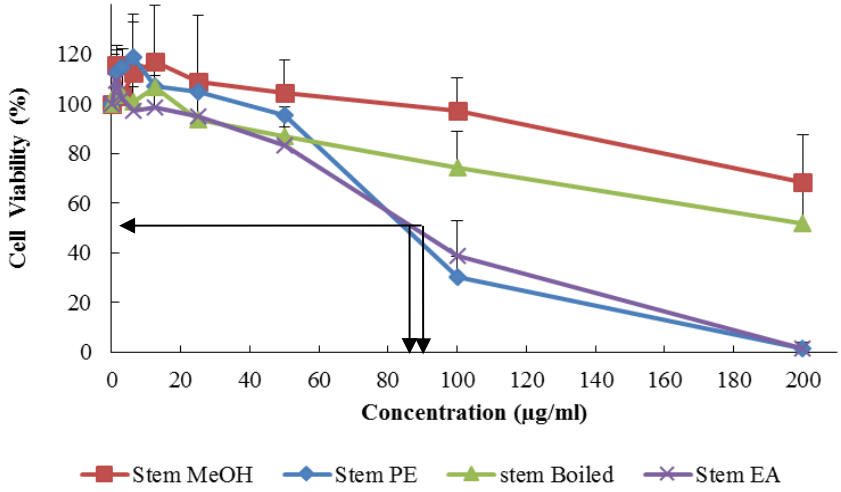

(C)

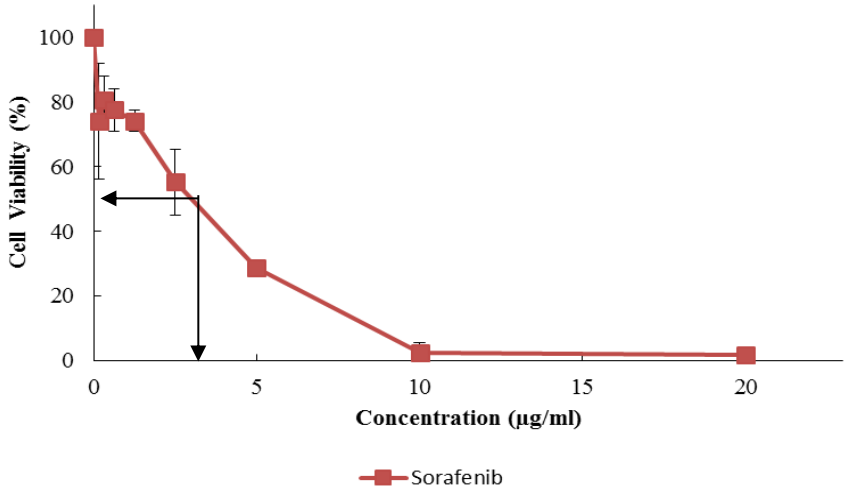

Figure 4.2: Extract concentration response curve of HepG2 cancer cell line treated with (A)bark extracts &exudates, (B) stem extracts, and (C) Sorafenib

4.3.3 Selection of the CCL Extracts for the Microarray Gene Expression Assay

Bark-PE extract was selected for subsequent extract-treated assay due to its wide availability and comparatively low IC_{50} value compared with other extracts.

4.4 Microarray Gene Expression Assays

4.4.1 Observations of Gene Expression among Sample Arrays

There were 1957 significantly regulated genes which are involved in various pathways (Appendix E). The total number of upregulated genes and downregulated genes for treated samples versus untreated samples at different time-points are tabulated in Table 4.3. The following observations were derived:

a) The number of genes down-regulated for extract-treated samples at all the time points was more apparent than the untreated samples.

b) The number of genes down-regulated for untreated samples was not significant at all time-points.

c) The number of genes up-regulated for untreated samples is much lesser than the number of treated samples, except C24.

d) The number of genes up-regulated and down-regulated for extract-treated samples was at the peak at time points of 12 and 18 hours.

Among all the pathways, the well-studied signalling pathways for cancer were analysed and their significant genes are tabulated at respective tables and figures as the following:

a) p53 signalling pathway (Table 4.5&Figure 4.3),

b) Cell cycle (Table 4.6& Figure 4.4),

c) Hedgehog signalling pathway (Table 4.7& Figure 4.5),

d) MAPK signalling pathway (Table 4.8& Figure 4.6),

e) mTOR signalling pathway (Table 4.9& Figure 4.7),

f) TGF-β signalling pathway (Table 4.10& Figure 4.8),

g) ErbB signalling pathway (Table 4.11& Figure 4.9),

h) Notch signalling pathway (Table 4.12& Figure 4.10),

i) VEGF signalling pathway (Table 4.13& Figure 4.11),

j) JAK-STAT signalling pathway (Table 4.14& Figure 4.12),

k) WNT signalling pathway (Table 4.15& Figure 4.13),

l) Toll-like receptor signalling pathway (Table 4.16& Figure 4.14),

m) Nod-like receptor signalling pathway (Table 4.17& Figure 4.15),

n) RIG-like receptor signalling pathway (Table 4.18& Figure 4.16),

o) Chemokine signalling pathway (Table 4.19& Figure 4.17),

p) Cytokine-cytokine receptor interaction (Table 4.20& Figure 4.18),

q) T cell receptor signalling pathway (Table 4.21& Figure 4.19),

r) B cell receptor signalling pathway (Table 4.22& Figure 4.20),

s) Apoptosis (Table 4.23& Figure 4.21),

t) Adherens junction signalling pathway (Table 4.24& Figure 4.22),

u) Focal adhesion (Table 4.25& Figure 4.23) and

v) Natural killer cell cytotoxicity (Table 4.26& Figure 4.24).

The significant differentially expressed genes, including genes showing expression with more than two-fold-changes or showing relatively significant

expressions in treated sample versus untreated samples, among these pathways were selected and tabulated in Table 4.4. Some genes were noted in various pathways due to the crosstalk of these genes among the pathways.

4.4.2 Pathway Analysis from Statistics among Sample Arrays

The tables (Table 4.5 - 4. 26) and graphs (Figure 4.3-4.24) revealed that there were genes regulated by extracts to different extents in various pathways. As summarized in Table 4.4, more regulated genes were observed in cytokine-cytokine receptor interaction, focal adhesion, chemokine signalling, JAK-STAT, MAPK, cell cycle and P53 signalling pathways. The least number of regulated genes were observed in Hedgehog, mTOR, B cell, apoptosis, Notch, WNT, VEGF, Toll-like, Nod-like, RIG-like signalling pathway. Genes in T-cell pathway was not significantly regulated. However, some genes were manually selected for this pathway for discussion due to the stark contrast of expression between treated samples and untreated samples. While a moderate number of genes were observed in other pathways, including TGF-β , ErbB, adherens junction, natural killer cell cytotoxicity.

From these tabulated tables and figures, significant downregulated or upregulated genes in various pathways were noted as follows (more details would be elaborated in the discussion section):

a) p53 signalling pathway (Table 4.5 & Figure 4.3)

Among the downregulated and upregulated genes, SFN and Serpine1 were More significantly downregulated, especially at the early timepoints.

b) Cell cycle (Table 4.6 & Figure 4.4)

RBL1 and SKP2 were significantly upregulated towards the late timepoints while WEE1 was significantly downregulated, especially at the early timepoints.

c) Hedgehog signalling pathway (Table 4.7 & Figure 4.5)

WNT11 was significantly downregulated from timepoint of 12 hours to 24 hours.

d) MAPK signalling pathway (Table 4.8 & Figure 4.6)

MAP2K6 was more significantly upregulated while DUSP5 was more downregulated significantly across all timepoints among all.

e) mTOR signalling pathway (Table 4.9 & Figure 4.7)

DDIT4 was more significantly downregulated across all the timepoints.

f) TGF-β signalling pathway (Table 4.10 & Figure 4.8)

ID1 and ACVR1 were more significantly downregulated among all the samples.

g) ErbB signalling pathway (Table 4.11 & Figure 4.9)

AREG, EREG and SOS1 were significantly downregulated across the timepoints, compared with timepoints of untreated samples.

h) Notch signalling pathway (Table 4.12 & Figure 4.10)

JAG1 was significantly downregulated across all the timepoints, compared with timepoints of untreated samples.

i) VEGF signalling pathway (Table 4.13 & Figure 4.11)

Cross-talk effect of MAPK13 was seen in this pathway. It was significantly downregulated across all the timepoints.

j) JAK-STAT signalling pathway (Table 4.14 & Figure 4.12)

IL11, LIF, PIM1, SPRY4 were seen downregulated significantly, especially IL11, which was downregulated in a much larger scale.

k) WNT signalling pathway (Table 4.15 & Figure 4.13)

WNT11 and FOSL1 were significantly downregulated.

l) Toll-like receptor signalling pathway (Table 4.16 & Figure 4.14)

MAP2K6 was significantly upregulated while MAPK13 was significantly downregulated. Downregulation of IL8 was also seen at all timepoints.

m) Nod-like receptor signalling pathway (Table 4.17 & Figure 4.15) &RIG-like receptor signalling pathway (Table 4.18 & Figure 4.16)

Cross-talk effect of MAPK13 was also seen in these pathways. It was significantly downregulated across all the timepoints, along with the significant downregulation of IL8.

n) Chemokine signalling pathway (Table 4.19 & Figure 4.17)

CCL20 and BCAR1 were significantly downregulated across all timepoints.

o) Cytokine-cytokine receptor interaction (Table 4.20 & Figure 4.18)

Along with the downregulation of LIF and CCL20, the downregulation of IL8, IL11, and IL6R were significantly observed while TNFSF10 and TNFRSF19 were seen upregulated significantly.

p) T cell receptor signalling pathway (Table 4.21 & Figure 4.19)

Cross-talk effect of MAPK13 was seen in this pathway. It was significantly downregulated across all the timepoints. Downregulation of SOS1 was observed across all the timepoints.

q) B cell receptor signalling pathway (Table 4.22 & Figure 4.20)

Cross-talk effect of MAPK13 was seen in this pathway. Apart from the downregulation of SOS1, CD22 was seen downregulated significantly across all the timepoints.

r) Apoptosis (Table 4.23 & Figure 4.21)

Besides the upregulation of TNFSF10, IRAK2 was seen significantly downregulated across the timepoints.

s) Adherens junction signalling pathway (Table 4.24 & Figure 4.22)

The upregulation of CDH1 and significant downregulation of SNAI2across timepoints were observed.

t) Focal adhesion (Table 4.25 & Figure 4.23)

Along with the downregulation of SOS1, the significant downregulationsof ZYX, VASP and BCAR1 were observed across the timepoints.

u) Natural killer cell cytotoxicity (Table 4.26 & Figure 4.24)

Significant downregulation of SOS1 and upregulation of TNFSF10 were observed across the timepoints.

Table 4.3 Differential gene analysis between samples at different time-point versus control at 0 hour (C0)

	Number of gene up-regulated				
Time-point (Hour)	**6**	**12**	**18**	**24**	**48**
Treated Sample (D6, D12, D18, D24, D48)	260	482	387	229	174
Untreated Sample (C6, C12, C18, C24, C48)	13	92	101	238	57

	Number of gene down-regulated				
Time-point (Hour)	**6**	**12**	**18**	**24**	**48**
Treated Sample (D6, D12, D18, D24, D48)	117	149	165	117	71
Untreated Sample (C6, C12, C18, C24, C48)	4	6	7	1	3

* Gene transcripts with ANOVA *P*-value < 0.05 and expression fold-change >2 or fold change <-2 for each timepoint are considered significant

Table 4.4: Gene differentially regulated versus control 0 hours after treated with bark-PE for 6, 12, 18, 24, and 48 hours, respectively

Biological Pathway	Up-Regulation	Down-Regulation
P53 pathway (Table 4.5 & Figure 4.5)	CCNE2, SESN3, THBS1, SESN1*	SFN, GADD45B, SERPINE1, SESN2, CDKN1A*
Cell Cycle (Table 4.6 & Figure 4.6)	SKP2, CCNE2, RBL1, CDC6, CDC7	TGFB1, CDKN2B, GADD45B, SFN, WEE1, CDC25B, CDKN1A*
Hedgehog Signalling pathway (Table 4.7 & Figure 4.7)	SMO, STK36	WNT11
MAPK pathway (Table 4.8 & Figure 4.8)	MAP2K6	MAPK13, CACNA1H, SOS1, RRAS, DUSP5, DUSP6, DUSP8, SRF, TGFB1, GADD45B, JUND, CDC25B, JUN*, EGFR*
mTOR Signalling pathway (Table 4.9 & Figure 4.9)		DDIT4, RICTOR*, PIK3CA*
TGF-β Signalling pathway (Table 4.10 & Figure 4.10)	THBS1	IDI, TGFB1, RBL1, CDKN2B, FST, ACVR1
ERBB signalling pathway (Table 4.11 & Figure 4.11)		AREG, EREG, SOS1, JUN*, EGFR*, PIK3CA*, CDKN1A*
Notch signalling Pathway (Table 4.12 & Figure 4.12)	NUMB*	JAG1, HES1
VEGF signalling pathway (Table 4.13 & Figure 4.13)		MAPK13, PIK3CA*
JAK-STAT signalling pathway (Table 4.14 & Figure 4.14)	PRLR	IL11, LIF, IL6R, PIM1, SOS1, SPRY4, PI3KCA*
WNT signalling pathway (Table 4.15 & Figure 4.15)		WNT11, FOSL1, JUN*, LRP5*
Toll-like receptor signalling pathway (Table 4.16 & Figure 4.16)	MAP2K6	MAPK13, IL8, PI3KCA*, JUN*
Nod-like receptor signalling pathway (Table 4.17 & Figure 4.17)	NAIP	MAPK13, IL8,
RIG like receptor signalling pathway (Table 4.18 & Figure 4.18)		MAPK13, IL8
Chemokine Signalling pathway (Table 4.19 & Figure 4.19)		CCL20, SOS1, BCAR1, ARRB2, PI3KCA*, CCR6*, PARD3*
Cytokine-cytokine receptor interaction(Table 4.20 & Figure 4.20)	KITLG, PRLR TNFRSF19, TNFSF10	IL8, CCL20, IL11, IL6R, LIF, TGFB1, ACVR1, EGFR*, CCR6*
T cell receptor signalling pathway (Table 4.21 & Figure 4.21)		MAPK13, SOS1, JUN*, PI3KCA*, LCK*
B cell receptor signalling pathway (Table 4.22 & Figure 4.22)		CD22, SOS1, JUN*, PI3KCA*
Apoptosis signalling pathway (Table 4.23 & Figure 4.23)	TNFSF10	IRAK2, PI3KCA*
Adherens junctions signalling (Table 4.24 & Figure 4.24)		CDH1,SNAI2, EGFR*, PARD3*
Focal adhesion (Table 4.25 & Figure 4.25)		ZYX, BCAR1, SOS1, VASP, MYL9, EGFR*, PI3KCA*, JUN*
Natural Killer Cell Cytotoxicity (Table 4.26 & Figure 4.26)	TNFSF10	SOS1, LCK*, PI3KCA*

***Gene with fold-change of expression < 2 but were relatively significant versus untreated time-points**

Table 4.5: The list of genes which are significantly expressed (>2-fold change) or relatively significantly expressed* (timepoints vs timepoint 0) in p53 signalling pathway

Transcription Cluster ID	Entrez ID	Gene Name	Gene Symbol	D6	D12	D18	D24	D48	C6	C12	C18	C24	C48	Biological Function
16661314	2810	Stratifin	SFN	-2.97	-6.25	-4.81	-6.59	-4.03	-1.3	-1.52	-1.66	-1.47	-1.25	Regulation of protein
16856803	4616	Growth arrest and DNA-damage-inducible, beta	GADD45B	-2.65	-2.41	-2.71	-2.65	-2.69	-1.34	-1.16	-1.02	1.17	1.04	Cell development/ differentiation; Apoptosis
17079293	9134	Cyclin E2	CCNE2	1.27	1.42	1.75	2.24	2.18	-1.13	1.18	1.25	1.12	1.36	Control of the cell cycle at the late G1 and early S phase
17049676	5054	Serpin peptidase inhibitor, clade E (nexin, plasminogen activator inhibitor type 1), member 1	Serpine1	-4.9	-5.06	-4.64	-4.82	-3.08	-1.63	-1.02	1.07	1.95	2.27	Serine-type endopeptidase inhibitor activity
16799315	7057	Thrombospondin 1	THBS1	-1.98	1.04	1.49	1.99	2.32	-1.07	1.43	1.63	1.75	1.47	Cell to cell interaction
16661544	83667	Sestrin 2	SESN2	-1.43	-1.68	-2.9	-2.37	-2.42	-1.66	-1.57	-1.31	-1.42	-1.38	Cell cycle arrest
16743432	143686	Sestrin 3	SESN3	1.33	1.46	1.63	2.13	1.92	1.07	1.2	-1.05	1.02	1.06	Cell growth
17008007	1026	Cyclin-dependent kinase inhibitor 1A (p21, Cip1)	CDKN1A*	-1.85	-1.51	-1.64	-1.52	-1.85	-1.1	-1.06	-1.17	1.19	1.23	Cell cycle arrest
17022362	27244	Sestrin 1	SESN1*	1.21	1.42	1.43	1.51	1.47	-1.11	-1.13	-1.15	-1.12	-1.09	Cell growth

Table 4.6: The list of genes which are significantly expressed (>2-fold change) or relatively significantly expressed* (timepoints vs timepoint 0) in cell cycle

Transcription Cluster ID	Entrez ID	Gene Name	Gene Symbol	D6	D12	D18	D24	D48	C6	C12	C18	C24	C48	Biological Function
16919044	5933	Retinoblastoma-like 1 (p107)	RBL1	1.26	1.6	1.65	1.76	3.05	-1.15	-1.08	1.18	1.34	1.27	Proliferation, Differentiation
16872551	7040	Transforming growth factor, beta 1	TGFB1	-1.77	-2.02	-1.71	-2.02	-1.52	-1.47	-1.31	-1.52	-1.29	-1.16	Proliferation, Differentiation
16984032	6502	S-phase kinase-associated protein 2 (p45)	SKP2	1.51	2.32	3.14	4.43	4.04	-1	-1.03	1.04	-1.24	-1.09	G1/S transition of mitoric cell cycle
17079293	9134	Cyclin E2	CCNE2	1.27	1.42	1.75	2.24	2.18	-1.13	1.18	1.25	1.12	1.36	Control of the cell cycle at the late G1 and early S phase
17092901	1030	Cyclin-dependent kinase inhibitor 2B (p15, inhibits CDK4)	CDKN2B	-1.67	-1.74	-1.75	-2.09	-1.45	-1.38	-1.49	-1.14	-1.32	1.13	Cell cycle arrest
16834056	990	Cell division cycle 6 homolog (S. cerevisiae)	CDC6	1.43	1.88	1.95	2.25	3.68	1.03	1.26	1.17	1.21	1.12	DNA replication
16667037	8317	Cell division cycle 7 homolog (S. cerevisiae)	CDC7	1.22	2.06	1.42	1.7	1.72	-1.07	1.12	1.21	1.61	1.29	DNA replication
16856803	4616	Growth arrest and DNA-damage-inducible, beta	GADD45B	-2.65	-2.41	-2.71	-2.65	-2.69	-1.34	-1.16	-1.02	1.17	1.04	Cell development/differentiation; Apoptosis
16661314	2810	Stratifin	SFN	-2.97	-6.25	-4.81	-6.59	-4.03	-1.3	-1.52	-1.66	-1.47	-1.25	Regulation of protein
16721835	7465	WEE1 homolog (S. pombe)	WEE1	-3.35	-1.73	-1.54	-1.37	-1.46	-1.25	-1.09	1.16	1.09	1.16	G2 to M transition
16911040	994	Cell division cycle 25 homolog B (S. pombe)	CDC25B	-1.06	-1.47	-1.97	-2.03	-1.33	-1.01	-1.39	-1.56	-1.29	-1.26	Catalytic activity
17008007	1026	Cyclin-dependent kinase inhibitor 1A (p21, Cip1)	CDKN1A*	-1.85	-1.51	-1.64	-1.52	-1.85	-1.1	-1.06	-1.17	1.19	1.23	Cell cycle arrest

Table 4.7: The list of genes which are significantly expressed (>2-fold change) or relatively significantly expressed* (timepoints vs timepoint 0) in Hedgehog signalling pathway

Transciption Cluster ID	Entrez ID	Gene Name	Gene Symbol	D6	D12	D18	D24	D48	C6	C12	C18	C24	C48	Biological Function
17051392	6608	Smoothened homolog (Drosophila)	SMO	1.43	1.89	1.77	1.83	2.01	1.38	1.1	-1.11	1.04	1.06	Cell proliferation
16890998	27148	Serine/threonine kinase 36, fused homolog (Drosophila)	STK36	1.9	2.55	1.66	2.02	2.99	1.51	1.62	1.62	2.65	1.66	Catalytic activity
16742340	7481	Wingless-type MMTV integration site family, member 11	WNT11	-1.8	-3.22	-3.01	-3.4	-2.49	-1.15	-1.1	-1.07	-1.31	1.07	Cell development

Table 4.8: The list of genes which are significantly expressed (>2-fold change) or relatively significantly expressed* (timepoints vs timepoint 0) in MAPK signalling pathway

Transcription Cluster ID	Entrez ID	Gene Name	Gene Symbol	D6	D12	D18	D24	D48	C6	C12	C18	C24	C48	Biological Function
16814584	8912	Calcium channel, voltage-dependent, T type, alpha 1H subunit	CACNA1H	-1.25	-1.82	-2.83	-1.85	-2.3	-1.15	1.33	1.19	1.12	1.12	Cell growth
16896710	6654	Son of sevenless homolog 1 (Drosophila)	SOS1	-2.67	-2.17	-2.89	-2.28	-1.4	-1.87	-1.05	1.14	1.36	1.03	Apoptosis
16874339	6237	Related RAS viral (r-ras) oncogene homolog	RRAS	-1.97	-2.31	-2.19	-2	-3.41	-1.46	-1.71	-2.08	-2.02	-1.6	Promotes focal adhension formation
16709128	1847	Dual specificity phosphatase 5	DUSP5	-5.39	-5.15	-7.57	-7.36	-12	-1.31	-1.22	-1.22	-1.12	-1.28	Tyrosine/serine / thereonince phosphatase activity
16768297	1848	Dual specificity phosphatase 6	DUSP6	-2.12	-1.69	-1.83	-1.98	-1.47	-1.18	-1.06	1.02	-1.1	-1.41	Tyrosine/ serine / thereonince phosphatase activity
16734271	1850	Dual specificity phosphatase 8	DUSP8	-2.68	-2.29	-1.78	-1.76	-2.67	-1.43	-1.08	-1.07	1.01	-1	Tyrosine/ serine/ thereonince phosphatase activity
17008856	6722	Serum response factor (c-fos serum response element-binding transcription factor)	SRF	-2.05	-1.76	-1.31	-1.33	-1.52	-1.27	-1.35	-1.33	-1.36	-1.34	Transcription factor
16872551	7040	Transforming growth factor, beta 1	TGFB1	-1.77	-2.02	-1.71	-2.02	-1.52	-1.47	-1.31	-1.52	-1.29	-1.16	Proliferation, Differentiation
16856803	4616	Growth arrest and DNA-damage-inducible, beta	GADD45B	-2.65	-2.41	-2.71	-2.65	-2.69	-1.34	-1.16	-1.02	1.17	1.04	Cell cycle
16870384	3727	Jun D proto-oncogene	JUND	-2.07	-2.09	-1.76	-1.92	-2.18	-1.45	-1.16	-1.16	-1.24	-1.31	Cell proliferation
17007910	5603	Mitogen-activated protein kinase 13	MAPK13	-1.58	-2.07	-2.23	-2.37	-1.97	-1.12	-1.2	-1.1	-1.02	1.08	Protein Binding
16837348	5608	Mitogen-activated protein kinase kinase 6	MAP2K6	1.2	3.93	5.78	5.15	3.27	1.23	-1.1	-1.28	-1.72	-1.5	Protein Binding
16911040	994	Cell division cycle 25 homolog B (S. pombe)	CDC25B	-1.06	-1.47	-1.97	-2.03	-1.33	-1.01	-1.39	-1.56	-1.29	-1.26	Catalytic activity
16687875	3725	Jun oncogene	JUN*	-1.83	-1.6	-1.7	-1.7	-1.42	-1.17	1.21	1.1	1.35	1.3	Transcription factor
17046135	1956	Epidermal growth factor receptor (erythroblastic leukemia viral (v-erb-b) oncogene homolog, avian)	EGFR*	-1.14	-1.15	-1.76	-1.6	-1.26	1.04	1.43	1.15	1.79	1.29	Cell growth , differentiation

Table 4.9: The list of genes which are significantly expressed (>2-fold change) or relatively significantly expressed* (timepoints vs timepoint 0) in mTOR signalling pathway

Transcription Cluster ID	Entrez ID	Gene Name	Gene Symbol	D6	D12	D18	D24	D48	C6	C12	C18	C24	C48	Biological function
16705961	54541	DNA-damage-inducible transcript 4	DDIT4	-1.53	-1.7	-2.69	-3.28	-2.24	-1.44	-1.07	-1.28	-1.28	-1.57	Cell proliferation
16995551	253260	RPTOR independent companion of MTOR, complex 2	RICTOR*	-1.25	-1.31	-1.71	-1.72	-1.73	-1.12	-1.04	1.09	1.28	-1.05	Protein binding
16948209	5290	phosphoinositide-3-kinase, catalytic, alpha polypeptide	PIK3CA*	-1.41	-1.51	-1.58	-1.72	-1.37	-1.23	-1.15	-1.19	-1.01	-1.29	Protein binding

Table 4.10: The list of genes which are significantly expressed (>2-fold change) or relatively significantly expressed* (timepoints vs timepoint 0) in TGF-βsignalling pathway

Transcription Cluster ID	Entrez ID	Gene Name	Gene Symbol	D6	D12	D18	D24	D48	C6	C12	C18	C24	C48	Biolgical Function
16912362	3397	Inhibitor of DNA binding 1, dominant negative helix-loop-helix protein	ID1	-1.55	-1.6	-1.55	-2.02	-1.08	-1.18	-1.2	-1.33	-1.1	-1.25	Protein Binding
16799315	7057	Thrombospondin 1	THBS1	-1.98	1.04	1.49	1.99	2.32	-1.07	1.43	1.63	1.75	1.47	Cell to cell interaction
16872551	7040	Transforming growth factor, beta 1	TGFB1	-1.77	-2.02	-1.71	-2.02	-1.52	-1.47	-1.31	-1.52	-1.29	-1.16	Proliferation, Differentiation
16919044	5933	Retinoblastoma-like 1 (p107)	RBL1	1.26	1.6	1.65	1.76	3.05	-1.15	-1.08	1.18	1.34	1.27	Cell division regulator
17092901	1030	Ccyclin-dependent kinase inhibitor 2B (p15, inhibits CDK4)	CDKN2B	-1.67	-1.74	-1.75	-2.09	-1.45	-1.38	-1.49	-1.14	-1.32	1.13	Cell Cycle Arrest
16984730	10468	Follistatin	FST	-2	-1.73	-1.28	-1.33	1.48	1.28	1.25	1.18	1.24	1.37	Cell Differentiation
16903969	90	Activin A receptor, type I	ACVR1	-1.3	-1.55	-1.74	-2.08	-1.35	-1.26	1.01	1.02	1.04	1.05	G1/S transition of mitotic cell cycle

Table 4.11: The list of genes which are significantly expressed (>2-fold change) or relatively significantly expressed* (timepoints vs timepoint 0) in ERBB signalling pathway

Transcription Cluster ID	Entrez ID	Gene Name	Gene ID	D6	D12	D18	D24	D48	C6	C12	C18	C24	C48	Biological Function
16967863	374	Amphiregulin	AREG	-4.1	-4.17	-4.37	-4.44	-3.85	-1.19	-1.08	1.35	1.56	1.86	Protein Binding
16967843	2069	Epiregulin	EREG	-2.66	-2.54	-2.19	-3.41	-2.28	-1.07	-1.04	1.38	1.19	2.2	Cell proliferation /Angiogenesis
16896710	6654	Son of sevenless homolog 1 (Drosophila)	SOS1	-2.67	-2.17	-2.89	-2.28	-1.4	-1.87	-1.05	1.14	1.36	1.03	Apoptosis
17046135	1956	Epidermal growth factor receptor (erythroblastic leukemia viral (v-erb-b) oncogene homolog, avian)	EGFR*	-1.14	-1.15	-1.76	-1.6	-1.26	1.04	1.43	1.15	1.79	1.29	Cell growth, differentiation
16687875	3725	Jun oncogene	JUN*	-1.83	-1.6	-1.7	-1.7	-1.42	-1.17	1.21	1.1	1.35	1.3	Transcription factor
16948209	5290	Phosphoinositide-3-kinase, catalytic, alpha polypeptide	PIK3CA *	-1.41	-1.51	-1.58	-1.72	-1.37	-1.23	-1.15	-1.19	-1.01	-1.29	Protein binding
17008007	1026	Cyclin-dependent kinase inhibitor 1A (p21, Cip1)	CDKN1A*	-1.85	-1.51	-1.64	-1.52	-1.85	-1.1	-1.06	-1.17	1.19	1.23	Cell cycle arrest

Table 4.12: The list of genes which are significantly expressed (>2-fold change) or relatively significantly expressed* (timepoints vs timepoint 0) in Notch signalling pathway

Transcription Cluster ID	Entrez ID	Gene Name	Gene Symbol	D6	D12	D18	D24	D48	C6	C12	C18	C24	C48	Biological Function
16917183	182	Jagged 1 (Alagille syndrome)	Jag1	-2.28	-2.28	-2.12	-2.01	-1.74	1.34	1.56	1.84	1.72	1.63	Protein binding
16949759	3280	Hairy and enhancer of split 1, (Drosophila)	HES1	-2.17	-1.67	-1.46	-1.38	-1.14	-1.16	1.04	1.06	1.06	-1.14	Cell proliferation
16786239	8650	Numb homolog (Drosophila)	NUMB*	1.53	1.56	1.57	1.56	1.53	1.31	1.04	1.02	1.04	-1.07	Cell development/ differentiation

Table 4.13: The list of genes which are significantly expressed (>2-fold change) or relatively significantly expressed* (timepoints vs timepoint 0) in VEGF signalling pathway

Transcription Cluster ID	Entrez ID	Gene Name	Gene Symbol	D6	D12	D18	D24	D48	C6	C12	C18	C24	C48	Biological Function
17007910	5603	Mitogen-activated protein kinase 13	MAPK13	-1.58	-2.07	-2.23	-2.37	-1.97	-1.12	-1.2	-1.1	-1.02	1.08	cell cycle
16948209	5290	Phosphoinositide-3-kinase, catalytic, alpha polypeptide	PIK3CA*	-1.41	-1.51	-1.58	-1.72	-1.37	-1.23	-1.15	-1.19	-1.01	-1.29	protein binding

Table 4.14: The list of genes which are significantly expressed (>2-fold change) or relatively significantly expressed* (timepoints vs timepoint 0) in JAK-STAT signalling pathway

Transcription Cluster ID	Entrez ID	Gene Name	Gene Symbol	D6	D12	D18	D24	D48	C6	C12	C18	C24	C48	Biological Function
16875754	3589	Interleukin 11	IL11	-12.4	-15.12	-12.85	-15.27	-8.35	-1.92	-1.56	-1.59	-1.03	-1.13	Cell proliferation
16933760	3976	Leukemia inhibitory factor (cholinergic differentiation factor)	LIF	-4.53	-3.99	-4.53	-4.51	-2.64	-1.13	1.02	1.28	1.73	1.32	Cell differentiation
16671457	3570	Interleukin 6 receptor	IL6R	-1.32	-2.09	-2.46	-2.31	-2.2	1.15	1.24	1.17	1.2	1.31	Cytokine binding
16995177	5618	Prolactin receptor	PRLR	1.3	2.09	1.6	1.85	1.36	1.28	1.2	-1.1	-1.06	-1.03	Protein binding
17008092	5292	Pim-1 oncogene	PIM1	-1.98	-2.95	-3.14	-3.72	-4.7	1.12	1.26	-1.03	1.14	-1.14	Cell proliferation
16896710	6654	Son of sevenless homolog 1 (Drosophila)	SOS1	-2.67	-2.17	-2.89	-2.28	-1.4	-1.87	-1.05	1.14	1.36	1.03	Apoptosis
17001063	81848	Sprouty homolog 4 (Drosophila)	SPRY4	-3.27	-2.22	-2.75	-3	-2.55	-1.29	1.11	-1.08	1.15	-1.23	Protein binding
16948209	5290	Phosphoinositide-3-kinase, catalytic, alpha polypeptide	PI3KCA	-1.41	-1.51	-1.58	-1.72	-1.37	-1.23	-1.15	-1.19	-1.01	-1.29	Protein binding

Table 4.15: The list of genes which are significantly expressed (>2-fold change) or relatively significantly expressed* (timepoints vs timepoint 0) in WNT signalling pathway

Transcription Cluster ID	Entrez ID	Gene Name	Gene Symbol	D6	D12	D18	D24	D48	C6	C12	C18	C24	C48	Biological Function
16742340	7481	Wingless-type MMTV integration site family, member 11	WNT11	-1.8	-3.22	-3.01	-3.4	-2.49	-1.15	-1.1	-1.07	-1.31	1.07	Cell development
16740630	8061	FOS-like antigen 1	FOSL1	-4.3	-4.66	-3.5	-3.16	-2.51	-1.83	-1.11	-1.12	-1.07	1.23	Transcription factor
16687875	3725	Jun oncogene	JUN*	-1.83	-1.6	-1.7	-1.7	-1.42	-1.17	1.21	1.1	1.35	1.3	Transcription factor
16728066	4041	Low density lipoprotein receptor-related protein 5	LRP5 *	-1.45	-1.61	-1.83	-1.76	-1.48	-1.13	-1.01	-1.1	-1.08	-1.14	Transcription factor

Table 4.16: The list of genes which are significantly expressed (>2-fold change) or relatively significantly expressed* (timepoints vs timepoint 0) in Toll-like receptor signalling pathway

Transcription Cluster ID	Entrez ID	Gene Name	Gene Symbol	D6	D12	D18	D24	D48	C6	C12	C18	C24	C48	Biological Function
16837348	5608	Mitogen-activated protein kinase kinase 6	MAP2k6	1.2	3.93	5.78	5.15	3.27	1.23	-1.1	-1.28	-1.72	-1.5	Protein binding
17007910	5603	Mitogen-activated protein kinase 13	MAPk13	-1.58	-2.07	-2.23	-2.37	-1.97	-1.12	-1.2	-1.1	-1.02	1.08	Cell cycle
16967771	3576	Interleukin 8	IL8	-3.89	-2.38	-1.69	-1.72	-1.34	-1.32	-1.04	-1.24	-1.18	1.02	Protein binding
16687875	3725	Jun oncogene	Jun*	-1.83	-1.6	-1.7	-1.7	-1.42	-1.17	1.21	1.1	1.35	1.3	Transcription factor
16948209	5290	Phosphoinositide-3-kinase, catalytic, alpha polypeptide	PI3KCA*	-1.41	-1.51	-1.58	-1.72	-1.37	-1.23	-1.15	-1.19	-1.01	-1.29	Protein binding

Table 4.17: The list of genes which are significantly expressed (>2-fold change) or relatively significantly expressed* (timepoints vs timepoint 0) in Nod-like receptor signalling

Transcription Cluster ID	Entrez ID	Gene Name	Gene Symbol	D6	D12	D18	D24	D48	C6	C12	C18	C24	C48	Biological Function
17007910	5603	Mitogen-activated protein kinase 13	MAPK13	-1.58	-2.07	-2.23	-2.37	-1.97	-1.12	-1.2	-1.1	-1.02	1.08	Cell cycle
16967771	3576	Interleukin 8	IL8	-3.89	-2.38	-1.69	-1.72	-1.34	-1.32	-1.04	-1.24	-1.18	1.02	Protein binding
16996983	4671	NLR family, apoptosis inhibitory protein	NAIP	2.53	2.22	2.33	1.92	2.3	1.28	1.55	1.64	1.8	1.39	Apoptosis

Table 4.18: The list of genes which are significantly expressed (>2-fold change) or relatively significantly expressed* (timepoints vs timepoint 0) in RIG-like receptor pathway

Transcription Cluster ID	Entrez ID	Gene Name	Gene Symbol	D6	D12	D18	D24	D48	C6	C12	C18	C24	C48	Biological Function
17007910	5603	Mitogen-activated protein kinase 13	MAPK13	-1.58	-2.07	-2.23	-2.37	-1.97	-1.12	-1.2	-1.1	-1.02	1.08	Cell cycle
16967771	3576	Interleukin 8	IL8	-3.89	-2.38	-1.69	-1.72	-1.34	-1.32	-1.04	-1.24	-1.18	1.02	Protein binding

Table 4.19: The list of genes which are significantly expressed (>2-fold change) or relatively significantly expressed* (timepoints vs timepoint 0 in chemokine signalling

Transcription Cluster ID	Entrez ID	Gene Name	Gene Symbol	D6	D12	D18	D24	D48	C6	C12	C18	C24	C48	Biological Function
16891774	6364	Chemokine (C-C motif) ligand 20	CCL20	-5.56	-5.12	-3.27	-4.03	-2.33	-1.36	1.13	1.59	-1.29	-1.44	Protein binding
16896710	6654	Son of sevenless homolog 1 (Drosophila)	SOS1	-2.67	-2.17	-2.89	-2.28	-1.4	-1.87	-1.05	1.14	1.36	1.03	Apoptosis
16828427	646079, 9564	Similar to breast cancer anti-estrogen resistance 1; breast cancer anti-estrogen resistance 1	BCAR1	-2.14	-1.97	-1.61	-2.11	-1.88	-1.23	-1.23	-1.36	-1.16	-1.19	Protein binding
16829835	409	Arrestin, beta 2	ARRB2	-1.24	-1.64	-1.61	-1.42	-2.17	-1.14	1.09	-1.06	-1.18	-1.05	Protein binding
17014651	1235, 81669	Cyclin L2; chemokine (C-C motif) receptor 6	CCR6*	-1.28	-1.14	-1.05	-1.06	-1.23	1.03	1.24	1.27	1.32	1.14	Protein binding
16948209	5290	Phosphoinositide-3-kinase, catalytic, alpha polypeptide	PI3KCA*	-1.41	-1.51	-1.58	-1.72	-1.37	-1.23	-1.15	-1.19	-1.01	-1.29	Protein binding
16713230	56288	Par-3 partitioning defective 3 homolog (*C. elegans*)	PARD3*	-1.28	-1.53	-1.8	-1.83	-1.62	-1.17	-1.16	-1.12	-1.07	-1.28	Protein binding

Table 4.20: The list of genes which are significantly expressed (>2-fold change) or relatively significantly expressed* (timepoints vs timepoint 0) in cytokine-cytokine receptor interaction

Transcription Cluster ID	Entrez ID	Gene Name	Gene Symbol	D6	D12	D18	D24	D48	C6	C12	C18	C24	C48	Biological Function
16967771	3576	Interleukin 8	IL8	-3.89	-2.38	-1.69	-1.72	-1.34	-1.32	-1.04	-1.24	-1.18	1.02	Cell proliferation
16891774	6364	Chemokine (C-C motif) ligand 20	CCL20	-5.56	-5.12	-3.27	-4.03	-2.33	-1.36	1.13	1.59	-1.29	-1.44	Protein binding
16875754	3589	Interleukin 11	IL11	-12.4	-15.12	-12.85	-15.27	-8.35	-1.92	-1.56	-1.59	-1.03	-1.13	Cell proliferation
16671457	3570	Interleukin 6 receptor	IL6R	-1.32	-2.09	-2.46	-2.31	-2.2	1.15	1.24	1.17	1.2	1.31	Protein binding
16933760	3976	Leukemia inhibitory factor (cholinergic differentiation factor)	LIF	-4.53	-3.99	-4.53	-4.51	-2.64	-1.13	1.02	1.28	1.73	1.32	Cell proliferation
16995177	5618	Prolactin receptor	PRLR	1.3	2.09	1.6	1.85	1.36	1.28	1.2	-1.1	-1.06	-1.03	Protein binding
16768270	4254	KIT ligand	KITLG	1.48	2.3	2.55	2.34	2.85	1.4	1.25	1.41	1.27	1.14	Protein binding
16961616	8743	Tumour necrosis factor (ligand) superfamily, member 10	TNFSF10	2.25	3.27	2.71	2.74	1.23	1.9	1.58	1.08	1.4	1.35	Protein binding
16773165	55504	Tumour necrosis factor receptor superfamily, member 19	TNFRSF19	1.17	2.53	2.68	2.89	2.91	-1.06	1.03	1.05	1.42	1.31	Cell death
16872551	7040	Transforming growth factor, beta 1	TGFB1	-1.77	-2.02	-1.71	-2.02	-1.52	-1.47	-1.31	-1.52	-1.29	-1.16	Proliferation, Differentiation
16903969	90	Activin A receptor, type I	ACVR1	-1.3	-1.55	-1.74	-2.08	-1.35	-1.26	1.01	1.02	1.04	1.05	Protein binding, G1/S transition of mitotic cell cycle
17014651	125, 81669	Cyclin L2; chemokine (C-C motif) receptor 6	CCR6*	-1.28	-1.14	-1.05	-1.06	-1.23	1.03	1.24	1.27	1.32	1.14	Protein binding
17046135	1956	Epidermal growth factor receptor (erythroblastic leukemia viral (v-erb-b) oncogene homolog, avian)	EGFR*	-1.14	-1.15	-1.76	-1.6	-1.26	1.04	1.43	1.15	1.79	1.29	Cell growth , differentiation

Table 4.21: The list of genes which are significantly expressed (>2-fold change) or relatively significantly expressed* (timepoints vs timepoint 0) in T cell receptor signalling pathway

Transcription Cluster ID	Entrez ID	Gene Name	Gene Symbol	D6	D12	D18	D24	D48	C6	C12	C18	C24	C48	Biological Function
17007910	5603	Mitogen-activated protein kinase 13	MAPK13	-1.58	-2.07	-2.23	-2.37	-1.97	-1.12	-1.2	-1.1	-1.02	1.08	Cell cycle
16896710	6654	Son of sevenless homolog 1 (Drosophila)	SOS1	-2.67	-2.17	-2.89	-2.28	-1.4	-1.87	-1.05	1.14	1.36	1.03	Apoptosis
16662052	3932	Lymphocyte-specific protein tyrosine kinase	LCK*	-1.3	-1.96	-1.69	-1.93	-1.9	-1.03	-1.1	-1.08	-1.01	1.04	Protein binding
16687875	3725	Jun oncogene	JUN*	-1.83	-1.6	-1.7	-1.7	-1.42	-1.17	1.21	1.1	1.35	1.3	Transcription factor
16948209	5290	Phosphoinositide-3-kinase, catalytic, alpha polypeptide	PI3KCA*	-1.41	-1.51	-1.58	-1.72	-1.37	-1.23	-1.15	-1.19	-1.01	-1.29	Protein binding

Table 4.22: The list of genes which are significantly expressed (>2-fold change) or relatively significantly expressed* (timepoints vs timepoint 0) in B cell receptor pathway

Transcription Cluster ID	Entrez ID	Gene Name	Gene Symbol	D6	D12	D18	D24	D48	C6	C12	C18	C24	C48	Biological Function
16860992	933	CD22 molecule	CD22	-1.08	-1.47	-2.43	-1.88	-2.4	1.01	1.27	1.2	1.13	1.12	Protein Binding
16896710	6654	Son of sevenless homolog 1 (Drosophila)	SOS1	-2.67	-2.17	-2.89	-2.28	-1.4	-1.87	-1.05	1.14	1.36	1.03	Apoptosis
16687875	3725	Jun oncogene	JUN*	-1.83	-1.6	-1.7	-1.7	-1.42	-1.17	1.21	1.1	1.35	1.3	Transcription factor
16948209	5290	Phosphoinositide-3-kinase, catalytic, alpha polypeptide	PI3KCA*	-1.41	-1.51	-1.58	-1.72	-1.37	-1.23	-1.15	-1.19	-1.01	-1.29	Protein Binding

Table 4.23: The list of genes which are significantly expressed (>2-fold change) or relatively significantly expressed* (timepoints vs timepoint 0) in apoptosis signalling pathway

Transcription Cluster ID	Entrez ID	Gene Name	Gene Symbol	D6	D12	D18	D24	D48	C6	C12	C18	C24	C48	Biological Function
16961616	8743	Tumour necrosis factor (ligand) superfamily, member 10	TNFSF10	2.25	3.27	2.71	2.74	1.23	1.9	1.58	1.08	1.4	1.35	Immune response
16937579	3656	Interleukin-1 receptor-associated kinase 2	IRAK2	-1.84	-1.97	-2.45	-2.42	-2.31	-1.23	-1.27	-1.18	-1.19	-1.26	Protein binding
16948209	5290	Phosphoinositide-3-kinase, catalytic, alpha polypeptide	PI3KCA*	-1.41	-1.51	-1.58	-1.72	-1.37	-1.23	-1.15	-1.19	-1.01	-1.29	Protein binding

Table 4.24: The list of genes which are significantly expressed (>2-fold change) or relatively significantly expressed* (timepoints vs timepoint 0) in adherens junction

Transcription Cluster ID	Entrez ID	Gene Name	Gene symbol	D6	D12	D18	D24	D48	C6	C12	C18	C24	C48	Biological Function
16820486	999	Cadherin 1, type 1, E-cadherin (epithelial)	CDH1	-1.21	1.61	2.14	1.95	1.39	-1.08	1.21	1.18	1.02	1.1	Cell adhesion
17077004	6591	Snail homolog 2 (Drosophila)	SNAI2	-3.37	-4.43	-6.21	-6.31	-4.37	-1.16	-1.13	-1.43	-1.55	-1.53	Transcription factor
16713230	56288	Par-3 partitioning defective 3 homolog (*C. elegans*)	PARD3*	-1.28	-1.53	-1.8	-1.83	-1.62	-1.17	-1.16	-1.12	-1.07	-1.28	Protein binding
17046135	1956	Epidermal growth factor receptor (erythroblastic leukemia viral (v-erb-b) oncogene homolog, avian)	EGFR*	-1.14	-1.15	-1.76	-1.6	-1.26	1.04	1.43	1.15	1.79	1.29	Cell growth , differentiation

Table 4.25: The list of genes which are significantly expressed (>2-fold change) or relatively significantly expressed* (timepoints vs timepoint 0) in focal adhesion

Transcription Cluster ID	Entrez ID	Gene Name	Gene Symbol	D6	D12	D18	D24	D48	C6	C12	C18	C24	C48	Biological Function
17052823	7791	Zyxin	ZYX	-2.93	-3.03	-2.39	-2.08	-2.41	-1.69	-1.31	-1.48	1.15	-1.15	Protein binding
16863307	7408	Vasodilator-stimulated phosphoprotein	VASP	-2.06	-2.32	-1.99	-2.41	-2.05	-1.16	-1.21	-1.49	-1.32	-1.35	Protein binding
16913341	10398	Myosin, light chain 9, regulatory	MYL9	-2.18	-1.79	-1.15	-1.12	-1.13	-1.24	-1.07	-1.07	1.12	1.14	Cell migration
16828427	646079, 9564	Similar to breast cancer anti-estrogen resistance 1; breast cancer anti-estrogen resistance 1	BCAR1	-2.14	-1.97	-1.61	-2.11	-1.88	-1.23	-1.23	-1.36	-1.16	-1.19	Protein binding
16896710	6654	Son of sevenless homolog 1 (Drosophila)	SOS1	-2.67	-2.17	-2.89	-2.28	-1.4	-1.87	-1.05	1.14	1.36	1.03	Apoptosis
16687875	3725	Jun oncogene	Jun*	-1.83	-1.6	-1.7	-1.7	-1.42	-1.17	1.21	1.1	1.35	1.3	Transcription factor
17046135	1956	Epidermal growth factor receptor (erythroblastic leukemia viral (v-erb-b) oncogene homolog, avian)	EGFR*	-1.14	-1.15	-1.76	-1.6	-1.26	1.04	1.43	1.15	1.79	1.29	Cell growth , differentiation
16948209	5290	Phosphoinositide-3-kinase, catalytic, alpha polypeptide	PI3KCA*	-1.41	-1.51	-1.58	-1.72	-1.37	-1.23	-1.15	-1.19	-1.01	-1.29	Protein binding

Table 4.26: The list of genes which are significantly expressed (>2-fold change) or relatively significantly expressed* (timepoints vs timepoint 0) in natural killer cell cytoxicity

Transciption Cluster ID	Entrez ID	Gene Name	Gene Symbol	D6	D12	D18	D24	D48	C6	C12	C18	C24	C48	Biological Function
16896710	6654	Son of sevenless homolog 1 (Drosophila)	SOS1	-2.67	-2.17	-2.89	-2.28	-1.4	-1.87	-1.05	1.14	1.36	1.03	Apoptosis
16961616	8743	Tumour necrosis factor (ligand) superfamily, member 10	TNFSF10	2.25	3.27	2.71	2.74	1.23	1.9	1.58	1.08	1.4	1.35	Protein binding
16662052	3932	Lymphocyte-specific protein tyrosine kinase	LCK*	-1.3	-1.96	-1.69	-1.93	-1.9	-1.03	-1.1	-1.08	-1.01	1.04	Protein binding
16948209	5290	Phosphoinositide-3-kinase, catalytic, alpha polypeptide	PI3KCA*	-1.41	-1.51	-1.58	-1.72	-1.37	-1.23	-1.15	-1.19	-1.01	-1.29	Protein binding

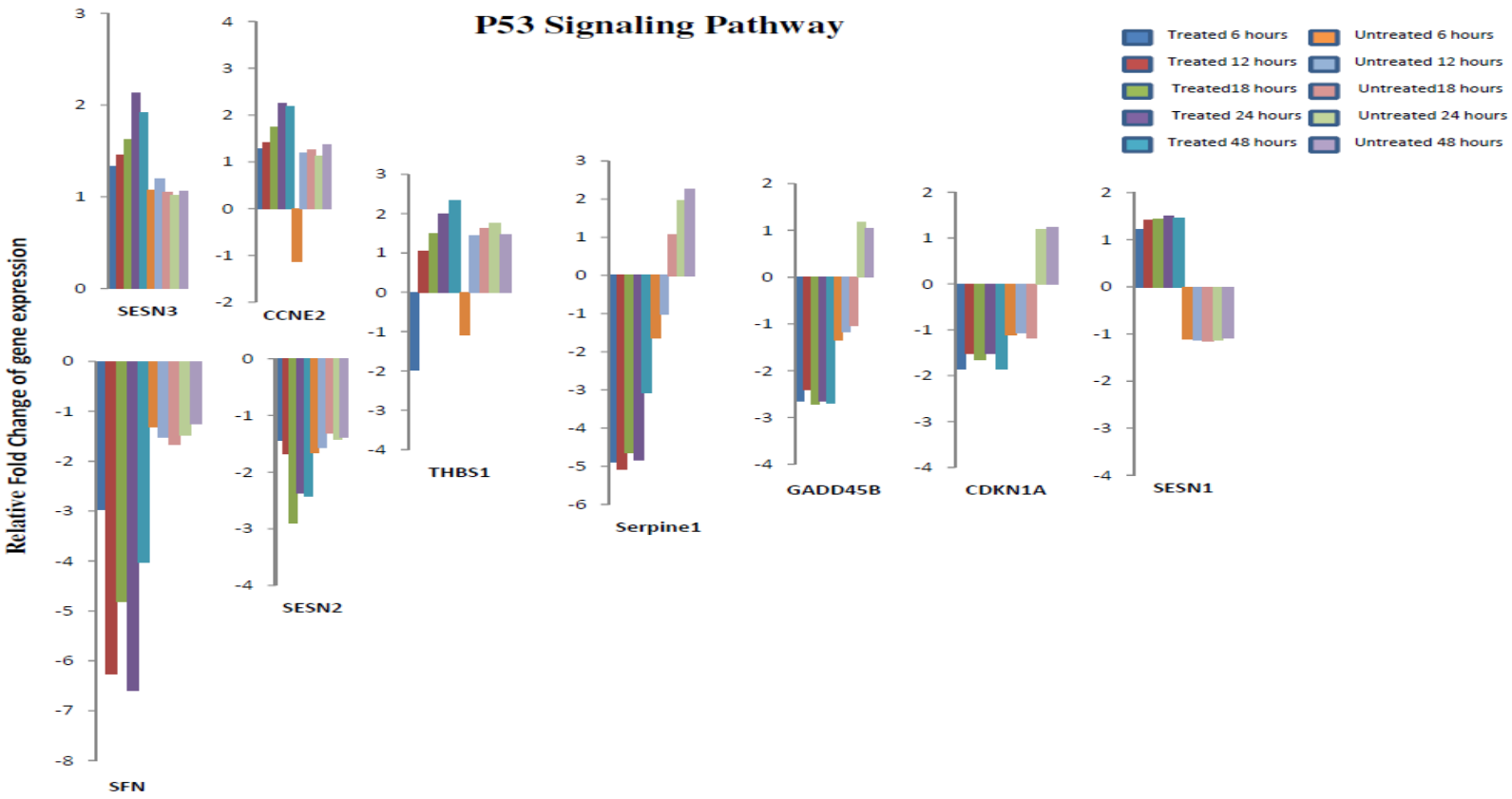

Figure 4.3: Genes identified in p53 singalling pathway with >2-fold-change or with relative significance compared with untreated samples at various time-points.

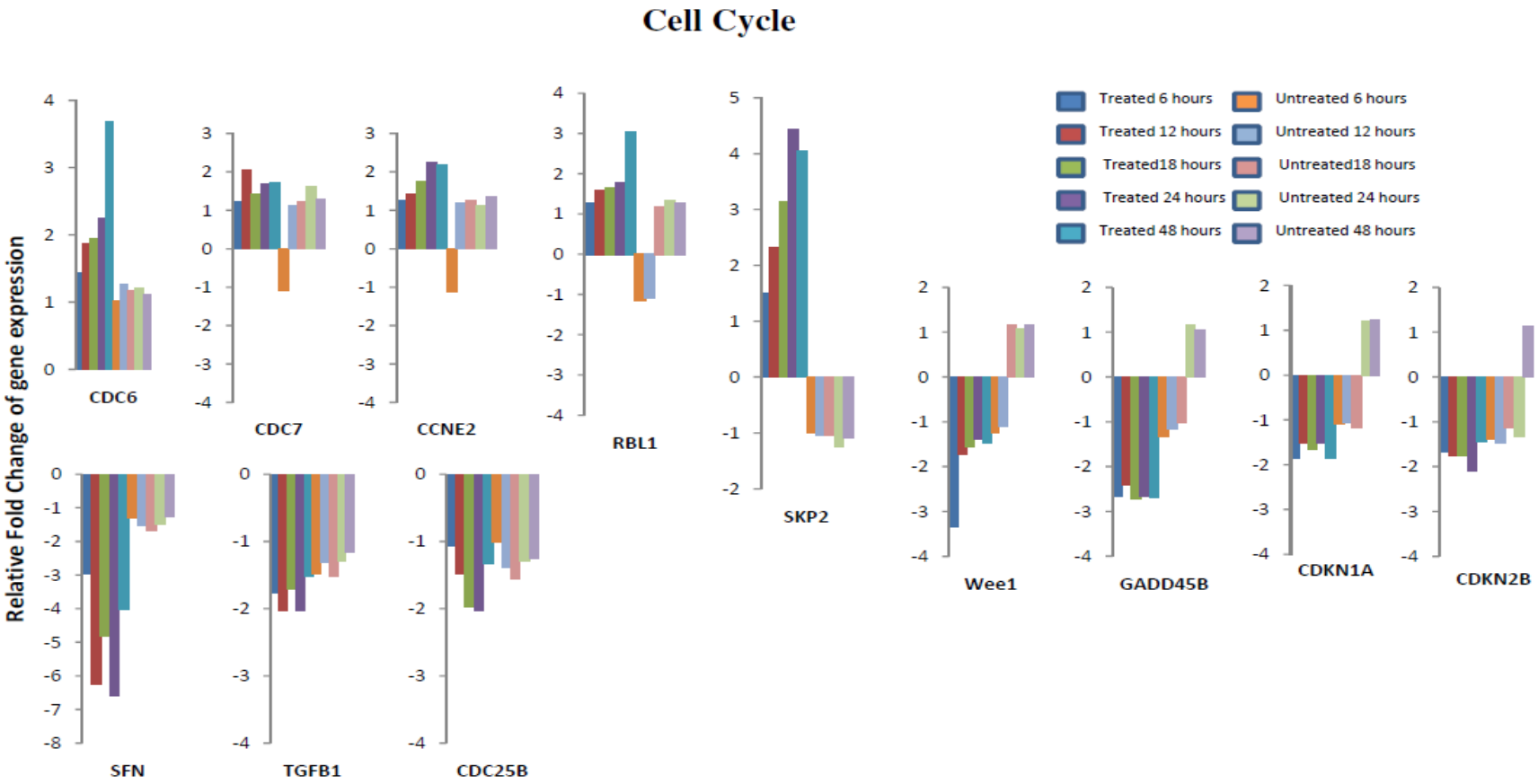

Figure 4.4: Genes identified in cell cycle with >2-fold-change or with relative significance compared with untreated samples with various time-points

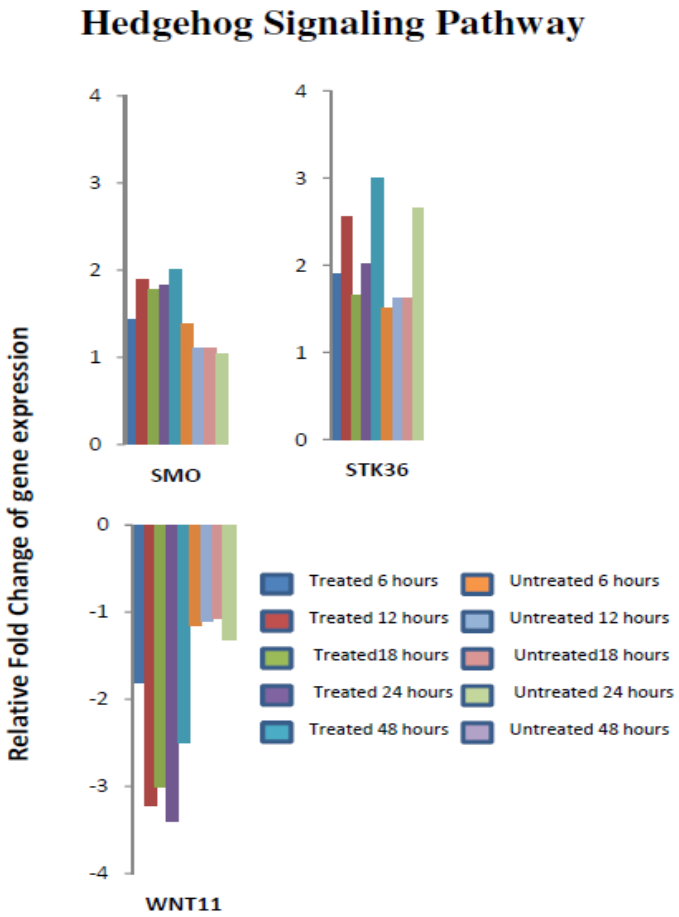

Figure 4.5: Genes identified in Hedgehog signalling pathway with >2-fold-change or with relative significance compared with untreated samples with various time-points

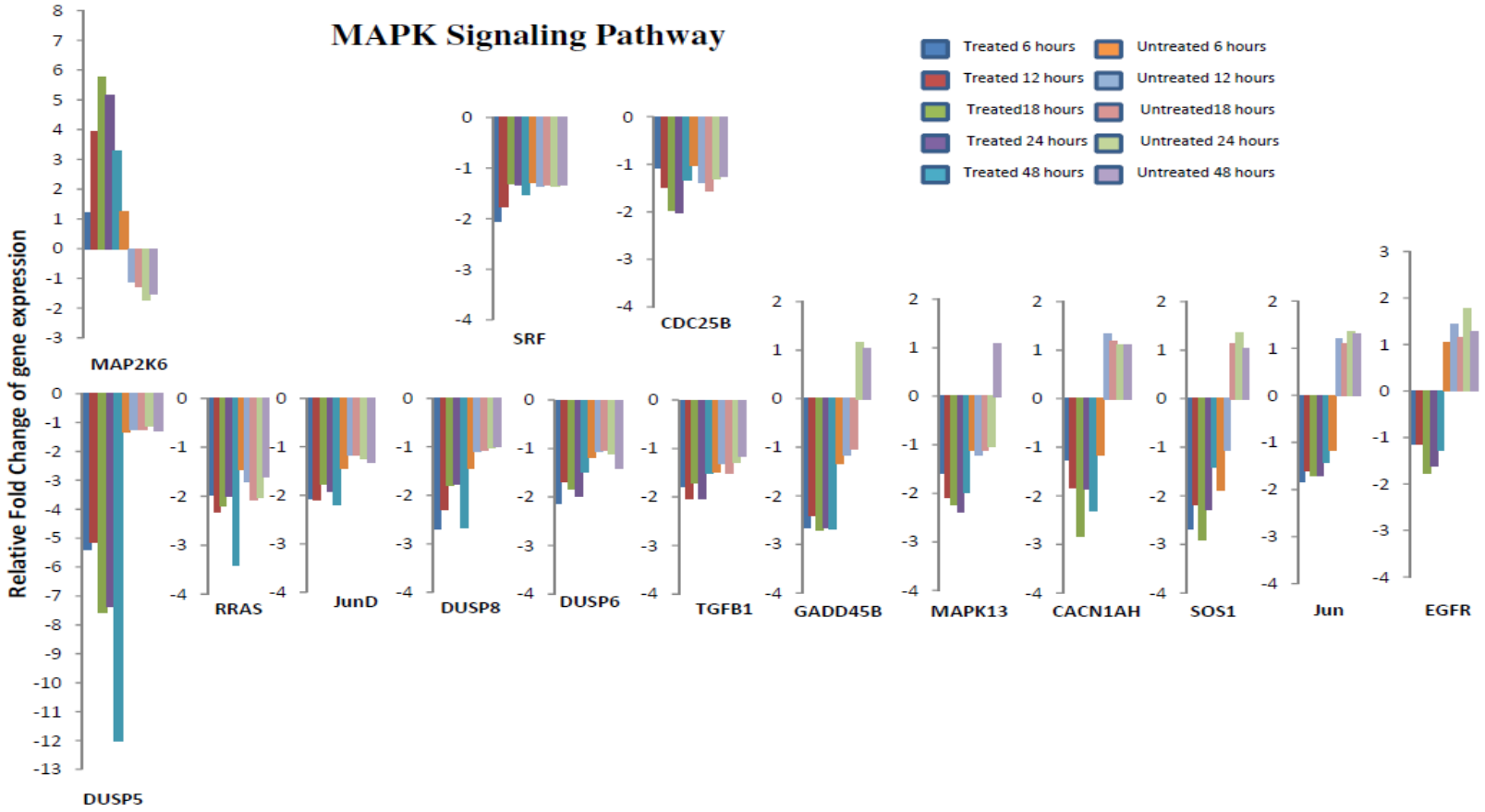

Figure 4.6: Genes identified in MAPK signalling pathway with >2-fold-change or with relative significance compared with untreated samples with various time-points

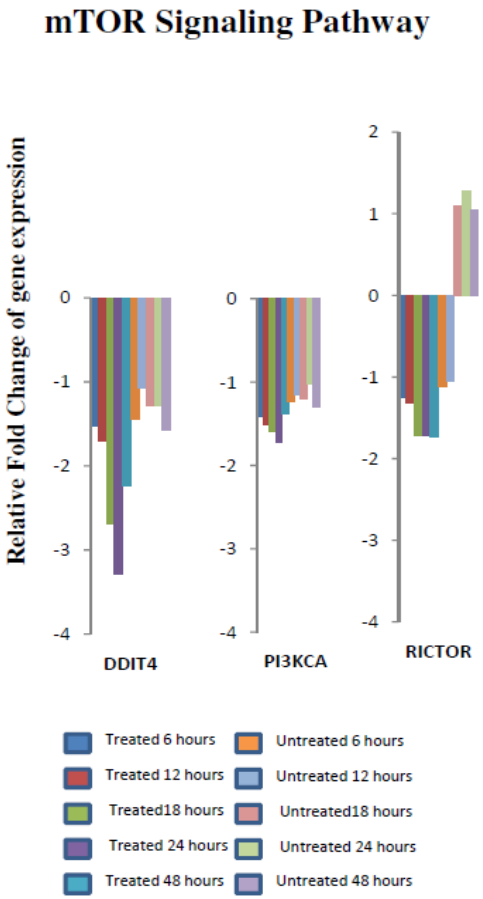

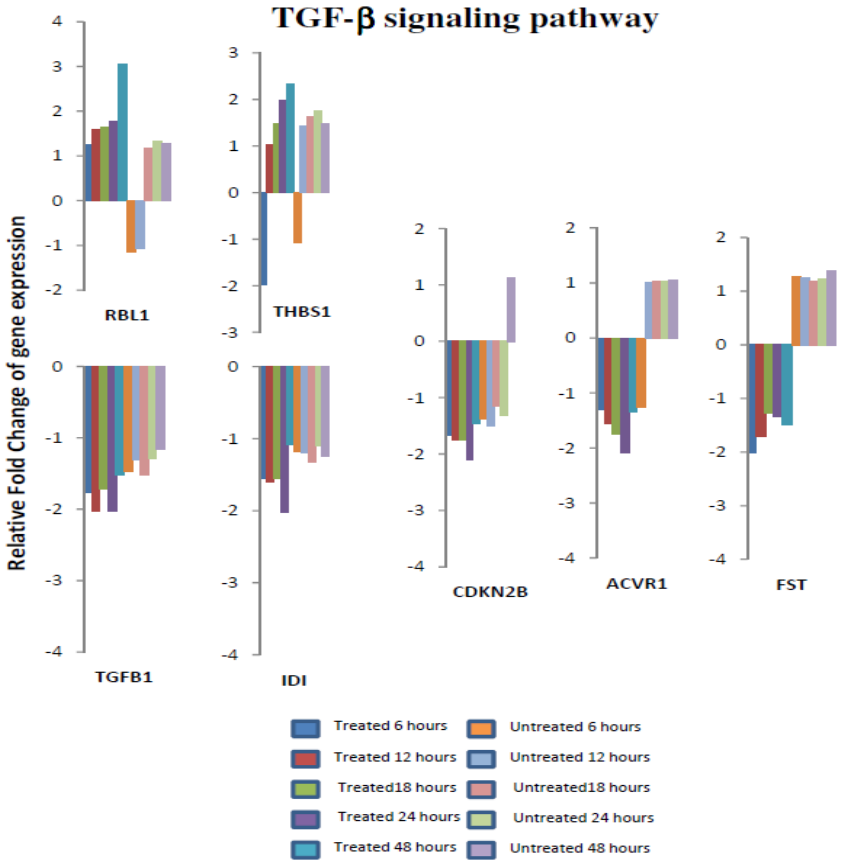

Figure 4.7 (Left) & Figure 4.8 (Right): Genes identified in mTOR signalling pathway & TGF-β signalling pathway with >2-fold-change or with relative significance compared with untreated samples with various time-points

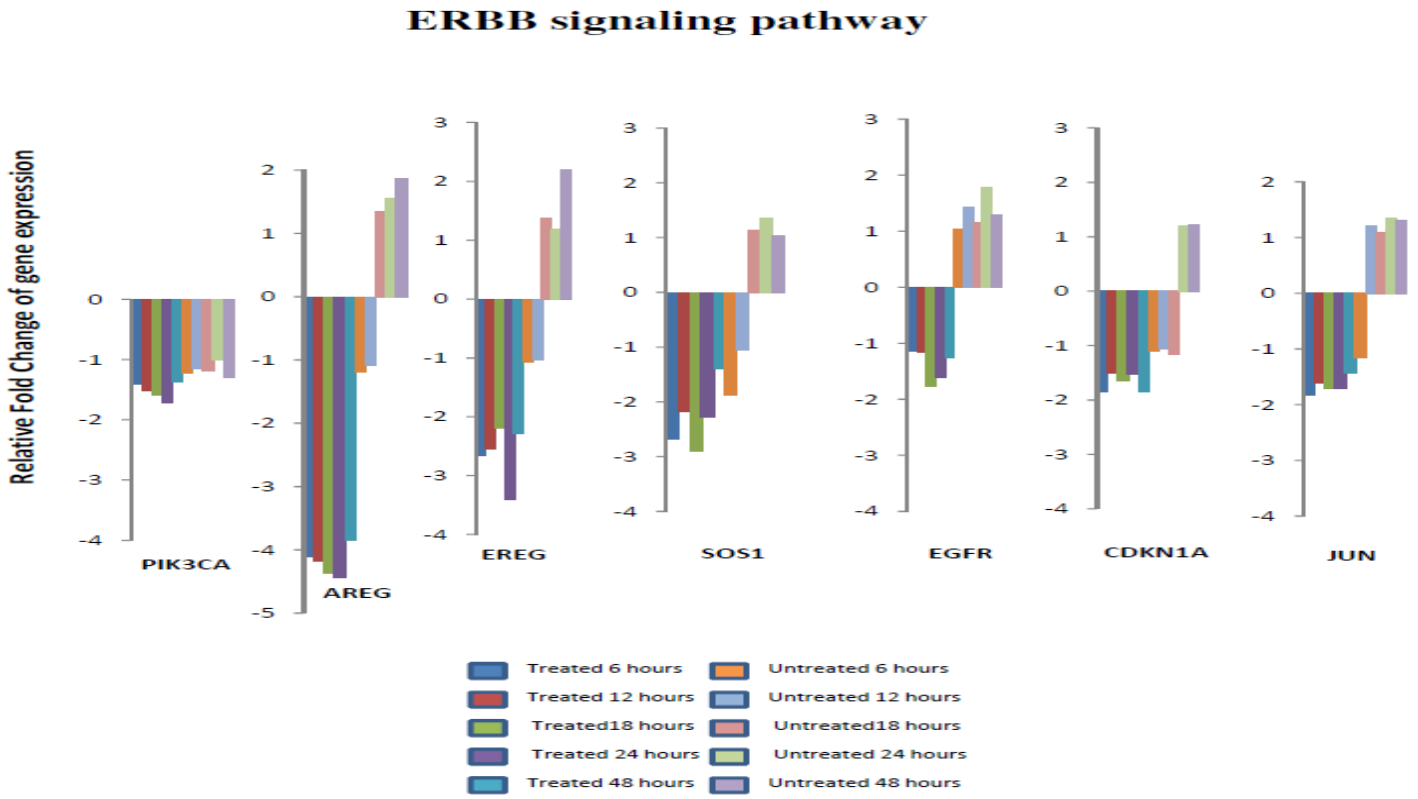

Figure 4.9: Genes identified in ERBB singalling pathway with >2-fold-change or with relative significance compared with untreated samples with various time-points

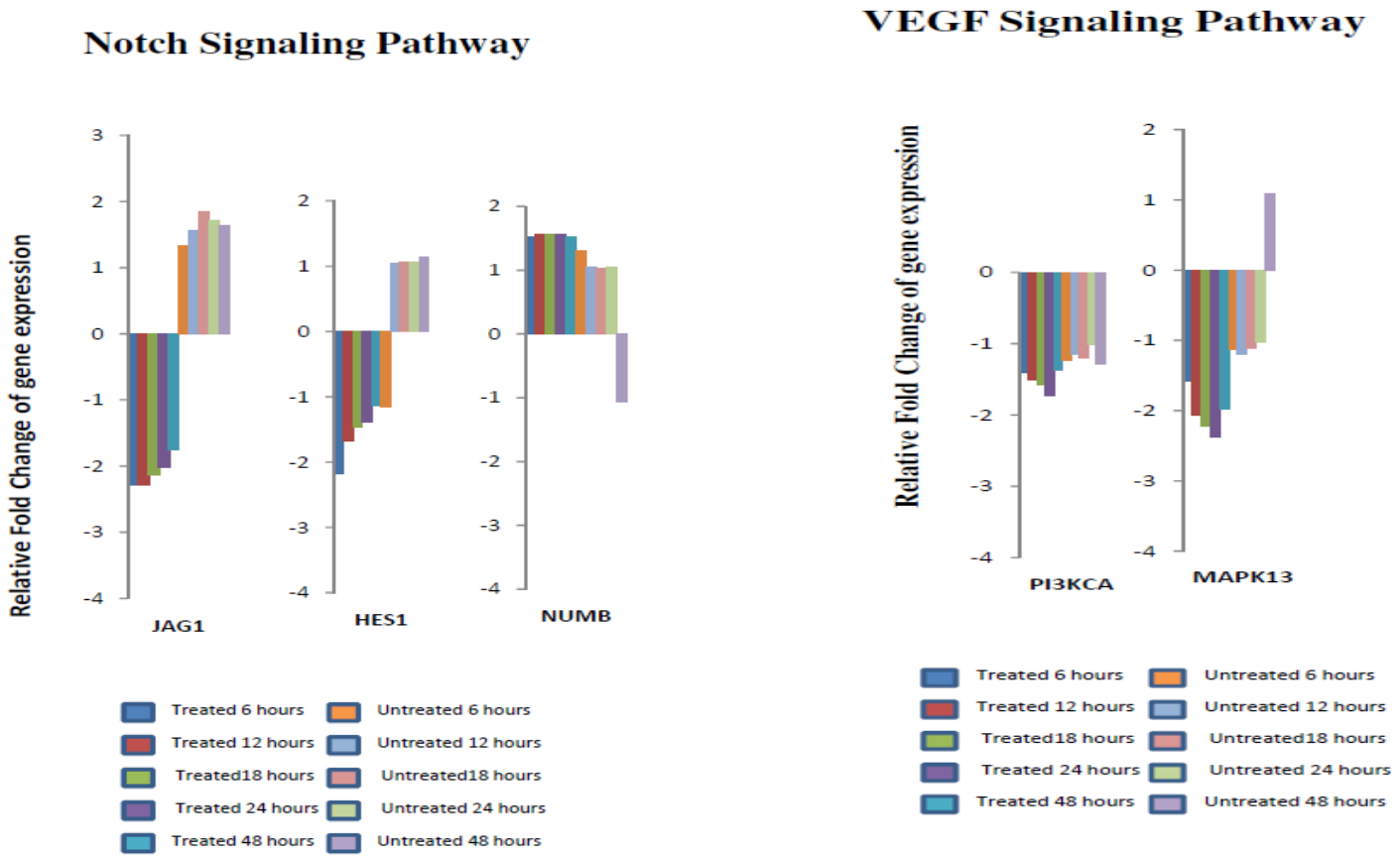

Figure 4.10and Figure 4.11: Genes identified in Notch signalling pathway and VEGF signalling pathway with >2-fold-change or with relative significance compared with untreated samples with various time-points

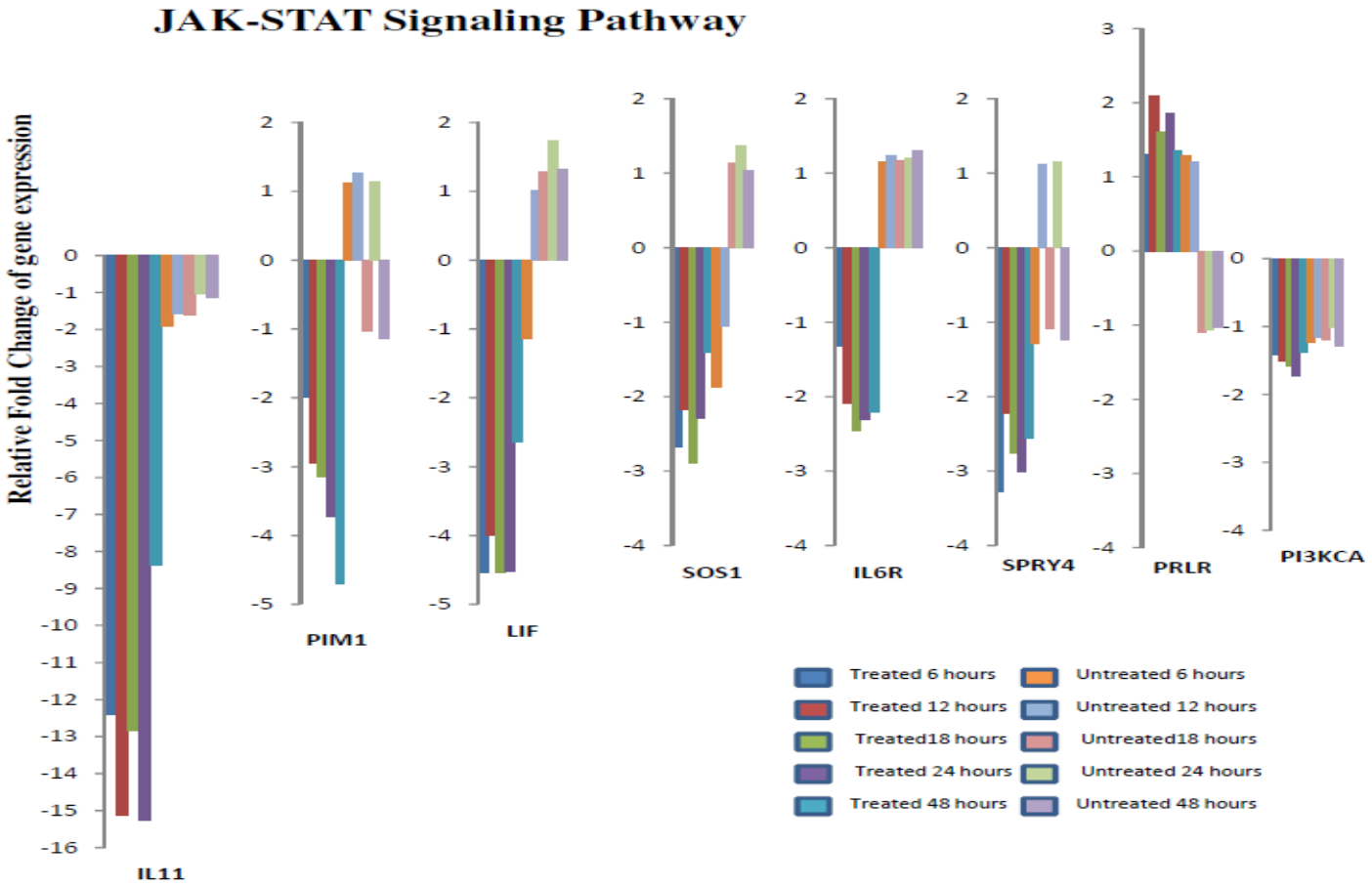

Figure 4.12: Genes identified in JAK-STAT signalling pathway with >2-fold-change or with relative significance compared with untreated samples with various time-points

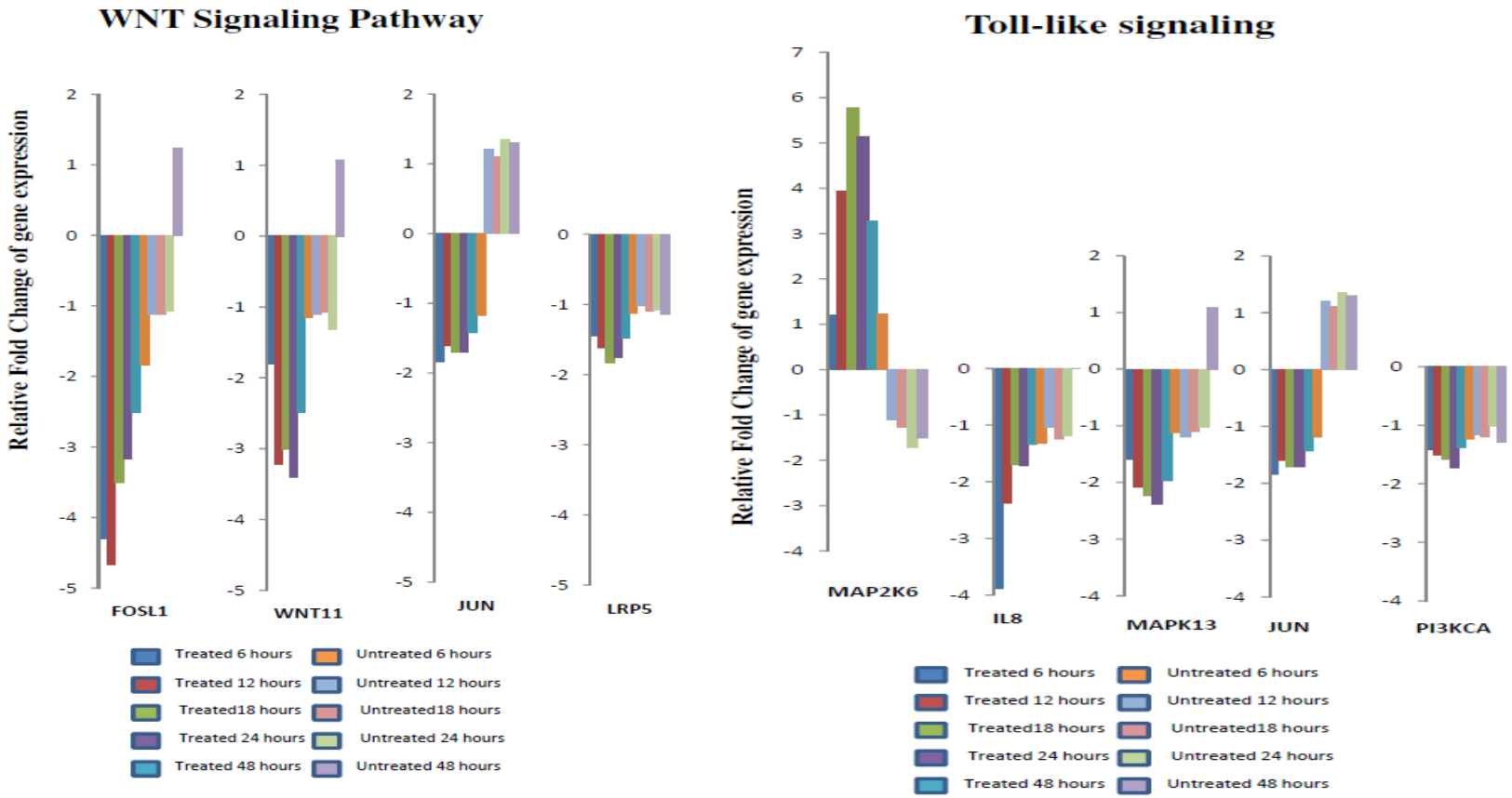

Figure 4.13and Figure 4.14: Genes identified in WNT signalling pathway and Toll-like signalling pathway with >2-fold-change or with relative significance compared with untreated samples with various time-points

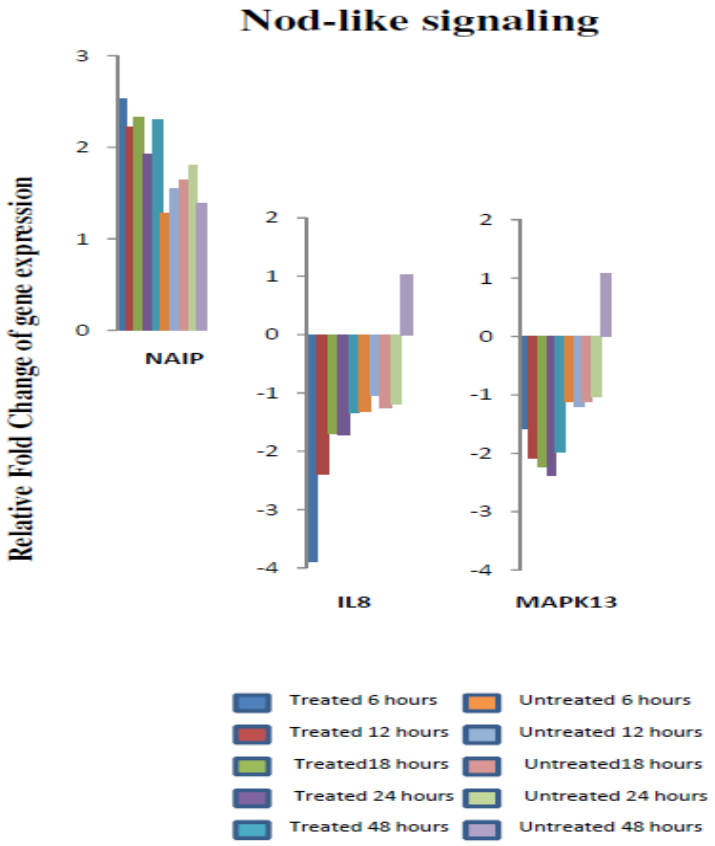

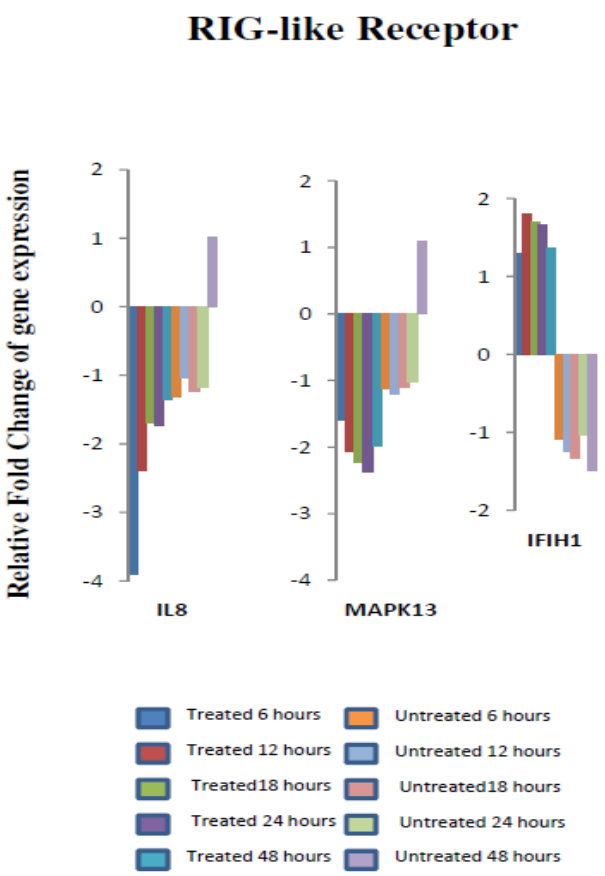

Figure 4.15and Figure 4.16: Genes identified in Nod -like receptor signalling pathway and RIG-like receptor signalling pathway with >2-fold-change or with relative significance compared with untreated samples at various time-points

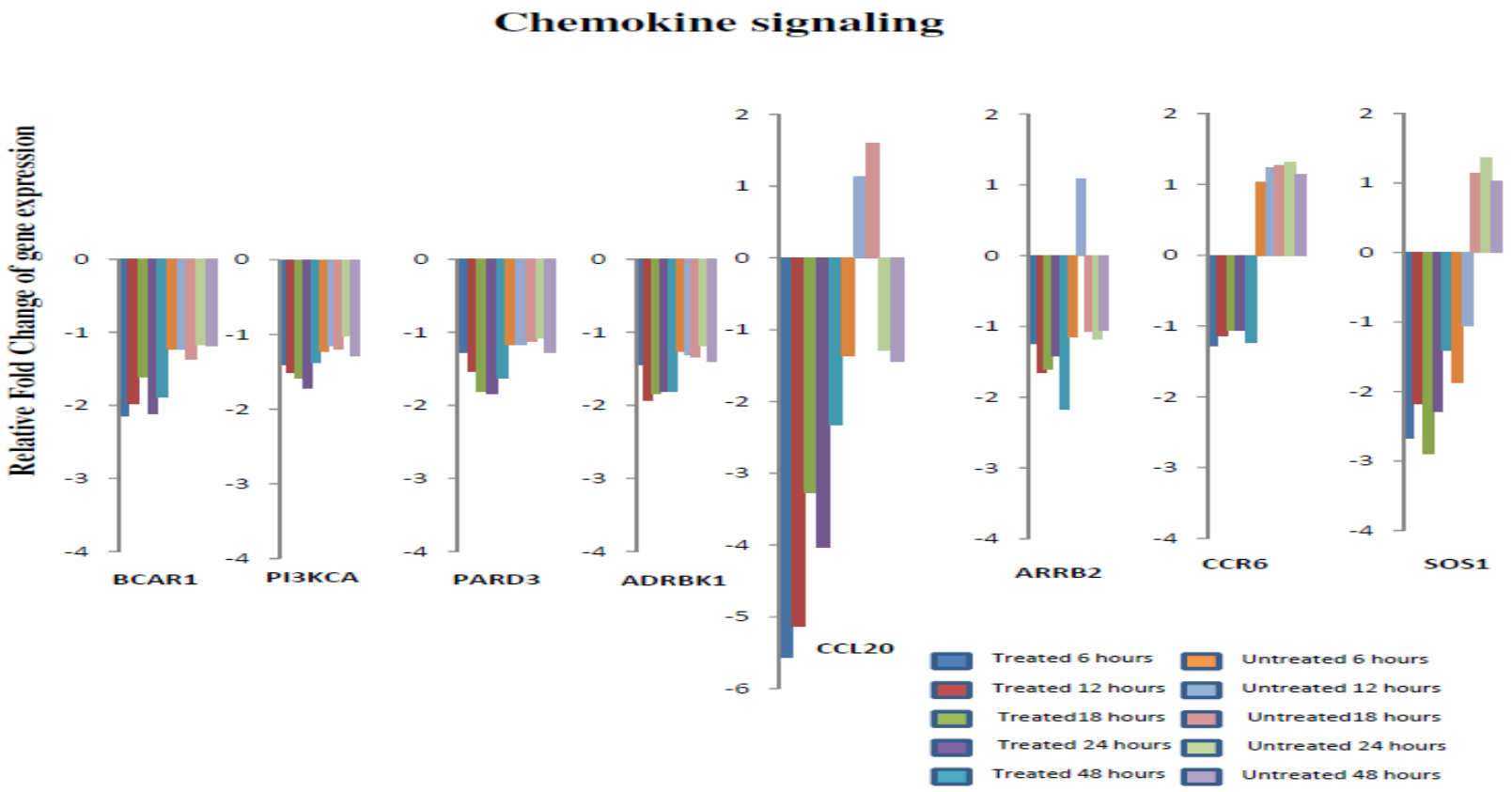

Figure 4.17: Genes identified in chemokine signalling pathway with >2-fold-change or with relative significance compared with untreated samples under various time-points

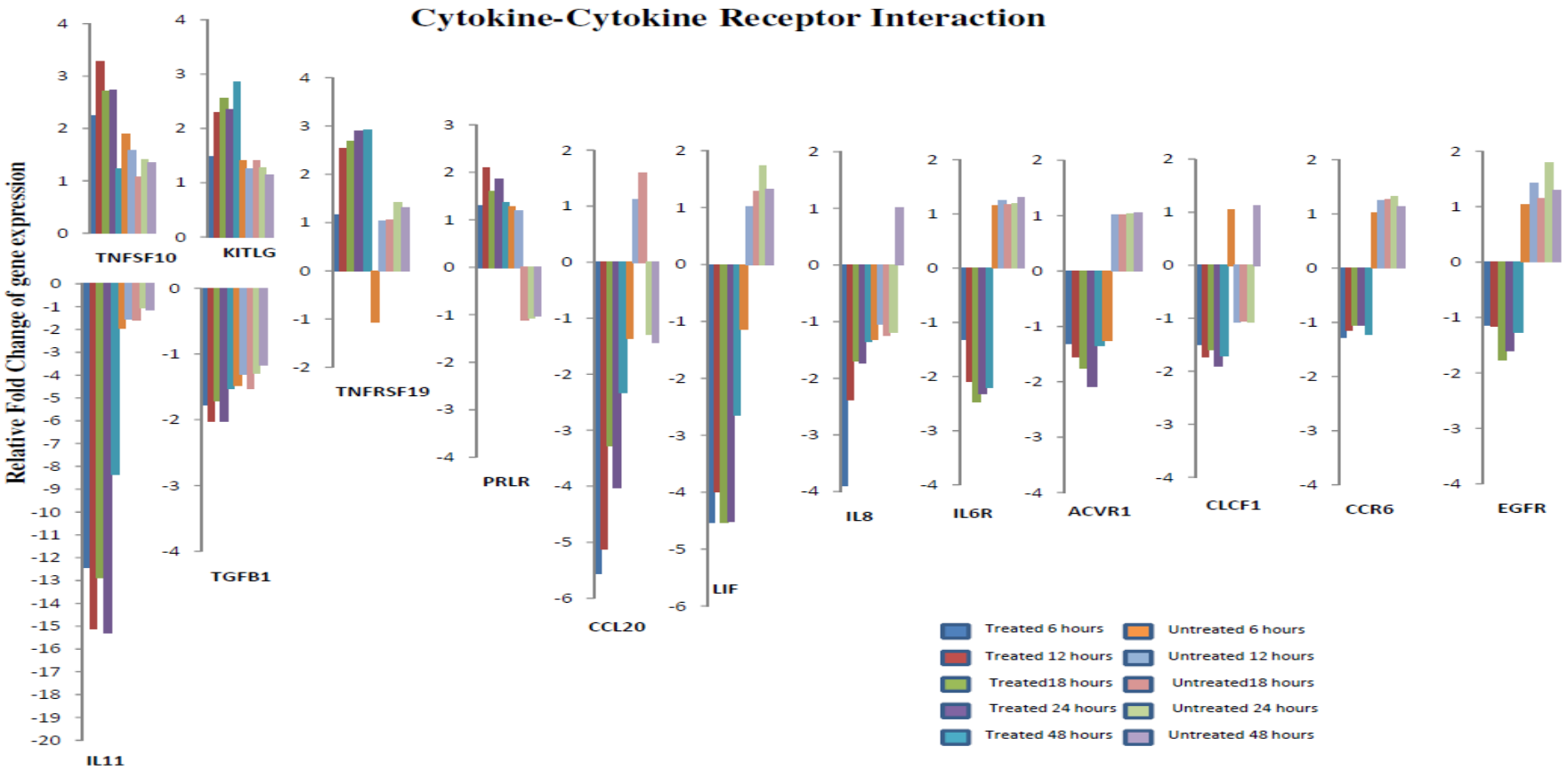

Figure 4.18: Genes identified in cytokine-cytokine receptor interaction with >2-fold-change or with relative significance compared with untreated samples under various time-points

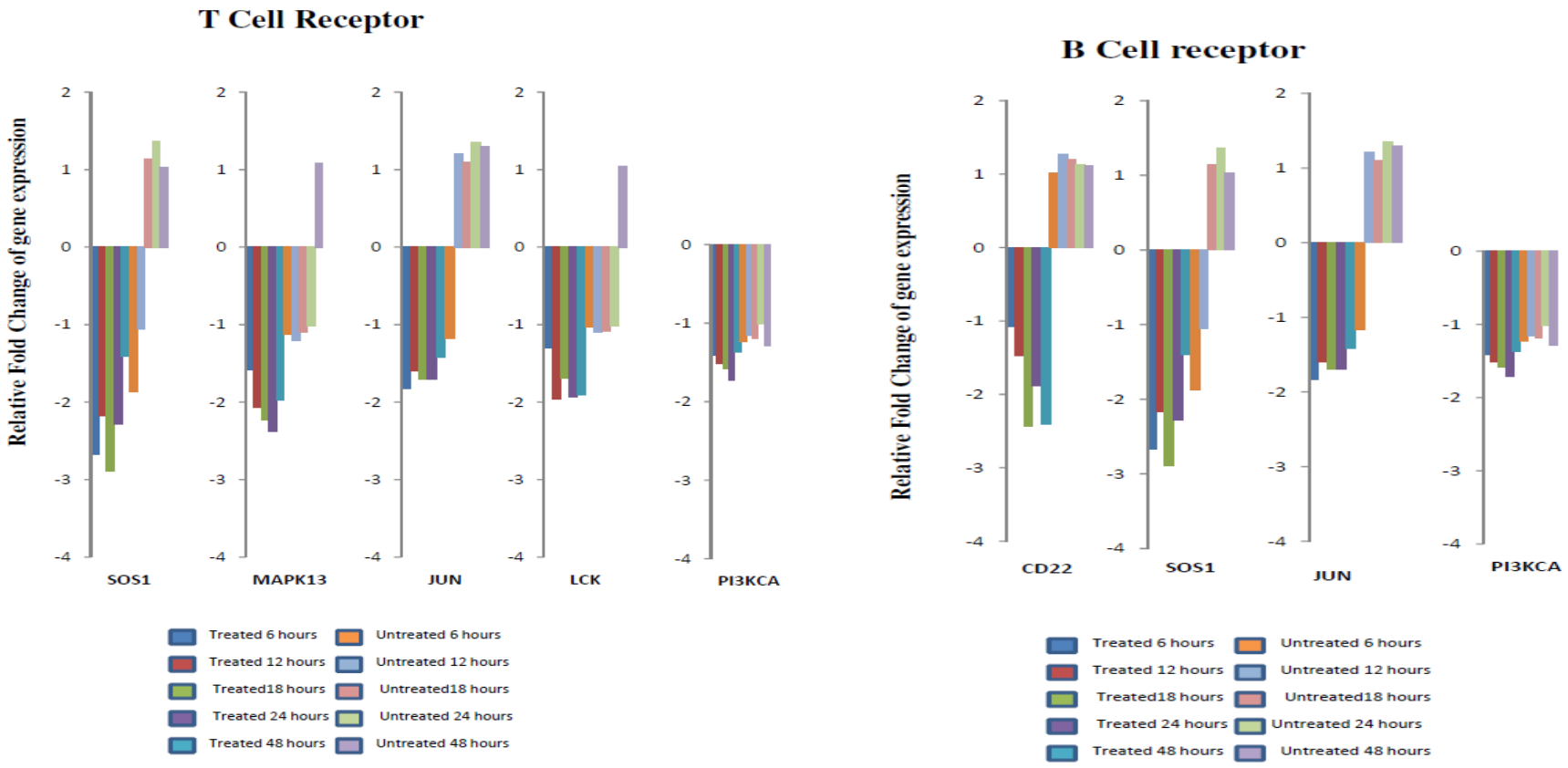

Figure 4.19and Figure 4.20: Genes identified in T-cell receptor signalling pathway and B-cell receptor signalling pathway with >2-fold-change or with relative significance compared with untreated samples under various time-points

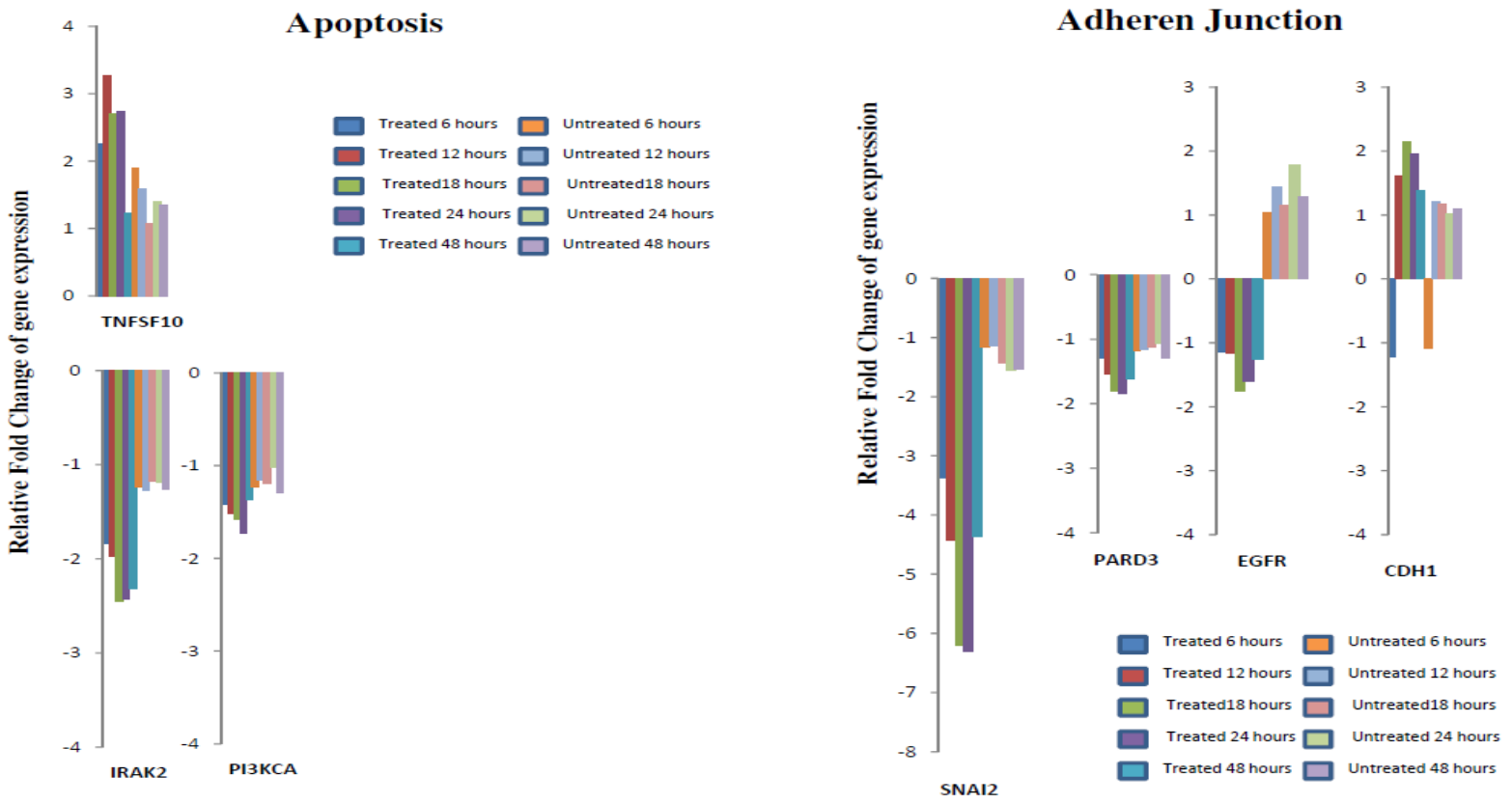

Figure 4.21 and Figure 4.22: Genes identified in Apoptosis signalling pathway and Adherens Junction with >2-fold-change or with relative significance compared with untreated samples under various time-points

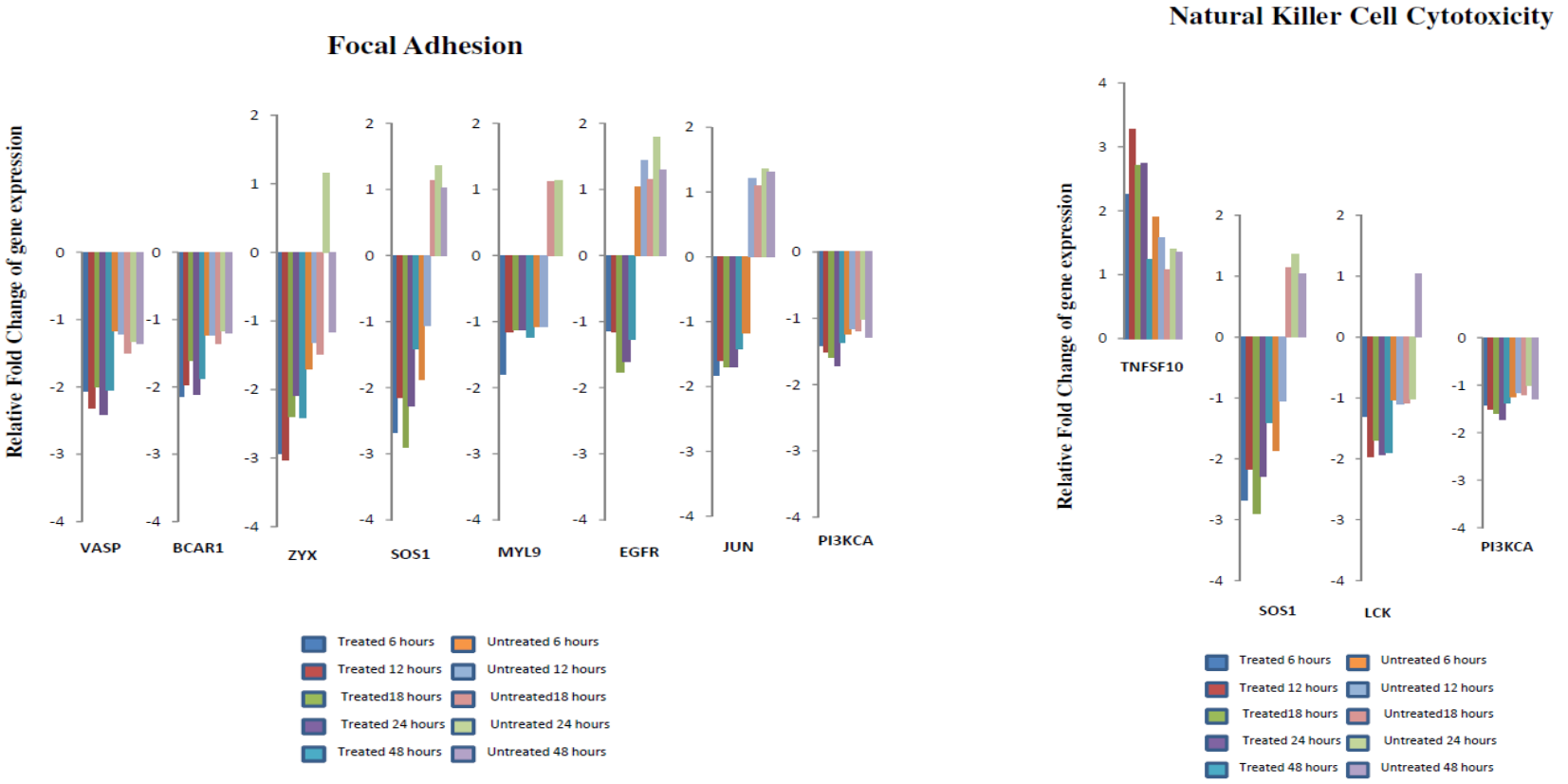

Figure 4.23 and Figure 4.24: Genes identified in Focal Adhesion signalling pathway and Natural Killer Cell Cytotoxicity signalling pathway with >2-fold-change or with relative significance compared with untreated samples under various time-points

4.5 Data Validation

4.5.1 Data Validation with Relative Real-time PCR Methodology

Real-time PCR has been widely used as a gold standard for validation of results obtained from microarrays based experiment. DNA microarrays provide an unprecedented capacity for whole genome profiling. However, the quality of gene expression data obtained from microarrays can vary greatly with platform and procedures used. Quantitative real-time PCR (qRT-PCR) is a commonly used validation tool for confirmation of gene expression results obtained from microarray analysis. However, microarray and qPCR data often result in certain level of disagreement.

Six genes were chosen based on their high fold-change value of differential expression, their genetic ontology and pathways. Among these, four significantly up-regulated genes (MAP2K, SKP2, PCY1B, and SLC2A2) and two significantly down-regulated genes (MMP3, SLC16A6) were selected for further validation. The mean values of gene expression of the fold-change for treated samples at different time-points (6, 12, 18, 24, and 48 hours) against the control group (0 hours) were derived and tabulated in Table 4.27.

The validation of microarray result by qRT-PCR results were carried out by plotting correlation chart of the gene expression of fold-change of microarray experiment and qRT-PCR approach (Figure 4.25 and Table 4.28). The measurement of the correlation value of these six genes has indicated the range of correlation from relatively acceptable correlation, 0.60, to good correlation,

0.947. This showed that the result of the microarray assay was consistent with the result of the qRT-PCR assay.

Table 4.27: Six genes selected for relative real-time PCR validation. Intensity level of gene expression is the criteria for selection

		Time Interval (Hours)						
Gene Symbol	**Gene Name**	**6**	**12**	**18**	**24**	**48**	**Gene Ontology**	**Pathway**
MAP2K	Mitogen-activated protein kinase kinase 6	1.2	3.93	5.78	5.15	3.27	Stress-induced cell cycle arrest, transcription activation and apoptosis	p38 MAP kinase mediated signal transduction pathway
SKP2	S-phase kinase-associated protein 2	1.51	2.32	3.14	4.43	4.04	Mitotic	Cell Cycle
PCYT1B	Phosphate cytidylyl transferase 1	1.63	2.55	4.11	3.84	3.96	Phosphatidylcholine biosynthesis from choline	CDP-choline pathway (TAS)
SLC2A2	Solute carrier family 2 (facilitated glucose transporter), member 2	2.11	4.72	5.58	8.61	5.9	Facilitative glucose transporter	Glucose transmembrane transporter activity
MMP3	Matrix metallo peptidase 3	-2.92	-6.56	-8.66	-8.53	-10.9	Extracellular matrix in normal physiological processes	GPCR pathway
SLC16A6	Solute carrier family 16, member 6	-16.48	-17.44	-18.02	-15.37	-6.97	Symporter activity and monocarboxylic acid transmembrane transporter activity	Proton-linked monocarboxylate transporter

Table 4.28: The relative fold change of the (A) upregulated genes and (B) downregulated genes for real-time PCR versus microarray assay

(A)

MAP2K6	Timepoint	**6hrs**	**12hrs**	**18hrs**	**24hrs**	**48hrs**
	Fold Change of Microarray	1.2	3.93	5.78	5.15	**3.27**
	Fold change of PCR	1.40	4.96	3.93	3.66	5.24
SKP2	Timepoint	**6hrs**	**12hrs**	**18hrs**	**24hrs**	**48hrs**
	Fold Change of Microarray	1.51	2.32	3.14	4.43	4.04
	Fold change of PCR	2.03	3.07	3.71	4.80	8.48
PCYT1B	Timepoint	**6hrs**	**12hrs**	**18hrs**	**24hrs**	**48hrs**
	Fold Change of Microarray	1.63	2.55	4.11	3.84	3.96
	Fold change of PCR	1.06	3.13	4.45	4.85	6.94
SLC2A2	Timepoint	**6hrs**	**12hrs**	**18hrs**	**24hrs**	**48hrs**
	Fold Change of Microarray	2.11	4.72	5.58	8.61	5.9
	Fold change of PCR	3.05	5.57	7.60	9.85	5.15

(B)

	Timepoint	**6hrs**	**12hrs**	**18hrs**	**24hrs**	**48hrs**
	Timepoint	**6hrs**	**12hrs**	**18hrs**	**24hrs**	**48hrs**
MMP3	Fold Change of Microarray	-2.92	-6.56	-8.66	-8.53	-10.9
	Fold change of PCR	1.00	0.44	0.23	0.10	0.03
	Timepoint	**6hrs**	**12hrs**	**18hrs**	**24hrs**	**48hrs**
SLC16A6	Fold Change of Microarray	-16.48	-17.44	-18.02	-15.37	-6.97
	Fold change of PCR	0.03	0.04	0.04	0.05	0.08

(A)

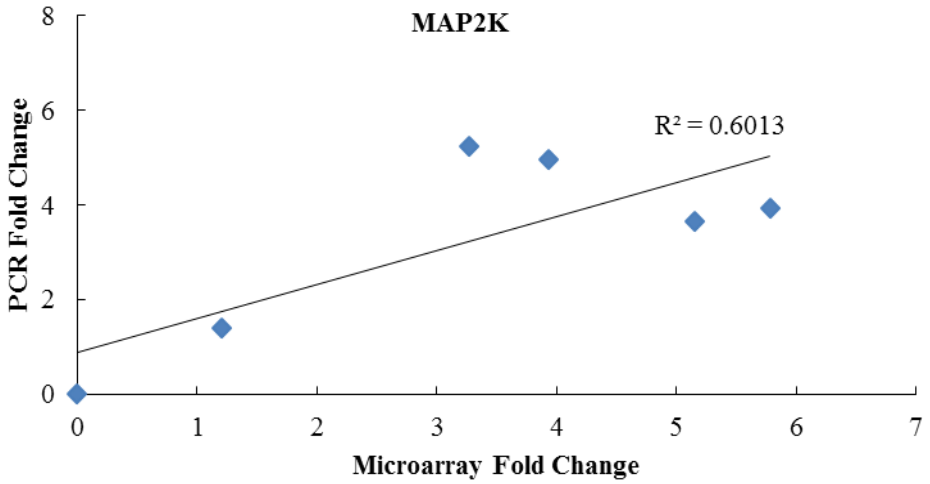

(B)

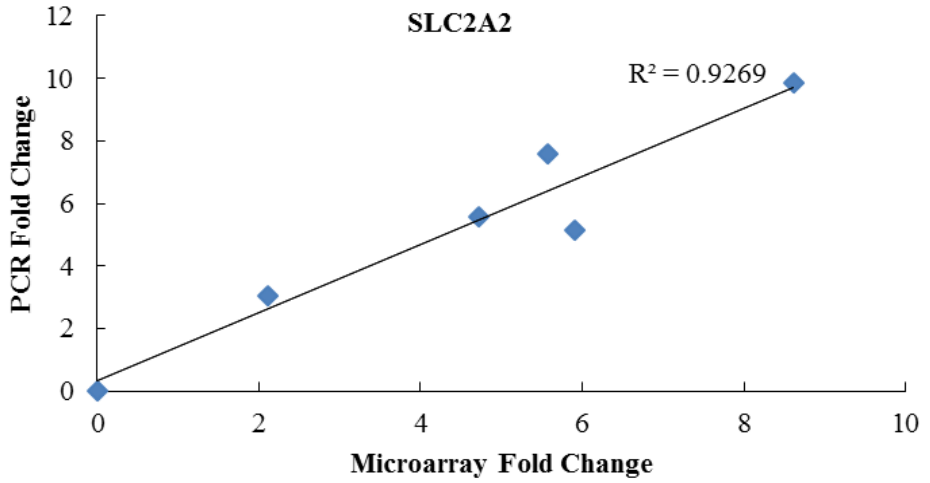

(C)

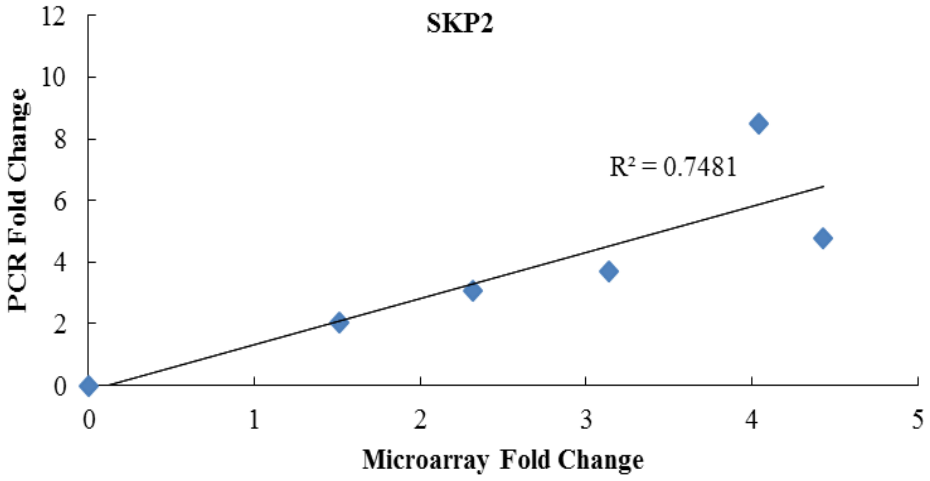

Figure 4.25: The correlation of real-time PCR result versus microarray resulton seven genes, namely (A) MAP2K, (B) SLC2A2, (C) SKP2, (D) PCYT1B, (E) SLC16A6, (F) MMP3

(D)

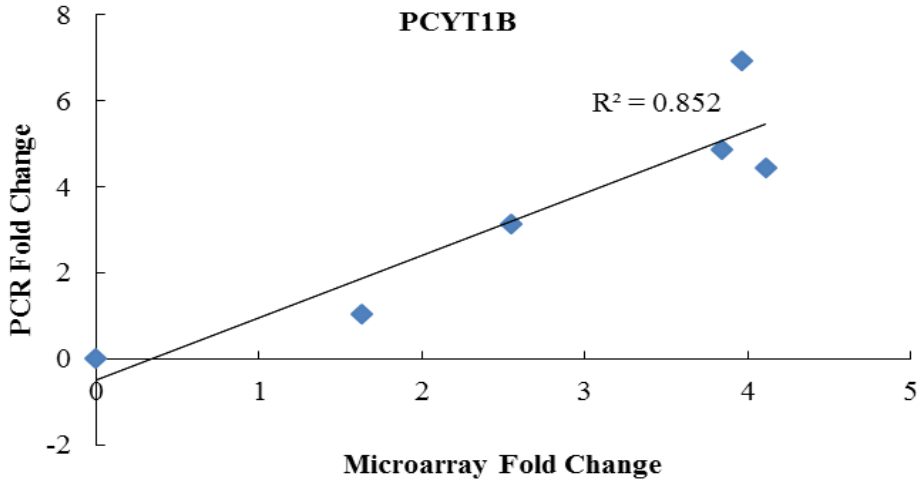

(E)

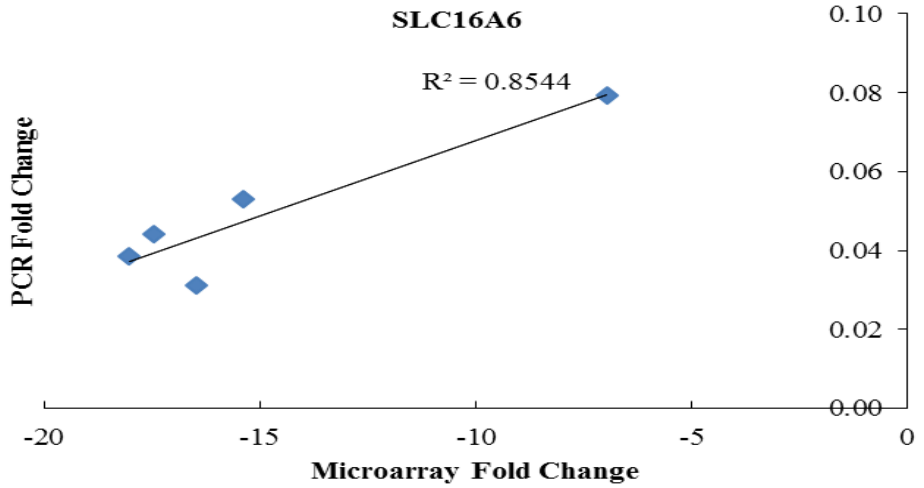

(F)

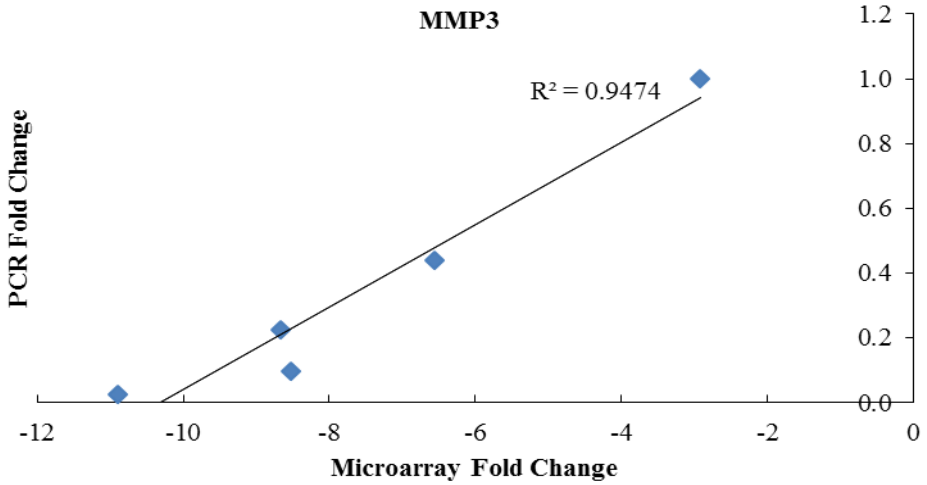

Figure 4.25(continued): The correlation of real-time PCR result versus microarray resulton seven genes, namely (A) MAP2K, (B) SLC2A2, (C) SKP2, (D) PCYT1B, (E) SLC16A6, (F) MMP3

4.5.2 Data Validation with Western Blot Approach

Following the qRT-PCR experiment, western blot assay was carried out to further validate the proteomic level of the genes. Theoretically, cellular protein levels are positively correlated with gene expression levels, but wide variation arises. It could be the result of difference in translational regulation, post-translational modification and protein or protein complexes stability (Grigoriev, 2001).

Accurate quantitation of sample loading into the gel for the western blot assay is a challenge. The signals of target proteins have to be normalized against the signal of housekeeping protein, such as GAPDH, which is in abundance in cells. However, the signal intensity of target proteins varies. The correlation of GADPH and those genes with less abundance may skew and show inconsistent results.

Antibodies of same six genes validated in qRT-PCR, including MAP2K, SKP2, PCYT1B, SLC2A2, MMP3 and SLC16A6 were selected for western blot assay to validate their expression at proteomic level. Their bands were detected in its respective western blot assay (Appendix D).

For the validation of protein, treated samples at time-points of 12 hours (D12), 24 hours (D24), 48 hours (D48) were placed along with untreated sample control 0 hour (C0) in the western blot assay (Figure 4.28). The signal intensity of the target proteins is consistent with the result of the RT-PCR result.

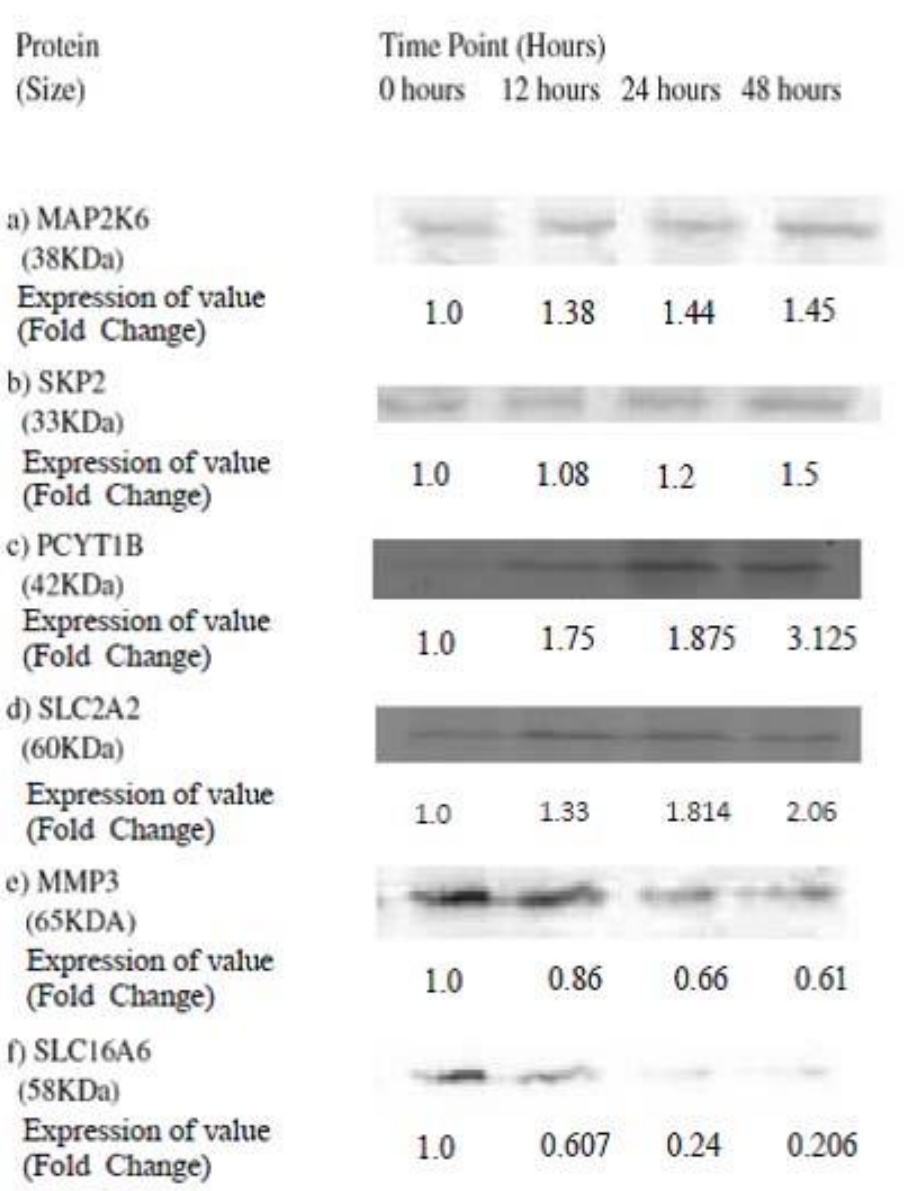

Figure 4.26: Western blot analysis of (A) MAP2K6, (B)SKP2, (C) PCYT1B, (D) SLC2A2, (E) MMP3 and (F) SLC16A6 proteins

4.6 Metabolite Identification

4.6.1 GC-MS Analysis

EI (Electron impact ionization) is the fundamental ionization mode for GCMS. Electron ionization typically is the first method of choice when screening samples and is applicable to the vast majority of analytes that can be analysed by gas chromatography. Fragmentation ions generated by GC-MS are analysed and possible metabolites are then identified.

TIC (total ion chromatogram) is a chromatogram created by summing up intensities of all mass spectral peaks belonging to the same scan, meaning that sample components and background noise are collected and included in the TIC. Due to some signals that are higher than the other, it could suppress small signals.

GC-MS analyses of bark-PE extract result in the identification of 13 compounds with match probability more than 650 (Figure 4.27; Table 4.29). However, the identification of these metabolites is tentative until they are confirmed with standards. These 13 metabolites belong to a diverse chemical class of diterpenes, sesquiterpenes, aldehyde, fatty acid, and essential oils. The main components were identified as Geranylgeraniol (28.38%), Hexadecanoic acid (9.46%), 17-Octadecynoic acid (4.18%), (E, E, E)-3,7,11,15-Tetramethylhexadeca-1,3,6,10,14-pentaene (2.01%) and Hexanedioic acid, mono(2-ethylhexyl) ester (1.9%). Diterpenes and sesquiterpenes make up 31.6% of the components in bark-PE.

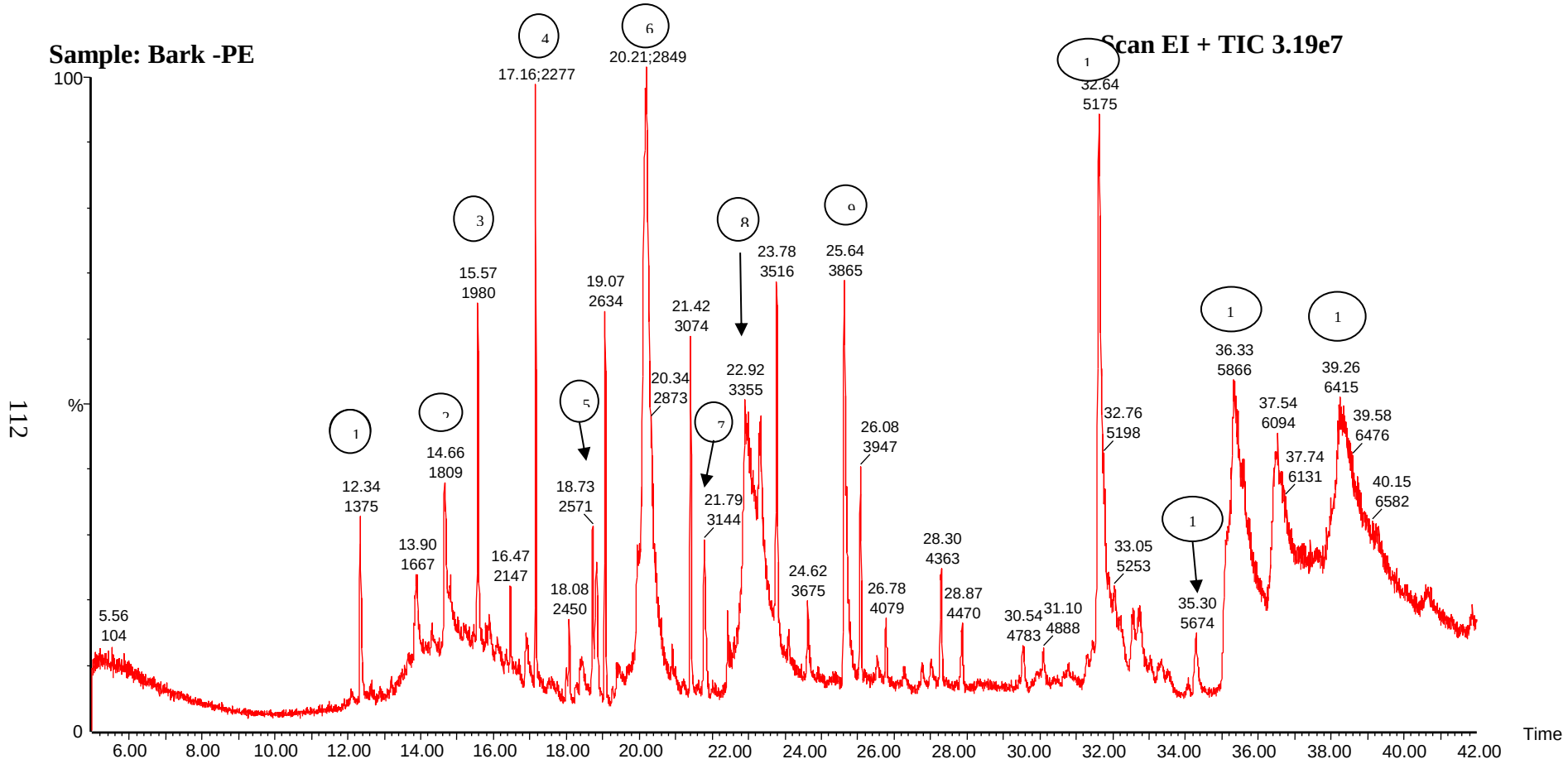

Figure 4.27: Typical total ion chromatograms from GC-MS analysis in EI-mode

Table 4.29: Metabolite profiling of bark-PE extract by GC-MS analysis

Item	Retention Time	Metabolite	Molecular Weight	Molecular Formula	Nature of Compound	Match	Area Percentage (%)
1	12.342	Naphthalene, 2,3,4,4a,5,6-hexahydro-1,4a-dimethyl-7-(1-methylethyl)-	204	$C_{15}H_{24}$	Sesquiterpene	695	0.555
2	14.66	3,5,9-Trimethyl-deca-2,4,8-trien-1-ol	194	$C_{13}H_{22}O$	essential oil	682	1.171
3	15.573	Heptasiloxane, hexadecamethyl-	533	$C_{16}H_{48}O_6Si_7$		650	1.028
4	17.159	Heptasiloxane, hexadecamethyl-	533	$C_{16}H_{48}O_6Si_7$		697	0.908
5	18.729	α-Farnesene	204	$C_{15}H_{24}$	Sesquiterpenes	729	0.394
6	20.214	Hexadecanoic acid, trimethylsilyl ester	328	$C_{19}H_{40}O2Si$	Palmitc acid, saturated fatty acid	686	9.457
7	21.789	11-Hexadecen-1-ol, (Z)-	240	$C_{16}H_{32}O$	Aldehyde, Pheromone	841	0.62
8	23.338	(E,E,E)-3,7,11,15-Tetramethylhexadeca-1,3,6,10,14-pentaene	272	$C_{20}H_{32}$	Diterpenes	718	2.011
9	25.639	Hexanedioic acid, mono(2-ethylhexyl) ester	258	$C_{14}H_{26}O_4$	Phtalate Ester	798	1.898
10	32.635	Geranylgeraniol	290	$C_{20}H_{34}O$	Diterpenoids	711	5.132
11	35.3	2-Methyl-3-(3-methyl-but-2-enyl)-2-(4-methyl-pent-3-enyl)-oxetane	222	$C_{15}H_{26}O$	Sesquiterpenoids	681	0.325
12	36.325	Geranylgeraniol	290	$C_{20}H_{34}O$	Diterpenoids	744	9.706
13	39.257	Geranylgeraniol	290	$C_{20}H_{34}O$	Diterpenoids	708	13.486

CHAPTER 5

DISCUSSION

5.1 Properties of Cancer Cells

During the last few decades, research has revealed that cancer is a dynamic disease involving changes in the genome. Advancement in technology allows researchers to have a better understanding of the pathogenesis of cancer in a precise and prompt manner.

Normal cell grows and divides to make a new cell. It dies in an orderly manner if any attempt to repair the damaged DNA fails. However, cancer cell does not die like it should. It could grow in a tremendous manner through a multistep, mutagenic process(Barrett, 1993). Its limitless replicative potential, self-sufficiency in growth signal, insensitivity to anti-growth signals and evasion of apoptosis allow it to proliferate and avoid being killed.

Its capability of forming new blood vessels, known as angiogenesis, allows its access to oxygen, nutrients and waste disposal. For cancer cell to grow, an angiogenic gene may be activated to make normally quiescent vasculature to continually expand new blood for the growth of tumour(Hanahan and Folkman, 1996).

Angiogenesis is critical for cancer development. Tumour cells need oxygen and nutrients for survival and proliferation. In order to get the adequate supply of oxygen and nutrients, they need to be within 100-200 μm from blood vessels(Carmeliet and Jain, 2000). For solid tumours smaller than 1-2 mm^3, the blood vessels are not established or vascularized. However, for those beyond the critical volume of 2 mm^3, new blood vessels are established to supply oxygen and nutrients and remove metabolic wastes (Hawkins, 1995).

This ultimately also leads the cell to metastasize to the distal part of the body. It evades immune detection, survive and proliferate. Cancer cell acquires a competitive advantage by gene mutation in order to grow faster, survive longer and produce more offspring than the normal cell. These genetic alterations involve the gain-of-function mutation, amplification, or overexpression of key oncogenes together with the loss-of-function mutation, deletion, or epigenetic silencing of key tumour suppressors. Despite the difficulties, many of the genes that are repeatedly mutated in human cancers have been identified over the last few decades. It has reached a common understanding that cancer is caused by some corrupted cellular genes, known as oncogenes, to survive longer than it should and proliferate aberrantly. The genesis and progression of a tumour are further complicated by inactivation of some identified tumour suppressor genes. These genes act to prevent any aberrant cell growth and survival or genomic instability. This inactivation could be caused by gene deletion, inactivating mutation, or epigenetic silencing, which results in the removal of restraints, leading to tumorigenesis (Hanahan and Weinberg, 2011).

The stochastic accumulation of these genetic alterations in cancer-critical genes, including oncogenes and tumour suppressors, progressively contribute to the evolution of cancer from a benign expansion of cells to an invasive and metastatic tumour. The discovery of these cancer-critical geneses of great clinical interest is target for cancer therapeutics. The inhibition of these oncogenes can lead to tumour cell death, differentiation, arrest, or senescence. The results of this cancer therapeutics have been encouraging. It includes the successful imatinib or Gleevec for the protein kinase oncogenes BCR-ABL, Gefitinib and Erlotinib for EGFR and Trastuzumab for Her2 (Roberts and Der, 2007; Sharma and Settleman, 2007; Luo et al., 2009).

Germline mutations in tumour suppressor genes p53 and Rb leave affected individual, particularly susceptible to the development of cancers by reducing the number of somatic mutations required for a cell to become malignant(Thomas and Balan, 2012). Scientists have been exploring to reintroduce tumour suppressor genes into a tumour, leading to tumour regression. However, the effort in restoring in these genes is still lagging behind the study in oncogenes due to its difficulty(Luo et al., 2009).

Any possible cure of cancer must show differential toxicity toward cancer cells relative to normal cells. Cancer evolves from the stepwise accumulation of genetic aberration. Despite the multitude of genetic and epigenetic alteration in cancers, its growth and survival can be implicated by the gain of single oncogene or loss of single tumour suppressor. These unique properties of cancer cells not shared by normal cells could be explored for their

detriment. Bernard Weinstein described this as oncogene addiction, which would have the tumour maintenance depended on the continued activity of certain oncogene or loss of certain tumour suppressor gene (Weinstein, 2002).

In principle, cancer cells can be induced to undergo apoptosis, necrosis, senescence, or differentiation leading to its demise. Cancer cells have the capabilities of rewiring pathways for growth and survival that underlie the malignant phenotype. Any successful therapy is to identify the critical nodes in the oncogenic network, which will lead to its cessation of the tumorigenesis. This provides cues for molecular targeted therapy in cancers (Weinstein and Joe, 2006).

5.2 Cytotoxic effects of CCL on HepG2 and its Regulation on Cancer Pathways

To determine the significantly regulated pathways, the genes obtained in this study were mapped to the Kyoto Encyclopaedia of Genes and Genomes (KEGG) pathways. The bark-PE extract used in this study showed a differential gain or loss of expression upon HepG2 cells relative to untreated HepG2 at time-points of 0, 6, 12, 18, 24 and 48 hours.

Various pathways were confirmed based on KEGG pathways in the DAVID Bioinformatic Tool, where its functional annotation tool identified the KEGG pathways showing an enrichment or loss of these genes and the probability of that pathway was significantly regulated.

5.2.1 p53 Signalling Pathway

Stresses, both intrinsic and extrinsic to the cell, can act upon the p53 pathway (Appendix C-1). p53 is the major cellular stress responder for intrinsic stress signals while NF-κB is the major stress responder for extrinsic stress signals, such as infectious diseases, cytokine signals, etc., activating the genes of the innate and adaptive immune responses (Lane and Levine, 2010). p53 pathway oversees the DNA replication, chromosome segregation and cell division. The integrity of the DNA is affected by stresses, such as Gamma or UV irradiation, alkylation of bases, depurination of DNA or its reaction with oxidative free radicals. In response to these stresses, the genes and its products in the cascades of p53 pathway are activated by post-translational modifications, leading to cell cycle arrest which induces cell senescence or cellular apoptosis (Vogelstein et al., 2000; Harris and Levine, 2005).

Metastasis of cancer, the migration of its cell from one organ to another distant organ, is related to the poor prognosis of various cancers. This cellular migration involves the complex barrier changes by interactions of structural components of the extracellular matrix (ECM) and surface binding element, namely integrins. It is noted that several proteases and protease inhibitors, including plasminogen activator inhibitor type-1 (*PAI-1*) or Serpine1, urokinase plasminogen activator (*μPA*) interact with several cell surface receptors, like μPA receptor (*μPAR*) and transduce intracellular signals that significantly affect other proliferative pathways (Czekay et al., 2011).

Plasminogen activator inhibitors (*PAI*s) are classified as a subgroup of the serine protease inhibitor (serpine) superfamily. It may have a role in regulating tumour invasion, angiogenesis and metastasis. The overexpression of *PAI-1* together with *μPA, μPAR* were found in HCC compared with those of cancer-adjacent tissue and normal liver tissue. This suggests that the increased *PAI-1*in HCC is related to the invasiveness, metastasis, and prognosis of HCC (Zheng et al., 2000). It concurs with Czekay that the deficiencies in *PAI-1* levels correlate with significantly reduced epithelial cell migration and tumour progression (Czekay et al., 2011). The down-regulations of *PAI-1*were observed across all the time-points of extract-treated HepG2 compared with time-points of untreated HepG2 in this study (Table 4.5; Figure 4.3). The high negative fold changes in all time-points of extract-treated HepG2 indicated that growth of HepG2 was suppressed significantly.

Sestrins are part of the antioxidant defence system. It helps inhibit cell proliferation and suppress mTOR activity in the liver following genotoxic and ER stress. The appearance of cancer cells triggers the expression of antioxidant proteins. Studies showed that active *RAS* oncogene downregulates *SESN1* and *SESN3* (Budanov and Karin, 2008; Lee et al., 2013). In this study, the significant up-regulations of *SESN3* were observed across all the time-points of extract-treated HepG2 compared with time-points of untreated HepG2 (Table 4.5; Figure 4.3), while SESN1 showed relatively higher fold changes (<2) in all time-points of extract-treated HepG2 indicated that growth of HepG2 was suppressed significantly.

Study has shown that *SESN2* activates p21 network and regulates hepatocyte proliferation and tumour development in mice with liver injury (Buitrago-Molina et al., 2013). The down-regulation of *SESN2* in all time-points of the extract-treated HepG2 indicated its suppression effect on the growth of HepG2 (Table 4.5; Figure 4.3).

5.2.2 Cell Cycle Signalling Pathway

All cancers share the common characteristic of a disordered cell cycle that is characterized by rapid and uncontrolled cell growth. Thus, targeting the molecules that regulate the cell cycle has become a major thrust in the development of anticancer therapeutics (Toogood, 2002) (Appendix C-2).

Overexpression or amplification of *SKP2* has been documented in various human cancers, including HCC, prostate cancer, breast cancer, lymphoma, small cell lung cancer, oral squamous cell carcinoma, and colorectal carcinoma. It correlates with their poor prognosis. This suggests that *SKP2* may be associated with the growth and expansion of tumour cells (Gstaiger et al., 2001; Zhang et al., 2003; Huang et al., 2005; Calvisi et al., 2009). *SKP2* is a downstream effector of multiple pathways, including H-Ras, AKT, JAK/STAT, and Wnt/β-catenin, which are commonly seen in human hepatocarcinogenesis (Thorgeirsson and Grisham, 2002). It is believed that its up-regulation may positively associate with cellular transformation and tumour progression.Study has shown that HBx selectively binds to *SKP2*, in which *SKP2* substrate proteins may be the natural targets of HBV during viral infection (Kalra and Kumar,

2006). Therefore, *SKP2* may be a therapeutic target for HBV-related HCC (Huang et al., 2011).The increased expression of *SKP2* was noticed across all time-points for extract-treated HepG2 compared with untreated HepG2 (Table 4.6; Figure 4.4). This indicated that the extract induced proliferation and accelerated the division of the HepG2 cells.

SKP2 is associated with the down-regulation of cell cycle regulators, including *CCKN1A (p21WAF1/CIP1*) during HCC pathogenesis. *CCKN1A*, cyclin kinase inhibitor, is an important regulator of cell cycle progression and proliferation. It is down-regulated in HCC and its deficiency can cooperate with other oncogenic mutations to enhance carcinogenesis (Calvisi et al., 2009).On the contrary, study of Marhenke et al (2014) has shown that loss of *CCKN1A* delays tumour development in the liver and expression of *CCKN1A* in HCC is associated with shorter survival (Marhenke et al., 2014). *CDKN2B (P15),*cyclin-dependent kinase inhibitor, was found to be downregulated in the cancerous tissues in most of HCC (Qin et al., 2004). In this study, the down-regulations of the *CCKN1A* and CCKN2B were observed across all the treated HepG2 cell line at all time-points compared with time-points of untreated HepG2 (Table 4.6; Figure 4.4). The downregulation of *CCKN2B* may suggest that proliferation of HepG2 cells was not suppressed.

Defects in the growth arrest DNA damage-inducible gene 45 (*GADD45*) pathway can be related to the initiation and progression of malignancies. In a study done by Qiu et al. (2003), the expression of *GADD45β* in HCC as well as HepG2 and Hep3B was down-regulated while other cancer tissues, including

colon cancer, breast cancer, prostate cancer, squamous cell cancer, and lymphoma were strongly stained. This may suggest that decreased expression of *GADD45β* is specific to HCC (Qiu et al., 2003). Similarly, the decreased *GADD45β* expression is seen in those infected by hepatitis C virus, and is associated with hyper-methylation of the *GADD45β* promoter upon viral infection (Higgs et al., 2010).

In cancer cells, the activation of *GADD45* proteins induces pro-apoptotic pathways. While in some normal cell lines, *GADD45* proteins play a role in pro-survival pathways. The main target of *GADD45*-mediated cell cycle arrest is CDK1/Cyclin B1 complex, a guard for the G2/M checkpoint. This cell cycle arrest leads to a reduced cell proliferation rate, in both normal and cancer cells without evidence of apoptosis inductions (Jin et al., 2002). Down-regulation of *GADD45* genes may be related to methylation of its promoter region, which contribute to the alteration in its expression. Targeting this process is the anti-cancer mechanism used by chemotherapeutic drugs (Tamura et al., 2012).

In studies of Alexey et al, *GADD45* may have dual roles in apoptosis and cell survival. The excessive DNA damage beyond a certain threshold may trigger apoptosis. *GADD45* proteins exert a pro-apoptotic function for irreparable damage while the *GADD45α* and *GADD45β* proteins act as anti-apoptotic agents for moderate DNA damage and increase hematopoietic cell survival under UV-irradiation or treatment with certain chemotherapeutic drugs (Moskalev et al., 2012). The significant down-regulations of *GADD45β* were observed across all

the time-points of extract-treated HepG2 compared with time-points of untreated HepG2 in this study (Table 4.6; Figure 4.4).

Stratifin (*SFN* or *14-3-3*) plays an active role in different steps of cancer development. It regulates many cellular processes in cancer biology, including apoptosis and cell cycle checkpoints. *14-3-3σ* is one of seven human 14-3-3 genes that only show induction after DNA damage. Transcriptional expression of *14-3-3σ* is directly activated by the p53 tumour suppressor protein. This p53-mediated induction of *14-3-3σ* is essential for the maintenance of a stable G2/M arrest after DNA damage (Samuel et al., 2001).However, the expression of *14-3-3σ* is down-regulated by CpG methylation in several types of human cancer, including prostate, lung, breast and several types of skin cancer (Yang et al., 2003; Lodygin and Hermeking, 2006). It is also reported that hyper-methylation and the resulting loss of expression of the *14-3-3σ* gene are the most common abnormalities in HCC. This gives the cue in its role in the development and progression of HCC (Iwata et al., 2000). On contrary to earlier reports, the studies done by Liu et al. (2014) indicate that *14-3-3σ* overexpression promotes tumour progression in HCC (Chen et al., 2010; Liu et al., 2014). These results, suggesting a "bipolar" role for *14-3-3σ*. The significant down-regulations of *SFN* were significantly observed across all the time-points of extract-treated HepG2 compared with time-points of untreated HepG2 in this study (Table 4.6; Figure 4.4).

WEE1 kinase is one of the key proteins in maintaining G2 arrest for DNA repair. Damaged normal cells are repaired during G1-arrest, while cancer cells may rely on G2-arrest, due to its deficiency in G1-arrest. Besides overexpressed in advanced HCC compared with noncancerous cirrhotic tissue, *WEE1* is also overexpressed in various cancer types (Masaki et al., 2003; Lee et al., 2011). *WEE1* silencing significantly increases the expression of p53 and p21 in *WEE1*-deficient HepG2 cells and subsequently lead to cell cycle arrest and induction of apoptosis (Lee et al., 2011). The down-regulations of *WEE1* were observed across all the time-points of extract-treated HepG2 compared with time-points of untreated HepG2 in this study (Table 4.6; Figure 4.4). This may suggest that the extract has suppressed the proliferation of HepG2. The *RBL1* gene is a known tumour suppressor protein which regulates cell cycle. The up-regulations of *RBL1* were significantly observed across all the time-points of extract-treated HepG2 compared with time-points of untreated HepG2 in this study (Table 4.6; Figure 4.4). This may suggest that the extract has suppressed the proliferation of HepG2.

Cell division cycle 25 homolog phosphatases (*CDC25*) are important activators of the Cdk/cyclins. Its isoform, *CDC25A* controls both the G1-to-S and G2-to-M transitions, whereas *CDC25B* and *CDC25C* are regulators of the G2-to-M transition. Over-expressions of *CDC25A* and *CDC25B*, are often associated with malignant tumours with poorer prognosis (Kristjansdottir and Rudolph, 2004). *CDC25B* is highly regulated by phosphorylation via several protein kinases in different pathways, including AKT, CDK/cyclin, p38, which in turn regulate *CDC25B* activity. It was identified as one of most significantly

overexpressed genes in HCC compared with non-tumour liver (Yan et al., 2008).

The down-regulations of CDC25B were observed across all the time-points of extract-treated HepG2 compared with time-points of untreated HepG2 in this study (Table 4.6; Figure 4.4). This may suggest that the extract has inhibited the growth of HepG2.

CDC6 and *CDC7* are essential regulators of DNA replication. *CDC6* is upregulated during the G1 phase of the cell cycle while *CDC7* is upregulated during S phase. Overexpression of *CDC6* and *CDC7* may indicate the progression of the tumour. The significant up-regulations of *CDC6*& *CDC7* were observed across all the time-points of extract-treated HepG2 compared with time-points of untreated HepG2 in this study (Table 4.6; Figure 4.4). This may suggest that the extract has promoted the proliferation of HepG2.

The role of *CCNE2* on HCC is not known although high level of expression of *CCNE2* in many cancers (Sieuwerts et al., 2006). In this experiment, the up-regulations of *CCNE2* were observed across all the time-points of extract-treated HepG2 compared with time-points of untreated HepG2 (Table 4.6; Figure 4.4).

5.2.3 Hedgehog Signalling Pathway

The Hedgehog (Hh) signalling pathway plays important role in embryonic development (Appendix C-3). However, studies also show that it has been involved in the development of multiple malignancies (Lappano and Maggiolini, 2012).

In the absence of Hh ligand, Hh receptor Patched (Ptch) keeps down the activity of Smoothened (SMO), G-protein-coupled receptors. Following Hh ligand binding to Ptch, the repression of SMO is released and the downstream transcription factors, including glioma-associated oncogene homologue (Gli), are stimulated (Merchant and Matsui, 2010).The overexpression of Hh ligands has been identified in tumours. This suggests its role in cell proliferation and survival. The Hh signalling pathway also interacts with other signalling pathways commonly implicated in human cancers, such as PI3K,WNT, and VEGF (Scales and de Sauvage, 2009; Gupta et al., 2010; Merchant and Matsui, 2010).

Hh signalling is dysregulated in human hepatocarcinogenesis. In studies by Sicklick et al. (2006) using HCC cell lines (HepG2 and Hep3B) show that overexpression of both *SMO* and SMO-mediated *c-Myc* play critical role in hepatocarcinogenesis and suggests that *SMO* is a prognostic factor in HCC tumorigenesis (Sicklick et al., 2006). The up-regulations of *SMO* were observed across all the time-points of extract-treated HepG2 compared with time-points of untreated HepG2 in this study (Table 4.7; Figure 4.5). This may suggest that extract may help HepG2 proliferate.

WNT11 was significantly up-regulated in a number of tumours. Up-regulation of *WNT11* might play an important role in human carcinogenesis through activation of the WNT signalling pathway (Kirikoshi et al., 2001). The down-regulations of *WNT11* were observed across all the time-points of extract-treated HepG2 compared with time-points of untreated HepG2 (Table 4.7;

Figure 4.5). This may suggest that extract help suppress the proliferation of HepG2.

5.2.4 MAPK Signalling Pathway

Mitogen-activated protein kinases (MAPKs) are a highly-conserved family of serine/threonine protein kinases involved in a variety of fundamental cellular processes such as proliferation, differentiation, motility, stress response, apoptosis, and survival (Appendix C-4). MAPK signalling pathway is a three-tiered cascade. The extracellular stimuli, including mitogens, cytokines, growth factors, and environmental stressors activate kinases of MAPKK pathway. They phosphorylate and in turn activate a downstream MAPK kinase (MAPKK), which subsequently phosphorylates and activates MAPKs. The classic MAP kinase family includes extracellular signal-regulated kinases (ERK), c-Jun NH2-terminal kinases (JNK), and p38-MAP kinases. Among the three MAPKs, ERKs are activated by the broad range of cytokines and growth factors and play an important role in cell growth and differentiation. JNKs and p38 MAPKs are stress-activated MAPKs and mainly activated by pro-inflammatory cytokines, such as tumour necrosis factor α (TNFα), or other stresses. After activated, stress-activated MAPKs phosphorylate specific serine/threonine residues of target substrates and trigger downstream cellular functions, such as cell death, survival, proliferation, migration, and inflammation (Yan et al., 1994; Xia et al., 2007; Nakagawa and Maeda, 2012).

MAPK phosphatases (MKPs) are one of the subgroups of DUSPs. *DUSP5, DUSP6* and *DUSP8* are known tumour suppressor or negative

regulators of MAPK activity (Kidger and Keyse, 2016). In this study, significant down-regulations of *DUSP5, DUSP6* and *DUSP8* were observed across all the time-points of extract-treated HepG2 compared with time-points of untreated HepG2 (Table 4.8; Figure 4.6). This may suggest that the extract promotes the proliferation of HepG2.

The ERK pathway is ubiquitous and can be activated by various receptors, particularly RTKs. Upon docking with the activated receptors, SOS1 and GRB2 activate the small GTPase RAS (*HRAS, NRAS* and *KRAS*). All RAS protein family members belong to a class of protein called small GTPase. *RAS* is the most common oncogenes in human cancer. Activated RAS activates several downstream effectors, such as serine–threonine kinase RAF-1, phosphoinositide 3′-kinase (PI3K), and RalGDS. These downstream effectors in turn activate several signalling cascades, leading to activation of certain genes which is favourable for cancer growth, including growth factors like transforming growth factor-α and vascular endothelial growth factor (*VEGF*) (Adjei, 2001).*RAF-1* in turn activates the ERK pathway. Studies show that MAPK/ERK was upregulated in human HCC. However, *EGFR* triggers the activation on *RAS*, which in turn, activates this RAF-MAPK-ERK. ERK activation, in turn, also promotes upregulated expression of EGFR ligands, promoting an autocrine growth loop critical for tumour growth. Thus, the EGFR-RAS-RAF-MEK-ERK signalling network has been the focus of research for cancer treatment (Roberts and Der, 2007). The obvious down-regulations of *SOS1* were observed across all the time-points of extract-treated HepG2 compared with time-points of untreated HepG2 in this study (Table 4.8; Figure

4.6). It may suggest that extract induced apoptosis in HegG2. However, the role of *RRAS* in cancer was not widely studied. The down-regulations of *RRAS* were observed across all the time-points of extract-treated HepG2 compared with time-points of untreated HepG2 in this study (Table 4.8; Figure 4.6).

HCCs show lower p38 MAPK and MKK6 activity than non-tumorigenic tissues supporting the observation that increased p38 MAPK activity induces apoptosis in hepatoma cell lines (Iyoda et al., 2003; Min et al., 2011). This suggests that diminished p38 MAPK and MKK6 activities may account for the resistance to apoptosis, leading to unrestricted cell growth of human HCC (Koul et al., 2013). The significant down-regulations of *P38* and up-regulations of *MKK6* were observed across all the time-points of extract-treated HepG2 compared with time-points of untreated HepG2 (Table 4.8; Figure 4.6). This may suggest that counteraction or neutralization of effects of both genes on the growth of HepG2.

The AP-1 transcription factor plays active roles in cell growth and proliferation. It is composed primarily of members of the *JUN* and *FOS* families of proteins. *JUND* is also part of the member of AP-1 transcription factor. *JUN* and *JUND* encode a central component of AP-1 transcription factors. They are the major regulators of the proliferative and stress responses of mammalian cells leading to oncogenesis. They are downregulated in response to osmotic stress, indicating that their downregulation promotes apoptosis (Xia et al., 2007; Nakagawa and Maeda, 2012). The significant down-regulations *JUND* were observed across all the time-points of extract-treated HepG2 compared with

time-points of untreated HepG2 (Table 4.8; Figure 4.6). This may suggest that extract promoted apoptosis and suppressed the growth of HepG2.

Serum response factor (*SRF*), transcriptional regulator, is frequently activated in hepatocellular carcinoma (HCC). Study showed that SRF-active mice developed hyperproliferative liver nodules that progressed to lethal HCC (Ohrnberger et al., 2015). The down-regulations of *SRF* were observed across all the time-points of extract-treated HepG2 compared with time-points of untreated HepG2 (Table 4.8; Figure 4.6). This may suggest that the extract suppressed the growth of HepG2.

CACNA1H was not well studied in most of the cancer type. However, it was detected in breast cancer(Asaga et al., 2006).The down-regulations of *CACNA1H* across all the time-points of extract-treated HepG2 compared with time-points of untreated HepG2 may potentially shed some lights on its suppression effect on cancer cell (Table 4.8; Figure 4.6).

5.2.5 mTOR Signalling Pathway

mTOR is a serine/threonine protein kinase that regulates cell growth, cell proliferation, cell motility, cell survival, protein synthesis, autophagy, and transcription (Appendix C-5). The mTOR signalling is activated in many tumour types. It contains a number of tumour suppressor genes, including *PTEN, LKB1, TSC1,* and*TSC2,* and a number of proto-oncogenes including *PI3K, AKT,* and*eIF4E* (Law, 2005). Over-activation of mTOR signalling significantly

contributes to the initiation and development of tumours including breast, prostate, lung, melanoma, bladder, brain, and renal carcinomas (Xu et al., 2014).

Comprised of mTOR and a regulatory associated protein of mTOR (RAPTOR), mTOR complex 1 (mTORC1) is a downstream target of AKT. It acts as a central regulator of cell growth and proliferation and regulates protein synthesis and allows progression from G1 to S phase of the cell. While mTOR complex 2 (mTORC2), formed by mTOR, RICTOR and PRR5/GβL, activates AKT and plays important role of mTOR pathway activation in human HCC (Villanueva et al., 2008).

In a study by Kimball and Jefferson (2012), DNA-damage-inducible transcript 4 (*DDIT4*) is rapidly induced in response to a wide variety of situations, including hypoxia conditions, food deprivation, or during glucocorticoid treatment. They deplete intracellular ATP or cause DNA damage (Kimball and Jefferson, 2012). The significant down-regulations of *DDIT4* were observed across all the time-points of extract-treated HepG2 compared with time-points of untreated HepG2 in this study (Table 4.9; Figure 4.7). This may suggest that extract may help reduce oxidative stress and suppress the growth of HepG2.

5.2.6 TGF-β Signalling Pathway

Transforming growth factor-β (TGF-β) is known as a multifunctional polypeptide that controls proliferation, differentiation, embryonic development,

angiogenesis, wound healing and other functions in many cell types (Massagué, 2008; Appendix C-6).

TGF-β and its receptors are widely expressed in all tissues. Low expression of *TGF-β* has been noticed in diseases like hyper-proliferative disorders, tumour formation, inflammation, and autoimmune diseases while higher expression is observed in diseases involved immunosuppression and tumour metastasis. Thus, *TGF-β* plays a dual role in human cancers, acting both as a tumour suppressor and as a promoter of tumour metastasis. It acts as a tumour suppressor in normal epithelial cells and in early stage of tumour progression while inducing many activities that lead to growth, invasion and metastasis of cancer cells in advanced cancer (Derynck et al., 2001; Mishra et al., 2005; Lebrun, 2012).

TGF-β triggers signalling cascade and promotes liver fibrosis, cirrhosis and subsequent progression to HCC (Giannelli et al., 2011; Stauffer et al., 2012). The other observation also suggests that the association of *TGF-β* with cancer is strongest in the most advanced stages of tumour progression. The cancer cells in advanced stages secrete larger amounts of *TGF-β* than their normal cell. However, *TGF-β* is highly protective against cancer in the early stage (Yasmin Anum et al., 2009; Nagaraj and Datta, 2010). These observations could be reconciled with other findings and provide a clue about its roles in anti-tumour and pro-tumour at different stages of HCC progression (Lebrun, 2012;Capece et al., 2013).

TGF-β also plays an important role in tumour progression as an effector in the microenvironment of epithelial-to-mesenchymal transition (EMT), which is conducive for cancer metastasis. *TGF-β*, along with others including *VEGF*, *ErbB/EGF*, *WNT*, interleukin 6 (*IL-6*), *IL-8, IL-11, IL-1*, insulin-like growth factor I & II *(IGF I & II*), platelet-derived growth factor (*PDGF*) and hedgehog (HH) signalling pathways have been identified as the important EMT and mesenchymal-to-epithelial transition(MET) effectors for bone metastasis formation (Katoh and Katoh, 2008; Scheel and Weinberg, 2012; Demirkan, 2013). The down-regulations of *TGF-β* were observed across all the time-points of extract-treated HepG2 compared with time-points of untreated HepG2 in this study (Table 4.10; Figure 4.8).

TGF-β mediates G1 cell cycle arrest. It induces CDK inhibitors and downregulates downstream transcription factors, which are inhibitors of differentiation, including c-*Myc*, *ID1* and *ID2*. However, in most of the tumour, *TGF-β* is not able to downregulate c-Myc and ID proteins (Sheen et al., 2013). The down-regulations of *ID1*were observed across all the time-points of extract-treated HepG2 compared with time-points of untreated HepG2 in this study (Table 4.10; Figure 4.8). This may suggest that the extract suppressed the growth of HepG2.

High expression of thrombospondin 1 (*THBS1*) is associated with tumour invasiveness and progression in HCC. It is believed that *THBS1* is a proangiogenic factor that stimulates angiogenesis in HCC (Poon et al., 2004). In this study, fold-change of gene expression at a time-point 6, 12 and 18 hours of

treated samples is less than untreated samples', while time-point 24 and 48 hours of treated samples exhibit higher fold-change compared with untreated samples'. This may suggest that suppression effect of extract was more effective for shorter intervals in the study (Table 4.10; Figure 4.8).

Study showed that follistatin (*FST*) is overexpressed in rodent liver tumours (Rossmanith et al., 2002) . The downregulations of FST across all the time-points of extract-treated HepG2 compared with time-points of untreated HepG2 in this experiment may indicate the suppression of HepG2 by the extract (Table 4.10; Figure 4.8).

Activin A type I receptor gene (*ACVR1*) plays an essential role in the development of cancer. Increased expression of *ACVR1*, along with its downstream genes like *IL-8*, was associated with shorter survival in HCC cases (Li et al., 2015). The down-regulations of ACVR1 were observed across all the time-points of extract-treated HepG2 compared with time-points of untreated HepG2 in this study (Table 4.10; Figure 4.8). This may suggest that the extract suppressed the growth of HepG2.

5.2.7 ErbB Signalling Pathway

Erythroblastic Leukemia Viral Oncogene Homolog (ErbB) or EGF Epidermal Growth Factor (EGF) family of transmembrane Receptor Tyrosine Kinases (RTKs) plays an important role during the growth and development of

a number of organs. They stimulate cell growth, proliferation, survival and differentiation. The ErbB family of proteins contains four receptor tyrosine kinases: namely EGFR/ErbB1, ErbB2/HER2, ErbB3/HER3 and ErbB4/HER4. They are structurally related to the epidermal growth factor receptor (EGFR) in which EGFR is its first discovered member. They play a well-established role in various types of cancer while ErbB2 is the most well-studied and mutated in many epithelial tumours (Hynes and MacDonald, 2009).

The ErbB pathway is also believed to have contributed to the occurrence of inflammation (Appendix C-7). The development of HCC is associated with persistent and chronic liver inflammation. Inflammatory cytokines and their receptors play vital roles in the development and progression of HCC. Besides ErbB pathway, they also activate other signalling pathways, including mitogen activated protein kinase (MAPK) and PI3K pathways, which in turn stimulate cellular responses such as survival, proliferation, and migration (Bischoff et al., 2015).

Increased levels of ErbB1 and ErbB3 expression are found to be associated with more aggressive tumours, including the poorly differentiated HCC (Berasain et al., 2007).*AREG, EREG* are part of the EGFR family. They were significantly down-regulated across all the time-points of extract-treated HepG2 compared with time-points of untreated HepG2 in this study (Table 4.11; Figure 4.9). This may suggest that extract promotes the apoptosis of HepG2.

5.2.8 Notch Signalling Pathway

There are four membrane receptors (Notch1-4) in Notch signalling and are activated by their binding to three Delta-like ligands (Dll1, Dll3, and Dll4), and two ligands of the Jagged family (Jag1 and Jag2). Direct cell-cell contact is a pre-requisite for the activation of Notch signalling (Appendix C-8).

Seven key signal transduction pathways that control cell communication during animal development have been identified: WNT, TGF-β, Hedgehog (Hh), RTK, nuclear receptor, JAK/STAT, and Notch signalling. Intriguingly, Notch is the only pathway that relies on cell-cell contact (Guo et al., 2014). Ligand binding activates Notch through proteolysis and endocytosis of the receptor. Notch receptors interact with ligands on a neighbouring cell, which lead to Notch intracellular domain before entering the nucleus and activating the transcription of target genes (Gordon et al., 2008; Fortini, 2009).

Notch signalling is frequently dysregulated and overactivated across many cancers, including breast cancer, medulloblastoma, colorectal cancer, non-small cell lung carcinoma (NSCLC), melanoma, and T-cell acute lymphoblastic leukaemia (T-ALL). It leads to poorer prognosis for patients. Recent studies show that Notch signalling increases tumour cell proliferation, maintains a significant cancer stem-cell pool, induces epithelial-mesenchymal transition (EMT) and promotes chemo-resistance (Capaccione and Pine, 2013; Ranganathan et al., 2011)

Tumours grow due to aberrantly overexpressed Notch Ligand, such as *JAG1* and defective inhibitors, such as *FBXW7, NUMB,* or *DELTEX*(Strazzabosco and Fabris, 2012). In the study done by Huntzicker et al. (2015) also shows similar results. The inhibition of *NOTCH2* and *JAG1* reduces tumour burden by eliminating highly malignant HCC-like and cholangiocarcinoma-like tumours. This comes to a consistent conclusion that *JAG1* plays important role in the development of HCC (Huntzicker et al. 2015). The down-regulations of the *JAG1* were observed across all the time-points of extract-treated HepG2 compared with time-points of untreated HepG2 (Table 4.12; Figure 4.10). This may suggest that the extract inhibited the proliferation of HepG2.

The downstream target gene of Notch signalling, *HES1*, was significantly overexpressed in HCC-like nodules and tumours (Villanueva et al., 2012; Huntzicker et al., 2015). Different phase of clinical trial for cancer treatment targeting *HES1* has been carried out (Morell and Strazzabosco, 2014).The down-regulations of *HES1* were observed across all the time-points of extract-treated HepG2 compared with time-points of untreated HepG2 in this study (Table 4.11; Figure 4.9). This may suggest that the extract promoted differentiation and inhibited tumorigenesis of HepG2 cell.

5.2.9 VEGF Signalling Pathway

The production of VEGF is stimulated by upstream activators, including environmental cues, growth factors, oncogenes, cytokines, and hormones. The binding of VEGF to its receptors on the surface of endothelial cells activates

intracellular tyrosine kinases, triggering multiple downstream signals that promote angiogenesis (Appendix C-9).

Expression of *VEGF* was observed in the HCC tumour and occludin disassembly in the normal liver parenchyma next to the tumour and it steadily increases with the progression of the hepatocarcinogenic process from a normal liver, to a dysplastic nodule, to HCC (Yamaguchi et al., 1998;Schmitt et al., 2004; Wu and Li, 2012b). In addition to its known angiogenic properties, studies suggest that *VEGF* may promote HCC spreading into the normal liver parenchyma. The VEGF pathway is clearly important for HCC pathogenesis, providing a cue for the development of *VEGF* antagonists for tumour therapy (Martin and Jiang, 2009). In this study, not much variation of expression of *VEGF* was observed (Table 4.13; Figure 4.11). This may suggest that the extract did not affect the expression level of *VEGF* in HepG2.

5.2.10 JAK-STAT Signalling Pathway

Janus associated kinase-signal transducer and activator of transcription (JAK-STAT) pathway regulates the transduction of extracellular signals from cytokines and growth factors (Appendix C-10). It is involved in proliferation, differentiation, migration, apoptosis, and cell survival.

The binding of IL-6 to its receptor, IL-6R, which leads to dimerization of gp130, initiates JAK-STAT signalling. IL-6 is a known type I cytokine produced by macrophages, endothelial cells and activated T cells. The binding complex then binds to JAK family before it phosphorylates and activates STAT3

and STAT1, which in turn regulate the downstream transcription factors(Heinrich et al., 2003; Furqan et al., 2013).

Overexpression of *IL-6* has been observed in many cancers, including breast, renal cell, colon, prostate, bladder and B-cell malignancies, especially myeloma and HCC. Elevated serum levels of IL-6 are related to poorer prognosis in all these tumour types. Secretion of high level IL-6 may serve as an autocrine growth factor for cancer cell to survive. It is believed as a potent inducer of both RAS and JAK-STAT pathways which are universally activated in human HCC (Trikha et al., 2003; Calvisi et al., 2006). *IL-6*, along with *TNF-α*, are identified as tumour promoting cytokines and work with latent transcription factors such as *STAT3* and *NF-κB* (Stauffer et al., 2012). *NF-κB* has been known as intracellular signalling effector for many proinflammatory cytokines. It has been implicated in the development of cancer and activated by the underlying inflammation during malignant progression. Studies show that *STAT3* and *NF-kB* are strongly linked to HCC development, in which *STAT3* is activated by the upregulated *IL-6*. STAT3-positive HCC tumour tend to be more aggressive (He and Karin, 2011). Corticosteroids are effective agents against myeloma due to its effective inhibition on IL-6. Effort of developing IL-6 ligand-binding antibodies and IL-6R blocking antibodies has proven positive. The growth of tumour is inhibited by using these antibodies alone or in combination with cytotoxic chemotherapies (Lee and Margolin, 2011; Sansone and Bromberg, 2012). The significant down-regulations of *IL-6R* were observed across all the time-points of extract-treated HepG2 compared with time-points of untreated

HepG2 (Table 4.14; Figure 4.12). This may suggest that extract induced apoptosis of HepG2.

IL11 is overexpressed in inflammatory HCC. It is released from dying hepatocytes to facilitate its proliferation to neighbouring cells by inducing STAT3 pathway (Ernst and Putoczki, 2014).The overexpression of *IL-11*and *IL-6* is observed in tumour epithelial cell. It correlates with staging of tumour (Necula et al., 2012). Along with *OSM* and *IL-6, LIF* was upregulated in higher grade prostatic carcinoma (Richards, 2013). The significant down-regulations of *IL-11*and *LIF* were observed across all the time-points of extract-treated HepG2 compared with time-points of untreated HepG2 in this study (Table 4.14; Figure 4.12). This may suggest that extract effectively inhibited the survival and proliferation of HepG2.

Overexpression of *PIM1*, proto-oncogenic protein, could be observed in tumour. When it is overexpressed, it inhibits apoptosis, promotes cell proliferation and genomic instability. However, its expression in normal tissues is nearly undetectable (Magnuson et al., 2010). *PIM1* expression was induced through downstream effectors or cytokines such as IL-6, IL-3, GM-CSF, and G-CSF. *PIM1* expression is not only regulated at the transcriptional, but also at the post-transcriptional, translational and post-translational levels (Brault et al., 2010). The significant down-regulations of *PIM1* were observed across all the time-points of extract-treated HepG2 compared with time-points of untreated HepG2 (Table 4.14; Figure 4.12). This may suggest that extract inhibited tumorigenesis of HepG2 cells.

Sprouty proteins are important modulators of MAPK/ERK pathway and mediate a crosstalk among different signalling pathways for a coordinated cellular response. *SPRY2*, sprouty protein, was among the genes found to be downregulated in HCC compared with non-tumour liver. However, *SPRY1* was found significantly upregulated and *SPRY4* was found significantly downregulated compared with non-tumour tissues (Fong et al., 2006; Masoumi-Moghaddam et al., 2014). The significant down-regulations of SPRY4 were observed across all the time-points of extract-treated HepG2 compared with time-points of untreated HepG2 (Table 4.14; Figure 4.12). This may suggest that stimulation of MAPK and the promotion of survival of HepG2 cells by the extract. However, the extract did not affect the expression level of SPRY1 at all timepoints. This may indicate that the extract may not induce the growth of HepG2 cells.

5.2.11 WNT Signalling Pathway

Besides RAS/RAF/MEK/ERK pathway, PI3K/AKT/mTOR pathway, JNK pathway and NF-κB pathway, WNT signalling pathway has been identified as one of oncogenic pathways being responsible for initiating and sustaining HCC (Fatima et al., 2011).

There are three different pathways for WNT receptor activation, including canonical Wnt/β-catenin cascade, noncanonical planar cell polarity (PCP) pathway, and Wnt/Ca2+ pathway (Appendix C-11). However, Wnt/β-catenin signalling is more broadly studied compared with the others.

The Wnt/β-catenin signalling plays important roles in the development of most organ systems, especially the liver. Canonical Wnt/β-catenin signalling pathway works through its formation of three distinct protein complexes: the ligand-receptor complex, the β-catenin destruction complex, and the β-catenin/TCF transcription complex (Takigawa and Brown, 2008).

In the absence of Wnt ligands, β-catenin is continually degraded in the cytoplasm. The pathway is only activated when a Wnt ligand binds to the one of the members of extracellular frizzled (FZD) receptor and its co-receptor low-density lipoprotein receptor-related protein 5 or 6 (LRP5/6), leading to the phosphorylation of LRP5/6 with the protein dishevelled (DVL) and recruitment of axin and GSK3β to the receptor, which in turn disrupts the formation of the β-catenin destruction complex. This allows non-phosphorylated β-catenin to be accumulated and transported to the nucleus before forming complexes with the TCF/LEF transcription factors and activating *WNT* target genes, such *c-Myc* and cyclin D1 which are implicated in cell proliferation, anti-apoptosis, and angiogenesis (Giles et al., 2003; Clevers, 2006; Gordon and Nusse, 2006; Fatima et al., 2011).

Besides *c-Myc* and cyclin D1, there are other oncogenes involved in this pathway, such as conductin (*AXIN2*), matrix metalloproteinase-7 (*MMP-7*), FRA-1 (*FOSL1*), *JUN, uPAR*, and immunoglobulin transcription factor-2 (*ITF-2*) (Giles et al., 2003). The significant down-regulations of *FOSL1* was observed across all the time-points of extract-treated HepG2 compared with time-points

of untreated HepG2 (Table 4.15; Figure 4.13). This may suggest that the extract suppressed the growth of HepG2.

Accumulated β-catenin is seen in gastrointestinal and liver cancers and 50-70 % of HCC has high levels of β-catenin in the cytoplasm and in the nucleus. It is believed that the TGFβ-mediated loss of E-cadherin results in the release of β-catenin from cell-cell contacts and both contribute to the modulation of HCC (Nejak-Bowen and Monga, 2008). Overexpression of *c-Myc* and cyclin D1 in HCC, along with high level of β-catenin, has a poor prognosis(Fatima et al., 2011). In some studies, *FZD* has been found consistently overexpressed in several mouse models of HCC.*DKK1*, an inhibitor of canonical Wnt signalling, is under-expressed in HCC. It binds specifically to *LRP5/6* and stops Wnt-mediated signal transduction (Takigawa and Brown, 2008). There were not many variations (< 2) in the expression of *β-catenin, c-Myc, FZD, DVL* and *DKK1* across all time-points in this study. This may suggest that the extract maintained the level of these proteins while suppressing the level of *FOSL1*, *LRP5* and *WNT11*.

5.2.12 Toll-like Receptor Signalling Pathway

There are four main groups of pattern recognition receptors identified: Toll-like receptors (TLR), NOD-like receptors (NLR), RIG-I-like receptors and C-type lectin receptors. Studies have shown that infectious agents could cause human cancer. These agents could be recognized by pattern recognition receptors (PRR), including TLRs and NODs. This suggests that TLRs and NODs play a major role in the immune response against biological carcinogens.

Together with other PRRs, TLR initiates both pathogen-specific and cell type-specific host immune responses to fight infections. Interleukin-1β (IL-1β) is a pro-inflammatory cytokine playing major role in innate and adaptive immunity. Being the earliest cytokines released in the early stage of inflammation, it regulates the activation of inflammation by inducing other cytokines, such as IL-6, TNF-α, and IL-1α to be released. IL-1β is commonly overexpressed in many tumours and used as a potential prognosis indicator for cancer patients. The inflammatory response triggered by an infection is part of normal host defence to kill the pathogens. However, these pathogens get around host immunity and cause consistent infections leading to chronic inflammation. The chronic inflammation is characterized by the continued expression of cytokines and the recruitment of immune cells to the organs. It is one of the key environmental risk factors associated with cancers (Kutikhin and Yuzhalin, 2012).

Inflammatory microenvironment constitutes one of the important elements of all tumours. It involves innate immune cells and adaptive immune cells on top of cancer cell and its surrounding stroma. Innate immune cells are mainly made up of macrophages, neutrophils and NK cells while adaptive immune cells are made up of T and B lymphocytes. This microenvironment provides important cytokines, chemokines, growth factors and others which contribute to the growth of cancer cells. TLRs are involved in sensing endogenous danger signals by invading microorganism and initiate early innate immune response to these invading pathogens. There were the first PRR identified before PRRs other than TLRs were identified to be also involved in pathogen-associated molecular patterns (PAMPs) recognition. PAMPs include

various bacterial cell wall components such as lipopolysaccharide (LPS), peptidoglycan (PGN), lipopeptides, flagellin, as well as bacterial DNA, single-stranded (ss) RNA and double-stranded (ds) RNA. There are more than ten TLRs identified in human to detect various PAMPs derived from viruses, bacteria, mycobacteria, fungi and parasites. This list of TLRs will get longer (Akira et al., 2006).

Upon recognition of PAMPs, TLRs recruit appropriate adaptor molecules for one of its two distinct pathways: a MyD88-dependent pathway, which is used by all TLRs with the exception of TLR3, leading to the production of inflammatory cytokines through NF-κB and MAPK activation, or a MyD88-independent pathway associated with the stimulation of IFN-β and the maturation of dendritic cells (Appendix C-12). As a result, neutrophils are recruited and macrophages are activated for the killing of the infected pathogens (Kawai and Akira, 2011).

Downstream genes of MyD88-dependent pathway include transcription factor AP-1 (*JUN), IL-6, IL-8*, interferon-α (*IFN-α*). IL-8 is a chemokine produced by macrophages and mostly present at epithelial and endothelial cells. It transactivates EGFR, promoting the downstream activation of MAPK signalling, which is involved in cell proliferation and cell survival (Waugh and Wilson, 2008). Studies show that expression of IL-8 and MyD88 correlates with the angiogenesis, tumorigenicity and metastasis of tumours. Patients with high plasma IL-8 and MyD88 have a poor prognosis and higher recurrence rate(Liang et al., 2013;Lu et al., 2015).

Cancer growth is believed to be driven by a population of tumour-initiating cells (TICs), type of stem-like cells. Studies show that TIC population derived from HCC is characterized by membrane expression of CD133, in which upregulated expression of IL-8 in CD133 liver TICs is observed. It induces tumour angiogenesis, and initiates tumours (Tang et al., 2012). The significant down-regulations of IL-8 were observed across all the time-points of extract-treated HepG2 compared with time-points of untreated HepG2. No much fold-change variation (< 2) in the expression of MyD88, together with down-regulation of IL-8, may suggest that the extract suppressed proliferation of HepG2. The up-regulation of the MAP2K6 also showed the effect of the extract in the suppression of proliferation of HepG2 (Table 4.16; Figure 4.14).

5.2.13 NOD-like Receptor Signalling Pathway

Recent studies show that NOD-like receptors (NLRs) have been involved in infections, cancer, autoimmune disease and inflammatory disorders. Among infection-related neoplasms, gastric cancer, hepatocellular carcinoma (HCC), and cervical cancer are more prevalent. Persistent infection of *Helicobacter pylori* in the stomach, HBC and HCV in the liver, and human papilloma virus in cervix uteri of women are linked to them, respectively. Researches show that inflammation caused by bacteria and viruses increases cancer risk (de Martel and Franceschi, 2009).

Like TLRs, upon activation, NLRs, by interacting with receptor-interacting protein 2 (RIP2), activate the downstream pathways, NF-κB and

MAPK signalling which are common pathways for cancers (Di Virgilio, 2013) (Appendix C-13). RIP2 is needed to produce pro-inflammatory and anti-microbial molecules. It recruits TGFβ-activated kinase1 (TAK1) before forming protein complexes which in turn activate the target genes in NF-κB and MAPK pathways (Saxena and Yeretssian, 2014). However, this result is contradicting with other murine studies by Zhang and Chin (2014), larger orthotopic bladder tumours developed in the absence of RIP2 while tumour metastases in both the lung and kidneys were observed. In this study, down-regulations of RIP2 were observed across all the time-points of extract-treated HepG2 compared with time-points of untreated HepG2 (Table 4.17; Figure 4.15).

High level expression of NAIP has been reported in prostate cancer cell line, breast cancer patients and bone marrow of AML (Mazrouei et al., 2012). However, there is no study related to NAIP on HCC. In this study, up-regulations of NAIP were observed across all the time-points of extract-treated HepG2 compared with time-points of untreated HepG2 (Table 4.17; Figure 4.15).

5.2.14 RIG-I-like Receptor Signalling Pathway

While there is increasing number of research to investigate the association of TLRs and NLRs with the progression of cancer, the research analysing the correlation between RIG-I like receptor (RLR) and cancer is scarce. This happens to the research of C-type lectin receptor too.

RIG-I is one of the sensors for host recognition of RNA virus infection. Upon activation, it triggers downstream signalling and induce type I IFN

production (Appendix C-14). So far the studies showed contradictory in results on the association of RLR with cancers as well as other diseases (Chistiakov, 2010; Kutikhin and Yuzhalin, 2012).

However, significant down-regulation of IL-8 in this pathway may suggest that extract trigger the apoptosis of the HepG2. It is interesting to note the crosstalk of P38 in Toll-like, NOD-like and RIG-like pathways. As discussed, down-regulation of P38 may promote the proliferation of HepG2 (Table 4.18; Figure 4.16).

5.2.15 Chemokine Signalling Pathway

Chemokines are involved in innate and adaptive immunity. The innate immune response is mediated by neutrophils, monocytes, dendritic cells (DC) and natural killer (NK) cells while naïve and memory CD4 and CD8 cells and immature DCs are involved in the adaptive immune response. Chemokines have been implicated in chronic inflammation, tumorigenesis and metastasis, as well as autoimmune diseases (Raman et al., 2011) (Appendix C-15).

According to the presence of its cysteine residues in conserved locations, chemokines and their receptors are divided into four families: namely CXC, CC, CX3C and C, where C represents the cysteine and X represents non-cysteine amino acids (Zlotnik and Yoshie, 2000). Approximately 20 chemokine receptors and 50 chemokines have been identified in humans (Sarvaiya et al., 2013).

The expression of chemokines and their receptors is significantly changed in various cancers. In studies related to the expression profiles of various chemokines and their receptors in tumour and its neighbouring tissues from HCC patients, all kinds of chemokines are found to express in both normal liver and HCC tissues. However, CCL20 has been the only chemokine showing significant upregulation in HCC tissues. Further analysis also showed that in CCL20 has higher expression in grade III HCC tumour tissues in comparison to grade II tumours HCC tumour tissues (Rubie et al., 2006). This suggests that the CCL20/CCR6 system is implicated in hepatocarcinogenesis. Observation by Chen et al. (2011) showed CCR6/CCL20 has elevated expression in HCC tumour tissues. Studies also showed CCR6 has been involved in intra-hepatic metastasis of HCC and used as potential prognostic factors for HCC (Huang and Geng, 2010). In this study, the significant down-regulations of CCL20 and CCR6 were observed across all the time-points of extract-treated HepG2 compared with time-points of untreated HepG2 (Table 4.19; Figure 4.17). This may suggest that the extract exhibit inhibitory effect on the hepatocarcinogenesis of HepG2.

G protein-coupled receptors (GPCRs) are the families of membrane receptors playing vital role in cellular differentiation and proliferation. Its kinases (GRKs), together with the β-arrestin (ARRB) used as scaffolds, are involved in the desensitization process of GPCRs. The GPCR- β-arrestins complex in turn activates the downstream signalling, including ERK1/2, PI3K-AKT, NF-kB pathways, which are implicated in HCC. (Vroon et al., 2006; Sobolesky and Moussa, 2013).

β-arrestins (ARRB) regulate processes in cancer cell migration, invasion and metastasis.High level of ARRB is observed in advanced stage of breast cancer tissues compared to early stage disease. In another study, ARRB1 is overexpressed in HCC, NSCLC tumour and their para-cancerous tissues (Bagnato et al., 2005; Sobolesky and Moussa, 2013; Yang et al., 2015). The down-regulations of *ARRB2* were observed across all the time-points of extract-treated HepG2 compared with time-points of untreated HepG2 (Table 4.19; Figure 4.17). Combining the effect of the significant down-regulations of*BCAR1* and*PARD3,* which were also implicated in focal adhesion signalling pathway (5.2.21), and adherens junctions signalling pathway (5.2.20), it may significantly suppress invasion and migration of the HepG2 cells.

5.2.16 Cytokine-Cytokine Receptor Interaction Signalling Pathway

Cytokines are released in response to cellular stresses, including infection or inflammation (Appendix C-16). They are the important proteins, allowing the immune cells of the innate immune response and adaptive immune response to communicate with each other to fight infections and other pathologies.

Common cytokines include chemokines, lymphokines, interleukins, interferons, tumour necrosis factor and others. Different names were derived from their functionality. For examples, cytokines with chemtactic activities is called chemokines while cytokines secreted by lymphocytes are called

lymphokine. Similarly, cytokines secreted by leukocyte are called interleukin, and cytokines secreted by monocytes is called monokine.

Excessive immune cell infiltration to the inflammation site leading to increased cytokine level could be seen if the inflammation persists. This inflammatory microenvironment allows stressed cells to release free radicals, such as reactive oxygen species (ROS) and nitric oxide (NO) reactive species which in turn cause further DNA damage leading to possible gene mutations. This host response to persistent higher cytokine expression has the impact on the formation and progression of the cancer. However, inflammation plays contradictory roles in tumour development. It promotes anti-tumour immune responses and also has the potential to support tumour growth and metastases (Kutikhin and Yuzhalin, 2012).

There are diverse groups of peptides and glycoproteins that are secreted by different hematopoietic cells, such as lymphocytes, monocytes, and granulocytes. Some are proinflammatory or anti-inflammatory. They mediate the intercellular signalling to regulate homeostasis of the immune system in a multifaceted and efficient manner. In order to function properly, cytokines must bind to specific extracellular receptors. Some cytokines have a dedicated receptor while others may have shared receptors (Schreiber and Walter, 2010).

In humans, *TNFRSF19 (TROY)* is mainly expressed in the brain and prostate while having low expression in other normal organs, including heart, lung, liver, thymus, uterus, skeletal muscle, spleen, colon, testis, kidney, and

peripheral blood lymphocytes. In various studies, it is highly expressed in glioblastoma specimens, colorectal cancer cell lines and carcinomas (Paulino et al., 2010; Schon et al., 2014). However, there is not much study of *TNFRSF19* in HCC. In this study, up-regulations of *TNFRSF19* were observed across all the time-points of extract-treated HepG2 compared with time-points of untreated HepG2 (Table 4.20; Figure 4.18).

Prolactin (PRL) is a multifunctional peptide hormone secreted by the anterior pituitary gland. In addition to its lactation, it regulates differentiation, proliferation. Its receptor (PRLR), part of the class 1 cytokine receptor family, is found in various human tissues, including liver, gastrointestinal tract, pancreas, and lung. The interaction of PRL and its receptor activates Janus kinase 2 (JAK2) which in turn promotes HCC proliferation. High level of PRL and PRLR is observed in HCC patients, predicting poor prognosis in these patients (Yeh et al., 2012). On the other hand, similar observation on its role is seen in the tumorigenesis of breast and prostate (Damiano et al., 2013). In this study, up-regulations of *PRLR* were observed across all the time-points of extract-treated HepG2 compared with time-points of untreated HepG2 (Table 4.20; Figure 4.18).

KIT is part of the PDGFR family with stem cell factor (SCF) as its ligand. SCF is encoded by the protooncogene *KIT* and involved in cellular proliferation and anti-apoptotic functions. It is found upregulated in various malignant tumours, including ovarian cancer, breast cancer, lung cancer, prostate cancer, leukaemia (Liu et al., 2009a). A significant amount of both *SCF* and *KIT* have

been found in the liver. This high amount could be related to its self-regenerating capability liver cells have. However, high expression of both is found implicated in the neoplastic processes in the liver. Their proliferative capability is mediated by *IL6. IL6* induced the production of SCF (Ren et al., 2008). In this study, up-regulations of *KIT* were observed across all the time-points of extract-treated HepG2 compared with time-points of untreated HepG2 (Table 4.20; Figure 4.18). It may indicate its stronger self-regenerating capability or progression of HepG2.

However, the significant down-regulation of *IL-8, IL-11, CCL20, IL-6R, LIF, ACVR1,* and *TNFSF10* were recorded in this study for this pathway and might suggest its suppression effect on HepG2.

5.2.17 B-cell Receptor Signalling Pathway

B cells provide first line of defence by producing antibodies and protection from invading pathogen or disease. CD22 is a B lymphocyte–specific phosphoglycoprotein and is highly expressed on the B cell surface. Besides its function as a cell adhesion molecule, CD22 also modulates signal transduction through the B-cell receptor (Appendix C-18).

CD22 is expressed on the malignant cells in more than 90 % of B lymphoid malignancies, including acute lymphoblastic leukaemia, non-Hodgkin lymphoma (Sapra et al., 2013). Similar to TCR, B cell receptor (BCR) induces the P13K, NF-kB, and AP1 signalling pathway. However, the mechanism of BCR on the liver cancer is less studied.

The down-regulations of *CD22* were observed across all the time-points of extract-treated HepG2 compared with time-points of untreated HepG2 (Table 4.22; Figure 4.20).

5.2.18 Apoptosis Signalling Pathway

Apoptosis is a controlled form of cell death. Normal cell going through regulated apoptotic cell death sees its chromatin condensed, membrane blebbed, and cell shrunk. It has its pivotal role in controlling irregular cell proliferation through either its extrinsic pathway or intrinsic pathway (Appendix C-19).

External pathway is mediated by death receptors on the cell membrane while internal pathway, associated with mitochondria, is initiated by the intracellular signals controlled by Bcl-2 family. Both pathways cause the activation of "initiator" caspases, which then activate "effector" caspases. The caspase cascade can be activated upon death receptor triggering. Caspases are cysteine-dependent, aspartate-specific proteases and are regulated at a posttranslational level which ensures that they can be rapidly activated (Falschlehner et al., 2007). TNFSF10 or TNF-related apoptosis inducing ligand (TRAIL), tumour necrosis factor α (TNFα) and FAS ligand are the ligand involved in the initiation of the external pathway.

Tumour necrosis factor (TNF) and TNF receptor (TNFR) superfamily are involved cell survival, programmed cell death, inflammation, and

differentiation. It is a type II transmembrane protein related to the TNF superfamily. The cancer patients with higher TRAIL have a better prognosis (Liu et al., 2005). TRAIL is mainly found on the surface of natural killer cells (NK), cytotoxic T lymphocytes, macrophages and dendritic cells. The study found that human soluble TRAIL is present at extremely high levels in human colostrum. It is known that the first secretion from the mammary glands after giving birth is rich in antibodies. Antibodies acquired through colostrum at birth are critical to the health of new-born. TRAIL might have a significant role in mediating the anti-cancer activity of human milk (Davanzo et al., 2013).

TRAIL functions as a tumour suppressor and induce apoptosis in tumour cell without affecting normal cells. It is secreted by normal tissues as part of natural immune responses. It suppresses tumour metastasis (Kemter et al., 2005; Refaat et al., 2014). It is regulated by two death receptors, *TRAIL* receptors 1 and 2 (TRAIL-R1and TRAIL-R2), and two decoy receptors: TRAIL-R3and TRAIL-R4. TRAIL-Rs are also implicated in most human HCC (Fabregat et al., 2007). The significant up-regulations of *TRAIL* were observed across all the time-points of extract-treated HepG2 compared with time-points of untreated HepG2 (Table 4.23; Figure 4.21). This may suggest that extract inhibit the metastasis and promote differentiation of the HepG2 cells.

TRAIL signalling does not only lead to the activation of effector caspases and subsequent initiation of apoptosis, but also induce non-apoptotic pathways, involving the activation of NF-kB, AKT and MAPKs pathway (Falschlehner et al., 2007). Interleukin-1 receptor-associated kinases 2 (*IRAK2*) is known to induce NF-κB activation through various TLRs. Activation of *IRAK2*promotes

carcinogenesis. It plays an important role in inflammatory responses which are critical for elimination of viruses, bacteria, and cancer cells, as well as for wound healing. It can be initiated from Toll-like receptors (TLRs) or from the interleukin-1 family receptors (IL-1R) (Jain et al., 2014). The significant down-regulations of *IRAK2* were observed across all the time-points of extract-treated HepG2 compared with time-points of untreated HepG2 (Table 4.23; Figure 4.21). The upregulation of *TRAIL* and downregulation of *IRAK2* may suggest that the extract promotes the apoptosis of HepG2.

5.2.19 Adherens Junction Signalling Pathway

The adherens junction (AJ) provides adhesive contacts between neighbouring epithelial cells. It helps maintain tissue architecture and integrity. It also controls the cell motility and proliferation. As a classical cadherin family of Ca2+-dependent adhesion proteins, E-cadherin (*CDH1*) is an essential transmembrane protein, which initiates intercellular contacts in adherens junction. The binding of E-cadherin with the cytoplasmic catenin family members, including p120-catenin, β-catenin and α-catenin forms the actin cytoskeleton and regulate the signalling pathway (Appendix C-20). Major changes in the cytoskeleton structure or loss of cell-cell adhesion or change of expression level in these proteins indicates the disruption to the stability of the AJ (Meng and Takeichi, 2009).

Down-regulation of *CDH1* expression disrupts the structure of AJ and help tumour cell proliferate and metastasize to distal cells. Gain of expression of *CDH1* on cancer cell help restore the AJ and decrease proliferation of cancer cell

(Conacci-Sorrell et al., 2002). Various studies on the epithelial derived tumours, especially breast cancer, show that loss in *CDH1* and its catenin members are associated with the advanced stages and poor prognosis (Hartsock and Nelson, 2008). Normal hepatocyte junctions help regulate the flow of molecules and maintain cellular polarity. However, studies show that the hepatocyte junctions have been compromised for HCC. The level of AJ expression is significantly lower for the advanced stage of HCC (Cao et al., 2007; Wickline et al., 2013). The expressions of *CDH1* swung from low negative fold-change to significant positive fold-change in this study may indicate that hepatocyte junctions had been re-built and proliferation of HepG2 decreased (Table 4.24; Figure 4.22).

SNAIL (SNAI1) and *SLUG* (SNAI2) genes play important roles in cancer progression by suppressing the E-Cadherin and inducing the EMT, which results in the acquisition of an invasive, mesenchymal phenotype by epithelial cells. With its upregulation, it inhibits cell cycle and prevents cell death. However, the high level of β-catenin may impair E-cadherin expression. HCC show high level of β-catenin (Fabregat, 2009). The TGF-β family of signalling molecules has been involved in the upregulation of *SNAIL* and *SLUG* as well as in EMT. The dual roles of TGF-β in tumour suppression and tumour promotion just make this pathway highly complex (Dhasarathy et al., 2011). The significant downregulations of the *SLUG* across all the time-points of the treated HepG2 compared with time-points of untreated HepG2 (Table 4.24; Figure 4.22) indicate the proliferation of HepG2 was suppressed.

5.2.20 Focal Adhesion Signalling Pathway

Focal adhesion (FA) is a dynamic protein complexes through which the signalling events of interacting cell link to the ECM. The degradation of ECM is observed in cancer invasion and metastasis. Cell invasion is a driving force in malignant tumour diseases. Changes of contact of cell-cell and cell to ECM adhesions, including changes of adhesion strength among cells or detachment of cell from cytoskeletal structure, facilitate the invasion of cancer cells. It correlate to the malignancy of cancer (Mierke, 2008).FA is the important link between the actin cytoskeleton of the cell and its plasma membrane. This physical interaction allows cells to communicate with their external environment and trigger various responses, including cell attachment, migration, proliferation, differentiation, and death. The proteins of FA are consistently associating with or disassociating from it so that the signal is transmitted to different parts of the cell. Different components are involved in the formation of the FA, including scaffolding molecules, GTPases, and enzymes such as kinases, phosphatases, proteases, and lipases (Appendix C-21).

Focal adhesion kinase (FAK) is phosphorylated and coupled with some downstream effectors for various pathways for different responses. FAK overexpression results in increased cell motility and suppresses apoptosis. Multiple downstream signalling pathways, including PI3K/AKT and BCAR1/Rac-1, are identified to mediate FAK regulation of migration of various normal cells as well as invasion and metastasis of cancer cells (Wozniak et al., 2004).

The study showed that HCC samples with positive expression of *BCAR1* had worse pathohistological grades and TNM stages than samples with a negative expression of *BCAR1*. It leads to the activation of the Ras family GTPases, which plays a significant role in cancer progression. The patients with positive expression of *BCAR1* had higher chances to develop regional nodal metastasis and worse prognosis. The upregulation of *BCAR1* expression can loosen the contact of cell-cell or cell-ECM adhesion which in turn enhances cell migration from HCC. Furthermore, this type of *BCAR1* phenotype HCC coming with lower expression of E-cadherin and abnormal expression of β-catenin proliferate faster and provide poorer prognosis. Same observation derived from breast cancer samples, high level of *BCAR1* is positively correlated with the clinical stage of samples (Wozniak et al., 2004;Guo et al., 2008). The significant down-regulations of BCAR1 were observed across all the time-points of extract-treated HepG2 compared with time-points of untreated HepG2 (Table 4.25; Figure 4.23). This may suggest that the extract suppressed proliferation of HepG2.

ZYX is believed to have played an important role through its interaction with integrins at FA. *ZYX* suppression inhibits cell growth. It is recruited from cytoplasm to integrin-mediated focal complexes, which is converted into FA. *ZYX* is overexpressed in most of HCC cases. Similar observations are found in the melanoma samples (Sy et al., 2006). The significant down-regulations of ZYX were observed across all the time-points of extract-treated HepG2 compared with time-points of untreated HepG2 (Table 4.25; Figure 4.23). This may suggest that the extract suppressed proliferation of HepG2.

VASP promotes tumour growth by regulating focal adhesion dynamics within the tumour microenvironment (Tu et al., 2015). Studies showed that *VASP* proteins were found to be overexpressed in breast and colorectal cancers (Stevenson et al., 2012). The significant down-regulations of *VASP* were observed across all the time-points of extract-treated HepG2 compared with time-points of untreated HepG2 (Table 4.25; Figure 4.23). It may suggest that the extract suppressed proliferation of HepG2 in this pathway.

5.2.21 Natural Killer Cells Mediated Cytotoxicity Signalling Pathway

NK cells are known to provide a first line of defence against invading infectious microbes and tumour cells. Most of them locate at peripheral blood, lymph nodes, spleen, and bone marrow and migrate towards inflammation by chemoattractant. NK cells are unique compared with other immune cells. They can recognize stressed cells in the absence of antibodies and MHC before reacting promptly. Their role is critical because stressed cells without MHC 1 markers may skip the scrutiny by other immune cells, such as T lymphocyte cells, let alone the destruction of these stressed cells. Mature NK cells have large amounts of cytotoxic granules containing perforin and granzymes. Upon stimulation of cytokines, such as IL-2, IL-12, IL-15, IL-18, IL-21 and type I IFNs, NK cell transforms itself into lymphokine-activated killer (LAK) cells and form synapses with stressed cells and release the perforin and granzyme to lyse the stressed target. NK cells can initiate the transduction of death signals within target cells through death receptor/ligand ligation (Appendix C-22).

Clinical studies show that using the approaches of therapeutic cytokines via NK cells activate their differentiation and functions which in turn leads to a more efficient elimination of tumour growth (Cheng et al., 2013; Wang et al., 2015). *TRAIL* in NK cells, along with *FASL*, can trigger apoptosis in target cells (Ames et al., 2009).As discussed, the downregulations of *TRAIL* across all time points may indicate that the pathway was suppressed.

5.3 Cytotoxic effects of CCL on HepG2 and its Regulation on Selective Genes

Although not expressing fold-change>2 or <-2, some of genes did show relatively significant fold-change if the timepoints of treated samples were compared with untreated samples'. These genes, including *PI3KCA, EGFR, PARD3, LCK, NUMB, RICTOR, LRP5* and *JUN*, were studied due to its significant roles played in the progression of HCC.

PI3KCA is an oncogene of Phosphatidylinositol 3-kinase (PI3K) pathway, main effector pathways of *RAS, which* regulates cell growth, cell cycle entry, cell survival, cytoskeleton reorganization, and metabolism. In normal cells, the activity of PI3Ks is tightly regulated by internal signals, like phosphatase and tensin homolog (*PTEN*). *PI3KCA* triggers various signalling pathway which may lead to cell growth and proliferation (Jun et al., 1999; Engelman et al., 2006). This deregulation of the PI3K signalling pathway may lead to mutations of receptor tyrosine kinases (RTKs), such as *EGFR* and *HER2* which are positively associated with development in one-third of human cancers

(Thomas et al., 2007; Engelman, 2009; Liu et al., 2009b). In this study, *PI3KCA* is relatively down-regulated across all the time-points of extract-treated HepG2 compared with time-points of untreated HepG2 (Table 4.9; Figure 4.7). This may suggest that an extract has the suppressive effect on the HepG2.

JUN, AP-1 transcription factor, plays an active role in cell growth and proliferation. It is the major regulators of the proliferative and stress responses of mammalian cells leading to oncogenesis. It is downregulated in response to osmotic stress and its downregulation promotes apoptosis (Xia et al., 2007; Nakagawa and Maeda, 2012). The relatively down-regulating *JUN* were observed across all the time-points of extract-treated HepG2 compared with time-points of untreated HepG2 (Table 4.8; Figure 4.6). This may suggest that extract promoted apoptosis and suppressed the growth of HepG2.

EGF and *EGFR* were overexpressed in many cancers, such as breast, lung and liver cancers. Overexpression of *EGFR* has been observed in around 40-70 % of conventional HCC with poorer prognosis in most studies (Feitelson et al., 2004; Buckley et al., 2008). EGF could be produced by autocrine and paracrine from HCCs and overexpression of *EGF/EGFR* might be associated with poor prognosis of patients with HCC (Berasain et al., 2009). Studies done by Huang et al. (2014) provide evidence that *EGF* plays an initial role in the development of the inflammation and in the promotion of cancer cells from low metastatic potentials into high metastatic potential. The *EGFR* pathway has been possibly involved in an increasing number of inflammatory mediators and in extensive crosstalk with other signalling pathways. The banding of *EGF* and *EGFR* could trigger signal transduction cascade in various cancer pathways,

including ERK-PI3K-AKT pathway, the RAS/RAF/MEK /MAPK pathway and NF-κB pathway (Buckley et al., 2008). The relatively down-regulating of *EGFR* were observed across all the time-points of extract-treated HepG2 compared with time-points of untreated HepG2 (Table 4.11; Figure 4.9). It may indicate that the extract suppressed the proliferation of HepG2.

Partitioning defective 3 (*PARD3*) is a crucial component of partitioning-defective complex proteins in AJ. Besides controlling cell polarity, it helps in cell migration and facilitates cancer cell in EMT. EMT has been postulated to play an important role in cancer metastasis. The study shows that up-regulation of *PARD3* expression in primary tumours has poor five-year overall survival rates. It also shows its association with distant metastasis of cancer and poor survival rates in HCC patients. It could be a novel prognostic biomarker and therapeutic target for HCC (Jan et al., 2013). The relatively down-regulating of *PARD3* were observed across all the time-points of extract-treated HepG2 compared with time-points of untreated HepG2 (Table 4.24; Figure 4.22). It may indicate migration of HepG2 in EMT was disrupted.

LCK, down-stream Src family kinase, is activated after T-cell receptor (TCR) is bound by antigen presented in the major histocompatibility complex (MHC) and in turn phosphorylate ZAP-70, which activate the mitogen-activated protein kinases (MAPKs) pathway, including ERK, JNK and p38. *LCK* plays an essential role in the maturation of developing lymphoid cells. High expressions of *LCK* are found in metastatic cancers compared to their primary cancer (Choi et al., 2012).

T cell or T lymphocytes, both CD4+ T helper cells (Th) and CD8+ cytotoxic T cells, are involved in killing tumour cells. It is activated in response to pathogens via TCR (Appendix C-17). TCR stimulation triggers various pathways, which in turn activates their downstream effectors, including *JUN*, nuclear factor of activated T cells (*NFAT*) and *NF-κB*. The presence of T cell in cancer areas is correlated with a favourable prognosis in many cancers. Studies show the high expression of CD8+ in HCC provide positive prognosis while low expression of CD4+ contribute to the malignancy of the cirrhosis and HCC (Thompson et al., 2010).

Effector lymphocytes (CD4, cytotoxic CD8 cells) and regulatory T cells (Tregs) are found in low amount in the human liver. CD4+CD25+ Tregs, the most common Tregs, shut the immune response after invading antigens are eliminated. Tregs attenuate the inflammation of hepatitis by suppressing the CD4 and CD8. The presence of Tregs is positively correlated with disease severity. Higher expression of Tregs is observed in advanced stages of HCC compared with initial stages of HCC. Reduction of CD8 is noted in tumours while Tregs is highly expressed (Oo and Sakaguchi, 2013; Sachdeva et al., 2015).

Cellular signalling that is mediated by the Raf-1 and VEGF pathways have been implicated in the molecular pathogenesis of hepatocellular carcinoma(Llovet et al., 2008). Sorafenib acts by inhibiting VEGFRs and PDGFRs and reduces the phosphorylation of ZAP70 by inhibiting the

phosphorylation of *LCK*. By activating T-cell signalling, it inhibits the recruitment of ZAP70 and phosphorylation of *LCK* and *ITAM* (Zhao et al., 2008). In this study, relatively down-regulating LCK were observed across all the time-points of extract-treated HepG2 compared with time-points of untreated HepG2 (Table 4.21; Figure 4.19; Table 4.26; Figure 4.24). This may suggest that extract suppressed the growth of HepG2.

Relatively up-regulating *NUMB*, tumour inhibitor of NOTCH pathway, were observed across all the time-points of extract-treated HepG2 compared with time-points of untreated HepG2 (Strazzabosco and Fabris, 2012; Table 4.12; Figure 4.10). This may suggest that extract suppressed the growth of HepG2.

Together with *mTOR* and *PRR5/GβL, RICTOR* activates *AKT* and plays important role of mTOR pathway activation in human HCC (Villanueva et al., 2008). The relatively down-regulating *RICTOR* was observed across all the time-points of extract-treated HepG2 compared with time-points of untreated HepG2 (Table 4.9; Figure 4.7). This may suggest that extract may suppress the growth of the HepG2.

Lack of phosphorylation of *LRP5/6* with the protein dishevelled (*DVL*) in WNT pathway, WNT pathway is not activated (Giles et al., 2003; Clevers, 2006; Gordon and Nusse, 2006; Fatima et al., 2011). The relatively down-regulating *LRP5* of WNT pathway were observed across all the time-points of extract-treated HepG2 in this experiment may suggest that less downstream

oncogenes in WNT pathway were activated (Table 4.15; Figure 4.13). This, in turn, suppressed the proliferation of HepG2.

5.4 Properties of metabolites and their anti-tumour activities

In decades, attempts have been put in to categorize some anti-tumour components derived from plants or TCM herbs by their chemical structures. Many different types of phytochemicals have been derived from these natural products. The major groups of them include alkaloids, terpenes, phenolic compounds, steroids and their corresponding glycosides as well as saccharides (including polysaccharides), amino acids and peptides. The chemical structures of these reagents decide or affect their activities in various cancer pathways (Xia, et al., 2014). The high abundance of diterpenes and sesquiterpenes in bark-PE extract may indicate that they may play a significant role in inhibiting the growth or proliferation of HepG2 in this study.

The classification of terpenes depends on the number of isoprene units (C_5H_8) present in the skeleton of the product. It is the building block for various terpenes. Diterpenes ($C_{20}H_{32}$) are composed of four isoprene units. Dimerization of two isoprene units is called monoterpenes ($C_{10}H_{16}$). Having extra isoprene units sequentially, sesquiterpenes ($C_{15}H_{24}$), diterpenes ($C_{20}H_{32}$), sesterterpenes ($C_{25}H_{40}$), triterpenes ($C_{30}H_{48}$) and tetraterpenes ($C_{40}H_{64}$) are formed respectively although their biosynthetic routes of forming are different (Lanzotti, 2013).

Terpenoids is one of the largest group of natural products, with 40,000 individual compounds identified. Besides its anti-microbial, anti-fungal, anti-

parasitic, antiviral, anti-allergenic, anti-spasmodic, anti-hyperglycemic, anti-inflammatory, and immunomodulatory properties, terpenoids have also exhibited its properties in inhibiting the growth of cancer cells. With the diverse array of terpenoid structures and functions, it is believed that terpenoids have a lot medical benefits which could be further explored (Thoppil & Bishayee, 2011).

Classified separately from terpenes, steroids, which are widely used in the cancer treatment, belong to the group of isoprenoids as they originate from triterpenes. During the process of the biosynthesis, its structure deviated from the isoprene units with loss of carbon or various chemical reactions. Therefore, they are classified separately from terpenes. Hundreds of steroids are widely found in plants, animals and fungi. All steroids are synthesized from lanosterol, a type of sterol in animal cells and fungi, or from cycloartenol in plants cells. Both lanosterol and cycloartenol are in turn synthesized from the triterpene squalene (Summons, et al., 2006).

Geranylgeraniol was found abundant in this plant extract. It is a diterpenoid which is an important molecule in the synthesis of various terpenes, including the acylation of proteins and the synthesis of retinol, retinal and phytol. They are critical for the formation of various vitamins, including vitamins A, E and K. Together with hexadecanoic acid, a saturated fatty acid, they showed anti-fungal and anti-microbial, anti-inflammatory functions (Nair et al., 1984; Karau et al., 2015). Research showed that sufficient production of diterpenes or diterpenoids in macrophages produced sizable pro-inflammatory cytokines for innate immune responses after detection of microbial infection(Kim et al., 2013).

Taxol, which is widely used as chemotherapy agents for various cancer treatment, including breast cancer, ovarian carcinoma, melanoma and lung cancer, is a diterpenoid with a taxadiene core (Rowinsky, 1997).

Studies showed that diterpenes exhibited their anti-tumour activities and led to the decrease in cell proliferation and DNA damage. Besides exhibiting anti-angiogenic and anti-inflammatory properties in epidemiological studies, they have also showed their anti-proliferation activities against a panel of tumour cell lines (Cardenas, et al., 2011). Their inhibitory effects on hepatocarcinogenesis by apoptosis were also observed (Yan, et al, 2014; Thoppil & Bishayee, 2011; Vergara, et al, 2014; Petiwala & Johnson, 2015). The diterpenoids induce apoptosis and inhibit invasion of cancer cells via various pathways, including PI3K/AKT pathway, MAPK pathway, NF-κB pathway, HIF-1α pathway, FAK pathway (Xia, et al., 2014).

Sesquiterpenes have played important role in the prevention and reduction of carcinogenesis by increasing the ROS as well as involving in inflammatory response. They sensitize tumour cells to conventional drug treatments (Chadwick, et al., 2013). Studies have showed that sesquiterpenes extracted from chamomile and wild ginger exhibited anti-cancer activity in HCC. They suppressed liver carcinogenesisand showed efficacy against HCC (Thoppil & Bishayee, 2011). These sesquiterpenes blocked proliferation and invasion of cancer cells via various pathways, including AKT/GSK3β pathway, mTOR pathway, SMAD3 pathway, SNAIL/E-cadherin pathway, Notch-1 pathway and JNK pathway (Xia, et al., 2014).

The presence of these diverse chemical compounds in the extract of CCL may indicate their role in inhibiting the growth and proliferation of HepG2. Previous studies may have exhibited the inhibitory effects of individual chemical compound on the carcinogenesis. However, the synergistic effects of these compounds on the suppression of carcinogenesis were not much studied. The richness of various terpenes in the extract may have showed the collective effects of these chemical compounds in inhibiting the proliferation of HepG2 by suppressing various cancer pathways as shown in the study.

CHAPTER 6

CONCLUSION

With the concentration of 20.41µg/ml, Bark-PE extract exhibited highest inhibitory rate on HepG2. It regulated genes of various pathways in different extent.

Its inhibitory effect on biological function of cells was obvious. NK cells mediated cytotoxicity pathway, adherens junction, focal adhesion, chemokine signalling are significantly suppressed. The downregulated *LCK, SOS1, PI3KCA* and upregulating *TRAIL* in NK cells mediated cytotoxicity pathway indicate its inhibitory effect against the progression of the cancer. The downregulated *BRAC1, ZYX, VASP, JUN, JUN-D, EGFR, SOS, PI3K, PARD3, SLUG,* and upregulated *CDH1*in adherens junction and focal adhesion shed the similar light. Chemokine acted as a chemoattractant to guide the migration of cells was seen down-regulated, which may indicate the inhibitory effects of the extract on chemokine pathway too. This is reflected from its downregulated *CCL20/CCR6, IL-6R, β-arrestins, SOS1, BRCA1, ARRB2, IL-8, JUN, PARD3, and PI3KCA.*

The inhibitory effect of extract was also observed in the pathways which are widely implicated in cancers, including WNT pathway, Notch pathway, mTOR pathway, ErbB pathway, and Apoptosis. *WNT, LRP5/6* and *FRA-1*, genes of WNT pathway are significantly down-regulated along with *JUN*. The significantly down-regulated *DDIT4,* along with *PI3KCA* and *RICTOR*, also indicate its inhibitory effects on mTOR pathway. The notably down-regulated

EGFR, AREG, EREG and *SOS1* of ErbB pathway, along with *PI3KCA and JUN*, also indicate the inhibitory effect of extract on the development of HepG2. The down-regulated *JAG1, HES1* and up-regulated *NUMB* in Notch pathway also indicates the inhibitory effect of extract on the migration of HepG2. Its obvious inhibitory effect was also observed in apoptosis pathway with its significant upregulated *TRAIL* and down-regulated *IRAK2*. B cell pathway was obviously suppressed with its *CD22*, along with *SOS1, LCK*, and *PI3KCA* down-regulated.

The genes for pathways related to pattern recognition receptors, including Toll-like receptors (TLR), Nod-like receptors (NLR), and RIG-I-like receptors have indicated the inhibitory effects of extract on their respective pathways. The up-regulated *MKK6* and down-regulated *IL8, IL-6R, JUN, PI3KCA* of these pathways has indicated the suppression effect of the extract. However, the suppression effect of these pattern recognition receptors is counteracted by the cross-talk of down-regulated *P38* of MAPK pathway. Low expression of *P38* is common in HCC. This counteracting effect of cross-talk by *P38* also was observed in VEGF pathway and T-cell pathway although down-regulated *SOS1, JUN, PI3K, LCK* of these pathways has exerted inhibitory effects on growth of HepG2.

MAPK pathway is considered favourably suppressed by CCL. Its genes, including *EGFR, SOS1, CACNA1H, JUN, JUN-D* are downregulated while *MKK6* is upregulated. However, MAPK cascades usually do not operate individually, but communicate with each other or with different signalling pathways, generating a wide network. Through its wide range of cross-talk

possibilities with other pathways, including Toll-like, Nod-like, Rig-1 receptor pathways, VEGF pathway, T-cell pathway, via specifically down-regulated P38, may withhold the suppression effect of the extract on these pathways.

Cross-talk effect was also observed in cell cycle. Upregulation of *SKP2, CDC 6, CDC7* and down-regulation of *CDKN2B* may be conducive to the growth of HCC. However, while the upregulation of *RBL1* and downregulation of *WEE1* and *CDC25B*would inhibit the progression of HCC. *CDKN2B* have showed the cross-talk effect on TGF-β pathway. The up-regulation of *RBL1* and down-regulation of *ID1, ACVR1, FST* of TGF-β pathway have indicated the suppression effects of extracts on this pathway. Inhibitory effect was observed in JAK-STATS pathway with its downregulated *IL11, IL6R, PIM1, LIF*. These genes, together with *ACVR1*, also exerted its inhibitory effects on cytokine-cytokine receptor interaction pathway although the up-regulation of *PRLR* may indicate otherwise. The inhibitory effect of down-regulated *WNT11* in Hedgehog pathway was counteracted by the up-regulated *SMO*. Significant downregulated of *PAI-1, CDKN1A* and up-regulated *SESN1, SESN3* indicated its inhibitory effect in P53 pathway.

The suppressive effect of the bark-PE extraction HepG2 is obviously observed in the experiment. Genes highly expressed in hepatocellular carcinoma (HCC) that were observed to be down-regulated in this study include *IL8, IL11, IL6R, CCL20, LIF, ACVR1, SOS1, BCAR1, VASP, ZYX, CD22, SLUG, IRAK2, FOSL1, WNT11, PIM1, LIF, JAG1, HES1, AREG, EREG, DDIT4, IDI, FST, ACVR1, JUND, WEE1, JUN, LCK, EGFR, PI3KCA, RICTOR,* and *PARD3* while

genes expressed low in HCC that were observed to be up-regulated significantly, include *MKK6, RBL1, TRAIL, and TNSRSF19*. However, some genes, including *P38, SKP2* and *SMO*, exhibited cross-talks with some of the pathways and counteract their inhibitory effect.

This finding is significant since it indicates that CCL has the inhibitory effect on the HepG2. This provides the scientific proof for interested communities to exploit further on its potential use clinically. The high abundance of diterpenes and sesquiterpenes was noted in bark-PE extract. This indicates that they are likely the potent inhibitors of liver cancer. It also paves the way for future studies in CCL, including, but not limited to, identification of active compounds of CCL as potent anti-HCC agent, expansion of experiment for broader range of cancer cell lines and clinical study using CCL on HCC subjects.

REFERENCES

Adjei, A.A., 2001. Blocking oncogenic Ras signaling for cancer therapy. *Journal of the National Cancer Institute*, 93 (14), pp. 1062-1074.

Aggarwal, B.B., Vijayalekshmi, R.V. and Sung, B., 2009. Targeting inflammatory pathways for prevention and therapy of cancer: short-term friend, long-term foe. *Clinical Cancer Research*, 15 (2), pp. 425-430.

Akao, Y., Nakagawa, Y., Iinuma, M. and Nozawa, Y., 2008. Anticancer effects of xanthones from pericarps of mangosteen. *International Journal of Molecular Sciences*, 9 (3), pp. 355-370.

Akira, S., Uematsu, S. and Takeuchi, O., 2006. Pathogen recognition and innate immunity. *Cell*, 124 (4), pp. 783-801.

American Association for Cancer Research. 2015. AACR Cancer Progress Report 2015. *Clinical Cancer Research*, 21 (1), pp. S1-S128.

Ames, E., Hallett, W.H. and Murphy, W.J., 2009. Sensitization of human breast cancer cells to natural killer cell-mediated cytotoxicity by proteasome inhibition. *Clinical and Experimental Immunology*, 155 (3), pp. 504-513.

Asaga, S., et al., 2006. Identification of a new breast cancer-related gene by restriction landmark genomic scanning. *Anticancer Research*, 26 (1a), pp. 35-42.

Auffray, C., Imbeaud, S., Roux-Rouquié, M. and Hood, L., 2003. From functional genomics to systems biology: concepts and practices. *Comptes Rendus Biologies*, 326 (10–11), pp. 879-892.

Bagnato, A., Spinella, F. and Rosano, L., 2005. Emerging role of the endothelin axis in ovarian tumor progression. *Endocrine-Related Cancer*, 12 (4), pp. 761-772.

Barrett, J.C., 1993. Mechanisms of multistep carcinogenesis and carcinogen risk assessment. *Environmental Health Perspectives*, 100, pp. 9-20.

Bennett, G.J., Harrison, L.J., Sia, G.-L. and Sim, K.-Y., 1993. Triterpenoids, tocotrienols and xanthones from the bark of Cratoxylum Cochinchinense. *Phytochemistry*, 32 (5), pp. 1245-1251.

Berasain, C., Castillo, J., Prieto, J. and Avila, M.A., 2007. New molecular targets for hepatocellular carcinoma: the ErbB signaling system. *Liver International*, 27 (2), pp. 174-185.

Berasain, C., et al., 2009. The epidermal growth factor receptor: a link between inflammation and liver cancer. *Experimental Biology and Medicine*, 234 (7), pp. 713-725.

Berasain, C., et al., 2011. Epidermal growth factor receptor (EGFR) crosstalks in liver cancer. *Cancers*, 3 (2), pp. 2444-2461.

Bischoff, A., et al., 2015. A global microRNA screen identifies regulators of the ErbB receptor signaling network. *Cell Communication and Signaling*, 13 (5), pp. 1-15.

Boonnak, N., et al., 2009. Anti-Pseudomonas aeruginosa xanthones from the resin and green fruits of Cratoxylum cochinchinense. *Tetrahedron*, 65 (15), pp. 3003-3013.

Brault, L., et al., 2010. PIM serine/threonine kinases in the pathogenesis and therapy of hematologic malignancies and solid cancers. *Haematologica*, 95 (6), pp. 1004-1015.

Bruix, J. et al., 2001. Clinical management of hepatocellular carcinoma. Conclusions of the Barcelona-2000. *Journal of Hepatology*, 35, pp. 421-443.

Buckley, A.F., Burgart, L.J., Sahai, V. and Kakar, S., 2008. Epidermal growth factor receptor expression and gene copy number in conventional hepatocellular carcinoma. *American Journal of Clinical Pathology*, 129 (2), pp. 245-251.

Budanov, A.V. and Karin, M., 2008. The p53-regulated Sestrin gene products inhibit mTOR signaling. *Cell*, 134 (3), pp. 451-460.

Buitrago-Molina, L.E., et al., 2013. The degree of liver injury determines the role of p21 in liver regeneration and hepatocarcinogenesis in mice. *Hepatology*, 58 (3), pp. 1143-1152.

Calvisi, D.F., et al., 2006. Ubiquitous activation of Ras and Jak/Stat pathways in human HCC. *Gastroenterology*, 130 (4), pp. 1117-1128.

Calvisi, D.F., et al., 2009. SKP2 and CKS1 promote degradation of cell cycle regulators and are associated with hepatocellular carcinoma prognosis. *Gastroenterology*, 137 (5), pp. 1816-1826.e10.

Cao, Y., Chang, H., Li, L., Cheng, R.C. and Fan, X.N., 2007. Alteration of adhesion molecule expression and cellular polarity in hepatocellular carcinoma. *Histopathology*, 51 (4), pp. 528-538.

Capaccione, K.M. and Pine, S.R., 2013. The Notch signaling pathway as a mediator of tumor survival. *Carcinogenesis*, 34 (7), pp. 1420-1430.

Capece, D., et al., 2013. The inflammatory microenvironment in hepatocellular carcinoma: a pivotal role for tumor-associated macrophages. *BioMed Research International*, 2013, pp. 15.

Cardenas, C., Quesada, A. & Medina, M., 2011. Anti-Angiogenic and Anti-Inflammatory Properties of Kahweol, a Coffee Diterpene. *PLoS ONE*, 6(8), p. e23407.

Carmeliet, P. and Jain, R.K., 2000. Angiogenesis in cancer and other diseases. *Nature*, 407 (6801), pp. 249-257.

Cervello, M., et al., 2012. Molecular mechanisms of Sorafenib action in liver cancer cells. *Cell Cycle*, 11 (15), pp. 2843-2855.

Chen, K.J., et al., 2011. Selective recruitment of regulatory T cell through CCR6-CCL20 in hepatocellular carcinoma fosters tumor progression and predicts poor prognosis. *PloS One*, 6 (9), pp. e24671.

Chen, X.L., et al., 2010. Hepatocellular carcinoma-associated protein markers investigated by MALDI-TOF MS. *Molecular Medicine Reports*, 3 (4), pp. 589-596.

Cheng, A.L., et al., 2009. Efficacy and safety of Sorafenib in patients in the Asia-Pacific region with advanced hepatocellular carcinoma: a phase III randomised, double-blind, placebo-controlled trial. *The Lancet Oncology*, 10 (1), pp. 25-34.

Cheng, M., Chen, Y., Xiao, W., Sun, R. and Tian, Z., 2013. NK cell-based immunotherapy for malignant diseases. *Cellular & Molecular Immunology*, 10 (3), pp. 230-252.

Chistiakov, D.A., 2010. Interferon induced with helicase C domain 1 (IFIH1) and virus-induced autoimmunity: a review. *Viral Immunology*, 23 (1), pp. 3-15.

Choi, D.S., et al., 2012. Quantitative proteomics of extracellular vesicles derived from human primary and metastatic colorectal cancer cells. *Journal of Extracellular Vesicles*, 1, pp. 18704.

Clevers, H., 2006. Wnt/beta-catenin signaling in development and disease. *Cell*, 127 (3), pp. 469-480.

Conacci-Sorrell, M., Zhurinsky, J. and Ben-Ze'ev, A., 2002. The cadherin-catenin adhesion system in signaling and cancer. *The Journal of Clinical Investigation*, 109 (8), pp. 987-991.

Czekay, R.P., et al., 2011. PAI-1: An integrator of cell signaling and migration. *International Journal of Cell Biology*, 2011, pp. 9.

Damiano, J.S., et al., 2013. Neutralization of prolactin receptor function by monoclonal antibody LFA102, a novel potential therapeutic for the treatment of breast cancer. *Molecular Cancer Therapeutics*, 12 (3), pp. 295-305.

Davanzo, R., et al., 2013. Human colostrum and breast milk contain high levels of TNF-related apoptosis-inducing ligand (TRAIL). *Journal of Human Lactation*, 29 (1), pp. 23-25.

de Martel, C. and Franceschi, S., 2009. Infections and cancer: established associations and new hypotheses. *Critical Reviews in Oncology/Hematology*, 70 (3), pp. 183-194.

Demirkan, B., 2013. The roles of epithelial-to-mesenchymal transition (EMT) and mesenchymal-to-epithelial transition (MET) in breast cancer bone metastasis: potential targets for prevention and treatment. *Journal of Clinical Medicine*, 2 (4), pp. 264-282.

Derynck, R., Akhurst, R.J. and Balmain, A., 2001. TGF-beta signaling in tumor suppression and cancer progression. *Nature Genetics*, 29 (2), pp. 117-129.

Dhasarathy, A., Phadke, D., Mav, D., Shah, R.R. and Wade, P.A., 2011. The transcription factors Snail and Slug activate the transforming growth factor-beta signaling pathway in breast cancer. *PloS One*, 6 (10), pp. e26514.

Dhiman, R.K. and Chawla, Y.K., 2005. Herbal medicines for liver diseases. *Digestive Diseases and Sciences*, 50 (10), pp. 1807-1812.

Di Virgilio, F., 2013. The therapeutic potential of modifying inflammasomes and NOD-like receptors. *Pharmacological Reviews*, 65 (3), pp. 872-905.

Dou, S.S., et al., 2008. System biology and its application in compound recipe of traditional Chinese medicine study. *World Science and Technology*, 10 (2), pp. 116-121.

Engelman, J.A., 2009. Targeting PI3K signalling in cancer: opportunities, challenges and limitations. *Nature Reviews Cancer*, 9 (8), pp. 550-562.

Engelman, J.A., Luo, J. and Cantley, L.C., 2006. The evolution of phosphatidylinositol 3-kinases as regulators of growth and metabolism. *Nature Reviews Genetics*, 7 (8), pp. 606-619.

Ernst, M. and Putoczki, T.L., 2014. Molecular pathways: IL11 as a tumor-promoting cytokine-translational implications for cancers. *Clinical Cancer Research*, 20 (22), pp. 5579-5588.

Fabregat, I., 2009. Dysregulation of apoptosis in hepatocellular carcinoma cells. *World Journal of Gastroenterology*, 15 (5), pp. 513-520.

Fabregat, I., Roncero, C. and Fernandez, M., 2007. Survival and apoptosis: a dysregulated balance in liver cancer. *Liver International*, 27 (2), pp. 155-162.

Falschlehner, C., Emmerich, C.H., Gerlach, B. and Walczak, H., 2007. TRAIL signalling: decisions between life and death. *The International Journal of Biochemistry & Cell Biology*, 39 (7-8), pp. 1462-1475.

Fatima, S., Lee, N.P. and Luk, J.M., 2011. Dickkopfs and Wnt/β-catenin signalling in liver cancer. *World Journal of Clinical Oncology*, 2 (8), pp. 311-325.

Feitelson, M.A., Pan, J. and Lian, Z., 2004. Early molecular and genetic determinants of primary liver malignancy. *The Surgical Clinics of North America*, 84 (2), pp. 339-354.

Ferlay, J., et al., 2013, *GLOBOCAN 2012 V1.0, Cancer incidence and mortality worldwide* [Online]. Available at: http://globocan.iarc.fr [Accessed: 13 November 2015].

Fong, C.W., et al., 2006. Sprouty 2, an inhibitor of mitogen-activated protein kinase signaling, is down-regulated in hepatocellular carcinoma. *Cancer Research*, 66 (4), pp. 2048-2058.

Fortini, M.E., 2009. Notch signaling: the core pathway and its posttranslational regulation. *Developmental Cell*, 16 (5), pp. 633-647.

Furqan, M., Mukhi, N., Lee, B. and Liu, D., 2013. Dysregulation of JAK-STAT pathway in hematological malignancies and JAK inhibitors for clinical application. *Biomarker Research*, 1, pp. 5.

Ge, S.L., 2008. *Anti-cancer bioactive compounds of Cratoxylum cochinchinense.* PhD thesis, Shenyang Pharmaceutical University, China.

Giannelli, G., Mazzocca, A., Fransvea, E., Lahn, M. and Antonaci, S., 2011. Inhibiting TGF-beta signaling in hepatocellular carcinoma. *Biochimica et Biophysica Acta*, 1815 (2), pp. 214-223.

Giles, R.H., van Es, J.H. and Clevers, H., 2003. Caught up in a Wnt storm: Wnt signaling in cancer. *Biochimica et Biophysica Acta*, 1653 (1), pp. 1-24.

Gordaliza, M., 2007. Natural products as leads to anticancer drugs. *Clinical & Translational Oncology*, 9 (12), pp. 767-776.

Gordon, M.D. and Nusse, R., 2006. Wnt signaling: multiple pathways, multiple receptors, and multiple transcription factors. *Journal of Biological Chemistry*, 281 (32), pp. 22429-22433.

Gordon, W.R., Arnett, K.L. and Blacklow, S.C., 2008. The molecular logic of Notch signaling--a structural and biochemical perspective. *Journal of Cell Science*, 121 (Pt 19), pp. 3109-3119.

Grigoriev, A., 2001. A relationship between gene expression and protein interactions on the proteome scale: analysis of the bacteriophage T7 and the yeast Saccharomyces cerevisiae. *Nucleic Acids Research*, 29 (17), pp. 3513-3519.

Grivennikov, S.I., Greten, F.R. and Karin, M., 2010. Immunity, inflammation, and cancer. *Cell*, 140 (6), pp. 883-899.

Gstaiger, M., et al., 2001. SKP2 is oncogenic and overexpressed in human cancers. *PNAS*, 98 (9), pp. 5043-5048.

Guo, C., Liu, Q.G., Yang, W., Zhang, Z.L. and Yao, Y.M., 2008. Relation among p130Cas, E-cadherin and beta-catenin expression, clinicopathologic significance and prognosis in human hepatocellular carcinoma. *Hepatobiliary & Pancreatic Diseases International*, 7 (5), pp. 490-496.

Guo, H., et al., 2014. Targeting the Notch signaling pathway in cancer therapeutics. *Thoracic Cancer*, 5 (6), pp. 473-486.

Gupta, S., Takebe, N. and LoRusso, P., 2010. Targeting the Hedgehog pathway in cancer. *Medical Oncology*, 2 (4), pp. 237-250.

Hamid, A.S., Tesfamariam, I.G., Zhang, Y. and Zhang, Z.G., 2013. Aflatoxin B1-induced hepatocellular carcinoma in developing countries: Geographical distribution, mechanism of action and prevention. *Oncology Letters*, 5 (4), pp. 1087-1092.

Hanahan, D. and Folkman, J., 1996. Patterns and emerging mechanisms of the angiogenic switch during tumorigenesis. *Cell*, 86 (3), pp. 353-364.

Hanahan, D. and Weinberg, R.A., 2011. Hallmarks of cancer: the next generation. *Cell*, 144 (5), pp. 646-674.

Harris, S.L. and Levine, A.J., 2005. The p53 pathway: positive and negative feedback loops. *Oncogene*, 24 (17), pp. 2899-2908.

Hartsock, A. and Nelson, W.J., 2008. Adherens and tight junctions: structure, function and connections to the actin cytoskeleton. *Biochimica et Biophysica Acta*, 1778 (3), pp. 660-669.

Hawkins, M.J., 1995. Clinical trials of antiangiogenic agents. *Current Opinion in Oncology*, 7 (1), pp. 90-93.

He, G. and Karin, M., 2011. NF-kappaB and STAT3 - key players in liver inflammation and cancer. *Cell Research*, 21 (1), pp. 159-168.

Heinrich, P.C., et al., 2003. Principles of interleukin (IL)-6-type cytokine signalling and its regulation. *The Biochemical Journal*, 374 (Pt 1), pp. 1-20.

Higgs, M.R., Lerat, H. and Pawlotsky, J.-M., 2010. Downregulation of Gadd45beta expression by hepatitis C virus leads to defective cell cycle arrest. *Cancer Research*, 70 (12), pp. 4901-4911.

Hiotis, S.P., et al., 2012. Hepatitis B vs. hepatitis C infection on viral hepatitis-associated hepatocellular carcinoma. *BMC Gastroenterology*, 12, pp. 64.

Ho, C.K., Huang, Y.L. and Chen, C.C., 2002. Garcinone E, a xanthone derivative, has potent cytotoxic effect against hepatocellular carcinoma cell lines. *Planta Medica*, 68 (11), pp. 975-979.

Hoang, T.H., Cam, T.I. and Ha, V.S., 2006. Study on the ethyl acetate extract of the leaves from Cratoxylum cochinchinese (Lour.) Blume. *Tap Chi Hoa Hoc*, 44 (1), pp. 71-75.

Hu, C. and Xu, G., 2014. Metabolomics and traditional Chinese medicine. *Trends in Analytical Chemistry*, 61, pp. 207-214.

Huang, F. and Geng, X.P., 2010. Chemokines and hepatocellular carcinoma. *World Journal of Gastroenterology*, 16 (15), pp. 1832-1836.

Huang, H., et al., 2005. SKP2 inhibits FOXO1 in tumor suppression through ubiquitin-mediated degradation. *PNAS*, 102 (5), pp. 1649-1654.

Huang, P., et al., 2014. The role of EGF-EGFR signalling pathway in hepatocellular carcinoma inflammatory microenvironment. *Journal of Cellular and Molecular Medicine*, 18 (2), pp. 218-230.

Huang, Y., Tong, S., Tai, A.W., Hussain, M. and Lok, A.S., 2011. Hepatitis B virus core promoter mutations contribute to hepatocarcinogenesis by deregulating SKP2 and its target, p21. *Gastroenterology*, 141 (4), pp. 1412-1421.

Huntzicker, E.G., et al., 2015. Differential effects of targeting Notch receptors in a mouse model of liver cancer. *Hepatology*, 61 (3), pp. 942-952.

Hynes, N.E. and MacDonald, G., 2009. ErbB receptors and signaling pathways in cancer. *Current Opinion in Cell Biology*, 21 (2), pp. 177-184.

Iwata, N., et al., 2000. Frequent hypermethylation of CpG islands and loss of expression of the 14-3-3 sigma gene in human hepatocellular carcinoma. *Oncogene*, 19 (46), pp. 5298-5302.

Iyoda, K., et al., 2003. Involvement of the p38 mitogen-activated protein kinase cascade in hepatocellular carcinoma. *Cancer*, 97 (12), pp. 3017-3026.

Jain, A., Kaczanowska, S. and Davila, E., 2014. IL-1 receptor-associated kinase signaling and its role in inflammation, cancer progression, and therapy resistance. *Frontiers in Immunology*, 5, pp. 553.

Jan, Y.J., et al., 2013. Expression of partitioning defective 3 (Par-3) for predicting extrahepatic metastasis and survival with hepatocellular carcinoma. *International Journal of Molecular Sciences*, 14 (1), pp. 1684-1697.

Jin, S.L., Wang, N.L., Zhang, X., Dai, Y. and Yao, X.S., 2009. Two new xanthones from the stems of Cratoxylum cochinchinense. *Journal of Asian Natural Products Research*, 11 (4), pp. 322-325.

Jin, S., et al., 2002. GADD45-induced cell cycle G2-M arrest associates with altered subcellular distribution of cyclin B1 and is independent of p38 kinase activity. *Oncogene*, 21 (57), pp. 8696-8704.

Jun, T., Gjoerup, O. and Roberts, T.M., 1999. Tangled webs: evidence of cross-talk between c-Raf-1 and Akt. *Science's STKE*, 1999 (13), pp. Pe1.

Kalra, N. and Kumar, V., 2006. The X protein of hepatitis B virus binds to the F box protein SKP2 and inhibits the ubiquitination and proteasomal degradation of c-Myc. *FEBS Letters*, 580 (2), pp. 431-436.

Karau, G.M., Njagi, E.N.M., Machocho, A.K., Wangai, L.N. and Nthinga, M.J., 2015. Chemical composition and *in vitro* antioxidant activities of *Ocimum americanum*. *Advances in Analytical Chemistry*, 5 (2), pp. 42-49.

Kaseb, A.O., 2013. *Hepatocellular carcinoma-future outlook*, 1st ed. Croatia: InTech.

Katoh, Y. and Katoh, M., 2008. Hedgehog signaling, epithelial-to-mesenchymal transition and miRNA (review). *International Journal of Molecular Medicine*, 22 (3), pp. 271-275.

Kawai, T. and Akira, S., 2011. Toll-like receptors and their crosstalk with other innate receptors in infection and immunity. *Immunity*, 34 (5), pp. 637-650.

Kemter, E., et al., 2005. Molecular cloning, expression analysis and assignment of the porcine tumor necrosis factor superfamily member 10 gene (TNFSF10) to SSC13q34-->q36 by fluorescence in situ hybridization and radiation hybrid mapping. *Cytogenetic and Genome Research*, 111 (1), pp. 74-78.

Kew, M.C., 2003. Synergistic interaction between aflatoxin B1 and hepatitis B virus in hepatocarcinogenesis. *Liver International*, 23 (6), pp. 405-409.

Kidger, A.M. and Keyse, S.M., 2016. The regulation of oncogenic Ras/ERK signalling by dual-specificity mitogen activated protein kinase phosphatases (MKPs). *Seminars in Cell & Developmental Biology*, 50, pp. 125-132.

Kim, J., et al., 2013. Sufficient production of geranylgeraniol is required to maintain endotoxin tolerance in macrophages. *Journal of Lipid Research*, 54 (12), pp. 3430-3437.

Kimball, S.R. and Jefferson, L.S., 2012. Induction of REDD1 gene expression in the liver in response to endoplasmic reticulum stress is mediated through a PERK, eIF2alpha phosphorylation, ATF4-dependent cascade. *Biochemical and Biophysical Research Communications*, 427 (3), pp. 485-489.

Kimman, M., Norman, R., Jan, S., Kingston, D. and Woodward, M., 2012. The burden of cancer in member countries of the Association of Southeast Asian Nations (ASEAN). *Asian Pacific Journal of Cancer Prevention*, 13 (2), pp. 411-420.

Kirikoshi, H., Sekihara, H. and Katoh, M., 2001. Molecular cloning and characterization of human WNT11. *International Journal of Molecular Medicine*, 8 (6), pp. 651-656.

Koltai, H. and Weingarten-Baror, C., 2008. Specificity of DNA microarray hybridization: characterization, effectors and approaches for data correction. *Nucleic Acids Research*, 36 (7), pp. 2395-2405.

Koul, H.K., Pal, M. and Koul, S., 2013. Role of p38 MAP kinase signal transduction in solid tumors. *Genes & Cancer*, 4 (9-10), pp. 342-359.

Kristjansdottir, K. and Rudolph, J., 2004. Cdc25 phosphatases and cancer. *Chemistry & Biology*, 11 (8), pp. 1043-1051.

Kutikhin, A.G. and Yuzhalin, A.E., 2012. C-type lectin receptors and RIG-I-like receptors: new points on the oncogenomics map. *Cancer Management and Research*, 4, pp. 39-53.

Lane, D. and Levine, A., 2010. p53 Research: the past thirty years and the next thirty years. *Cold Spring Harbor Perspectives in Biology*, 2 (12), pp. a000893.

Lanzotti, V., 2013. Diterpenes for Therapeutic Use. Natural Products. pp. 3173-3191 .

Laphookhieo, S., Syers, J.K., Kiattansakul, R. and Chantrapromma, K., 2006. Cytotoxic and antimalarial prenylated xanthones from Cratoxylum cochinchinense. *Chemical & Pharmaceutical Bulletin*, 54 (5), pp. 745-747.

Lappano, R. and Maggiolini, M., 2012. GPCRs and cancer. *Acta Pharmacologica Sinica*, 33 (3), pp. 351-362.

Law, B.K., 2005. Rapamycin: an anti-cancer immunosuppressant? *Critical Reviews in Oncology/Hematology*, 56 (1), pp. 47-60.

Lebrun, J.J., 2012. The dual role of TGF in human cancer: from tumor suppression to cancer metastasis. *ISRN Molecular Biology*, 2012, pp. 28.

Lee, J.H., Budanov, A.V. and Karin, M., 2013. Sestrins orchestrate cellular metabolism to attenuate aging. *Cell Metabolism*, 18 (6), pp. 792-801.

Lee, S. and Margolin, K., 2011. Cytokines in cancer immunotherapy. *Cancers*, 3 (4), pp. 3856-3893.

Lee, Y.H., et al., 2011. Abstract 1644: siRNA targeting of cell cycle kinase Wee1 inhibits hepatocullar carconima growth in vitro and in vivo. *Cancer Research*, 71 (8 Supplement), pp. 1644.

Li, L., et al., 2015. Regulatory MiR-148a-ACVR1/BMP circuit defines a cancer stem cell-like aggressive subtype of hepatocellular carcinoma. *Hepatology*, 61 (2), pp. 574-584.

Li, X. and Li, Y.H., 1990. Guttiferae. *Popularis Sin*, 50 (2), pp. 1-112.

Liang, B., et al., 2013. Myeloid differentiation factor 88 promotes growth and metastasis of human hepatocellular carcinoma. *Clinical Cancer Research*, 19 (11), pp. 2905-2916.

Lindon, J.C., Holmes, E. and Nicholson, J.K., 2007. Metabonomics in pharmaceutical R&D. *The FEBS Journal*, 274 (5), pp. 1140-1151.

Liu, C.C., et al., 2014. 14-3-3σ induces heat shock protein 70 expression in hepatocellular carcinoma. *BioMed Central Cancer*, 14 (425), pp. 1-11.

Liu, L., et al., 2009a. MEK1-independent activation of MAPK and MEK1-dependent activation of p70 S6 kinase by stem cell factor (SCF) in ovarian cancer cells. *Biochemical and Biophysical Research Communications*, 382 (2), pp. 385-389.

Liu, M.S., 2003. Conservation and utilization of tropical medicine resources of Hainan island. *Molecular Plant Breeding*, 1 (5), pp. 791-794.

Liu, P., Cheng, H., Roberts, T.M. and Zhao, J.J., 2009b. Targeting the phosphoinositide 3-kinase pathway in cancer. *Nature Reviews Drug Discovery*, 8 (8), pp. 627-644.

Liu, X.Y., et al., 2005. Effective gene-virotherapy for complete eradication of tumor mediated by the combination of TRAIL (TNFSF10) and plasminogen k5. *Molecular Therapy*, 11 (4), pp. 531-541.

Liu, Y., et al., 2015. Interaction of key pathways in Sorafenib-treated hepatocellular carcinoma based on a PCR-array. *International Journal of Clinical and Experimental Pathology*, 8 (3), pp. 3027-3035.

Liu, Y. and Wu, F., 2010. Global burden of aflatoxin-induced hepatocellular carcinoma: a risk assessment. *Environmental Health Perspectives*, 118 (6), pp. 818-824.

Llovet, J.M., et al., 2008. Sorafenib in advanced hepatocellular carcinoma. *The New England Journal of Medicine*, 359 (4), pp. 378-390.

Lodygin, D. and Hermeking, H., 2006. Epigenetic silencing of 14-3-3sigma in cancer. *Seminars in Cancer Biology*, 16 (3), pp. 214-224.

Lopez-Terrada, D., Cheung, S.W., Finegold, M.J. and Knowles, B.B., 2009. HepG2 is a hepatoblastoma-derived cell line. *Human Pathology*, 40 (10), pp. 1512-1515.

Lu, C.C., et al., 2015. Upregulation of TLRs and IL-6 as a marker in human colorectal cancer. *International Journal of Molecular Sciences*, 16 (1), pp. 159-177.

Luo, G.A., Wang, Y.M., Liang, Q.L., Xie, Y.Y. and Xue-Mei, F., 2011. System medicine and translational medicine. *Mode of Traditional Chinese Medicine Materia Medica*, 13 (1), pp. 1-8.

Luo, J., Solimini, N.L. and Elledge, S.J., 2009. Principles of cancer therapy: oncogene and non-oncogene addiction. *Cell*, 136 (5), pp. 823-837.

Magnuson, N.S., Wang, Z., Ding, G. and Reeves, R., 2010. Why target PIM1 for cancer diagnosis and treatment? *Future Oncology*, 6 (9), pp. 1461-1478.

Mahabusarakam, W., Nuangnaowarat, W. and Taylor, W.C., 2006. Xanthone derivatives from Cratoxylum cochinchinense roots. *Phytochemistry*, 67 (5), pp. 470-474.

Mans, D.R., da Rocha, A.B. and Schwartsmann, G., 2000. Anti-cancer drug discovery and development in Brazil: targeted plant collection as a rational strategy to acquire candidate anti-cancer compounds. *The Oncologist*, 5 (3), pp. 185-198.

Marhenke, S., et al., 2014. p21 promotes sustained liver regeneration and hepatocarcinogenesis in chronic cholestatic liver injury. *Gut*, 63 (9), pp. 1501-1512.

Martin, T.A. and Jiang, W.G., 2009. Loss of tight junction barrier function and its role in cancer metastasis. *Biochimica et Biophysica Acta*, 1788 (4), pp. 872-891.

Masaki, T., et al., 2003. Cyclins and cyclin-dependent kinases: comparative study of hepatocellular carcinoma versus cirrhosis. *Hepatology*, 37 (3), pp. 534-543.

Masoumi-Moghaddam, S., Amini, A. and Morris, D.L., 2014. The developing story of Sprouty and cancer. *Cancer Metastasis Reviews*, 33 (2-3), pp. 695-720.

Massagué, J., 2008. TGFβ in Cancer. *Cell*, 134 (2), pp. 215-230.

Mazrouei, S., et al., 2012. Apoptosis inhibition or inflammation: the role of NAIP protein expression in Hodgkin and non-Hodgkin lymphomas compared to non-neoplastic lymph node. *Journal of Inflammation*, 9 pp. 4.

Meng, W. and Takeichi, M., 2009. Adherens junction: molecular architecture and regulation. *Cold Spring Harbor Perspectives in Biology*, 1 (6), pp. a002899.

Merchant, A.A. and Matsui, W., 2010. Targeting Hedgehog--a cancer stem cell pathway. *Clinical Cancer Research*, 16 (12), pp. 3130-3140.

Mierke, C.T., 2008. Role of the endothelium during tumor cell metastasis: is the endothelium a barrier or a promoter for cell invasion and metastasis? *Journal of Biophysics*, 2008, pp. 13.

Min, L., He, B. and Hui, L., 2011. Mitogen-activated protein kinases in hepatocellular carcinoma development. *Seminars in Cancer Biology*, 21 (1), pp. 10-20.

Mishra, L., Shetty, K., Tang, Y., Stuart, A. and Byers, S.W., 2005. The role of TGF-β and Wnt signaling in gastrointestinal stem cells and cancer. *Oncogene*, 24 (37), pp. 5775-5789.

Morell, C.M. and Strazzabosco, M., 2014. Notch signaling and new therapeutic options in liver disease. *Journal of Hepatology*, 60 (4), pp. 885-890.

Moskalev, A.A., et al., 2012. Gadd45 proteins: relevance to aging, longevity and age-related pathologies. *Ageing Research Reviews*, 11 (1), pp. 51-66.

Nagaraj, N.S. and Datta, P.K., 2010. Targeting the transforming growth factor-beta signaling pathway in human cancer. *Expert Opinion on Investigational Drugs*, 19 (1), pp. 77-91.

Nair, P.P., et al., 1984. Diet, nutrition intake, and metabolism in populations at high and low risk for colon cancer. Dietary cholesterol, beta-sitosterol, and stigmasterol. *The American Journal of Clinical Nutrition*, 40 (4 Suppl), pp. 927-930.

Nakagawa, H. and Maeda, S., 2012. Molecular mechanisms of liver injury and hepatocarcinogenesis: focusing on the role of stress-activated MAPK. *Pathology Research International*, 2012, pp. 14.

Necula, L.G., et al., 2012. IL-6 and IL-11 as markers for tumor aggressiveness and prognosis in gastric adenocarcinoma patients without mutations in Gp130 subunits. *Journal of Gastrointestinal and Liver Diseases*, 21 (1), pp. 23-29.

Nejak-Bowen, K. and Monga, S.P.S., 2008. Wnt/β-catenin signaling in hepatic organogenesis. *Organogenesis*, 4 (2), pp. 92-99.

Newman, D.J. and Cragg, G.M., 2012. Natural products as sources of new drugs over the 30 years from 1981 to 2010. *Journal of natural Products*, 75 (3), pp. 311-335.

Nguyen, H.D., et al., 2011. Xanthones from the twigs of Cratoxylum cochinchinense. *Phytochemistry Letters*, 4 (1), pp. 48-51.

Nguyen, L.H.D. and Harrison, L.J., 1999. Triterpenoid and xanthone constituents of Cratoxylum cochinchinense. *Phytochemistry*, 50 (3), pp. 471-476.

Ohrnberger, S., et al., 2015. Dysregulated serum response factor triggers formation of hepatocellular carcinoma. *Hepatology*, 61 (3), pp. 979-989.

Oo, Y.H. and Sakaguchi, S., 2013. Regulatory T-cell directed therapies in liver diseases. *Journal of Hepatology*, 59 (5), pp. 1127-1134.

Paulino, V.M., et al., 2010. TROY (TNFRSF19) is overexpressed in advanced glial tumors and promotes glioblastoma cell invasion via Pyk2-Rac1 signaling. *Molecular Cancer Research*, 8 (11), pp. 1558-1567.

Petiwala, S. & Johnson, J., 2015. Diterpenes from rosemary (Rosmarinus officinalis): Defining their potential for anti-cancer activity.. *Cancer Letters*, 367, pp. 93-102.

Phuwapraisirisan, P., Udomchotphruet, S., Surapinit, S. and Tip-Pyang, S., 2006. Antioxidant xanthones from Cratoxylum cochinchinense. *Natural Product Research*, 20 (14), pp. 1332-1337.

Poon, R.T., et al., 2004. Clinical significance of thrombospondin 1 expression in hepatocellular carcinoma. *Clinical Cancer Research*, 10 (12 Pt 1), pp. 4150-4157.

Purohit, V., Rapaka, R., Kwon, O.S. and Song, B.J., 2013. Roles of alcohol and tobacco exposure in the development of hepatocellular carcinoma. *Life Sciences*, 92 (1), pp. 3-9.

Qin, Y., Liu, J.Y., Li, B., Sun, Z.L. and Sun, Z.F., 2004. Association of low p16INK4a and p15INK4b mRNAs expression with their CpG islands methylation with human hepatocellular carcinogenesis. *World Journal of Gastroenterology*, 10 (9), pp. 1276-1280.

Qiu, W., et al., 2003. Down-regulation of growth arrest DNA damage-inducible gene 45beta expression is associated with human hepatocellular carcinoma. *The American Journal of Pathology*, 162 (6), pp. 1961-1974.

Ramadori, G. and Cameron, S., 2010. Effects of systemic chemotherapy on the liver. *Annals of Hepatology*, 9 (2), pp. 133-143.

Raman, D., Sobolik-Delmaire, T. and Richmond, A., 2011. Chemokines in health and disease. *Experimental Cell Research*, 317 (5), pp. 575-589.

Ranganathan, P., Weaver, K.L. and Capobianco, A.J., 2011. Notch signalling in solid tumours: a little bit of everything but not all the time. *Nature Reviews Cancer*, 11 (5), pp. 338-351.

Refaat, A., Abd-Rabou, A. and Reda, A., 2014. TRAIL combinations: The new 'trail' for cancer therapy (Review). *Oncology Letters*, 7 (5), pp. 1327-1332.

Ren, X., Hu, B. and Colletti, L., 2008. Stem cell factor and its receptor, c-kit, are important for hepatocyte proliferation in wild-type and tumor necrosis factor receptor-1 knockout mice after 70% hepatectomy. *Surgery*, 143 (6), pp. 790-802.

Ren, Y., et al., 2011. Cytotoxic and NF-kappaB inhibitory constituents of the stems of Cratoxylum cochinchinense and their semisynthetic analogues. *Journal of Natural Products*, 74 (5), pp. 1117-1125.

Richards, C.D., 2013. The enigmatic cytokine oncostatin M and roles in disease. *ISRN Inflammation*, 2013, pp. 23.

Roberts, P.J. and Der, C.J., 2007. Targeting the Raf-MEK-ERK mitogen-activated protein kinase cascade for the treatment of cancer. *Oncogene*, 26 (22), pp. 3291-3310.

Romero, I.G., Ruvinsky, I. and Gilad, Y., 2012. Comparative studies of gene expression and the evolution of gene regulation. *Nature Reviews Genetics*, 13 (7), pp. 505-516.

Rossmanith, W., et al., 2002. Follistatin overexpression in rodent liver tumors: a possible mechanism to overcome activin growth control. *Molecular Carcinogenesis*, 35 (1), pp. 1-5.

Rowinsky, E., 1997. The development and clinical utility of the taxane class of antimicrotubule chemotherapy agents. *Annual Review Of Medicine*, 48, pp. 353-374.

Rubie, C., et al., 2006. Enhanced expression and clinical significance of CC-chemokine MIP-3 alpha in hepatocellular carcinoma. *Scandinavian Journal of Immunology*, 63 (6), pp. 468-477.

Sachdeva, M., Chawla, Y.K. and Arora, S.K., 2015. Immunology of hepatocellular carcinoma. *World Journal of Hepatology*, 7 (17), pp. 2080-2090.

Safarzadeh, E., Sandoghchian Shotorbani, S. and Baradaran, B., 2014. Herbal medicine as inducers of apoptosis in cancer treatment. *Advanced Pharmaceutical Bulletin*, 4 (Suppl 1), pp. 421-427.

Samuel, T., et al., 2001. The G2/M regulator 14-3-3sigma prevents apoptosis through sequestration of Bax. *The Journal of Biological Chemistry*, 276 (48), pp. 45201-45206.

Sansone, P. and Bromberg, J., 2012. Targeting the interleukin-6/Jak/stat pathway in human malignancies. *Journal of Clinical Oncology*, 30 (9), pp. 1005-1014.

Sapra, P., et al., 2013. Long-term tumor regression induced by an antibody-drug conjugate that targets 5T4, an oncofetal antigen expressed on tumor-initiating cells. *Molecular Cancer Therapeutics*, 12 (1), pp. 38-47.

Sarvaiya, P.J., Guo, D., Ulasov, I., Gabikian, P. and Lesniak, M.S., 2013. Chemokines in tumor progression and metastasis. *Oncotarget*, 4 (12), pp. 2171-2185.

Saxena, M. and Yeretssian, G., 2014. NOD-like receptors: master regulators of inflammation and cancer. *Frontiers in Immunology*, 5, pp. 327.

Scales, S.J. and de Sauvage, F.J., 2009. Mechanisms of Hedgehog pathway activation in cancer and implications for therapy. *Trends in Pharmacological Sciences*, 30 (6), pp. 303-312.

Scheel, C. and Weinberg, R.A., 2012. Cancer stem cells and epithelial-mesenchymal transition: concepts and molecular links. *Seminars in Cancer Biology*, 22 (5-6), pp. 396-403.

Schmitt, M., Horbach, A., Kubitz, R., Frilling, A. and Haussinger, D., 2004. Disruption of hepatocellular tight junctions by vascular endothelial growth factor (VEGF): a novel mechanism for tumor invasion. *Journal of Hepatology*, 41 (2), pp. 274-283.

Schon, S., et al., 2014. Beta-catenin regulates NF-kappaB activity via TNFRSF19 in colorectal cancer cells. *International Journal of Cancer*, 135 (8), pp. 1800-1811.

Schreiber, G. and Walter, M.R., 2010. Cytokine-receptor interactions as drug targets. *Current Opinion in Chemical Biology*, 14 (4), pp. 511-519.

Sharma, S.V. and Settleman, J., 2007. Oncogene addiction: setting the stage for molecularly targeted cancer therapy. *Genes & Development*, 21 (24), pp. 3214-3231.

Sheen, Y.Y., Kim, M.J., Park, S.A., Park, S.Y. and Nam, J.S., 2013. Targeting the transforming growth factor-β signaling in cancer therapy.*Biomolecules & Therapeutics*, 21 (5), pp. 323-331.

Shibuya, M., 2011. Vascular endothelial growth factor (VEGF) and its receptor (VEGFR) signaling in angiogenesis: a crucial target for anti- and pro-angiogenic therapies. *Genes & Cancer*, 2 (12), pp. 1097-1105.

Shyur, L.F. and Yang, N.S., 2008. Metabolomics for phytomedicine research and drug development. *Current Opinion in Chemical Biology*, 12 (1), pp. 66-71.

Sicklick, J.K., et al., 2006. Dysregulation of the Hedgehog pathway in human hepatocarcinogenesis. *Carcinogenesis*, 27 (4), pp. 748-757.

Sieuwerts, A.M., et al., 2006. Which cyclin E prevails as prognostic marker for breast cancer? Results from a retrospective study involving 635 lymph node-negative breast cancer patients. *Clinical Cancer Research*, 12 (11 Pt 1), pp. 3319-3328.

Sobolesky, P.M. and Moussa, O., 2013. The role of beta-arrestins in cancer. *Progress in Molecular Biology and Translational Science*, 118, pp. 395-411.

Soepadmo, E. and Wong, K.M., 1995. *Tree flora of Sabah and Sarawak volume 1,* 1st ed. Malaysia: Joint publication of Sabah Forestry Department, Forest Research Institute Malaysia and Saraway Forestry Department.

Staib, F., Hussain, S.P., Hofseth, L.J., Wang, X.W. and Harris, C.C., 2003. TP53 and liver carcinogenesis. *Human Mutation*, 21 (3), pp. 201-216.

Stauffer, J.K., Scarzello, A.J., Jiang, Q. and Wiltrout, R.H., 2012. Chronic inflammation, immune escape, and oncogenesis in the liver: a unique neighborhood for novel intersections. *Hepatology*, 56 (4), pp. 1567-1574.

Stevenson, R.P., Veltman, D. and Machesky, L.M., 2012. Actin-bundling proteins in cancer progression at a glance. *Journal of Cell Science*, 125 (Pt 5), pp. 1073-1079.

Strazzabosco, M. and Fabris, L., 2012. Notch signaling in hepatocellular carcinoma: guilty in association! *Gastroenterology*, 143 (6), pp. 1430-1434.

Summons, R., Bradley, A., Jahnke, L. & Waldbauer, J., 2006. Steroids, triterpenoids and molecular oxygen. *Philosophical Transactions of the Royal Society B: Biological Sciences*, 361(1470), pp. 951-968.

Sy, S.M., et al., 2006. Novel identification of zyxin upregulations in the motile phenotype of hepatocellular carcinoma. *Modern Pathology*, 19 (8), pp. 1108-1116.

Takigawa, Y. and Brown, A.M., 2008. Wnt signaling in liver cancer. *Current Drug Targets*, 9 (11), pp. 1013-1024.

Tamura, R.E., et al., 2012. GADD45 proteins: central players in tumorigenesis. *Current Molecular Medicine*, 12 (5), pp. 634-651.

Tang, K.H., et al., 2012. CD133(+) liver tumor-initiating cells promote tumor angiogenesis, growth, and self-renewal through neurotensin/interleukin-8/CXCL1 signaling. *Hepatology*, 55 (3), pp. 807-820.

Tang, S.Y., Whiteman, M., Jenner, A., Peng, Z.F. and Halliwell, B., 2004a. Mechanism of cell death induced by an antioxidant extract of Cratoxylum cochinchinense (YCT) in Jurkat T cells: the role of reactive oxygen species and calcium. *Free Radical Biology & Medicine*, 36 (12), pp. 1588-1611.

Tang, S.Y., et al., 2004b. Characterization of antioxidant and antiglycation properties and isolation of active ingredients from traditional chinese medicines. *Free Radical Biology and Medicine*, 36 (12), pp. 1575-1587.

Thomas, M.B. and Abbruzzese, J.L., 2005. Opportunities for targeted therapies in hepatocellular carcinoma. *Journal of Clinical Oncology*, 23 (31), pp. 8093-108.

Thomas, R.K., et al., 2007. High-throughput oncogene mutation profiling in human cancer. *Nature Genetics*, 39 (3), pp. 347-351.

Thomas, S. and Balan, A., 2012. Retinoblastoma tumour suppresor gene: an overview. *Journal of Indian Academy of Oral Medicine and Radiology*, 24 (1), pp. 30-35.

Thompson, E.D., Enriquez, H.L., Fu, Y.X. and Engelhard, V.H., 2010. Tumor masses support naive T cell infiltration, activation, and differentiation into effectors. *The Journal of Experimental Medicine*, 207 (8), pp. 1791-1804.

Thoppil, R. and Bishayee, A., 2011. Terpenoids as potential chemopreventive and therapeutic agents in liver cancer. *World Journal of Hepatology*, 3(9), pp. 228-249.

Thorgeirsson, S.S. and Grisham, J.W., 2002. Molecular pathogenesis of human hepatocellular carcinoma. *Nature Genetics*, 31 (4), pp. 339-346.

Toogood, P.L., 2002. Progress toward the development of agents to modulate the cell cycle. *Current Opinion in Chemical Biology*, 6 (4), pp. 472-478.

Torre, L.A., et al., 2015. Global cancer statistics, 2012. *CA: A Cancer Journal for Clinicians*, 65 (2), pp. 87-108.

Trikha, M., Corringham, R., Klein, B. and Rossi, J.F., 2003. Targeted anti-interleukin-6 monoclonal antibody therapy for cancer: a review of the rationale and clinical evidence. *Clinical Cancer Research*, 9 (13), pp. 4653-4665.

Tu, K., et al., 2015. Vasodilator-stimulated phosphoprotein promotes activation of hepatic stellate cells by regulating Rab11-dependent plasma membrane targeting of transforming growth factor beta receptors. *Hepatology*, 61 (1), pp. 361-374.

Tyakht, A.V., et al., 2014. RNA-Seq gene expression profiling of HepG2 cells: the influence of experimental factors and comparison with liver tissue. *BMC Genomics*, 15 (1), pp. 1-9.

Udomchotphruet, S., Phuwapraisirisan, P., Sichaem, J. and Tip-pyang, S., 2012. Xanthones from the stems of Cratoxylum cochinchinense. *Phytochemistry*, 73, pp. 148-151.

Vergara, D., et al., 2014. Antitumor activity of the dietary diterpene carnosol against a panel of human cancer cell lines. *Food Function*, 5, pp. 1261-1269.

Villanueva, A., et al., 2012. Notch signaling is activated in human hepatocellular carcinoma and induces tumor formation in mice. *Gastroenterology*, 143 (6), pp. 1660-1669.e7.

Villanueva, A., et al., 2008. Pivotal role of mTOR signaling in hepatocellular carcinoma. *Gastroenterology*, 135 (6), pp. 1972-1983.

Vogelstein, B., Lane, D. and Levine, A.J., 2000. Surfing the p53 network. *Nature*, 408 (6810), pp. 307-310.

Vroon, A., Heijnen, C.J. and Kavelaars, A., 2006. GRKs and arrestins: regulators of migration and inflammation. *Journal of Leukocyte Biology*, 80 (6), pp. 1214-1221.

Wang, W., Erbe, A.K., Hank, J.A., Morris, Z.S. and Sondel, P.M., 2015. NK cell-mediated antibody-dependent cellular cytotoxicity in cancer immunotherapy. *Frontiers in Immunology*, 6 pp. 368.

Wang, Z., Wang, N., Chen, J. and Shen, J., 2012. Emerging glycolysis targeting and drug discovery from chinese medicine in cancer therapy. *Evidence-based Complementary and Alternative Medicine*, 2012, pp. 873175.

Waugh, D.J. and Wilson, C., 2008. The interleukin-8 pathway in cancer. *Clinical Cancer Research*, 14 (21), pp. 6735-6741.

Weinstein, I.B., 2002. Cancer. Addiction to oncogenes--the Achilles heal of cancer. *Science*, 297 (5578), pp. 63-64.

Weinstein, I.B. and Joe, A.K., 2006. Mechanisms of disease: oncogene addiction--a rationale for molecular targeting in cancer therapy. *Nature Clinical Practice Oncology*, 3 (8), pp. 448-457.

Wickline, E.D., Du, Y., Stolz, D.B., Kahn, M. and Monga, S.P., 2013. gamma-catenin at adherens junctions: mechanism and biologic implications in hepatocellular cancer after beta-catenin knockdown. *Neoplasia*, 15 (4), pp. 421-434.

Williams, J.H., et al., 2004. Human aflatoxicosis in developing countries: a review of toxicology, exposure, potential health consequences, and interventions. *The American Journal of Clinical Nutrition*, 80 (5), pp. 1106-1122.

Wozniak, M.A., Modzelewska, K., Kwong, L. and Keely, P.J., 2004. Focal adhesion regulation of cell behavior. *Biochimica et Biophysica Acta*, 1692 (2-3), pp. 103-119.

Wu, X. and Li, Y., 2012a. *Signaling pathways in liver cancer,* 1st ed. US: InTech.

Wu, X. and Li, Y., 2012b. Signaling pathways in liver cancer. In: Julianov, A. (ed.) *Liver tumors.* Croatia: InTech, pp. 37-58.

Xia, J.F., Liang, Q.L., Hu, P., Wang, Y.M. and Luo, G.A., 2009. Recent trends in strategies and methodologies for metabonomics. *Chinese Journal of Analytical Chemistry*, 37 (1), pp. 136-143.

Xia, J.F., et al., 2014. A map describing the association between effective components of traditional Chinese medicine and signaling pathways in cancer cells in vitro and in vivo.. *Drug Discoveries & Therapeutics,* 8(4), pp. 139-153.

Xia, Y., et al., 2007. MEKK1 mediates the ubiquitination and degradation of c-Jun in response to osmotic stress. *Molecular and Cellular Biology*, 27 (2), pp. 510-517.

Xu, K., Liu, P. and Wei, W., 2014. mTOR signaling in tumorigenesis. *Biochimica et Biophysica Acta- Reviews on Cancer*, 1846 (2), pp. 638-654.

Yamaguchi, R., et al., 1998. Expression of vascular endothelial growth factor in human hepatocellular carcinoma. *Hepatology*, 28 (1), pp. 68-77.

Yan, M., et al., 1994. Activation of stress-activated protein kinase by MEKK1 phosphorylation of its activator SEK1. *Letters to Nature*, 372 (6508), pp. 798-800.

Yan, X., Chua, M.S., He, J. and So, S., 2008. Small interfering RNA targeting CDC25B inhibits liver tumor growth in vitro and in vivo. *Molecular Cancer*, 7 (1), pp. 1-9.

Yan X.J., et al., 2014. Triterpenoids as reversal agents for anticancer drug resistance treatment. *Drug Discovery Today,* 19(4), pp. 482-488.

Yang, H.Y., Wen, Y.Y., Chen, C.H., Lozano, G. and Lee, M.H., 2003. 14-3-3 sigma positively regulates p53 and suppresses tumor growth. *Molecular and Cellular Biology*, 23 (20), pp. 7096-7107.

Yang, Y., et al., 2015. beta-Arrestin1 enhances hepatocellular carcinogenesis through inflammation-mediated Akt signalling. *Nature Communications*, 6, pp. 7369.

Yasmin Anum, M.Y., et al., 2009. Combined assessment of TGF-beta-1 and alpha-fetoprotein values improves specificity in the diagnosis of hepatocellular carcinoma and other chronic liver diseases in Malaysia. *The Medical Journal of Malaysia*, 64 (3), pp. 223-227.

Yeh, Y.T., Lee, K.T., Tsai, C.J., Chen, Y.J. and Wang, S.N., 2012. Prolactin promotes hepatocellular carcinoma through Janus kinase 2. *World Journal of Surgery*, 36 (5), pp. 1128-1135.

Yin, S.Y., Wei, W.C., Jian, F.Y. and Yang, N.S., 2013. Therapeutic applications of herbal medicines for cancer patients. *Evidence-based Complementary and Alternative Medicine*, 2013, pp. 302426.

Yu, H.Y., et al., 2009. Two new benzophenone glucosides from Cratoxylon cochinchinensis. *Chinese Chemical Letters*, 20 (4), pp. 459-461.

Zhang, H. and Chin, A.I., 2014. Role of Rip2 in development of tumor-infiltrating MDSCs and bladder cancer metastasis. *PloS One*, 9 (4), pp. e94793.

Zhang, H., et al., 2003. Mechanism of beta 1-integrin-mediated hepatoma cell growth involves p27 and S-phase kinase-associated protein 2. *Hepatology*, 38 (2), pp. 305-313.

Zhao, S., Fung-Leung, W.P., Bittner, A., Ngo, K. and Liu, X., 2014. Comparison of RNA-Seq and microarray in transcriptome profiling of activated T cells. *PloS One*, 9 (1), pp. e78644.

Zhao, W., Gu, Y.H., Song, R., Qu, B.Q. and Xu, Q., 2008. Sorafenib inhibits activation of human peripheral blood T cells by targeting LCK phosphorylation. *Leukemia*, 22 (6), pp. 1226-1233.

Zhu, C., Liang, Q.L., Wang, Y.M. and Luo, G.A., 2010. Integrated development of metabonomics and its new progress. *Chinese Journal of Analytical Chemistry*, 38 (7), pp. 1060-1068.

Zlotnik, A. and Yoshie, O., 2000. Chemokines: a new classification system and their role in immunity. *Immunity*, 12 (2), pp. 121-127.

APPENDICES

Appendix A-1

The Quality Assessment of Samples Running Microarray Assays

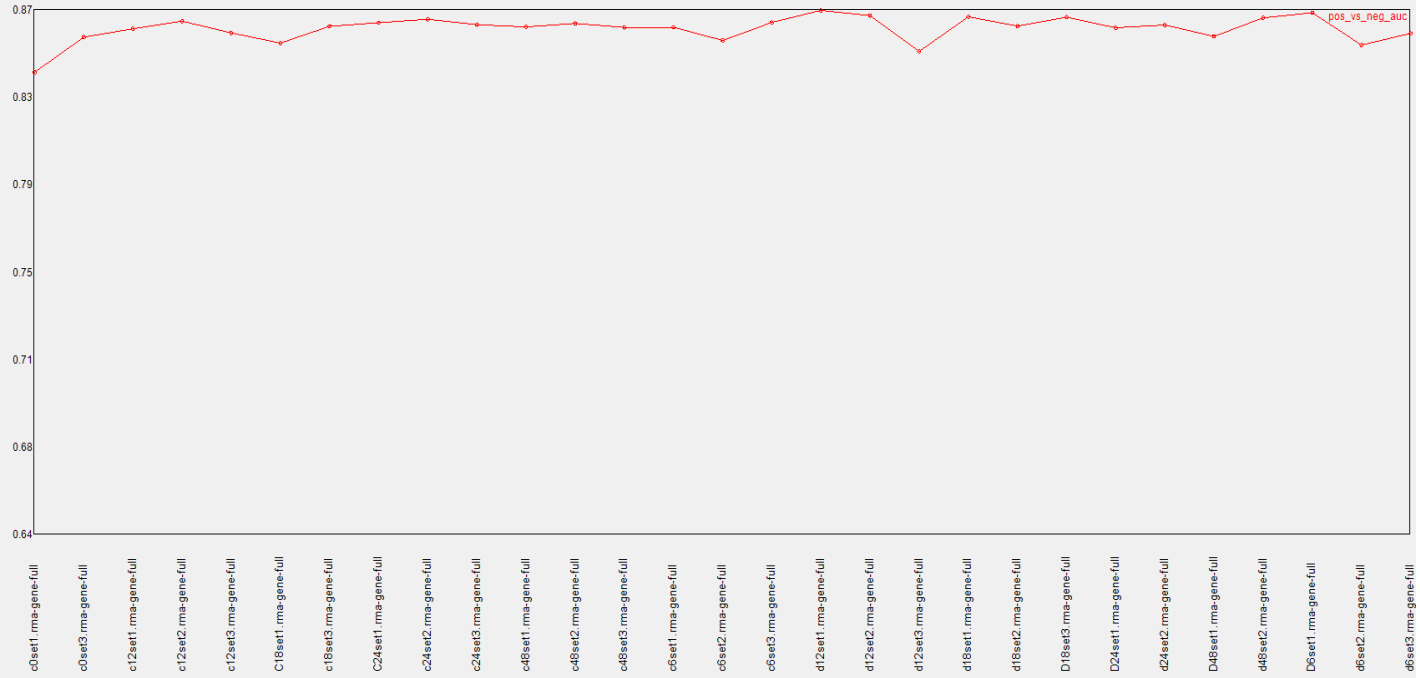

Appendix A-2

The Correlation Plot for Samples Running Microarray Assays

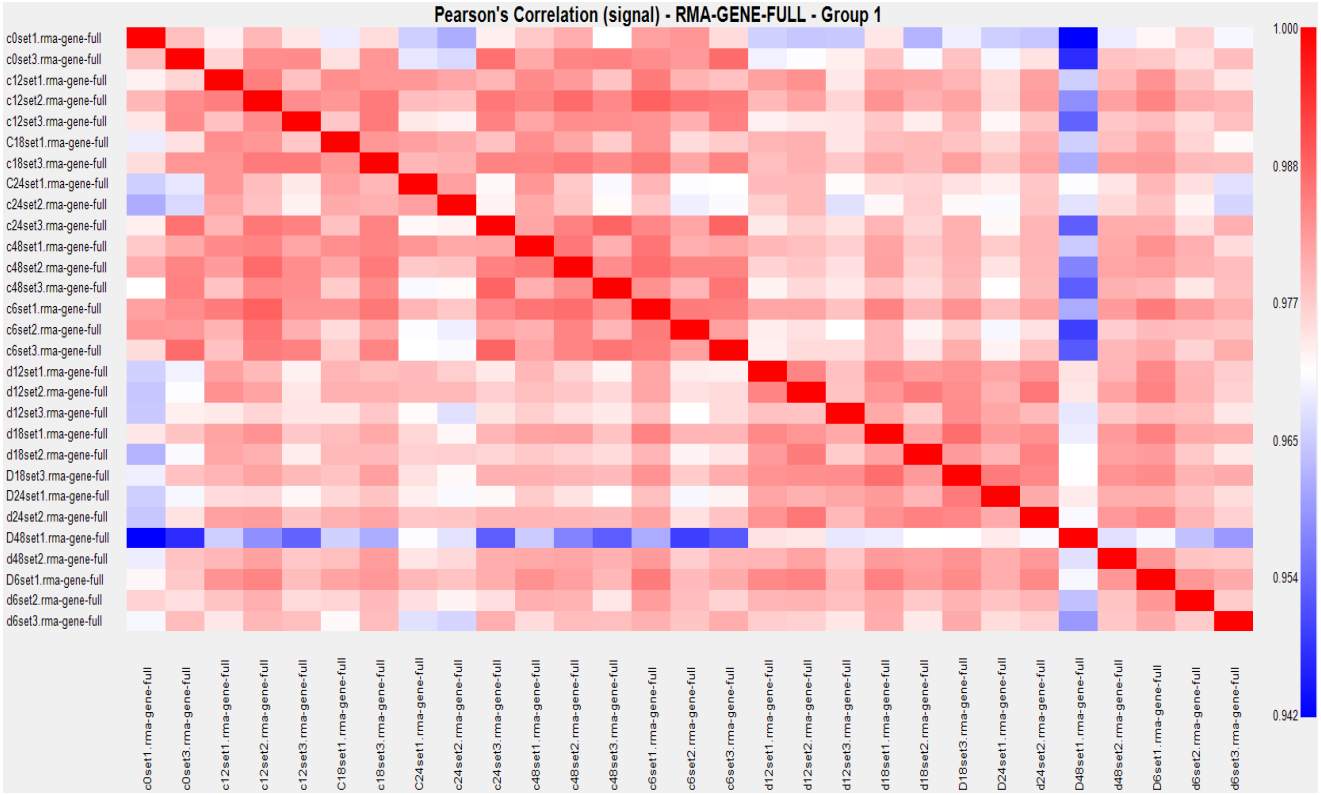

Appendix B

Preparation of Western Blot Buffer/Reagents

Acrylamide/bisacrylamide (30% T, 2.67% C)

Acrylamide/Bis (30 % T, 2.67 % C) was prepared by dissolving 87.6 g of acrylamide (R & M Chemicals) and 2.4 g of N, N-bis-methylene-acrylamide in distilled water. The volume was made up to 300 ml.

10 % Ammonium Persulfate (APS)

Exact 0.1 g of ammonium persulfate (Promega) was dissolved in 1 ml of distilled water. The solution was prepared fresh before use.

10 % Sodium Dodecyl Sulphate (SDS)

Exact 10 g of SDS (Bio Basic Inc) was dissolved in distilled water. The volume was made up to 100 ml.

5x Electrode (Running) Buffer

The 5x electrode/running buffer was prepared by mixing 60 g of Tris base, 288 g of glycine and 10 g of SDS with distilled water. The volume was made up to 2L. 1x running buffer was derived for gel running.

7.5 % Resolving Gel

Exact 3.75 ml of 30% acrylamide/bisacrylamide was mixed with 3.75 ml of 1.5 M Tris-HCl, pH 8.8 (Bio Rad), 150 µl of 10 % SDS, 7.5 µl of TEMED, 75 µl of 10 % APS, 7.28 ml of ddH_20 to make up to a total volume of 15 ml. It was immediately used after mixed.

4 % of Stacking Gel

Exact 1.98 ml of 30 % acrylamide/bisacrylamide was mixed with 3.78 ml of 0.5 M Tris-HCl, pH 6.8 (Bio Rad), 150 µl of 10 % SDS, 15 µl of TEMED, 75 µl of 10 % APS, 9 ml of ddH_20 to make up to a total volume of 15 ml. It was immediately used after mixed.

Water-Saturated *n*-Butanol

Exact 50 ml of *n*-butanol was mixed with 5 ml of distilled water. Only top phase of the mixture was used. It was kept at room temperature.

Blotting Buffer

Standard ready blotting buffer (Nacalai tesque, Japan) was used as transfer buffer. Alternatively, blotting buffer was prepared by mixing 30.3 g Tris [250 mM] and 144.1 g Glycine [1.92 M] to make up to 1L of 10X Tris/Glycine. Then, 125 ml of this 10X Tris/Glycine [25 mM Tris & 192 mM Glycine] was mixed with 313 ml Methanol [20%] and 812 ml H2O to make up to 1.25 liter of this transfer buffer.

Washing Buffer (10x TBST)

About 60.57 g of 0.5 M Tris, pH 7.5 base was mixed with 87.66 g of 1.5 M NaCl in the distilled water. The volume was made up to 1 L.

Appendix B - Continued

Washing Buffer (1X TBST)

Exact 100 ml of TBST 10x was then diluted with 900 ml of distilled water. 5ml of Tween was added into the diluted washing buffer.

Blocking Buffer

Blocking One (Nacalai tesque, Japan) was used as blocking buffer. Alternatively, blocking buffer was prepared by mixing 1X TBST with 5% w/v non-fat dry milk. For example, 150 ml 1X TBST was added with 7.5 g non-fat dry milk to mix well. Immersion of the membrane in Blocking One was for approximately 30 minutes.

Stripping Buffer

Exact 1.5 g of glycine was mixed with 0.1 g of SDS and 1 ml of Tween 20 in distilled water. The pH value was adjusted to pH 2.2. The volume was made up to 100 ml.

Appendix C-1

KEGG: P53 Signalling Pathway

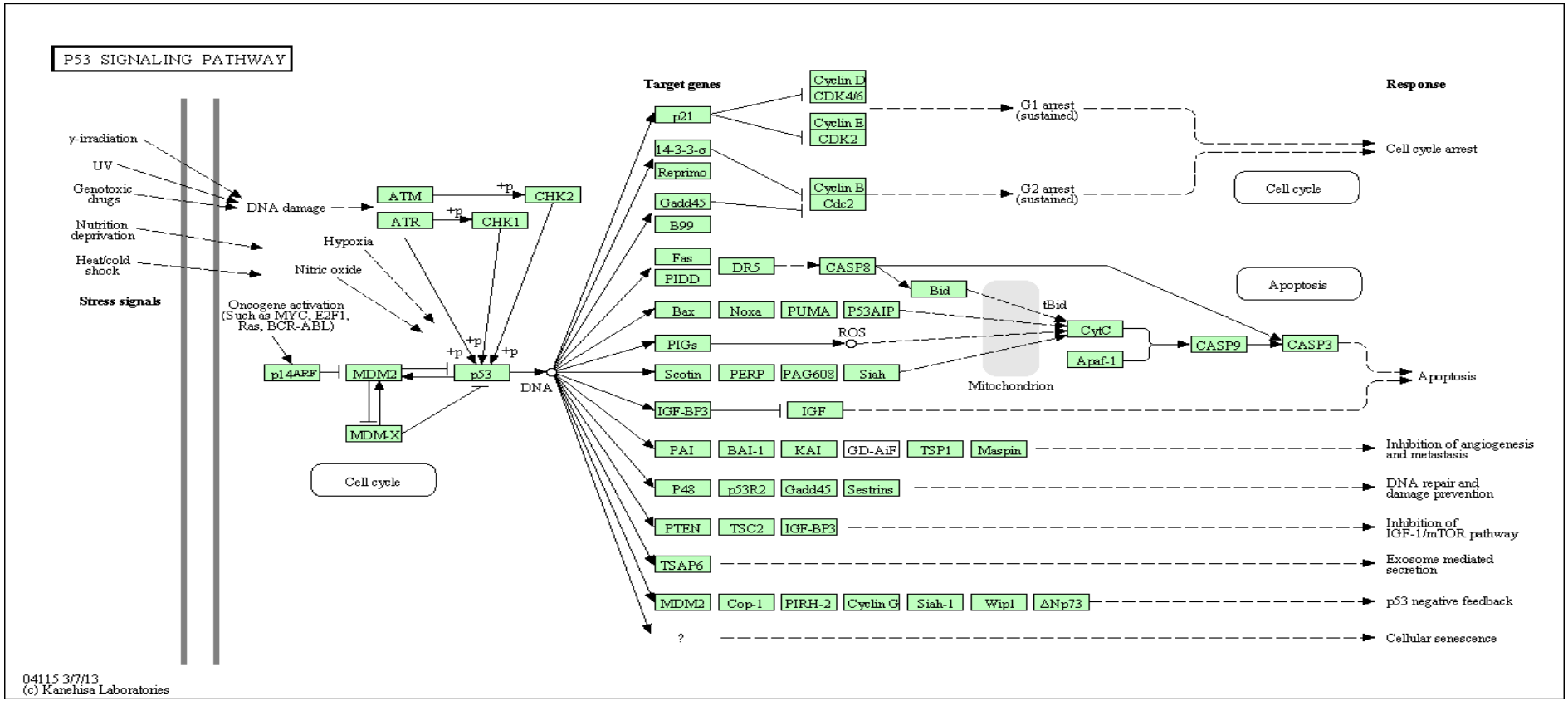

Appendix C-2

KEGG: Cell Cycle Signalling Pathway

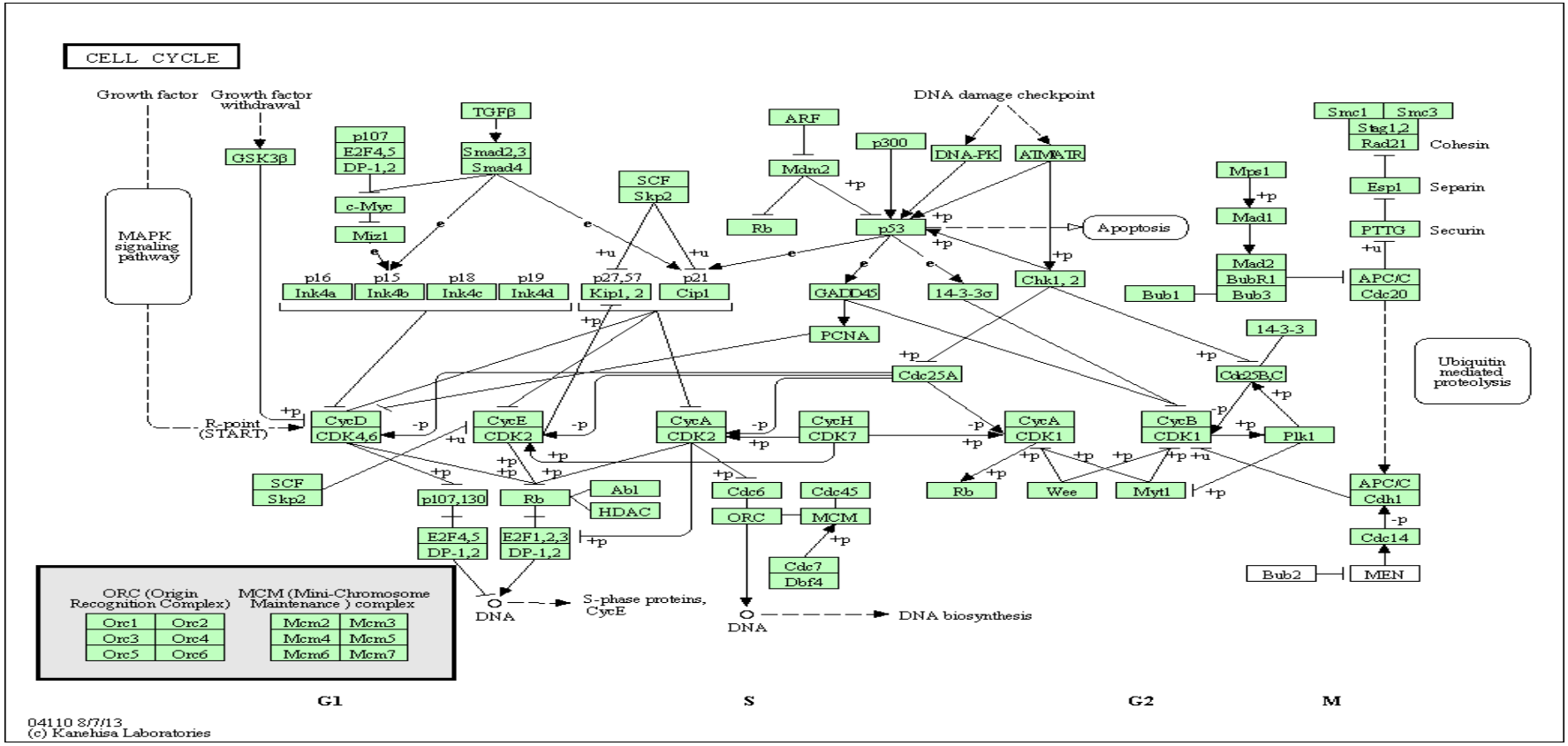
CELL CYCLE
Growth factor
Growth factor withdrawal
GSK3β
MAPK signaling pathway
R-point (START)
TGFβ
p107
E2F4,5
DP-1,2
Smad2,3
Smad4
c-Myc
Mizl
SCF
Skp2
ARF
Mdm2
p300
DNA-PK
ATM/ATR
DNA damage checkpoint
Rb
p53
Apoptosis
p16 Ink4a
p15 Ink4b
p18 Ink4c
p19 Ink4d
p27,57 Kip1, 2
p21 Cip1
GADD45
14-3-3σ
Chk1, 2
PCNA
Cdc25A
CycD CDK4,6
CycE CDK2
CycA CDK2
CycH CDK7
CycA CDK1
CycB CDK1
Plk1
Cdc25B,C
14-3-3
Mps1
Mad1
Mad2
BubR1
Bub3
Bub1
Smc1 Smc3
Stag1,2
Rad21
Cohesin
Esp1
Separin
PTTG
Securin
APC/C Cdc20
Ubiquitin mediated proteolysis
APC/C Cdh1
Cdc14
MEN
Bub2
p107,130
Abl
HDAC
Cdc6
Cdc45
ORC
MCM
Cdc7
Dbf4
E2F4,5
DP-1,2
E2F1,2,3
DP-1,2
Rb
Wee
Myt1
ORC (Origin Recognition Complex)
Orc1 Orc2
Orc3 Orc4
Orc5 Orc6
MCM (Mini-Chromosome Maintenance) complex
Mcm2 Mcm3
Mcm4 Mcm5
Mcm6 Mcm7
DNA
S-phase proteins, CycE
DNA biosynthesis
G1
S
G2
M
04110 8/7/13
(c) Kanehisa Laboratories

Appendix C-3

KEGG: Hedgehog Cancer Signalling Pathway

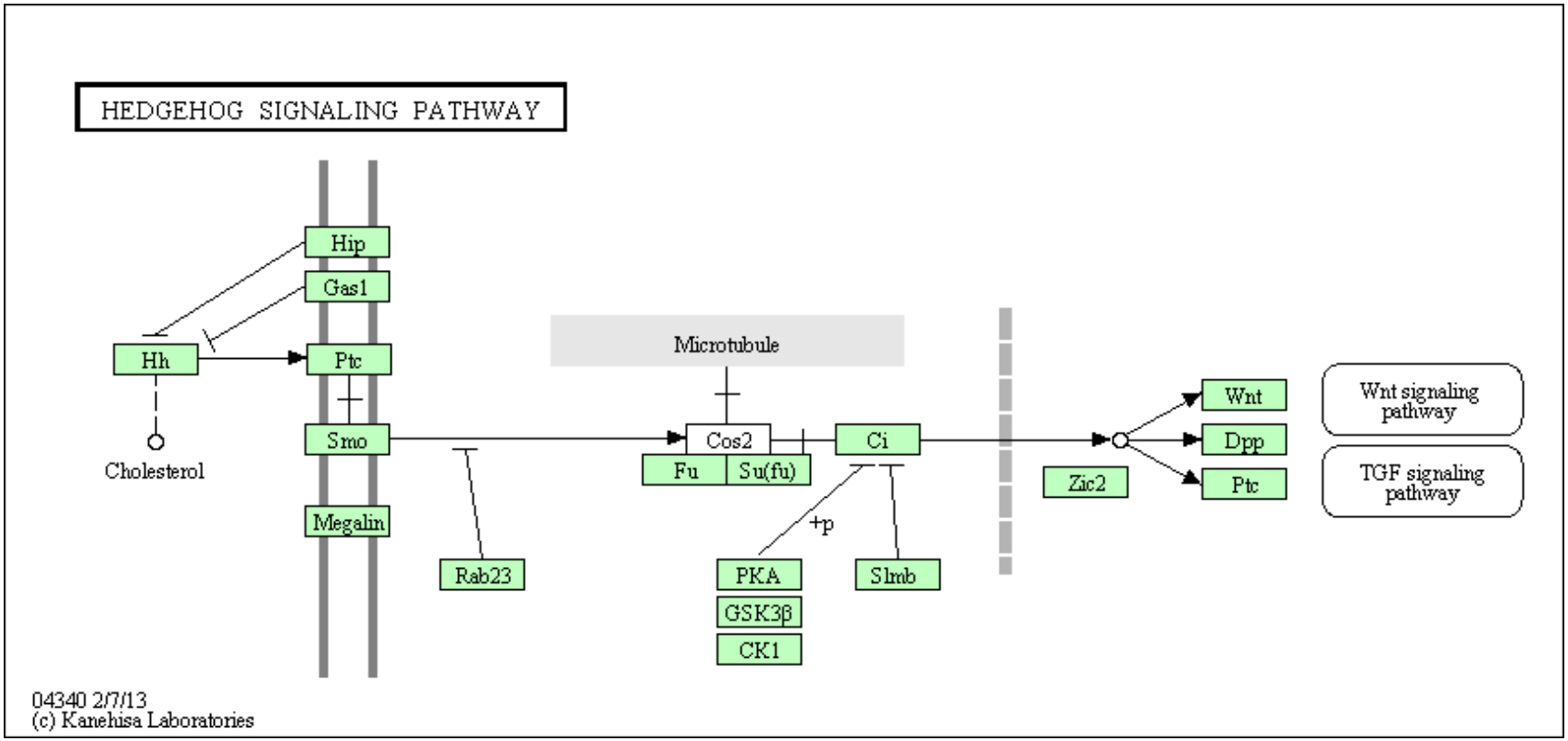

Appendix C-4

KEGG: MAPK Cancer Signalling Pathway

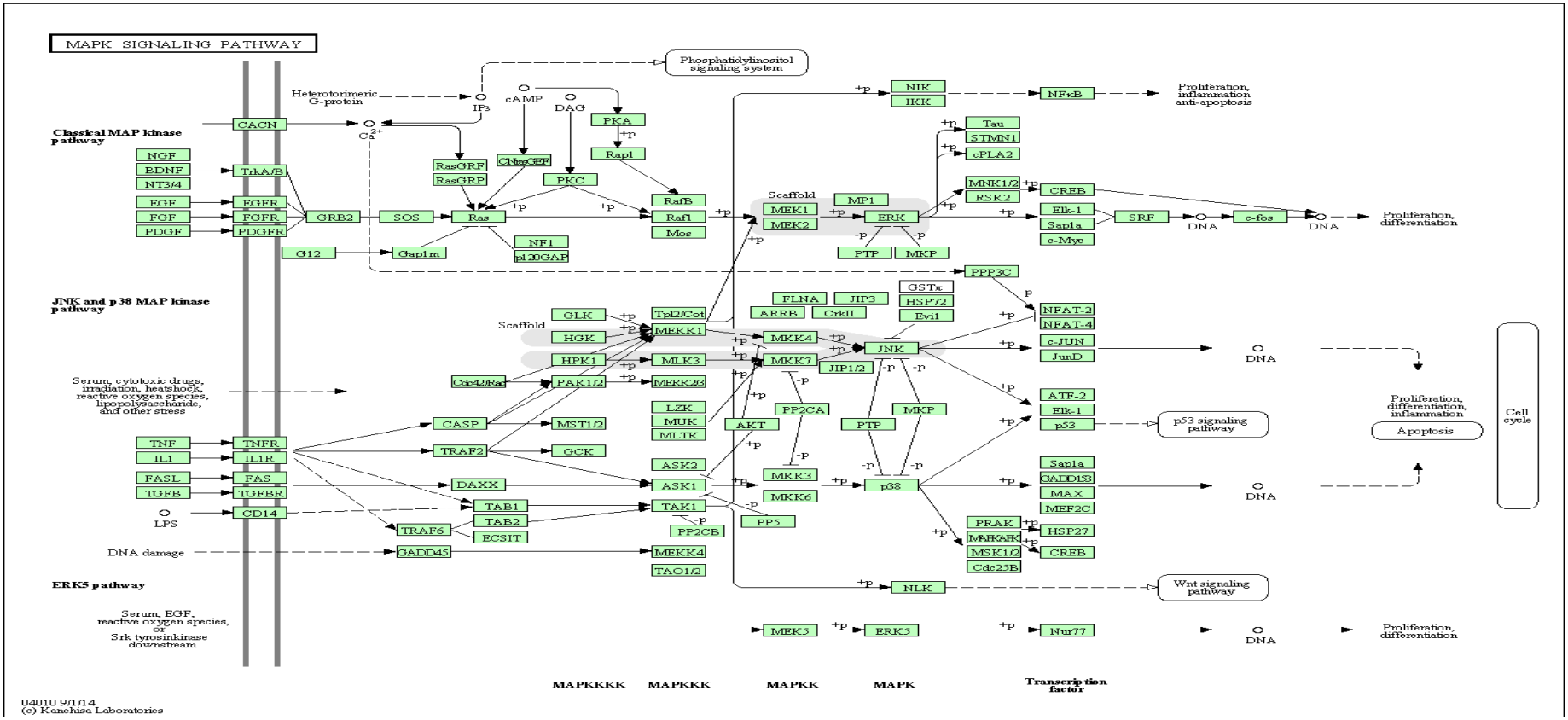

Appendix C-5

KEGG: mTOR Cancer Signalling Pathway

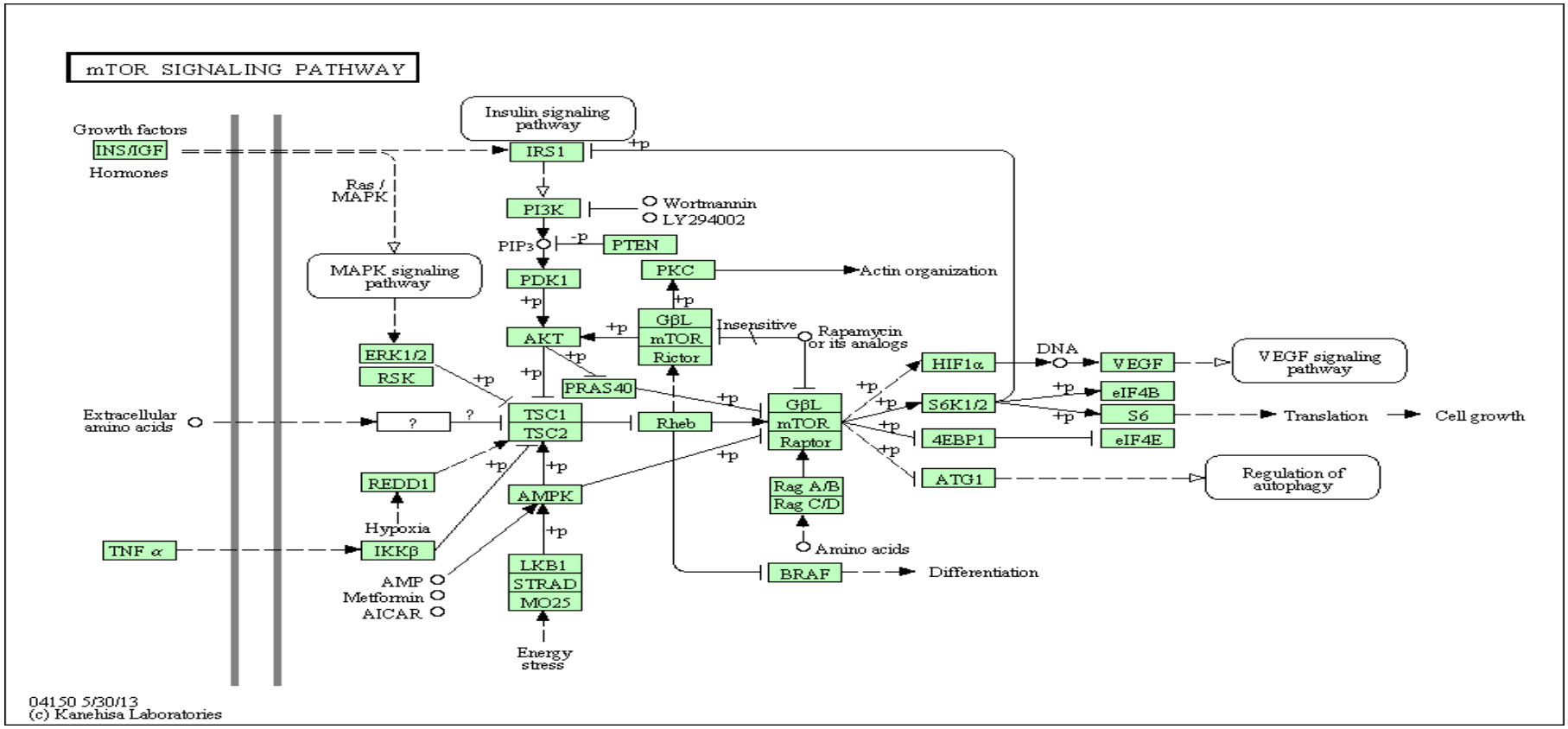

Appendix C-6

KEGG: TGF-β Cancer Signalling Pathway

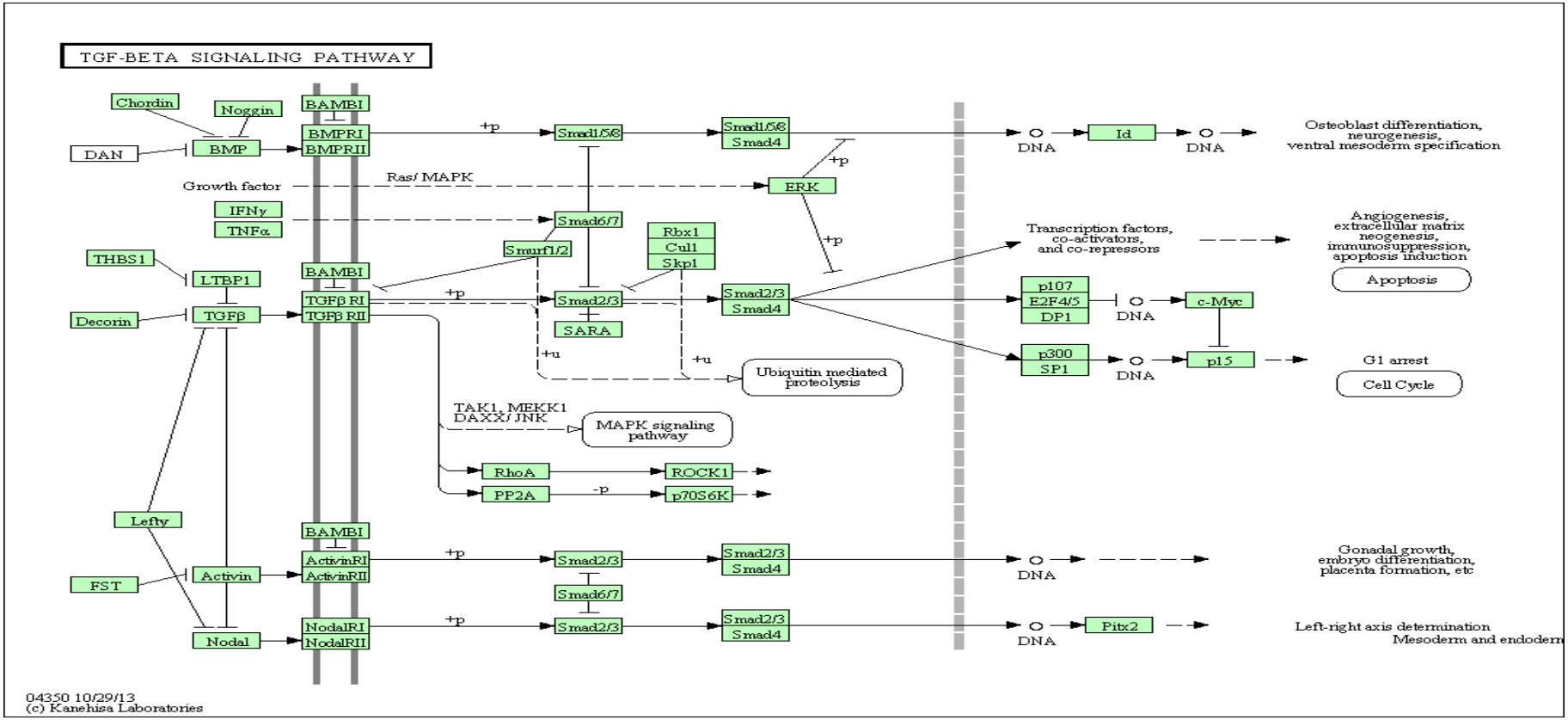

Appendix C-7

KEGG: ErbB Cancer Signalling Pathway

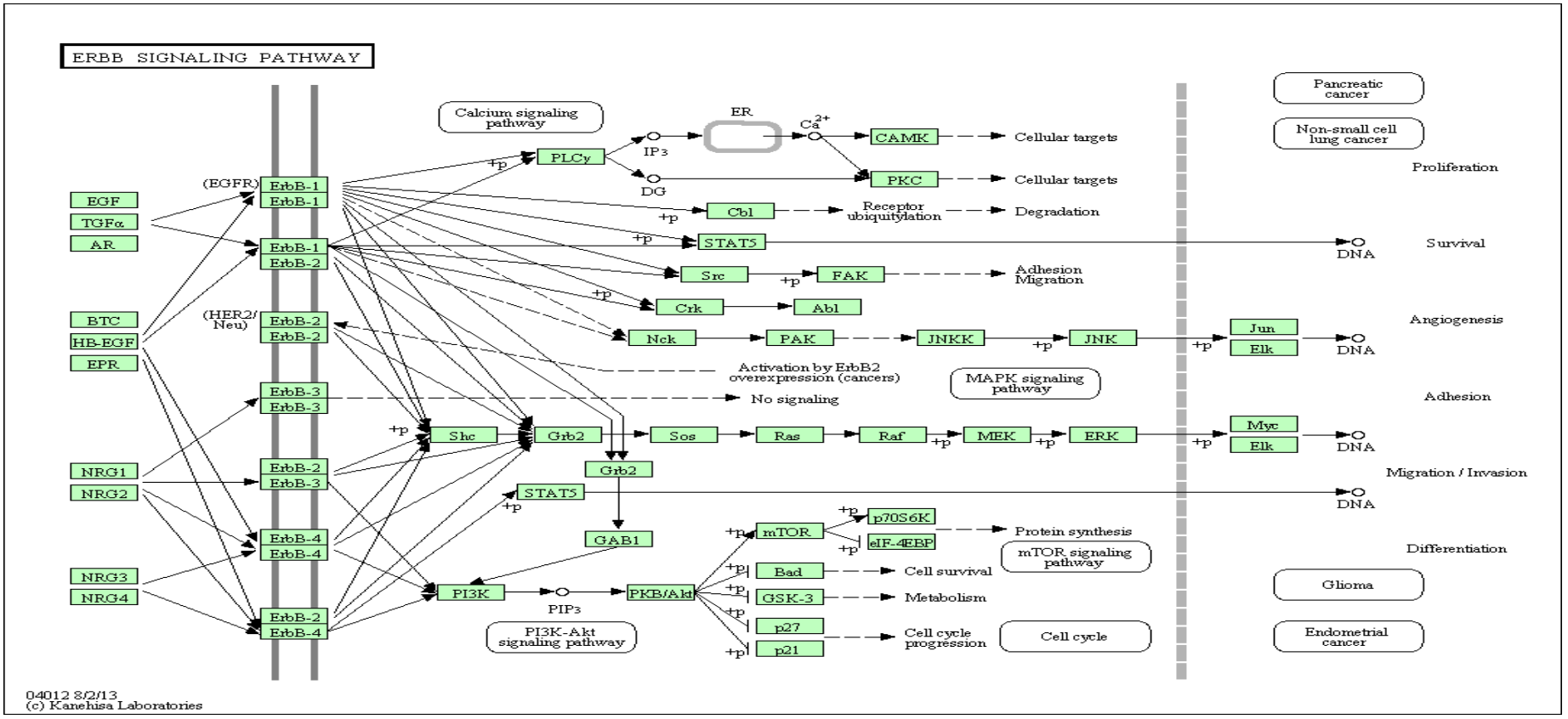

Appendix C-8

KEGG: Notch Cancer Signalling Pathway

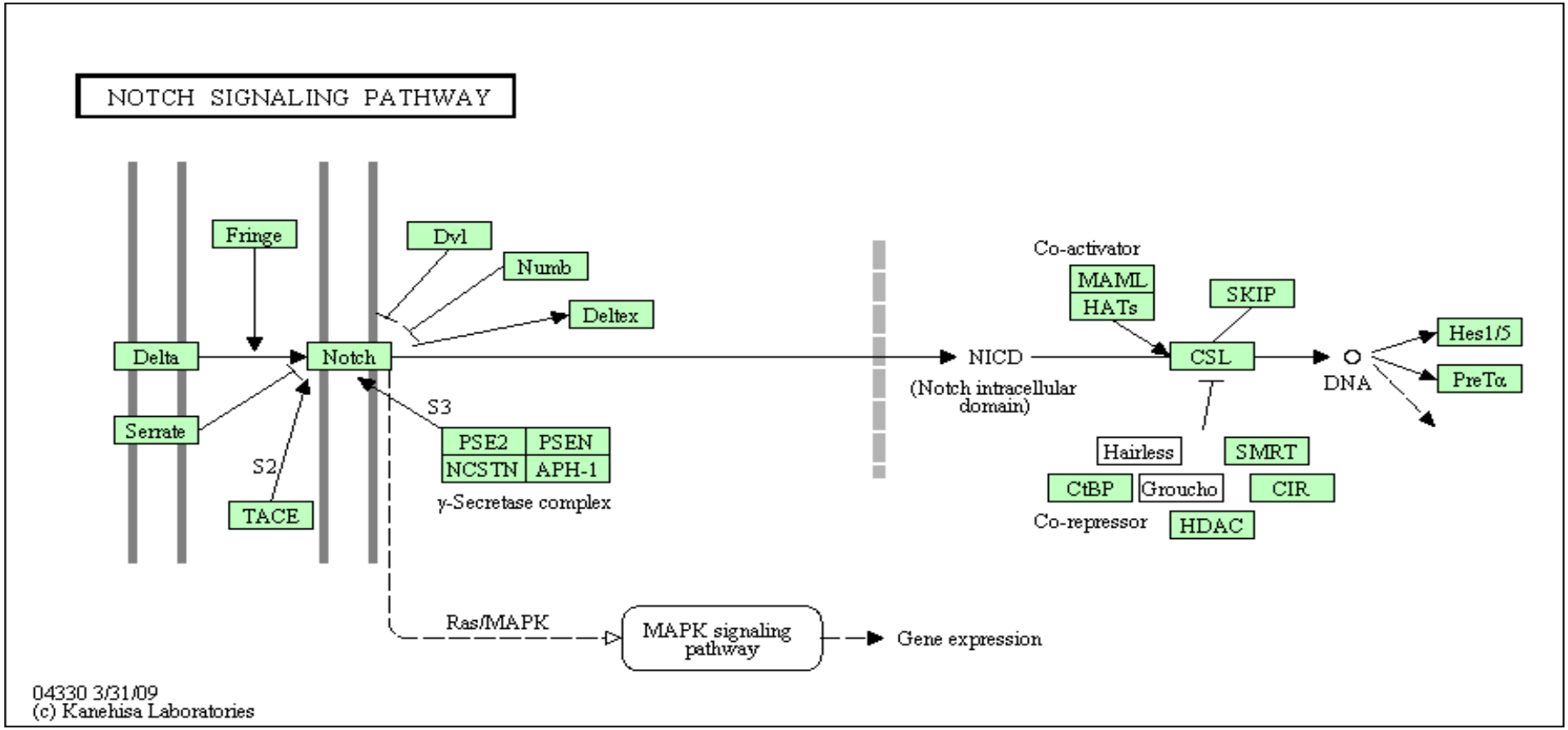

Appendix C-9

KEGG: VEGF Cancer SignallingPathway

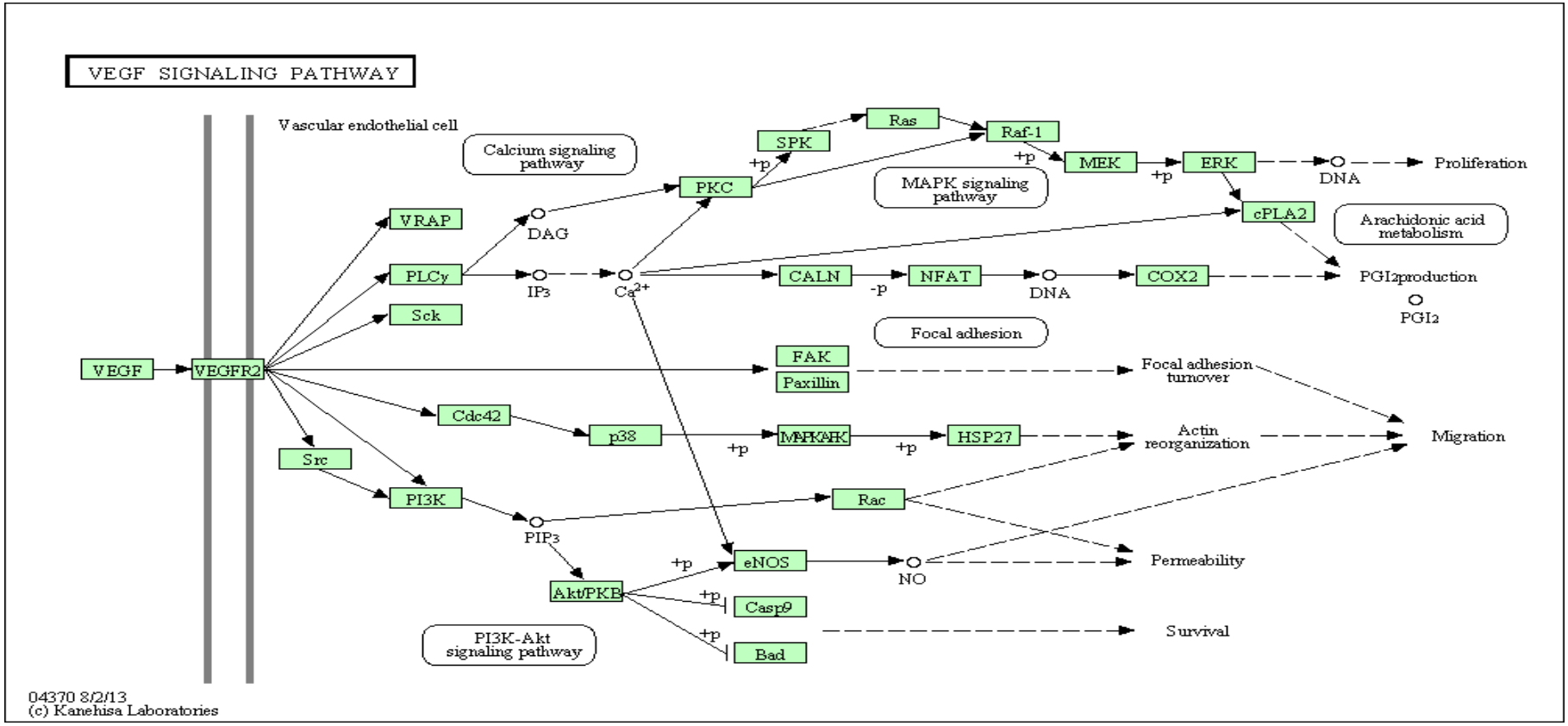

Appendix C-10

KEGG: JAK-STAT Cancer Signalling Pathway

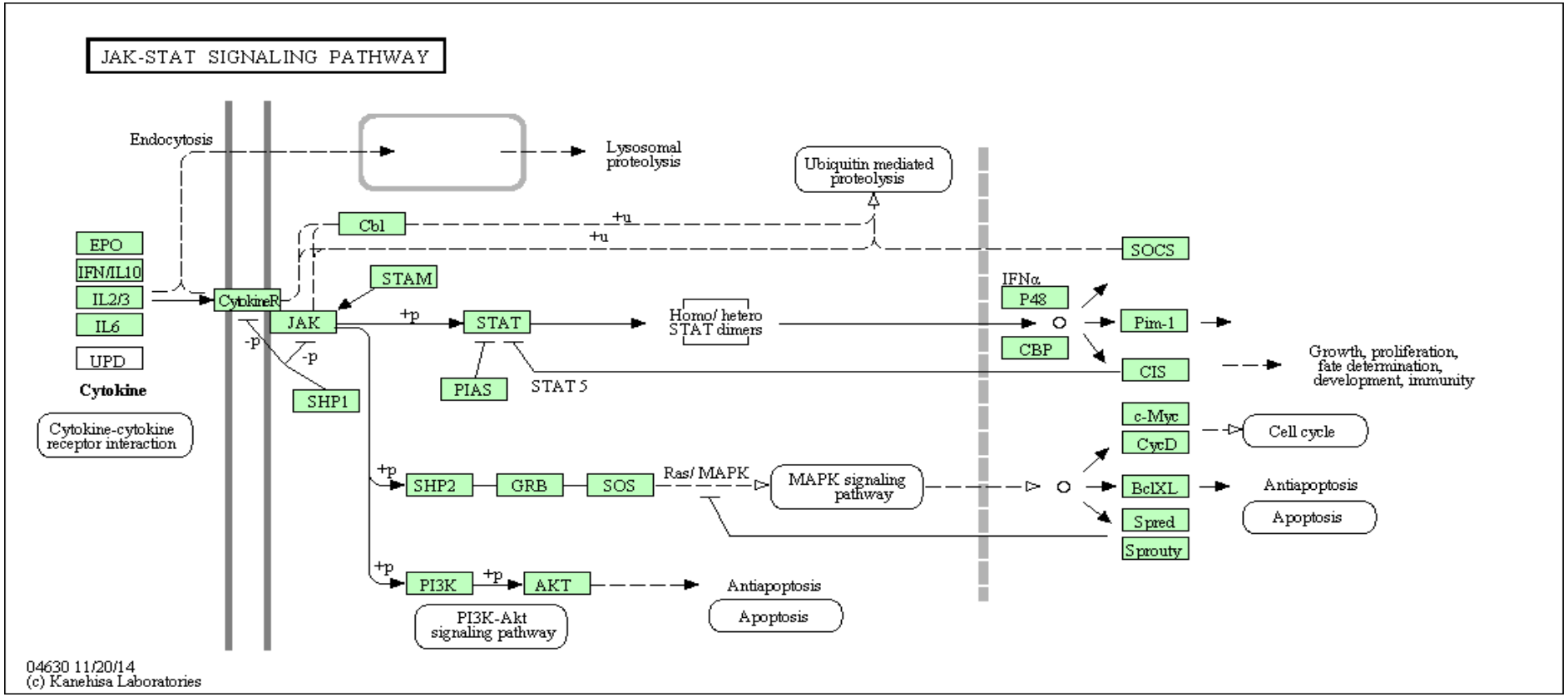

Appendix C-11

KEGG: WNT Cancer Signalling Pathway

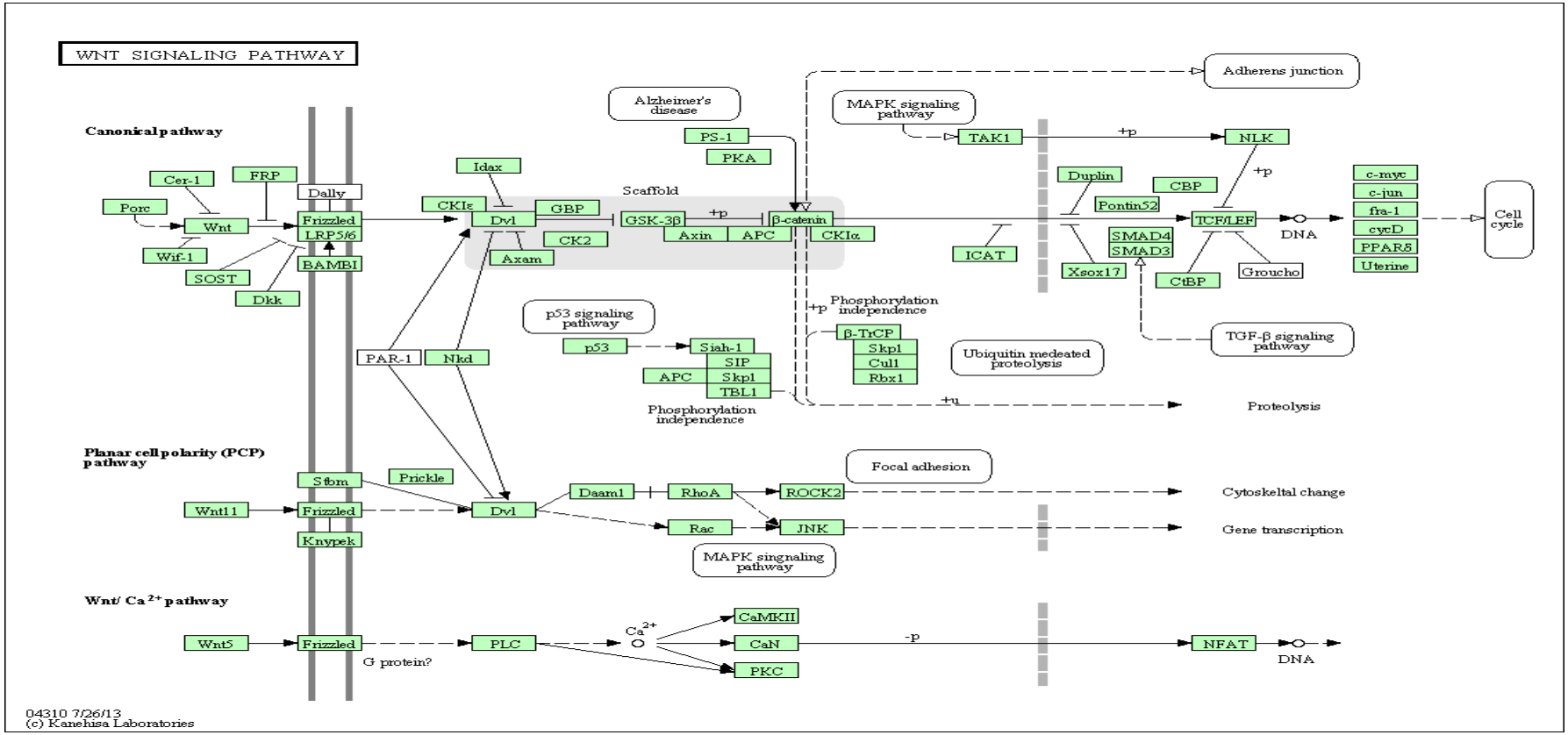

Appendix C-12

KEGG: Toll-Like Receptor Cancer Signalling Pathway

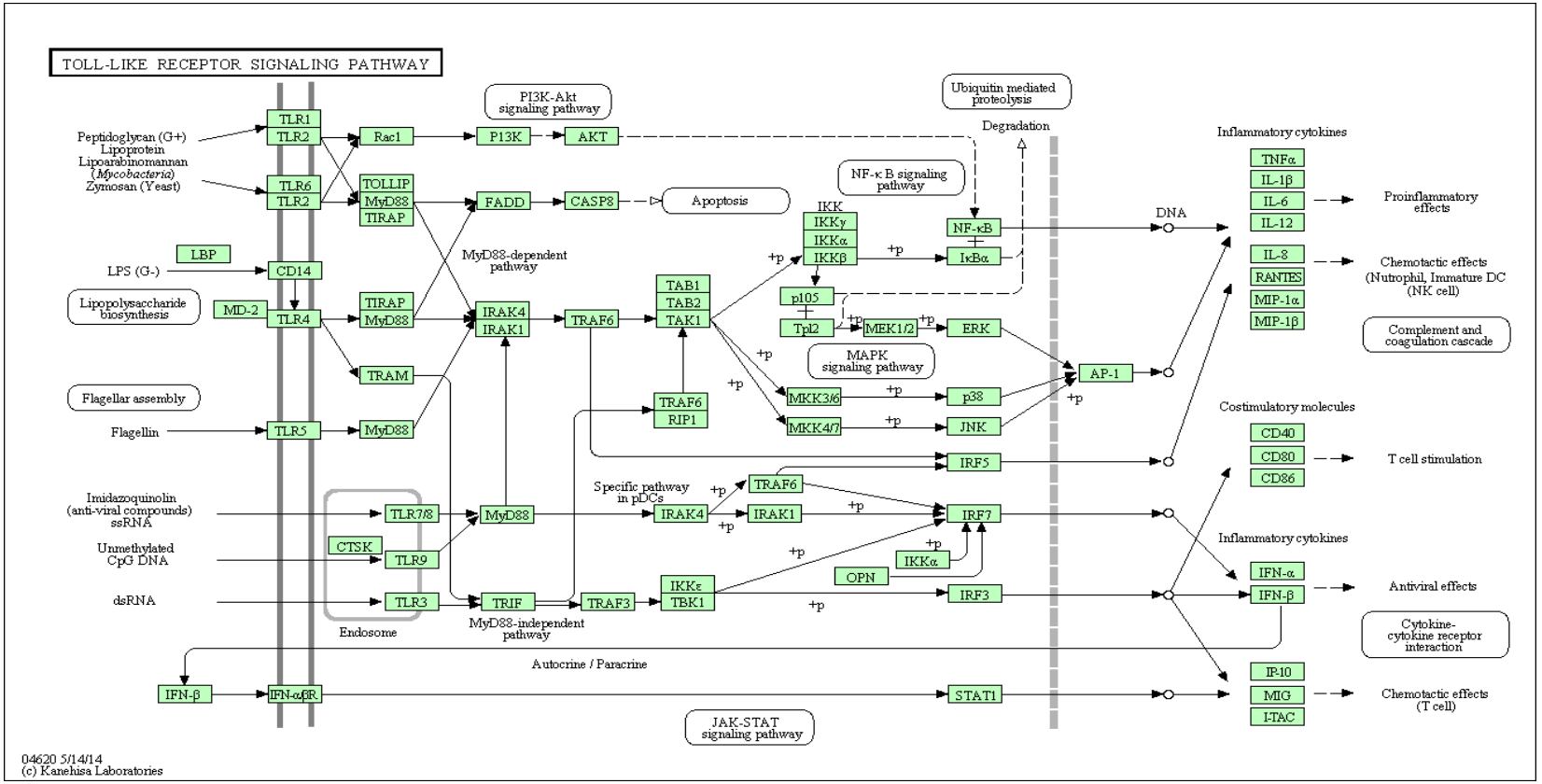

Appendix C-13

KEGG: Nod-Like Receptor Cancer Signalling Pathway

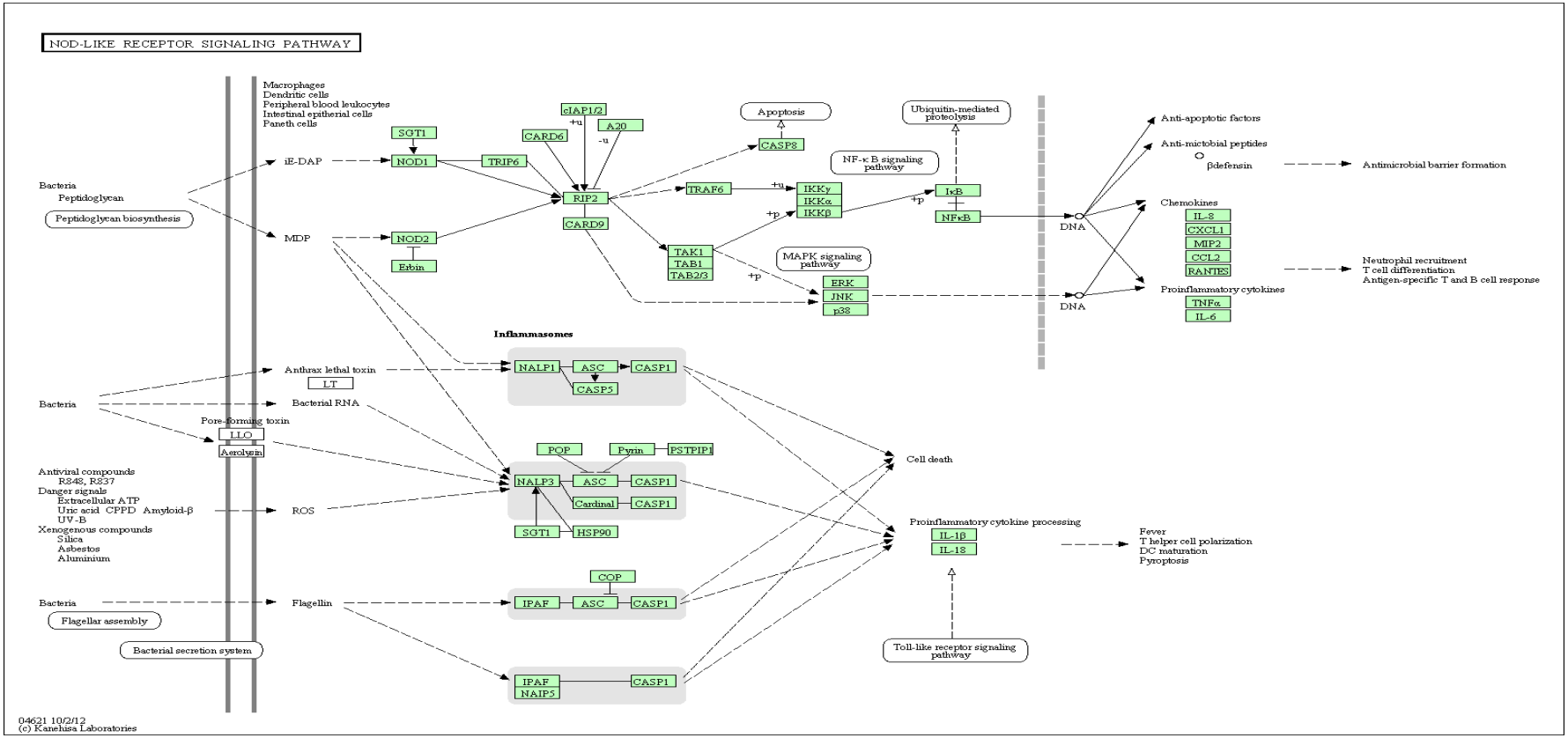

Appendix C-14

KEGG: RIG-1-Like Receptor Cancer Signalling Pathway

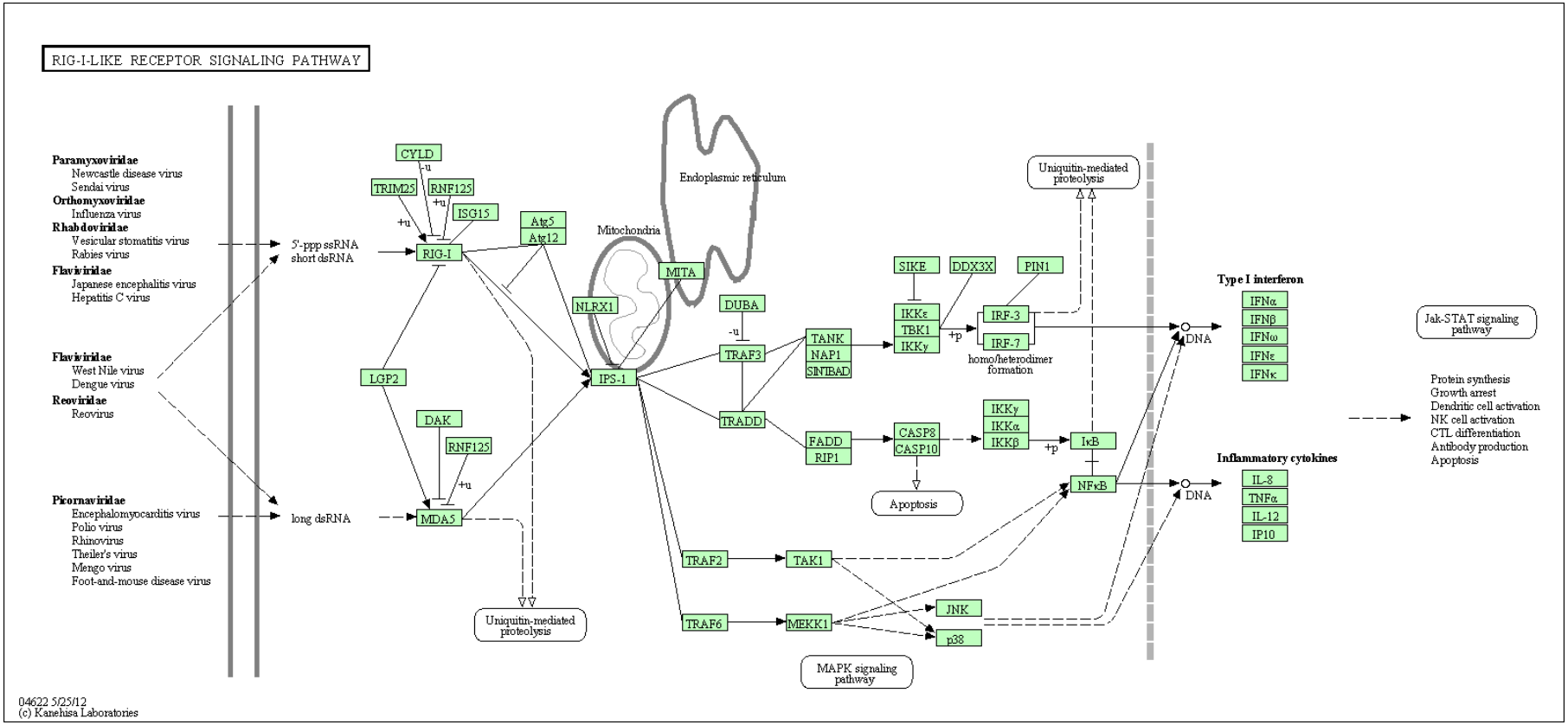

Appendix C-15

KEGG: Chemokine Cancer Signalling Pathway

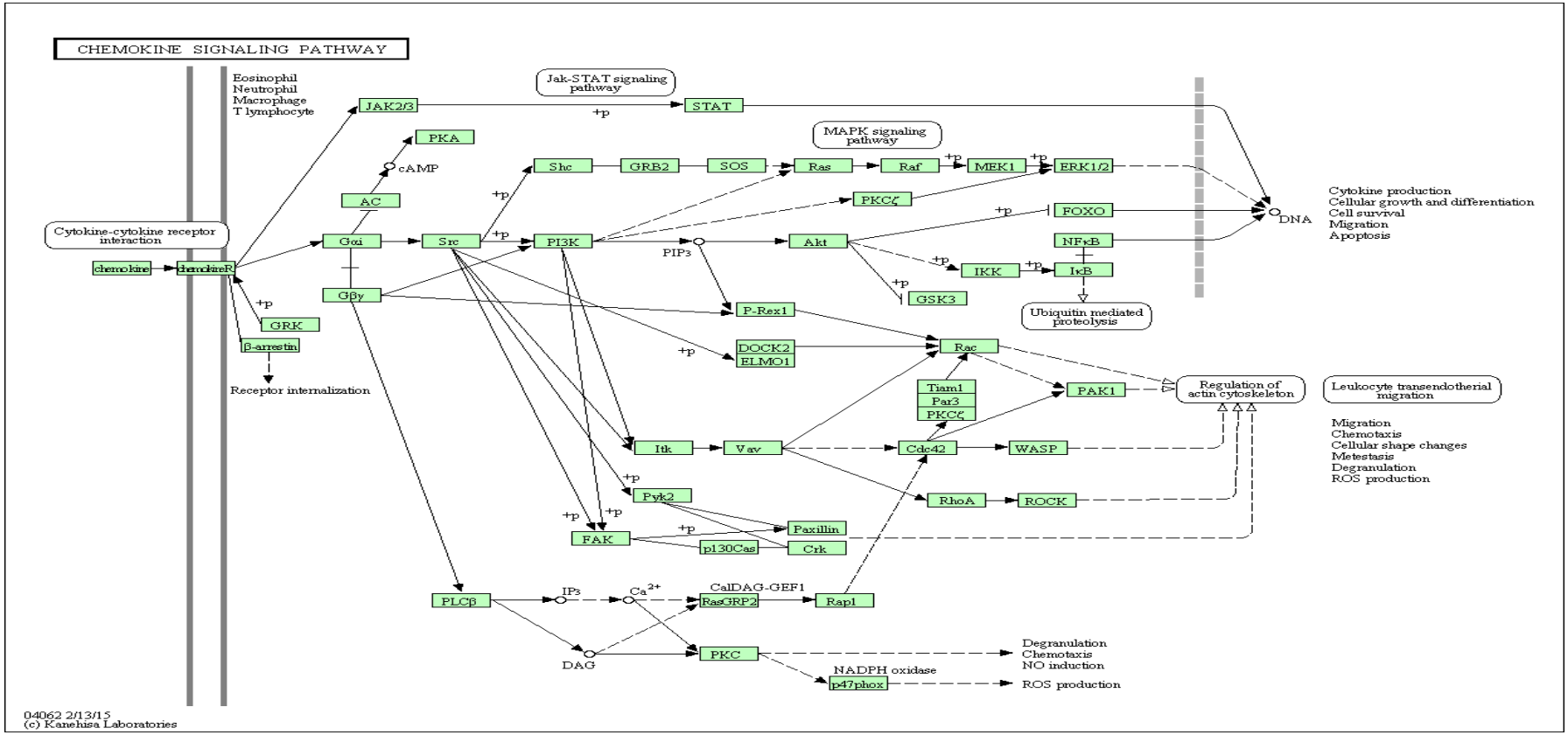

Appendix C-16

KEGG: Cytokine-Cytokine Receptor Interaction Cancer Signalling Pathway

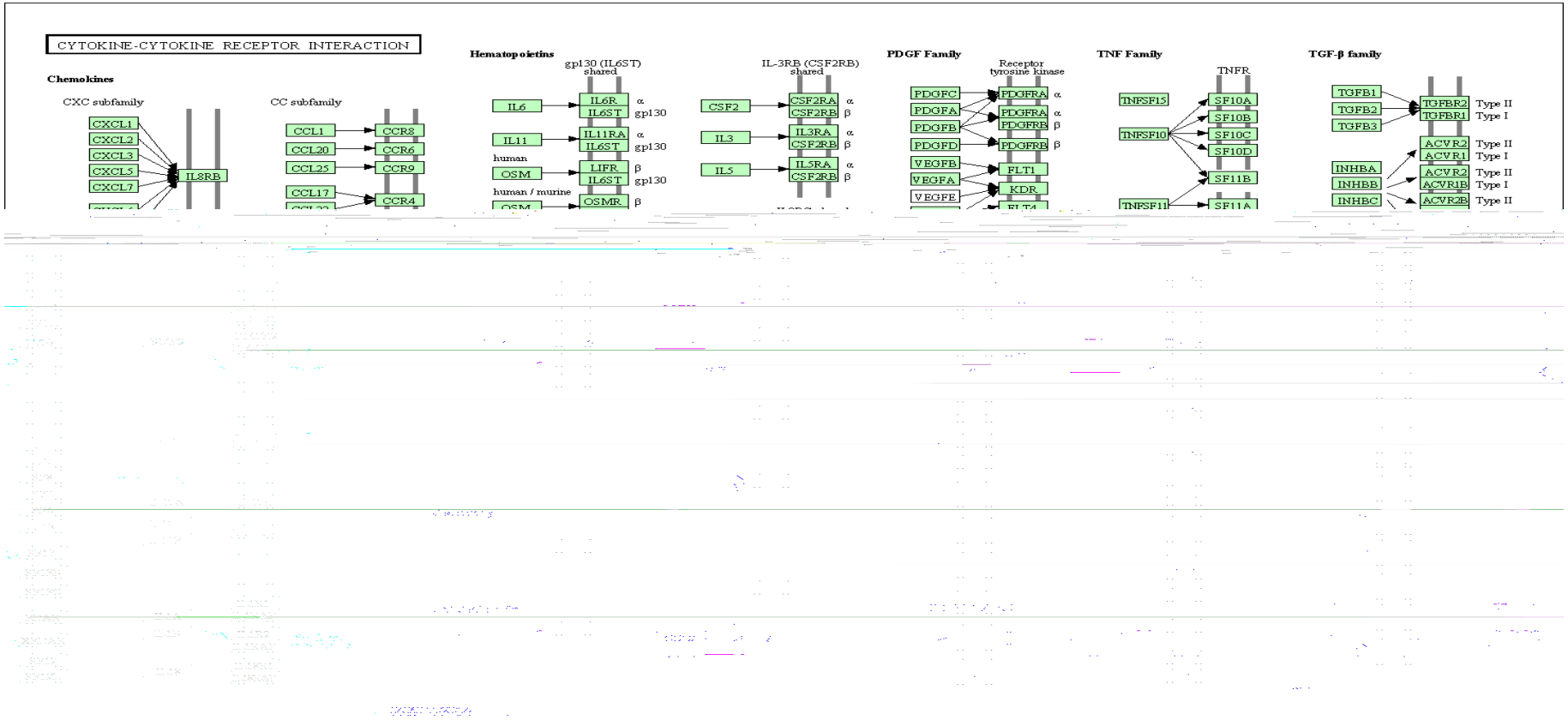

Appendix C-17

KEGG: T-Cell Receptor Cancer Signalling Pathway

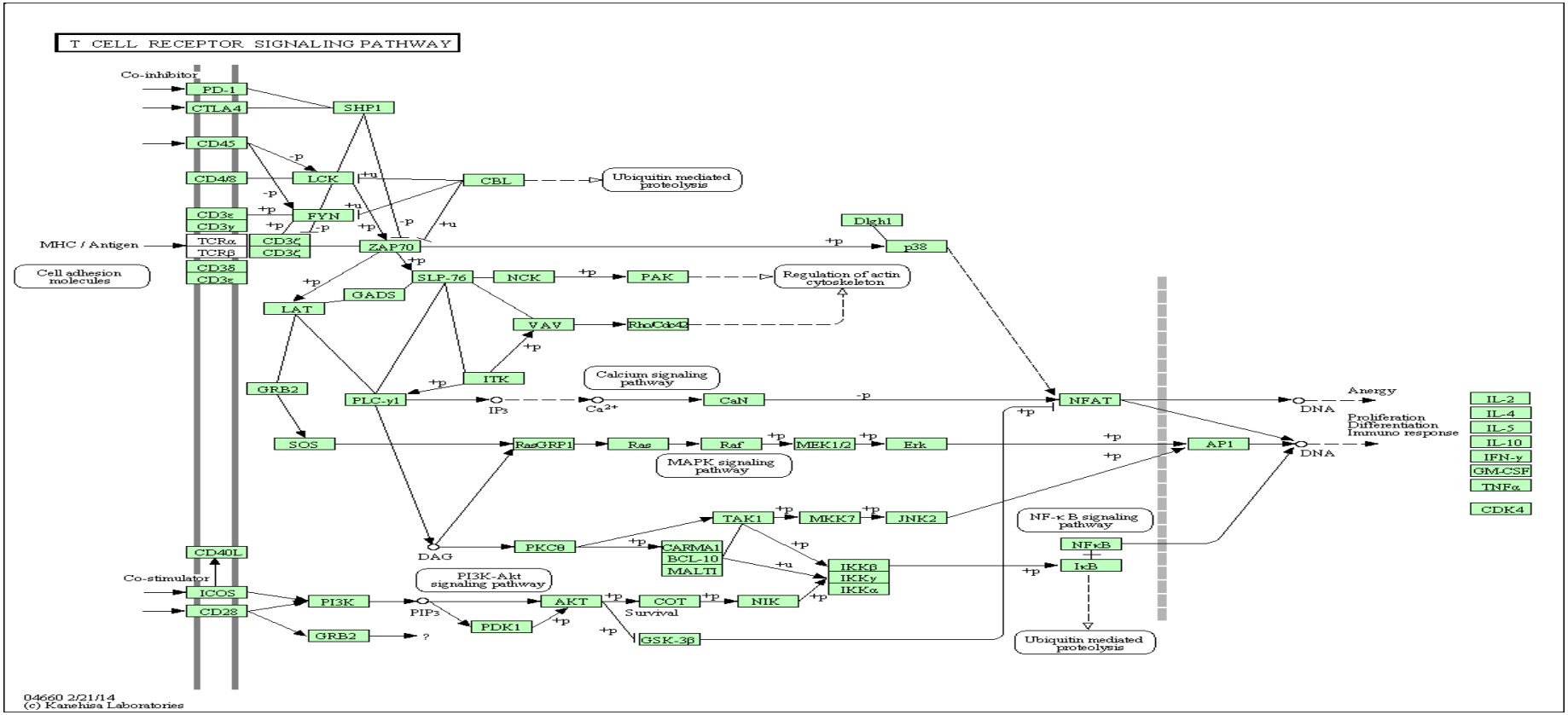

Appendix C-18

KEGG: B-Cell Receptor Cancer Signalling Pathway

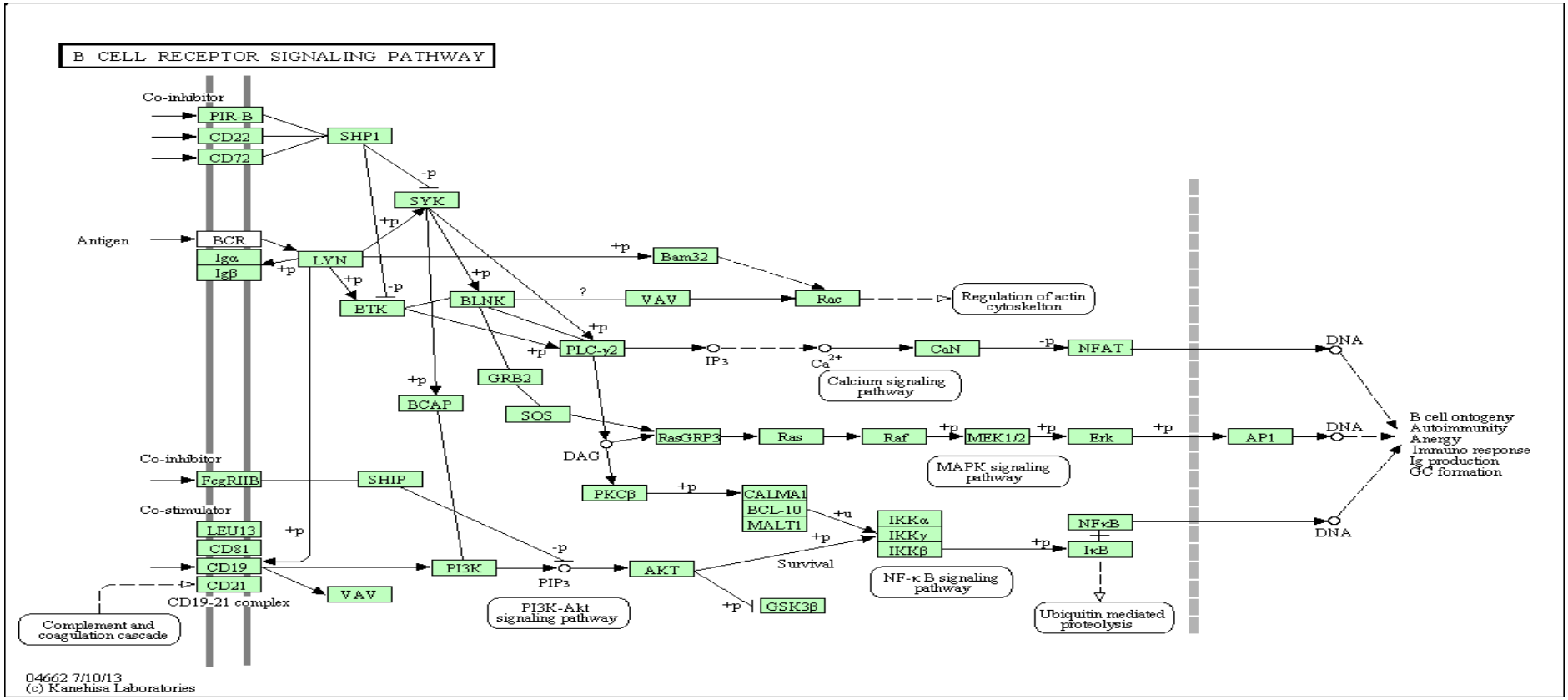

Appendix C-19

KEGG: ApoptosisCancer Signalling Pathway

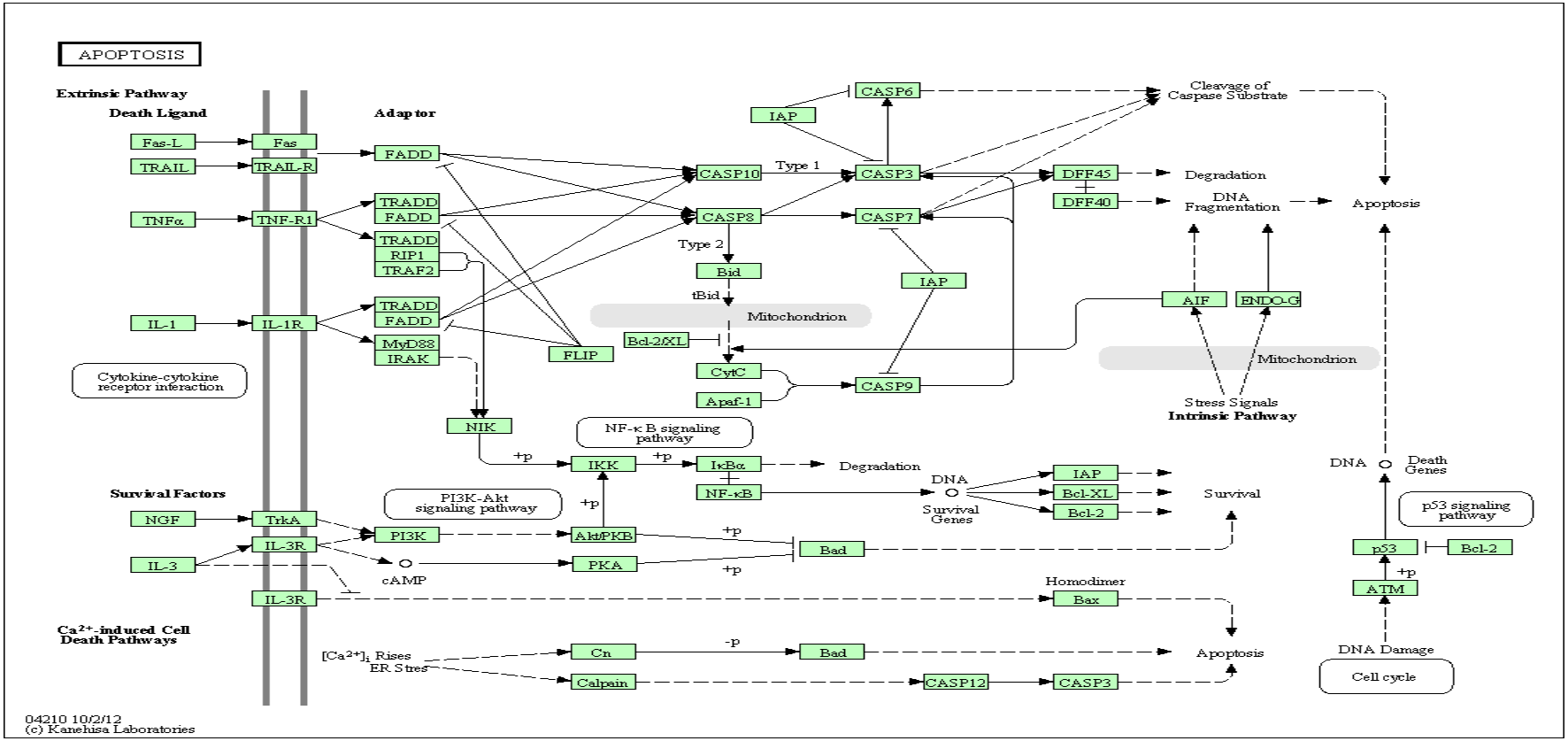

Appendix C-20

KEGG: Adherens Junction Cancer Signalling Pathway

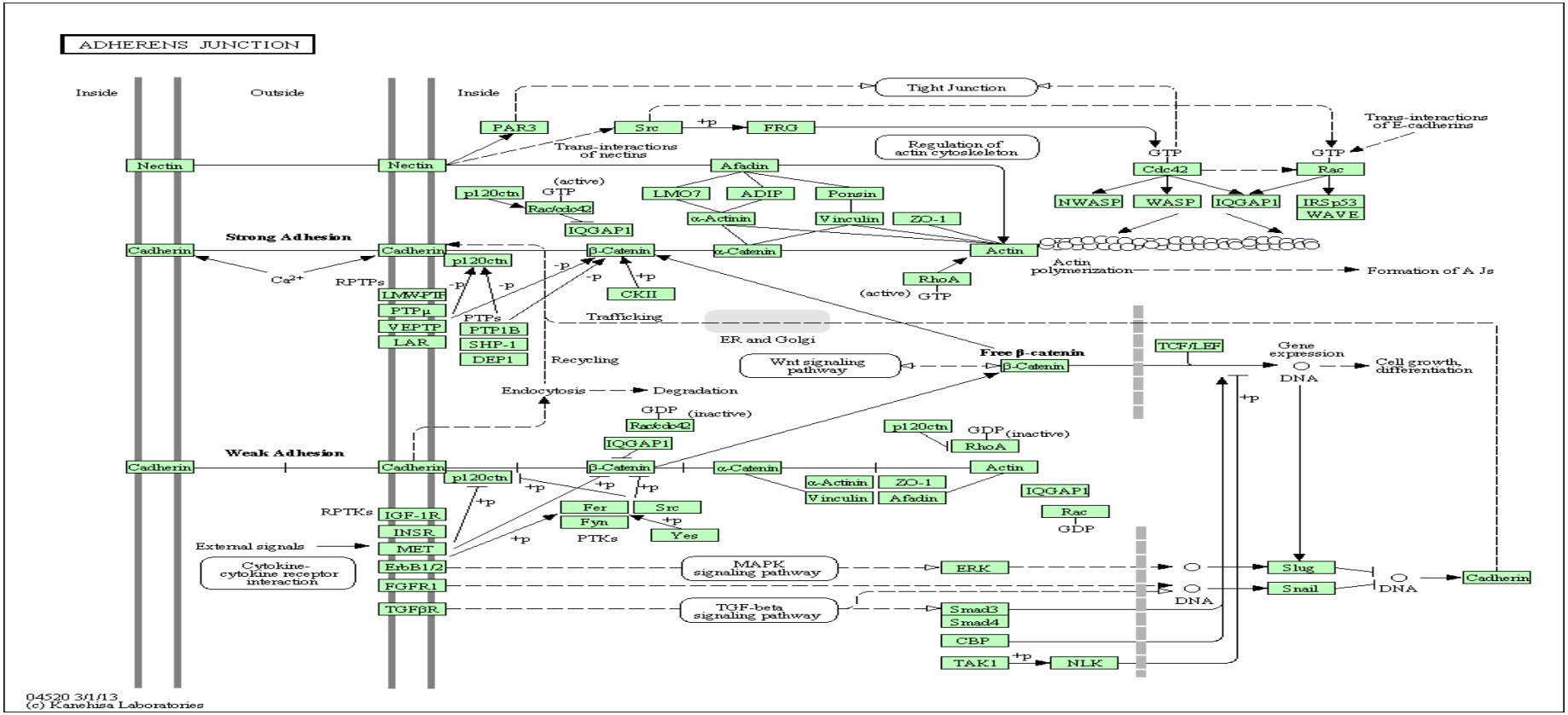

Appendix C-21

KEGG: Focal AdhesionCancer Signalling Pathway

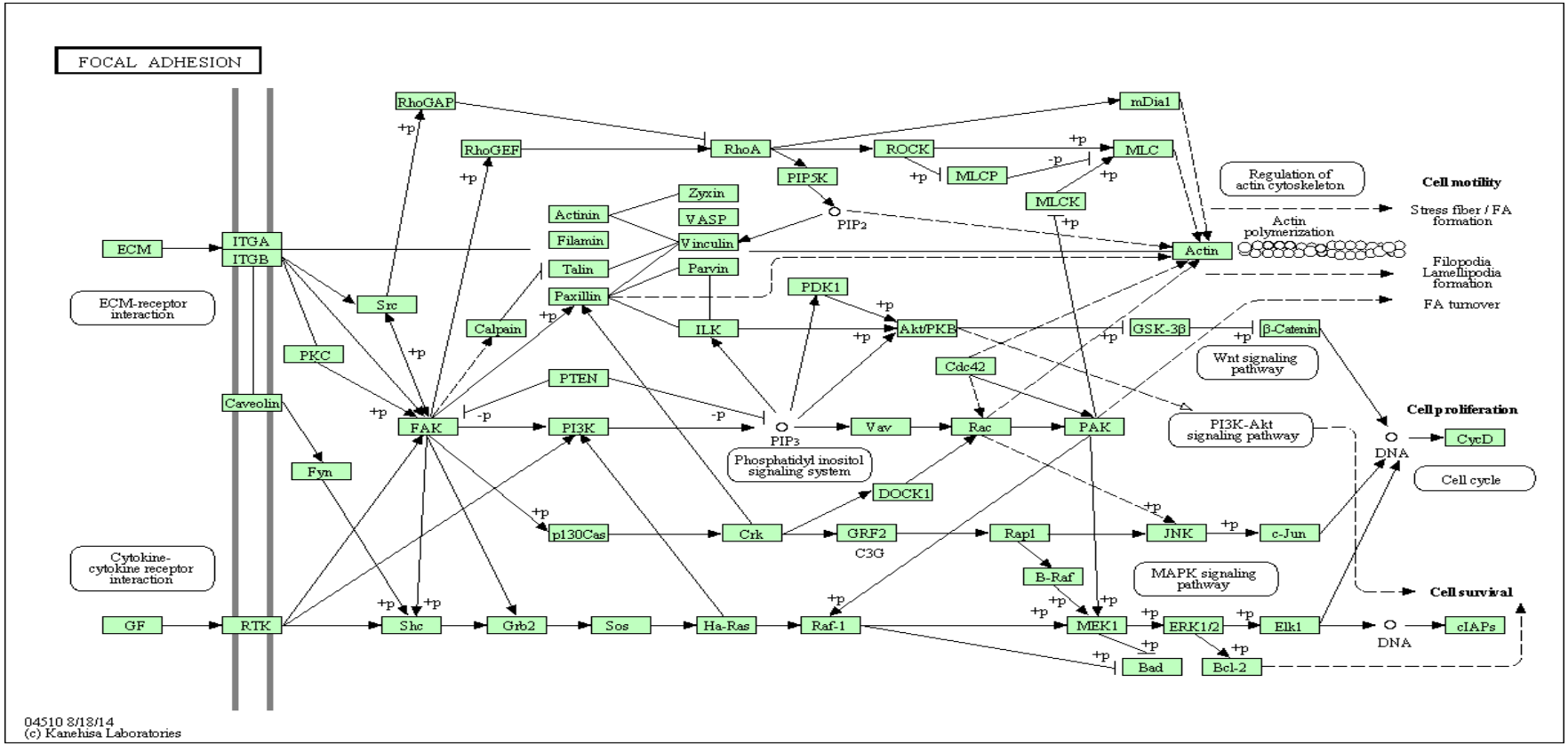

Appendix C-22

KEGG:Natural Killer Cell Mediated Cytotoxicity Cancer Signalling Pathway

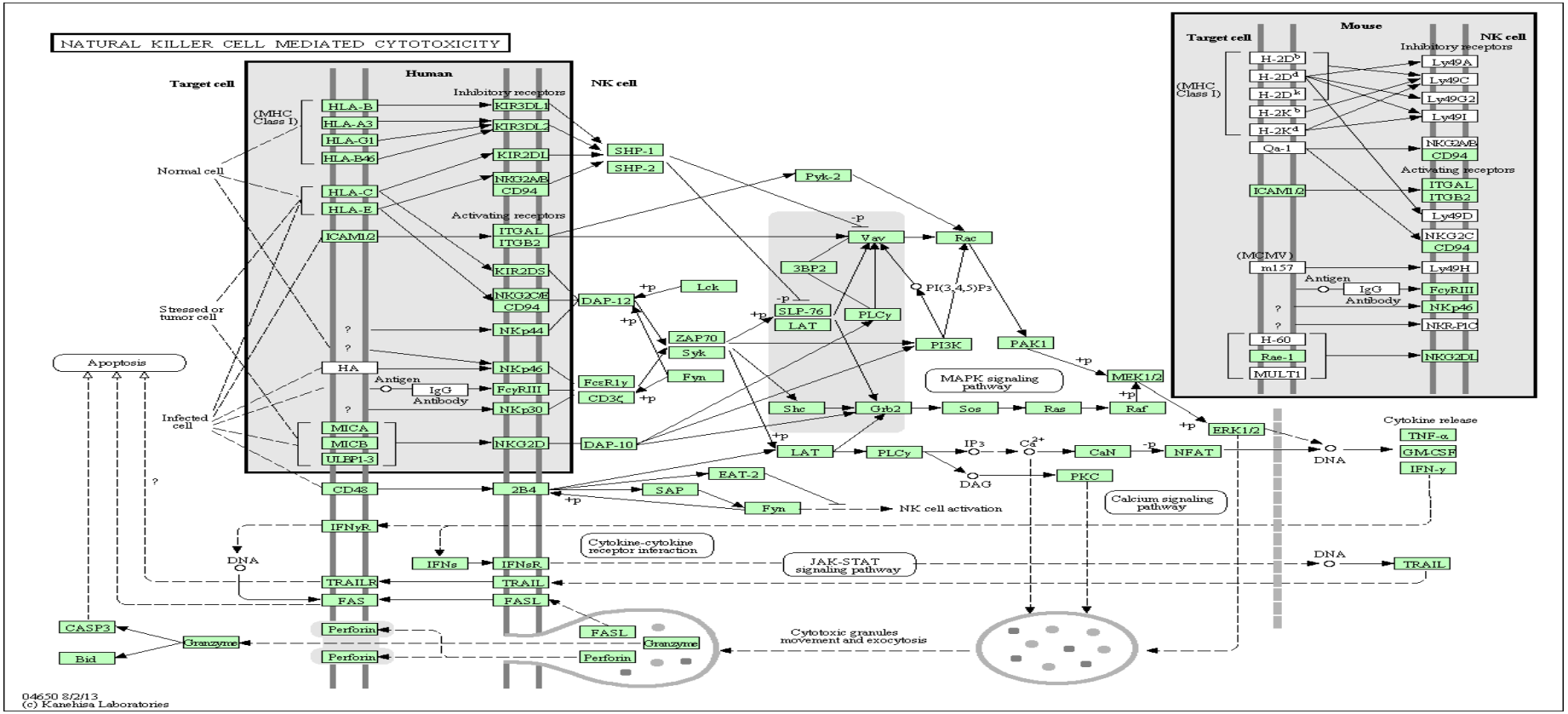

Appendix D

The Western Blot Assay for Verification of Proteins of Six Genes at Various Time Points. The Drug Ttreated Sample at Time Points of 12 hours, 24 hours and 48hours Versus Control 0 hour

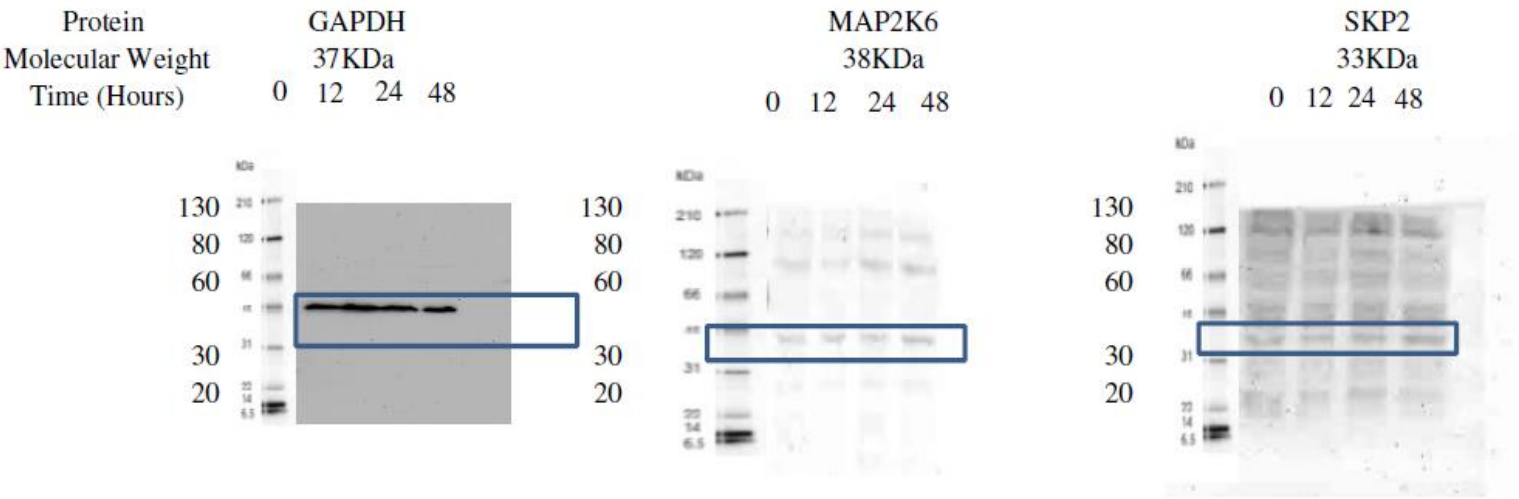

Appendix D Continued

The Western Blot Assay for Verification of Proteins of Six Genes at Various Time Points. The Drug Ttreated Sample at Time Points of 12 hours, 24 hours and 48 hours Versus Control 0 hour

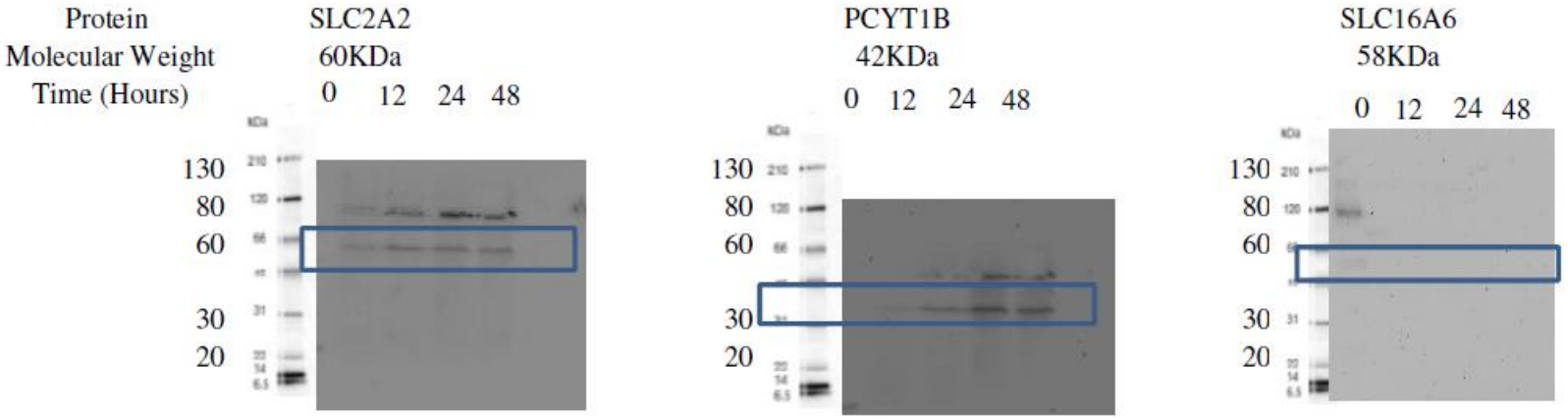

The Western Blot Assay for Verification of Proteins of Seven Genes at Various Time Points. The Drug Ttreated Sample at Time Points of 12 hours, 24 hours and 48 hours Versus Control 0 hour

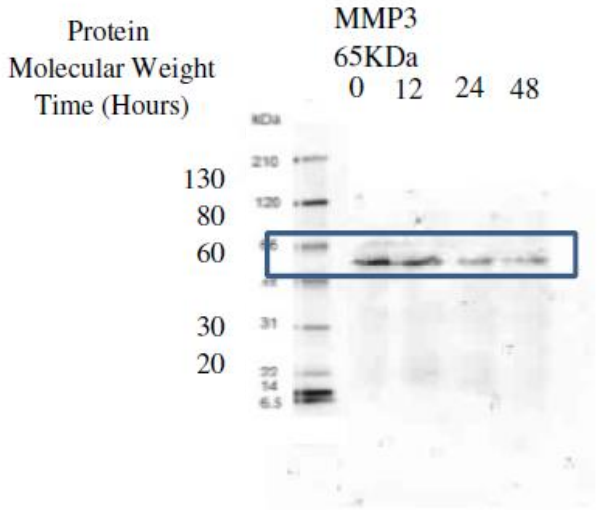

Appendix E

List of GeneswithExpressionFold-changes >2 and *P*-Value< 0.05 at Any Single Time-pointGenerated from DAVID Bioinformatics

OFFICIAL GENE SYMBOL	Name
WDR73	WD repeat domain 73
PABPC1	poly(A) binding protein, poly(A) binding protein, cytoplasmic 1
KLHL24	kelch-like 24 (Drosophila)
TTC21B	tetratricopeptide repeat domain 21B
RFC5	replication factor C (activator 1) 5, 36.5kDa
PAR1	Prader-Willi/Angelman region-1
TTR	transthyretin
DHRS4L2	dehydrogenase/reductase (SDR family) member 4 like 2
ARG2	arginase, type II
DKFZP434L187	hypothetical LOC26082
ADAM33	ADAM metallopeptidase domain 33
ADH5	alcohol dehydrogenase 5 (class III), chi polypeptide, pseudogene 4
PHTF2	putative homeodomain transcription factor 2
SCRN3	secernin 3
SKP2	S-phase kinase-associated protein 2 (p45)
GOLGA6L9	similar to golgi autoantigen, golgin subfamily a-like
GOLGA6L10	similar to golgi autoantigen, golgin subfamily a-like
LOC692247	hypothetical locus LOC692247
SERPINA7	serpin peptidase inhibitor, clade A (alpha-1 antiproteinase, antitrypsin), member 7
STC2	stanniocalcin 2
VCX2	variable charge, X-linked 2
JHDM1D	jumonji C domain containing histone demethylase 1 homolog D (S. cerevisiae)
IPW	imprinted in Prader-Willi syndrome (non-protein coding)
SPDYE1	speedy homolog E6 (Xenopus laevis)
SPDYE5	speedy homolog E6 (Xenopus laevis)
SPDYE6	speedy homolog E6 (Xenopus laevis)
ST7	suppression of tumourigenicity 7
PP13439	hypothetical LOC100128046
LOC100294341	similar to ADP-ribosylation factor-like 17
MIR1185-2	microRNA 1185-2
LSM5	LSM5 homolog, U6 small nuclear RNA associated (S. cerevisiae)
FNBP1L	formin binding protein 1-like
POTEB	POTE ankyrin domain family, member B

SLC25A14	solute carrier family 25 (mitochondrial carrier, brain), member 14
MYC	v-myc myelocytomatosis viral oncogene homolog (avian)
KIAA1984	KIAA1984; transmembrane protein 141
GPR75	G protein-coupled receptor 75
ACACA	acetyl-Coenzyme A carboxylase alpha
PTGIR	prostaglandin I2 (prostacyclin) receptor (IP)
ACSM3	acyl-CoA synthetase medium-chain family member 3
TRIB1	tribbles homolog 1 (Drosophila)
ZNF354A	zinc finger protein 354A
MT1A	metallothionein 1A
PCID2	PCI domain containing 2
CTGLF9P	centaurin, gamma-like family, member 9 pseudogene
G6PC	glucose-6-phosphatase, catalytic subunit
KRTAP9-6	keratin associated protein 9-6; keratin-associated protein 9-2-like 2-like
DAPK3	death-associated protein kinase 3
ANKRD1	ankyrin repeat domain 1 (cardiac muscle)
LY6G6E	lymphocyte antigen 6 complex, locus G6E
RPL23	ribosomal protein L23 pseudogene 6; ribosomal protein L23
CLDN25	claudin-like
FAM197Y5	similar to CYorf16 protein
IGLJ7	immunoglobulin lambda joining 7
JUNB	jun B proto-oncogene
IFIH1	interferon induced with helicase C domain 1
SNHG1	small nucleolar RNA host gene 1 (non-protein coding)
TPH1	tryptophan hydroxylase 1
ZNF783	zinc finger family member 783
PLSCR1	phospholipid scramblase 1
ZNF780A	zinc finger protein 780A
RPL7A	ribosomal protein L7a pseudogene 70
CYP21A2	cytochrome P450, family 21, subfamily A, polypeptide 2
MTG1	mitochondrial GTPase 1 homolog (S. cerevisiae)
RAD51AP1	RAD51 associated protein 1
SFN	stratifin
WDR6	WD repeat domain 6
RPL32	ribosomal protein L32
CREB3L4	cAMP responsive element binding protein 3-like 4
FAM122B	family with sequence similarity 122B
SGK223	homolog of rat pragma of Rnd2
SNORD47	small nucleolar RNA, C/D box 47
DPH5	DPH5 homolog (S. cerevisiae)
POLE	polymerase (DNA directed), epsilon
PDGFRL	platelet-derived growth factor receptor-like

ZNF90	zinc finger protein 90
RPL41	ribosomal protein L41
CTHRC1	collagen triple helix repeat containing 1
ZNF133	zinc finger protein 133
SERTAD1	SERTA domain containing 1
CDRT4	CMT1A duplicated region transcript 4
ZNF165	zinc finger protein 165
ATXN7L3	ataxin 7-like 3
FLJ45340	hypothetical LOC402483
CHMP1B	chromatin modifying protein 1B
CDKN2B	cyclin-dependent kinase inhibitor 2B (p15, inhibits CDK4)
SLC38A11	solute carrier family 38, member 11
FHL2	four and a half LIM domains 2
MAP1S	microtubule-associated protein 1S
SCN9A	sodium channel, voltage-gated, type IX, alpha subunit
GOT1	glutamic-oxaloacetic transaminase 1, soluble (aspartate aminotransferase 1)
COX19	COX19 cytochrome c oxidase assembly homolog (S. cerevisiae)
VMAC	vimentin-type intermediate filament associated coiled-coil protein
SNORD16	small nucleolar RNA, C/D box 16
MAFA	v-maf musculoaponeurotic fibrosarcoma oncogene homolog A (avian)
GPATCH2	G patch domain containing 2
MMP3	matrix metallopeptidase 3 (stromelysin 1, progelatinase)
GNA13	guanine nucleotide binding protein (G protein), alpha 13
PAGE2B	P antigen family, member 2B
ARL5B	ADP-ribosylation factor-like 5B
ALKBH6	alkB, alkylation repair homolog 6 (E. coli)
CEBPG	CCAAT/enhancer binding protein (C/EBP), gamma
TSNAX	translin-associated factor X
CLK1	CDC-like kinase 1
AGAP8	ArfGAP with GTPase domain, ankyrin repeat and PH domain 8
STAG3L3	stromal antigen 3-like 3
LOC440905	hypothetical LOC440905
L2HGDH	L-2-hydroxyglutarate dehydrogenase
HNRNPC	heterogeneous nuclear ribonucleoprotein C (C1/C2)
TRBV11-1	T cell receptor beta variable 11-1
CACYBP	similar to calcyclin binding protein; calcyclin binding protein
SOS1	son of sevenless homolog 1 (Drosophila)
FLJ31306	hypothetical LOC379025
FAM111B	family with sequence similarity 111, member B

SOLH	small optic lobes homolog (Drosophila)
TRA2A	transformer 2 alpha homolog (Drosophila)
DKFZP686I15217	hypothetical LOC401232
SUMO4	SMT3 suppressor of mif two 3 homolog 4 (S. cerevisiae)
LOC100132249	hypothetical LOC100132249
TMEM117	transmembrane protein 117
SNORA1	small nucleolar RNA, H/ACA box 1
FOXQ1	forkhead box Q1
RNASET2	ribonuclease T2
APTX	aprataxin
PUS10	pseudouridylate synthase 10
RNU7-35P	RNA, U7 small nuclear 35 pseudogene
ZNF331	zinc finger protein 331
SH3BP5	SH3-domain binding protein 5 (BTK-associated)
KIAA1009	KIAA1009
PCIF1	PDX1 C-terminal inhibiting factor 1
PFDN5	prefoldin subunit 5
GCLM	glutamate-cysteine ligase, modifier subunit
FAM92A1	family with sequence similarity 92, member A1
KRT84	keratin 84
NBEAL1	neurobeachin-like 1
PDCD6	programmed cell death 6
POTEE	POTE ankyrin domain family, member E
DZIP3	DAZ interacting protein 3, zinc finger
TRNT1	tRNA nucleotidyl transferase, CCA-adding, 1
C4BPB	complement component 4 binding protein, beta
LGR5	leucine-rich repeat-containing G protein-coupled receptor 5
LOC613037	nuclear pore complex interacting protein pseudogene
RHOF	ras homolog gene family, member F (in filopodia)
PPIL3	peptidylprolyl isomerase (cyclophilin)-like 3
LTB4R	leukotriene B4 receptor
ZNF283	zinc finger protein 283
EVL	Enah/Vasp-like
PCSK9	proprotein convertase subtilisin/kexin type 9
CPB2	carboxypeptidase B2 (plasma)
RIMBP3C	RIMS binding protein 3C
C6orf70	chromosome 6 open reading frame 70
PGAM1	phosphoglycerate mutase 1 (brain)
TRAV38-2DV8	T cell receptor alpha variable 38-2/delta variable 8
SCRN2	secernin 2
TOMM6	translocase of outer mitochondrial membrane 6 homolog (yeast)
ZSWIM6	zinc finger, SWIM-type containing 6
ATAD5	ATPase family, AAA domain containing 5
GOLGA5	golgi autoantigen, golgin subfamily a, 5
SLC7A5P2	SLC7A5 pseudogene

SNAR-G2	small ILF3/NF90-associated RNA G2
ANKRD18A	ankyrin repeat domain 18A
UPK3BL	uroplakin-like protein
MARK4	MAP/microtubule affinity-regulating kinase 4
ORAOV1	oral cancer overexpressed 1
MIR1224	microRNA 1224
CYCS	cytochrome c, somatic
KIF19	kinesin family member 19
LOC100132062	hypothetical LOC100132062
LOC100128288	hypothetical protein LOC100128288
TMEM135	transmembrane protein 135
ZNF337	zinc finger protein 337
C11orf39	chromosome 11 open reading frame 39
VASP	vasodilator-stimulated phosphoprotein
OR4F21	olfactory receptor, family 4, subfamily F, member 21
SYNJ2	synaptojanin 2
CDC42BPB	CDC42 binding protein kinase beta (DMPK-like)
PIK3CA	phosphoinositide-3-kinase, catalytic, alpha polypeptide
TRAJ28	T cell receptor alpha joining 28
LOC644961	similar to cytoplasmic beta-actin
RPL23AP7	ribosomal protein L23a pseudogene 7
MIR564	microRNA 564
FLJ20464	hypothetical protein FLJ20464
CCNL2	cyclin L2; chemokine (C-C motif) receptor 6
CDC34	cell division cycle 34 homolog (S. cerevisiae)
CENPC1	centromere protein C 1
PGM2L1	phosphoglucomutase 2-like 1
SNORD77	small nucleolar RNA, C/D box 77
YME1L1	YME1-like 1 (S. cerevisiae)
LOC440300	chondroitin sulfate proteoglycan 4 pseudogene
TSTD1	thiosulfate sulfurtransferase KAT, putative
ACSM1	acyl-CoA synthetase medium-chain family member 1
SNORA52	small nucleolar RNA, H/ACA box 52
OBP2B	odorant binding protein 2B
MLNR	motilin receptor
ZNF114	zinc finger protein 114
D2HGDH	D-2-hydroxyglutarate dehydrogenase
DGCR11	DiGeorge syndrome critical region gene 11
EDC3	enhancer of mRNA decapping 3 homolog (S. cerevisiae)
MAGOH	mago-nashi homolog, proliferation-associated (Drosophila)
STK36	serine/threonine kinase 36, fused homolog (Drosophila)
WIPI1	WD repeat domain, phosphoinositide interacting 1
ACOX2	acyl-Coenzyme A oxidase 2, branched chain
ELMOD2	ELMO/CED-12 domain containing 2

TOMM40L	translocase of outer mitochondrial membrane 40 homolog (yeast)-like
IGLJ3	immunoglobulin lambda joining 3
MT2A	metallothionein 2A
BRD1	bromodomain containing 1
TAC4	tachykinin 4 (hemokinin)
CYP24A1	cytochrome P450, family 24, subfamily A, polypeptide 1
LPPR1	plasticity related gene 3
NR1D1	nuclear receptor subfamily 1, group D, member 1
LOC100130428	IGYY565
FOXRED1	FAD-dependent oxidoreductase domain containing 1
FAM157B	family with sequence similarity 157, member B
LOC388242	coiled-coil domain containing 101 pseudogene
CHUK	conserved helix-loop-helix ubiquitous kinase
NKAP	NFKB activating protein
COG7	component of oligomeric golgi complex 7
NUMB	numb homolog (Drosophila)
LOC100288069	similar to hCG1640306
UCHL3	ubiquitin carboxyl-terminal esterase L3 (ubiquitin thiolesterase)
IGLJ5	immunoglobulin lambda joining 5 (non-functional)
POTEH	POTE ankyrin domain family, member H
DHCR7	7-dehydrocholesterol reductase
NCOR1	nuclear receptor co-repressor 1
SNORA11D	small nucleolar RNA, H/ACA box 11D
HCG9	HLA complex group 9
MYLK4	myosin light chain kinase family, member 4
TMEM144	transmembrane protein 144
NLGN4Y	neuroligin 4, Y-linked
F11R	F11 receptor
HNRNPA3	heterogeneous nuclear ribonucleoprotein A3
BOLA2	bolA homolog 2 (E. coli); bolA homolog 2B (E. coli)
SNRPE	small nuclear ribonucleoprotein polypeptide E-like 1
PRKY	protein kinase, Y-linked
PKD2	polycystic kidney disease 2 (autosomal dominant)
SCARNA17	small Cajal body-specific RNA 17
WDR52	WD repeat domain 52
GPR21	G protein-coupled receptor 21
PLAU	plasminogen activator, urokinase
DLEU2	deleted in lymphocytic leukemia 2 (non-protein coding)
SMO	smoothened homolog (Drosophila)
OPRL1	opiate receptor-like 1
ACPL2	acid phosphatase-like 2
ADAMTS4	ADAM metallopeptidase with thrombospondin type 1 motif, 4

SRF	serum response factor (c-fos serum response element-binding transcription factor)
DISC1	disrupted in schizophrenia 1
RTEL1	regulator of telomere elongation helicase 1
TNFRSF6B	tumour necrosis factor receptor superfamily, member 6b, decoy
LOC100130927	hypothetical protein LOC100130927
STEAP2	six transmembrane epithelial antigen of the prostate 2
ARPC1A	actin related protein 2/3 complex, subunit 1A, 41kDa
LGALS3	lectin, galactoside-binding, soluble, 3
ERN1	endoplasmic reticulum to nucleus signalling 1
TMEM97	transmembrane protein 97
ABCA11P	ATP-binding cassette, sub-family A (ABC1), member 11 (pseudogene)
SGCE	sarcoglycan, epsilon
ZNF658	zinc finger protein 658
RASGRF1	Ras protein-specific guanine nucleotide-releasing factor 1
DND1	dead end homolog 1 (zebrafish); similar to dead end homolog 1
KDM6B	lysine (K)-specific demethylase 6B
HIST1H2BI	histone cluster 1, H2bi
HIST1H2BG	histone cluster 1, H2bg
HIST1H2BC	histone cluster 1, H2bc
HIST1H2BE	histone cluster 1, H2be
HIST1H2BF	histone cluster 1, H2bf
LOC100130642	hypothetical LOC100130642
TNS4	tensin 4
ZNF776	zinc finger protein 776
C4orf36	chromosome 4 open reading frame 36
LOC493754	RAB guanine nucleotide exchange factor (GEF) 1 pseudogene
JUND	jun D proto-oncogene
ZNF224	zinc finger protein 224
RPS27	ribosomal protein S27 pseudogene 19
FLJ44342	hypothetical LOC645460
ANAPC4	anaphase promoting complex subunit 4
SNORD103A	small nucleolar RNA, C/D box 103A
FAM3C	family with sequence similarity 3, member C
RAB9B	RAB9B, member RAS oncogene family
SORBS2	sorbin and SH3 domain containing 2
CSGALNACT2	chondroitin sulfate N-acetylgalactosaminyltransferase 2
ADAMTS13	ADAM metallopeptidase with thrombospondin type 1 motif, 13
DDX11L1	similar to DEAD/H box polypeptide 11 like 9
SH2D7	SH2 domain containing 7
PLXNC1	plexin C1

ZMIZ1	zinc finger, MIZ-type containing 1
CELA3B	chymotrypsin-like elastase family, member 3B
HNRNPA2B1	heterogeneous nuclear ribonucleoprotein A2/B1
GATAD2A	GATA zinc finger domain containing 2A
CDC25B	cell division cycle 25 homolog B (S. pombe)
CHTF18	CTF18, chromosome transmission fidelity factor 18 homolog (S. cerevisiae)
SNRPG	small nuclear ribonucleoprotein polypeptide G
BRCA2	breast cancer 2, early onset
MGC2752	hypothetical LOC65996
ZNF789	zinc finger protein 789
CYR61	cysteine-rich, angiogenic inducer, 61
GLMN	glomulin, FKBP associated protein
HIBCH	3-hydroxyisobutyryl-Coenzyme A hydrolase
WIPF2	WAS/WASL interacting protein family, member 2
MIR933	microRNA 933
NCOR2	nuclear receptor co-repressor 2
RICTOR	RPTOR independent companion of MTOR, complex 2
DDX11	DEAD/H (Asp-Glu-Ala-Asp/His) box polypeptide 11
UBD	ubiquitin D
NPM1	nucleophosmin 1 (nucleolar phosphoprotein B23, numatrin) pseudogene 21
EIF2C2	eukaryotic translation initiation factor 2C, 2
DEFB113	defensin, beta 113
STX3	syntaxin 3
GPSM2	G-protein signalling modulator 2 (AGS3-like, C. elegans)
MIR421	microRNA 421
SNAI2	snail homolog 2 (Drosophila)
KDM4D	lysine (K)-specific demethylase 4D
VSNL1	visinin-like 1
MTRF1L	mitochondrial translational release factor 1-like
SLC37A4	solute carrier family 37 (glucose-6-phosphate transporter), member 4
CYP51A1	cytochrome P450, family 51, subfamily A, polypeptide 1
ERAP2	endoplasmic reticulum aminopeptidase 2
PPP4R4	protein phosphatase 4, regulatory subunit 4
NR0B2	nuclear receptor subfamily 0, group B, member 2
CDH26	cadherin-like 26
LOC553103	hypothetical LOC553103
FOXD4L6	forkhead box D4-like 6
RCAN3	RCAN family member 3
TRIM59	tripartite motif-containing 59
CARM1	coactivator-associated arginine methyltransferase 1

B3GNT3	UDP-GlcNAc:betaGal beta-1,3-N-acetylglucosaminyltransferase 3
DCDC5	doublecortin domain containing 5
RPL23AP32	ribosomal protein L23a pseudogene 32
SNORD75	small nucleolar RNA, C/D box 75
MT1X	metallothionein 1X
RNU7-11P	RNA, U7 small nuclear 11 pseudogene
CARD17	caspase recruitment domain family, member 17
OGFOD2	2-oxoglutarate and iron-dependent oxygenase domain containing 2
PRR4	proline rich 4 (lacrimal)
METRNL	meteorin, glial cell differentiation regulator-like
KCTD9	potassium channel tetramerisation domain containing 9
CSAD	cysteine sulfinic acid decarboxylase
PLCG1	phospholipase C, gamma 1
TMEM25	transmembrane protein 25
RPS2	ribosomal protein S2
FOXD4L5	forkhead box D4-like 5
SNORA70B	small nucleolar RNA, H/ACA box 70B (retrotransposed)
ABCA7	ATP-binding cassette, sub-family A (ABC1), member 7
STX16	syntaxin 16
PLEKHG2	pleckstrin homology domain containing, family G (with RhoGef domain) member 2
CCDC53	coiled-coil domain containing 53
ACVR1	activin A receptor, type I
CRIPAK	cysteine-rich PAK1 inhibitor
HES1	hairy and enhancer of split 1, (Drosophila)
SIGLEC15	sialic acid binding Ig-like lectin 15
C14orf145	chromosome 14 open reading frame 145
DLX2	distal-less homeobox 2
RNU7-77P	RNA, U7 small nuclear 77 pseudogene
CSNK1G3	casein kinase 1, gamma 3
SPAG4	sperm associated antigen 4
IL8	interleukin 8
CD46	CD46 molecule, complement regulatory protein
LOC644450	hypothetical protein LOC644450
TRAV1-2	T cell receptor alpha variable 1-2
PTPDC1	protein tyrosine phosphatase domain containing 1
ERCC1	excision repair cross-complementing rodent repair deficiency, complementation group 1
TUBB2A	tubulin, beta 2A
GSTO2	glutathione S-transferase omega 2
HERC2P5	hect domain and RLD 2 pseudogene 5
GLS	glutaminase
ZFP30	zinc finger protein 30 homolog (mouse)

FANCA	Fanconi anemia, complementation group A
ZNF614	zinc finger protein 614
HMGN3	high mobility group nucleosomal binding domain 3
B4GALT6	UDP-Gal:betaGlcNAc beta 1,4-galactosyltransferase, polypeptide 6
MTERFD3	MTERF domain containing 3
ANAPC10	anaphase promoting complex subunit 10
SNORA64	small nucleolar RNA, H/ACA box 64
LRRC25	leucine rich repeat containing 25
RNU7-72P	RNA, U7 small nuclear 72 pseudogene
LRP5	low density lipoprotein receptor-related protein 5
SLC6A14	solute carrier family 6 (amino acid transporter), member 14
NKAIN1	Na+/K+ transporting ATPase interacting 1
IFT80	intraflagellar transport 80 homolog (Chlamydomonas)
RNU7-47P	RNA, U7 small nuclear 47 pseudogene
C9orf3	chromosome 9 open reading frame 3
GDPD5	glycerophosphodiester phosphodiesterase domain containing 5
CCDC41	coiled-coil domain containing 41
GADD45B	growth arrest and DNA-damage-inducible, beta
CLEC18C	C-type lectin domain family 18, member C
MSTO2P	misato homolog 2 pseudogene
ASAP2	ArfGAP with SH3 domain, ankyrin repeat and PH domain 2
FAM133B	family with sequence similarity 133, member B pseudogene
MEX3C	mex-3 homolog C (C. elegans)
STMN1	stathmin 1
MBNL2	muscleblind-like 2 (Drosophila)
LRTOMT	leucine rich transmembrane and 0-methyltransferase domain containing
CHD2	chromodomain helicase DNA binding protein 2
LCK	lymphocyte-specific protein tyrosine kinase
AGAP11	ankyrin repeat and GTPase domain Arf GTPase activating protein 11
LOC100133032	hypothetical LOC100133032
TCEA1	transcription elongation factor A (SII), 1
TCEA1P2	transcription elongation factor A (SII), 1 pseudogene 2
BTAF1	BTAF1 RNA polymerase II
DCDC1	doublecortin domain containing 1
LOC90784	hypothetical protein LOC90784
GSTA3	glutathione S-transferase alpha 3
LOC100287628	hypothetical protein LOC100287628
AQP3	aquaporin 3 (Gill blood group)
CNP	2',3'-cyclic nucleotide 3' phosphodiesterase

PARD3	par-3 partitioning defective 3 homolog (C. elegans)
MAPK13	mitogen-activated protein kinase 13
WASH1	similar to WAS protein family homolog 1
MED13L	mediator complex subunit 13-like
SAT1	spermidine/spermine N1-acetyltransferase 1
ZNF280A	zinc finger protein 280A
CDHR3	hypothetical protein FLJ23834
SNORA27	small nucleolar RNA, H/ACA box 27
MTM1	myotubularin 1
SERINC2	serine incorporator 2
MIDN	midnolin
PNN	pinin, desmosome associated protein
BMS1P2	BMS1 pseudogene 2
MAT2A	methionine adenosyltransferase II, alpha
ARHGAP33	sorting nexin 26
ST7L	suppression of tumourigenicity 7 like
RALB	v-ral simian leukemia viral oncogene homolog B (ras related; GTP binding protein)
RNF19B	ring finger protein 19B
TREX1	three prime repair exonuclease 1
CCDC15	coiled-coil domain containing 15
CHKB-CPT1B	choline kinase-like, carnitine palmitoyltransferase 1B (muscle) transcription unit
GUSBP3	glucuronidase, beta pseudogene
CYTH2	cytohesin 2
TMPRSS9	transmembrane protease, serine 9
SOD2	superoxide dismutase 2, mitochondrial
DDX11L9	similar to DEAD/H box polypeptide 11 like 9
HGFAC	HGF activator
CEBPB	CCAAT/enhancer binding protein (C/EBP), beta
TM2D1	TM2 domain containing 1
OBFC1	oligonucleotide/oligosaccharide-binding fold containing 1
PIGZ	phosphatidylinositol glycan anchor biosynthesis, class Z
CHRD	chordin
LOC441259	PMS2 postmeiotic segregation increased 2 (S. cerevisiae)-like
KRT80	keratin 80
SCFV	single-chain Fv fragment
FKSG49	FKSG49
C5orf54	chromosome 5 open reading frame 54
HAUS4	HAUS augmin-like complex, subunit 4
CLMN	calmin (calponin-like, transmembrane)
SLC2A3	solute carrier family 2 (facilitated glucose transporter), member 3
MIRLET7E	microRNA let-7e
SESN1	sestrin 1

DCAF10	WD repeat domain 32
SNORD116-28	small nucleolar RNA, C/D box 116-28
XPNPEP3	X-prolyl aminopeptidase (aminopeptidase P) 3, putative
PRH1	proline-rich protein HaeIII subfamily 1
CCL20	chemokine (C-C motif) ligand 20
MIR34A	microRNA 34a
SERPINB2	serpin peptidase inhibitor, clade B (ovalbumin), member 2
MED8	mediator complex subunit 8
TTPA	tocopherol (alpha) transfer protein
CCDC138	coiled-coil domain containing 138
RSL24D1	ribosomal L24 domain containing 1
KLK11	kallikrein-related peptidase 11
SPDYE2	speedy homolog E2 (Xenopus laevis)
SNAR-C3	small ILF3/NF90-associated RNA C3
NAT9	N-acetyltransferase 9 (GCN5-related, putative)
FNDC4	fibronectin type III domain containing 4
PAR-SN	paternally expressed transcript PAR-SN
PDE4D	phosphodiesterase 4D
UGT2B28	UDP glucuronosyltransferase 2 family, polypeptide B28
MIR93	microRNA 93
ZFP36	zinc finger protein 36, C3H type, homolog (mouse)
RPL13AP6	ribosomal protein L13a pseudogene 6
PPP1R10	protein phosphatase 1, regulatory (inhibitor) subunit 10
ARHGAP11B	Rho GTPase activating protein 11B; Rho GTPase activating protein 11A
TIA1	TIA1 cytotoxic granule-associated RNA binding protein
AHI1	Abelson helper integration site 1
DQX1	DEAQ box RNA-dependent ATPase 1
RPL21	119; ribosomal protein L21 pseudogene 125
AK2	adenylate kinase 2
IRAK2	interleukin-1 receptor-associated kinase 2
RRAS	related RAS viral (r-ras) oncogene homolog
IL15RA	interleukin 15 receptor, alpha
OXER1	oxoeicosanoid (OXE) receptor 1
MTMR2	myotubularin related protein 2
ADAMTS6	ADAM metallopeptidase with thrombospondin type 1 motif, 6
CUL9	cullin 9
LONRF1	LON peptidase N-terminal domain and ring finger 1
SMYD4	SET and MYND domain containing 4
EP400NL	EP400 N-terminal like
EGR1	early growth response 1

GLUD1	glutamate dehydrogenase 1
BHLHE40	basic helix-loop-helix family, member e40
LOC729603	calcium binding protein P22 pseudogene
CACNA2D4	calcium channel, voltage-dependent, alpha 2/delta subunit 4
RPL36A	ribosomal protein L36a
HNRNPH2	heterogeneous nuclear ribonucleoprotein H2 (H')
IGKV1-8	immunoglobulin kappa variable 1-8
TAS1R1	taste receptor, type 1, member 1
FHL3	four and a half LIM domains 3
RHOT1	ras homolog gene family, member T1
MITD1	MIT, microtubule interacting and transport, domain containing 1
LIPG	lipase, endothelial
FADS2	fatty acid desaturase 2
PTAFR	platelet-activating factor receptor
MIR645	microRNA 645
ZNF594	zinc finger protein 594
GOLT1A	golgi transport 1 homolog A (S. cerevisiae)
MAFG	v-maf musculoaponeurotic fibrosarcoma oncogene homolog G (avian)
TAGLN	transgelin
C3orf35	chromosome 3 open reading frame 35
LOC728730	hypothetical LOC728730
MADD	MAP-kinase activating death domain
RAPH1	Ras association (RalGDS/AF-6) and pleckstrin homology domains 1
SERPINB9	serpin peptidase inhibitor, clade B (ovalbumin), member 9
SNORD44	small nucleolar RNA, C/D box 44
ETV3	ets variant 3
PRSS22	protease, serine, 22
ATF3	activating transcription factor 3
CD22	CD22 molecule
EME1	essential meiotic endonuclease 1 homolog 1 (S. pombe)
IL6R	interleukin 6 receptor
ZNF260	zinc finger protein 260
NBPF7	neuroblastoma breakpoint family, member 7
PTCD2	pentatricopeptide repeat domain 2
MIR623	microRNA 623
FAM197Y2	chromosome Y open reading frame 16
TEAD3	TEA domain family member 3
SNORD79	small nucleolar RNA, C/D box 79
ABCG5	ATP-binding cassette, sub-family G (WHITE), member 5
NVL	nuclear VCP-like
RGL1	ral guanine nucleotide dissociation stimulator-like 1

HOXD1	homeobox D1
MIR1304	microRNA 1304
PPIA	peptidylprolyl isomerase A (cyclophilin A)
ZNF768	zinc finger protein 768
MSTO1	misato homolog 1 (Drosophila)
C21orf90	chromosome 21 open reading frame 90
CROT	carnitine O-octanoyltransferase
SNORD33	small nucleolar RNA, C/D box 33
SNORD32A	small nucleolar RNA, C/D box 32A
CENPL	centromere protein L
ALS2CR8	amyotrophic lateral sclerosis 2 (juvenile) chromosome region, candidate 8
CPLX3	complexin 3
LOC728208	hypothetical protein LOC728208
SNORD5	small nucleolar RNA, C/D box 5
FLJ41757	hypothetical gene supported by AF086285
HNRNPA1	similar to heterogeneous nuclear ribonucleoprotein A1
RBM27	RNA binding motif protein 27
ZNF688	zinc finger protein 688; zinc finger protein 785
LOC100130015	hypothetical LOC100130015
DHX32	DEAH (Asp-Glu-Ala-His) box polypeptide 32
KRTAP10-7	keratin associated protein 10-7
TEX9	testis expressed 9
FAM138E	family with sequence similarity 138, member E
SERPINA4	serpin peptidase inhibitor, clade A (alpha-1 antiproteinase, antitrypsin), member 4
SLC16A6	solute carrier family 16, member 6
SLC37A2	solute carrier family 37 (glycerol-3-phosphate transporter), member 2
SUMO1	SUMO1 pseudogene 3
SLC7A11	solute carrier family 7, (cationic amino acid transporter, y+ system) member 11
MAP2K6	mitogen-activated protein kinase kinase 6
LOC728323	hypothetical LOC728323
PTGIS	prostaglandin I2 (prostacyclin) synthase
TRAM1	translocation associated membrane protein 1
LOC645166	lymphocyte-specific protein 1 pseudogene
ZSCAN16	zinc finger and SCAN domain containing 16
NQO1	NAD(P)H dehydrogenase, quinone 1
C9orf152	chromosome 9 open reading frame 152
DGCR8	DiGeorge syndrome critical region gene 8
FAM111A	family with sequence similarity 111, member A
FOSL1	FOS-like antigen 1
MLF1IP	MLF1 interacting protein
PHF11	PHD finger protein 11
ISX	intestine-specific homeobox

TNFRSF19	tumour necrosis factor receptor superfamily, member 19
LOC613038	coiled-coil domain containing 101 pseudogene
PLXNA2	plexin A2
AKR1D1	aldo-keto reductase family 1, member D1 (delta 4-3-ketosteroid-5-beta-reductase)
SYNE2	spectrin repeat containing, nuclear envelope 2
NUPR1	nuclear protein, transcriptional regulator, 1
KLF12	Kruppel-like factor 12
TMCC2	transmembrane and coiled-coil domain family 2
CADM1	cell adhesion molecule 1
IGHM	immunoglobulin heavy constant gamma 1 (G1m marker)
NPPC	natriuretic peptide precursor C
DNAJC5	DnaJ (Hsp40) homolog, subfamily C, member 5
DDC	dopa decarboxylase (aromatic L-amino acid decarboxylase)
ARHGAP27	Rho GTPase activating protein 27
RHBG	Rh family, B glycoprotein (gene/pseudogene)
MAGED4B	melanoma antigen family D, 4B; melanoma antigen family D, 4
MAGED4	melanoma antigen family D, 4B; melanoma antigen family D, 4
ZNF443	zinc finger protein 443
PLCD3	phospholipase C, delta 3
LOC729083	hypothetical protein LOC729083
LOC728724	hCG1814486
NQO2	NAD(P)H dehydrogenase, quinone 2
TPD52L2	tumour protein D52-like 2
CDO1	cysteine dioxygenase, type I
IGBP1	immunoglobulin (CD79A) binding protein 1
POM121L1P	POM121 membrane glycoprotein-like 1 (rat) pseudogene
ITPR2	inositol 1,4,5-triphosphate receptor, type 2
ACBD5	acyl-Coenzyme A binding domain containing 5
MIR27B	microRNA 27b
CARS	cysteinyl-tRNA synthetase
ABHD4	abhydrolase domain containing 4
GINS1	GINS complex subunit 1 (Psf1 homolog)
DDIT3	DNA-damage-inducible transcript 3
FATE1	fetal and adult testis expressed 1
MPPE1	metallophosphoesterase 1
PRMT7	protein arginine methyltransferase 7
SGTB	small glutamine-rich tetratricopeptide repeat (TPR)-containing, beta
IDS	iduronate 2-sulfatase
SNORD103B	small nucleolar RNA, C/D box 103B
TXNIP	thioredoxin interacting protein

TBC1D8	TBC1 domain family, member 8 (with GRAM domain)
TAF1D	TATA box binding protein (TBP)-associated factor, RNA polymerase I, D, 41kDa
SNORA32	small nucleolar RNA, H/ACA box 32
ACSS1	acyl-CoA synthetase short-chain family member 1
SH2B3	SH2B adaptor protein 3
UBE2G2	ubiquitin-conjugating enzyme E2G 2 (UBC7 homolog, yeast)
LOC643696	hypothetical LOC643696
MKRN3	makorin ring finger protein 3
TMCO6	transmembrane and coiled-coil domains 6
LOC440149	hypothetical LOC440149
PACS1	phosphofurin acidic cluster sorting protein 1
SNORD107	small nucleolar RNA, C/D box 107
SKIL	SKI-like oncogene
PION	pigeon homolog (Drosophila)
AGAP7	ArfGAP with GTPase domain, ankyrin repeat and PH domain 7
AREGB	amphiregulin; amphiregulin B
AREG	amphiregulin; amphiregulin B
POLE2	polymerase (DNA directed), epsilon 2 (p59 subunit)
MRPL45P2	mitochondrial ribosomal protein L45 pseudogene 2
MIR637	microRNA 637
NAMPTL	nicotinamide phosphoribosyltransferase-like
MPV17L	MPV17 mitochondrial membrane protein-like
UHRF2	ubiquitin-like with PHD and ring finger domains 2
PAQR5	progestin and adipoQ receptor family member V
SSH1	slingshot homolog 1 (Drosophila)
ZNF493	zinc finger protein 493
ADH4	alcohol dehydrogenase 4 (class II), pi polypeptide
ATP7B	ATPase, Cu++ transporting, beta polypeptide
LOC441124	hypothetical gene supported by AK093729; BX647918
DEFB103A	defensin, beta 103B; defensin, beta 103A
DEFB103B	defensin, beta 103B; defensin, beta 103A
EED	embryonic ectoderm development
C9orf173	hypothetical protein LOC441476
NDRG1	N-myc downstream regulated 1
DOC2GP	double C2, gamma pseudogene
CBWD1	COBW domain containing 6; COBW domain containing 1
CBWD6	COBW domain containing 6; COBW domain containing 1
SPG7	spastic paraplegia 7 (pure and complicated autosomal recessive)
SNORD80	small nucleolar RNA, C/D box 80
PRSS33	protease, serine, 33

SFI1	Sfi1 homolog, spindle assembly associated (yeast)
GLB1L	galactosidase, beta 1-like
KRT37	keratin 37
ZGPAT	zinc finger, CCCH-type with G patch domain
FAM27B	family with sequence similarity 27, member B
FAM27C	family with sequence similarity 27, member C
FAM27A	family with sequence similarity 27, member A
CISD2	CDGSH iron sulfur domain 2
TMEM18	transmembrane protein 18
GDPD1	glycerophosphodiester phosphodiesterase domain containing 1
PCBP1	poly(rC) binding protein 1
SNAR-C5	small ILF3/NF90-associated RNA C5
MT1G	metallothionein 1G
TCEA3	transcription elongation factor A (SII), 3
GLT8D1	glycosyltransferase 8 domain containing 1
APOF	apolipoprotein F
OSTF1	osteoclast stimulating factor 1
BMS1P7	BMS1 pseudogene 7
EIF1B	eukaryotic translation initiation factor 1B
DDX11L10	DEAD/H box polypeptide 11 like 11
MAP3K2	mitogen-activated protein kinase kinase kinase 2
MAFK	v-maf musculoaponeurotic fibrosarcoma oncogene homolog K (avian)
CLDN19	claudin 19
TRNP1	TMF1-regulated nuclear protein 1
CREBZF	CREB/ATF bZIP transcription factor
MKLN1	muskelin 1, intracellular mediator containing kelch motifs
PARG	similar to poly (ADP-ribose) glycohydrolase; poly (ADP-ribose) glycohydrolase
CYP4F12	similar to cytochrome P450, family 4, subfamily F, polypeptide 12
ITPR1	inositol 1,4,5-triphosphate receptor, type 1
LOC339260	hypothetical protein LOC339260
ACACB	acetyl-Coenzyme A carboxylase beta
ZNF440	zinc finger protein 440
DUT	deoxyuridine triphosphatase
LOC100129518	similar to hCG2029803
GRB10	growth factor receptor-bound protein 10
SNORD53	small nucleolar RNA, C/D box 53
THRA	thyroid hormone receptor, alpha (erythroblastic leukemia viral (v-erb-a) oncogene homolog, avian)
NAIP	NLR family, apoptosis inhibitory protein
SNAR-E	small ILF3/NF90-associated RNA E
SUB1	SUB1 homolog (S. cerevisiae)
ACTR3B	ARP3 actin-related protein 3 homolog B (yeast)
CASP8AP2	caspase 8 associated protein 2

MRPS6	mitochondrial ribosomal protein S6
TMEM218	transmembrane protein 218
MIR570	microRNA 570
HIST2H3PS2	histone cluster 2, H3, pseudogene 2
TTC30A	tetratricopeptide repeat domain 30A
SH3BGR	SH3 domain binding glutamic acid-rich protein
SMN2	survival of motor neuron 2, centromeric
SMN1	survival of motor neuron 1, telomeric
LUC7L3	cisplatin resistance-associated overexpressed protein
CRLF3	cytokine receptor-like factor 3
CSRNP1	cysteine-serine-rich nuclear protein 1
CREBBP	CREB binding protein
CAMLG	calcium modulating ligand
SESN2	sestrin 2
LOC441081	POM121 membrane glycoprotein (rat) pseudogene
NPIPL2	nuclear pore complex interacting protein-like 2
SH3RF1	SH3 domain containing ring finger 1
SETD1B	SET domain containing 1B
SLC2A10	solute carrier family 2 (facilitated glucose transporter), member 10
CFI	complement factor I
PPP1R1B	protein phosphatase 1, regulatory (inhibitor) subunit 1B
LOC100131655	hypothetical LOC100131655
C1orf220	chromosome 1 open reading frame 220
NBPF9	neuroblastoma breakpoint family, member 9
NBPF10	neuroblastoma breakpoint family, member 10
NBPF1	neuroblastoma breakpoint family, member 1
NBPF12	neuroblastoma breakpoint family, member 12
NBPF8	neuroblastoma breakpoint family, member 8
LOC81691	exonuclease NEF-sp
LOC338797	hypothetical LOC338797
SNHG10	small nucleolar RNA host gene 10 (non-protein coding)
SCARNA13	small Cajal body-specific RNA 13
HIVEP2	human immunodeficiency virus type I enhancer binding protein 2
LOC100288102	similar to Putative uncharacterized protein C20orf69
EPAS1	endothelial PAS domain protein 1
LOC100216546	hypothetical LOC100216546
FAM3B	family with sequence similarity 3, member B
OAS1	2',5'-oligoadenylate synthetase 1, 40/46kDa
SLC44A5	solute carrier family 44, member 5
SQRDL	sulfide quinone reductase-like (yeast)
LOC100272216	hypothetical LOC100272216
SENP7	SUMO1/sentrin specific peptidase 7
UBE2N	ubiquitin-conjugating enzyme E2N (UBC13 homolog, yeast)

UQCC	ubiquinol-cytochrome c reductase complex chaperone
CMIP	c-Maf-inducing protein
BMS1P6	BMS1 pseudogene 6
MAGI3	membrane associated guanylate kinase, WW and PDZ domain containing 3
AKR7L	aldo-keto reductase family 7-like
LRRC45	leucine rich repeat containing 45
HIST2H2BC	histone cluster 2, H2bc
MIR587	microRNA 587
RABGAP1	RAB GTPase activating protein 1
MMAB	methylmalonic aciduria (cobalamin deficiency) cblB type
UBE2B	ubiquitin-conjugating enzyme E2B (RAD6 homolog)
SUCLA2	succinate-CoA ligase, ADP-forming, beta subunit
NFE2L2	nuclear factor (erythroid-derived 2)-like 2
EREG	epiregulin
PINK1	PTEN induced putative kinase 1
GHRLOS	ghrelin opposite strand (non-protein coding)
NR3C1	nuclear receptor subfamily 3, group C, member 1 (glucocorticoid receptor)
MT1F	metallothionein 1F
ZNF664	zinc finger protein 664
LOC399753	hypothetical LOC399753
UCA1	urothelial cancer associated 1
TNFSF10	tumour necrosis factor (ligand) superfamily, member 10
SPATA5	spermatogenesis associated 5
LOC100292922	similar to hCG1644292
DHRS1	dehydrogenase/reductase (SDR family) member 1
LOC728715	similar to hCG38149
AIP	aryl hydrocarbon receptor interacting protein
SMOX	spermine oxidase
RB1CC1	RB1-inducible coiled-coil 1
MUC15	mucin 15, cell surface associated
STK40	serine/threonine kinase 40
L1CAM	L1 cell adhesion molecule
NFYC	nuclear transcription factor Y, gamma
MIR99B	microRNA 99b
THBS1	thrombospondin 1
CMC1	COX assembly mitochondrial protein homolog (S. cerevisiae)
PRAMEF16	PRAME family member 16
CCDC111	coiled-coil domain containing 111
HSD17B7	hydroxysteroid (17-beta) dehydrogenase 7
LOC728407	poly(ADP-ribose) glycohydrolase pseudogene

TWF1	twinfilin, actin-binding protein, homolog 1 (Drosophila)
NHLRC3	NHL repeat containing 3
C1orf159	chromosome 1 open reading frame 159
SGK494	uncharacterized serine/threonine-protein kinase SgK494
IFT172	intraflagellar transport 172 homolog (Chlamydomonas)
ANG	angiogenin, ribonuclease, RNase A family, 5
RRN3	RRN3 RNA polymerase I transcription factor homolog (S. cerevisiae)
SESN3	sestrin 3
CPT1B	choline kinase beta; carnitine palmitoyltransferase 1B (muscle)
CHKB	choline kinase beta; carnitine palmitoyltransferase 1B (muscle)
PRLR	prolactin receptor
CACNA1H	calcium channel, voltage-dependent, T type, alpha 1H subunit
IL11	interleukin 11
RPL37	ribosomal protein L37
ZRANB2	zinc finger, RAN-binding domain containing 2
HSD17B7P2	hydroxysteroid (17-beta) dehydrogenase 7 pseudogene 2
LOC219690	hypothetical protein LOC219690
FAM72C	family with sequence similarity 72, member C
HMGA1	hypothetical LOC100130009; high mobility group AT-hook 1
SLA2	Src-like-adaptor 2
LIX1L	Lix1 homolog (mouse)-like
LOC729737	hypothetical LOC729737
GOLGA6L3	hypothetical golgin-like LOC100133220
XPA	xeroderma pigmentosum, complementation group A
FLJ45513	hypothetical LOC729220
C3orf58	chromosome 3 open reading frame 58
KLF10	Kruppel-like factor 10
CYTH3	cytohesin 3
CYP4F3	cytochrome P450, family 4, subfamily F, polypeptide 3
FBXL21	F-box and leucine-rich repeat protein 21
MST1P2	macrophage stimulating, pseudogene 2
ETS2	v-ets erythroblastosis virus E26 oncogene homolog 2 (avian)
PPP1R2	protein phosphatase 1, regulatory (inhibitor) subunit 2
GSTP1	glutathione S-transferase pi 1
CHORDC1	cysteine and histidine-rich domain (CHORD)-containing 1
SNORD20	small nucleolar RNA, C/D box 20

WDR67	WD repeat domain 67
JUN	jun oncogene
C14orf1	chromosome 14 open reading frame 1
LRIG2	leucine-rich repeats and immunoglobulin-like domains 2
SPCS2	signal peptidase complex subunit 2 homolog (S. cerevisiae)
NR4A1	nuclear receptor subfamily 4, group A, member 1
KNTC1	kinetochore associated 1
TTC31	tetratricopeptide repeat domain 31
NPIPL3	nuclear pore complex interacting protein-like 3
ARHGEF17	Rho guanine nucleotide exchange factor (GEF) 17
KRTAP9-3	keratin associated protein 9-3
KLF6	Kruppel-like factor 6
CYTL1	cytokine-like 1
RGS10	regulator of G-protein signalling 10
SLC4A11	solute carrier family 4, sodium borate transporter, member 11
SNAR-D	small ILF3/NF90-associated RNA D
ACAD10	acyl-Coenzyme A dehydrogenase family, member 10
MYL5	myosin, light chain 5, regulatory
TMEM106C	transmembrane protein 106C
GOLGA6L5	golgi autoantigen, golgin subfamily a-like pseudogene
HMGA2	high mobility group AT-hook 2
EEF1A2	eukaryotic translation elongation factor 1 alpha 2
PTGR2	prostaglandin reductase 2
UBC	ubiquitin C
ATPBD4	ATP binding domain 4
GTF2IRD1	GTF2I repeat domain containing 1
TECPR1	tectonin beta-propeller repeat containing 1
MTRF1	mitochondrial translational release factor 1
KRTAP9-8	keratin associated protein 9-8
HCG23	HLA complex group 23
FKSG29	FKSG29
ZNF483	zinc finger protein 483
DDX11L2	hypothetical LOC84771
ESF1	ESF1, nucleolar pre-rRNA processing protein, homolog (S. cerevisiae)
LOC283587	hypothetical protein LOC283587
MIR608	microRNA 608
PNMA1	paraneoplastic antigen MA1
CLTCL1	clathrin, heavy chain-like 1
NFKBIZ	nuclear factor of kappa light polypeptide gene enhancer in B-cells inhibitor, zeta
LOC100132705	similar to immunoglobulin superfamily, member 3
SLC17A2	solute carrier family 17 (sodium phosphate), member 2

CD9	CD9 molecule
EBP	emopamil binding protein (sterol isomerase)
NMNAT3	nicotinamide nucleotide adenylyltransferase 3
F2RL1	coagulation factor II (thrombin) receptor-like 1
MNS1	meiosis-specific nuclear structural 1
MEF2D	myocyte enhancer factor 2D
SQSTM1	sequestosome 1
ANKRD20A3	ankyrin repeat domain 20 family, member A3
ANKRD20A2	ankyrin repeat domain 20 family, member A2
ANKRD20A1	ankyrin repeat domain 20 family, member A1
LOC402269	similar to SLC29A4 protein
SMA5	glucuronidase, beta pseudogene
CBX4	chromobox homolog 4 (Pc class homolog, Drosophila)
PVT1	Pvt1 oncogene (non-protein coding)
NLK	nemo-like kinase
MIR192	microRNA 192
LOC285758	hypothetical protein LOC285758
LOC100287934	similar to hCG2042721
ARL6IP6	ADP-ribosylation-like factor 6 interacting protein 6
RBM12B	RNA binding motif protein 12B
GEN1	Gen homolog 1, endonuclease (Drosophila)
LOC100129617	hypothetical protein LOC100129617
SNAR-C2	small ILF3/NF90-associated RNA C2
NPEPL1	aminopeptidase-like 1
NAT8B	N-acetyltransferase 8B (GCN5-related, putative, gene/pseudogene)
HIST1H2BM	histone cluster 1, H2bm
SNORD25	small nucleolar RNA, C/D box 25
TRIM50	tripartite motif-containing 50
SNORD72	small nucleolar RNA, C/D box 72
P2RX3	purinergic receptor P2X, ligand-gated ion channel, 3
CTH	cystathionase (cystathionine gamma-lyase)
OVOL2	ovo-like 2 (Drosophila)
LOC653501	zinc finger protein 658 pseudogene; zinc finger protein 658B
ZNF658B	zinc finger protein 658 pseudogene; zinc finger protein 658B
TMED6	transmembrane emp24 protein transport domain containing 6
TBC1D7	TBC1 domain family, member 7
AGPAT9	1-acylglycerol-3-phosphate O-acyltransferase 9
PCGF2	polycomb group ring finger 2
FOXD4L3	forkhead box D4-like 3
BARD1	BRCA1 associated RING domain 1
MPP1	membrane protein, palmitoylated 1, 55kDa
FAM72B	family with sequence similarity 72, member B
ZNF334	zinc finger protein 334

LRCH1	leucine-rich repeats and calponin homology (CH) domain containing 1
BRD2	bromodomain containing 2
PSIMCT-1	MCTS1 pseudogene
MRPL52	mitochondrial ribosomal protein L52
GATSL2	GATS protein-like 2
MYLK	myosin light chain kinase
ZNF26	zinc finger protein 26
SNORD35A	small nucleolar RNA, C/D box 35B; small nucleolar RNA, C/D box 35A
GPN3	GPN-loop GTPase 3
RNF146	ring finger protein 146
ZNF782	zinc finger protein 782
ZNF765	zinc finger protein 765
MGEA5	meningioma expressed antigen 5 (hyaluronidase)
BCL3	B-cell CLL/lymphoma 3
EEF1D	eukaryotic translation elongation factor 1 delta (guanine nucleotide exchange protein)
ZNF563	zinc finger protein 563
GNAI1	guanine nucleotide binding protein (G protein), alpha inhibiting activity polypeptide 1
SLC5A3	solute carrier family 5 (sodium/myo-inositol cotransporter), member 3
RSF1	remodeling and spacing factor 1
SMA4	glucuronidase, beta pseudogene
H3F3B	H3 histone, family 3B (H3.3B)
H3F3A	H3 histone, family 3A pseudogene
FAM197Y7	similar to CYorf16 protein
ESAM	endothelial cell adhesion molecule
MANF	mesencephalic astrocyte-derived neurotrophic factor
SNX12	sorting nexin 12
ZNF226	zinc finger protein 226
PPM1N	protein phosphatase 1B-like
GCFC1	chromosome 21 open reading frame 66
BCDIN3D	BCDIN3 domain containing
NDRG4	NDRG family member 4
KCMF1	potassium channel modulatory factor 1
RPL32P3	ribosomal protein L32 pseudogene 3
ZNF131	zinc finger protein 131
FLJ38717	FLJ38717 protein
MCL1	myeloid cell leukemia sequence 1 (BCL2-related)
HDAC5	histone deacetylase 5
ORMDL1	ORM1-like 1 (S. cerevisiae)
ZNF280D	zinc finger protein 280D
HDAC10	histone deacetylase 10
IDI1	isopentenyl-diphosphate delta isomerase 1

RNU105B	RNA, U105A small nucleolar; RNA, U105B small nucleolar
LOC729218	hypothetical LOC729218
TARBP1	TAR (HIV-1) RNA binding protein 1
TRGV4	T cell receptor gamma variable 4
SNORD34	small nucleolar RNA, C/D box 34
RPS25	ribosomal protein S25 pseudogene 8; ribosomal protein S25
NAGS	N-acetylglutamate synthase
YIPF2	Yip1 domain family, member 2
AKR7A3	aldo-keto reductase family 7, member A3 (aflatoxin aldehyde reductase)
GOLGA8DP	golgi autoantigen, golgin subfamily a, 8D
GOLGA8F	golgi autoantigen, golgin subfamily a, 8F
GOLGA8G	golgi autoantigen, golgin subfamily a, 8G
PDCD1	programmed cell death 1
ANKRD16	ankyrin repeat domain 16
RBL1	retinoblastoma-like 1 (p107)
ZNF703	zinc finger protein 703
OPTN	optineurin
ZNF625	zinc finger protein 625
NUP62CL	nucleoporin 62kDa C-terminal like
EWSR1	Ewing sarcoma breakpoint region 1
ARGLU1	arginine and glutamate rich 1
ZNF860	zinc finger protein 860
CD109	CD109 molecule
FLJ42393	hypothetical LOC401105
AIG1	androgen-induced 1
ELF5	E74-like factor 5 (ets domain transcription factor)
MYADM	myeloid-associated differentiation marker
SCGN	secretagogin, EF-hand calcium binding protein
ANKK1	ankyrin repeat and kinase domain containing 1
POU5F1	POU class 5 homeobox 1
GABPB1	GA binding protein transcription factor, beta subunit 1
RPL13A	ribosomal protein L13a
MAML2	mastermind-like 2 (Drosophila)
ALG12	asparagine-linked glycosylation 12, alpha-1,6-mannosyltransferase homolog (S. cerevisiae)
CDH15	cadherin 15, type 1, M-cadherin (myotubule)
PRKCI	protein kinase C, iota
LYPLAL1	lysophospholipase-like 1
LRRC61	leucine rich repeat containing 61
RPS15AP10	ribosomal protein S15a pseudogene 10
INPP1	inositol polyphosphate-1-phosphatase
PA2G4	proliferation-associated 2G4, 38kDa
NPFF	neuropeptide FF-amide peptide precursor
PCSK5	proprotein convertase subtilisin/kexin type 5

GPLD1	glycosylphosphatidylinositol specific phospholipase D1
MICALL1	MICAL-like 1
ADH6	alcohol dehydrogenase 6 (class V)
SNORD81	small nucleolar RNA, C/D box 81
NICN1	nicolin 1
CCDC84	coiled-coil domain containing 84
SLC2A11	solute carrier family 2 (facilitated glucose transporter), member 11
FBLIM1	filamin binding LIM protein 1
SARS	seryl-tRNA synthetase
SCAI	chromosome 9 open reading frame 126
SNORA2A	small nucleolar RNA, H/ACA box 2A; small nucleolar RNA, H/ACA box 2B
ARL17A	ADP-ribosylation factor-like 17 pseudogene 1; ADP-ribosylation factor-like 17
ARL17B	ADP-ribosylation factor-like 17 pseudogene 1; ADP-ribosylation factor-like 17
SNORA62	small nucleolar RNA, H/ACA box 62
SNORA6	small nucleolar RNA, H/ACA box 6
MTSS1L	metastasis suppressor 1-like
RNU7-25P	RNA, U7 small nuclear 25 pseudogene
LOC100133130	PRO1102
TTC6	tetratricopeptide repeat domain 6
RPL34	ribosomal protein L34
STX4	syntaxin 4
SNORD102	small nucleolar RNA, C/D box 102
CYP2A7P1	cytochrome P450, family 2, subfamily A, polypeptide 7 pseudogene 1
ZNF432	zinc finger protein 432
MSH2	mutS homolog 2, colon cancer, nonpolyposis type 1 (E. coli)
NAMPT	nicotinamide phosphoribosyltransferase
LMX1B	LIM homeobox transcription factor 1, beta
STRN	striatin, calmodulin binding protein
PABPC1L	poly(A) binding protein, cytoplasmic 1-like
SCML1	sex comb on midleg-like 1 (Drosophila)
MT4	metallothionein 4
FAM156B	family with sequence similarity 156, member B
FAM156A	family with sequence similarity 156, member A
FEM1A	fem-1 homolog a (C. elegans)
CEACAM19	carcinoembryonic antigen-related cell adhesion molecule 19
RAPGEF5	Rap guanine nucleotide exchange factor (GEF) 5
DUSP8	dual specificity phosphatase 8
DUSP5	dual specificity phosphatase 5
NOXA1	NADPH oxidase activator 1
MXD1	MAX dimerization protein 1

UNC5CL	unc-5 homolog C (C. elegans)-like
NBR2	neighbor of BRCA1 gene 2
FAM197Y3	similar to CYorf16 protein
HAMP	hepcidin antimicrobial peptide
RABGEF1	RAB guanine nucleotide exchange factor (GEF) 1
KIAA0247	KIAA0247
ATP6V1E2	ATPase, H+ transporting, lysosomal 31kDa, V1 subunit E2
LOC399744	hypothetical LOC399744
RASA4	RAS p21 protein activator 4; RAS p21 protein activator 4 pseudogene
SH3GLB1	SH3-domain GRB2-like endophilin B1
MDM1	Mdm1 nuclear protein homolog (mouse)
NPM2	nucleophosmin/nucleoplasmin, 2
RPL23AP79	ribosomal protein L23a pseudogene 79
FAM110C	family with sequence similarity 110, member C
GLS2	glutaminase 2 (liver, mitochondrial)
C1orf138	chromosome 1 open reading frame 138
PDXK	pyridoxal (pyridoxine, vitamin B6) kinase
U2AF1L4	U2 small nuclear RNA auxiliary factor 1-like 4
EFHC1	EF-hand domain (C-terminal) containing 1
KITLG	KIT ligand
LOC728819	hCG1645220
ZNF767	zinc finger family member 767
EIF5A2	eukaryotic translation initiation factor 5A2
ZNF117	zinc finger protein 117
TOX2	TOX high mobility group box family member 2
FES	feline sarcoma oncogene
LOC401180	similar to hCG1745223
AIM1	absent in melanoma 1
BTN3A1	butyrophilin, subfamily 3, member A1
DBI	diazepam binding inhibitor (GABA receptor modulator, acyl-Coenzyme A binding protein)
B4GALNT4	beta-1,4-N-acetyl-galactosaminyl transferase 4
BCAR1	breast cancer anti-estrogen resistance 1
BRPF3	bromodomain and PHD finger containing, 3
COG6	component of oligomeric golgi complex 6
PFKP	phosphofructokinase, platelet
MIR1306	microRNA 1306
BMS1P1	BMS1 pseudogene 1
PIF1	PIF1 5'-to-3' DNA helicase homolog (S. cerevisiae)
MIR1208	microRNA 1208
ARFRP1	ADP-ribosylation factor related protein 1
MYL9	myosin, light chain 9, regulatory
TTC39B	tetratricopeptide repeat domain 39B
RAP1GAP2	GTPase activating Rap/RanGAP domain-like 4
PIGN	phosphatidylinositol glycan anchor biosynthesis, class N

ZFYVE27	zinc finger, FYVE domain containing 27
SNORA21	small nucleolar RNA, H/ACA box 21
FLT3LG	fms-related tyrosine kinase 3 ligand
GPR157	G protein-coupled receptor 157
LCA5	Leber congenital amaurosis 5
DENND4A	DENN/MADD domain containing 4A
HMGN2	high-mobility group nucleosomal binding domain 2
ZNF519	zinc finger protein 519
USP25	ubiquitin specific peptidase 25
SNORD115-7	small nucleolar RNA, C/D box 115-7
SNORD115-13	small nucleolar RNA, C/D box 115-13
SNORD115-26	small nucleolar RNA, C/D box 115-26
LOC100129540	hypothetical LOC100129540
OR10Z1	olfactory receptor, family 10, subfamily Z, member 1
TEAD2	TEA domain family member 2
FLJ45445	hypothetical LOC399844
CCNB1IP1	cyclin B1 interacting protein 1
RIPK2	receptor-interacting serine-threonine kinase 2
C20orf132	chromosome 20 open reading frame 132
DTWD1	DTW domain containing 1
FAM120A	family with sequence similarity 120A
IRAK4	interleukin-1 receptor-associated kinase 4
PI4KAP2	phosphatidylinositol 4-kinase, catalytic, alpha pseudogene 2
N4BP2L2	NEDD4 binding protein 2-like 2
PTBP2	polypyrimidine tract binding protein 2
HPCA	hippocalcin
ADAT2	adenosine deaminase, tRNA-specific 2, TAD2 homolog (S. cerevisiae)
HMGN1	high-mobility group nucleosome binding domain 1
TBX3	T-box 3
C6orf48	chromosome 6 open reading frame 48
SNAR-C4	small ILF3/NF90-associated RNA C4
ERAP1	endoplasmic reticulum aminopeptidase 1
ANKZF1	ankyrin repeat and zinc finger domain containing 1
ATP6V1B1	ATPase, H+ transporting, lysosomal 56/58kDa, V1 subunit B1
SLC22A12	solute carrier family 22 (organic anion/urate transporter), member 12
TAS2R5	taste receptor, type 2, member 5
RNU7-29P	RNA, U7 small nuclear 29 pseudogene
NSMCE4A	non-SMC element 4 homolog A (S. cerevisiae)
TRUB2	TruB pseudouridine (psi) synthase homolog 2 (E. coli)
PI4K2B	phosphatidylinositol 4-kinase type 2 beta
ANKRD36B	ankyrin repeat domain 36B
BMS1P4	BMS1 pseudogene 4
POLQ	polymerase (DNA directed), theta

CDH1	cadherin 1, type 1, E-cadherin (epithelial)
ZNF84	zinc finger protein 84
FKBP11	FK506 binding protein 11, 19 kDa
KRTAP9-2	keratin associated protein 9-2
KRTAP9-9	keratin associated protein 9-9; keratin associated protein 9-2
LOC391322	similar to D-dopachrome tautomerase
LOC100130876	hypothetical LOC100130876
LIF	leukemia inhibitory factor (cholinergic differentiation factor)
ZNF738	zinc finger protein 738
GPR89B	G protein-coupled receptor 89B
GPR89A	G protein-coupled receptor 89A
RAPGEFL1	Rap guanine nucleotide exchange factor (GEF)-like 1
LOC100133161	hypothetical LOC100133161
BOK	BCL2-related ovarian killer
C2orf48	chromosome 2 open reading frame 48
UGT2B10	UDP glucuronosyltransferase 2 family, polypeptide B10
SLMO1	slowmo homolog 1 (Drosophila)
IGLV3-16	immunoglobulin lambda variable 3-16
SNHG12	small nucleolar RNA host gene 12 (non-protein coding)
ANGPT4	angiopoietin 4
LOC100287515	similar to zinc finger protein 26 (KOX 20)
ITPR3	inositol 1,4,5-triphosphate receptor, type 3
RPS28	ribosomal protein S28
STAT2	signal transducer and activator of transcription 2, 113kDa
SFTPB	surfactant protein B
MIR590	microRNA 590
WDR90	WD repeat domain 90
CENPI	centromere protein I
CREB3L3	cAMP responsive element binding protein 3-like 3
MORC3	MORC family CW-type zinc finger 3
ILDR1	immunoglobulin-like domain containing receptor 1
LOC728093	similar to Putative POM121-like protein 1-like
TRIM45	tripartite motif-containing 45
PLCH1	phospholipase C, eta 1
HERC2P2	hect domain and RLD 2 pseudogene 2
HERC2P3	hect domain and RLD 2 pseudogene 3
SH3YL1	SH3 domain containing, Ysc84-like 1 (S. cerevisiae)
FAM197Y1	similar to CYorf16 protein
ESYT1	family with sequence similarity 62 (C2 domain containing), member A
GRID2IP	glutamate receptor, ionotropic, delta 2 (Grid2) interacting protein
FAM102A	family with sequence similarity 102, member A

FAM95B1	family with sequence similarity 95, member B1
DAGLA	diacylglycerol lipase, alpha
PIGV	phosphatidylinositol glycan anchor biosynthesis, class V
ADHFE1	alcohol dehydrogenase, iron containing, 1
ZNF551	zinc finger protein 551
CYS1	cystin 1
MTHFD2	methylenetetrahydrofolate dehydrogenase (NADP+ dependent) 2
RPL4	ribosomal protein L4
ARL8A	ADP-ribosylation factor-like 8A
EPHX2	epoxide hydrolase 2, cytoplasmic
CCDC144NL	coiled-coil domain containing 144 family, N-terminal like
FAM197Y6	similar to CYorf16 protein
ARHGAP32	Rho GTPase-activating protein
ASNS	asparagine synthetase
LAIR2	leukocyte-associated immunoglobulin-like receptor 2
ALDOC	aldolase C, fructose-bisphosphate
CP	ceruloplasmin (ferroxidase)
TAS2R3	taste receptor, type 2, member 3
YARS	tyrosyl-tRNA synthetase
GATAD2B	GATA zinc finger domain containing 2B
CDCA7	cell division cycle associated 7
OSGIN2	oxidative stress induced growth inhibitor family member 2
MAPK12	mitogen-activated protein kinase 12
KLF7	Kruppel-like factor 7 (ubiquitous)
SLK	STE20-like kinase (yeast)
TARP	TCR gamma alternate reading frame protein
MORN1	MORN repeat containing 1
ZNF547	zinc finger protein 547
LOC90834	hypothetical protein BC001742
TADA2A	transcriptional adaptor 2 (ADA2 homolog, yeast)-like
TPT1	tumour protein, translationally-controlled 1
DKFZP586I1420	hypothetical protein DKFZp586I1420
KLF5	Kruppel-like factor 5 (intestinal)
TRPV1	transient receptor potential cation channel, subfamily V, member 1
PPP1R3F	protein phosphatase 1, regulatory (inhibitor) subunit 3F
STAG3L2	stromal antigen 3-like 2
STAG3L1	stromal antigen 3-like 1
LOC100130691	hypothetical LOC100130691
RNU7-57P	RNA, U7 small nuclear 57 pseudogene
KIAA0226	KIAA0226
NEK8	NIMA (never in mitosis gene a)- related kinase 8

TFE3	transcription factor binding to IGHM enhancer 3
MYO5A	myosin VA (heavy chain 12, myoxin)
HIST1H3H	histone cluster 1, H3h
HIST2H3A	histone cluster 2, H3a
HIST1H3J	histone cluster 1, H3j
HIST1H3G	histone cluster 1, H3g
HIST1H3F	histone cluster 1, H3F
HIST1H3C	histone cluster 1, H3c
HIST2H3D	histone cluster 2, H3d
HIST1H3E	histone cluster 1, H3e
HIST1H3A	hhistone cluster 1, H3a
HIST1H3I	histone cluster 1, H3i
HIST1H3D	histone cluster 1, H3d
HIST2H3C	histone cluster 2, H3c
HIST1H3B	histone cluster 1, H3b
NGEF	neuronal guanine nucleotide exchange factor
ACSS2	acyl-CoA synthetase short-chain family member 2
COL4A6	collagen, type IV, alpha 6
POLR2J3	polymerase (RNA) II (DNA directed) polypeptide J3
RUFY2	RUN and FYVE domain containing 2
ZFP36L1	zinc finger protein 36, C3H type-like 1
NR1H4	nuclear receptor subfamily 1, group H, member 4
FAM101A	family with sequence similarity 101, member A
GPR135	G protein-coupled receptor 135
WNT11	wingless-type MMTV integration site family, member 11
GAS5	growth arrest-specific 5 (non-protein coding)
ATG4A	ATG4 autophagy related 4 homolog A (S. cerevisiae)
TMEM82	transmembrane protein 82
SHB	Src homology 2 domain containing adaptor protein B
MVK	mevalonate kinase
TGFB1	transforming growth factor, beta 1
CBWD2	COBW domain containing 2
HSF2BP	heat shock transcription factor 2 binding protein
MIR2110	microRNA 2110
FBXO9	F-box protein 9
SEC16B	SEC16 homolog B (S. cerevisiae)
GLYCTK	glycerate kinase
TCP11L2	t-complex 11 (mouse)-like 2
RABEP1	rabaptin, RAB GTPase binding effector protein 1
F11	coagulation factor XI
PIP5K1A	phosphatidylinositol-4-phosphate 5-kinase, type I, alpha
FDPS	farnesyl diphosphate synthase (farnesyl pyrophosphate synthetase
RNASE4	ribonuclease, RNase A family, 4
GOLGA6L6	Putative golgin subfamily A member 6-like protein 6
RPLP1	ribosomal protein, large, P1

ANKRD12	ankyrin repeat domain 12
TRBV6-6	T cell receptor beta variable 6-6
PLEKHO1	pleckstrin homology domain containing, family O member 1
SLC25A3	solute carrier family 25 (mitochondrial carrier; phosphate carrier), member 3
LOC100132352	similar to hCG1989297
INPP5F	inositol polyphosphate-5-phosphatase F
NOL6	nucleolar protein family 6 (RNA-associated)
BRCA1	breast cancer 1, early onset
PGRMC2	progesterone receptor membrane component 2
RRAGB	Ras-related GTP binding B
LOC100132815	hypothetical protein LOC100132815
SIK3	serine/threonine-protein kinase QSK
SRXN1	sulfiredoxin 1 homolog (S. cerevisiae)
DDX59	DEAD (Asp-Glu-Ala-Asp) box polypeptide 59
MIR591	microRNA 591
MKL1	megakaryoblastic leukemia (translocation) 1
CDRT15L2	CMT1A duplicated region transcript 15-like 2
SCN1A	sodium channel, voltage-gated, type I, alpha subunit
C1orf35	chromosome 1 open reading frame 35
C11orf54	chromosome 11 open reading frame 54
SNORD27	small nucleolar RNA, C/D box 27
SNORA8	small nucleolar RNA, H/ACA box 8
SNORA18	small nucleolar RNA, H/ACA box 18
SPDYA	speedy homolog A (Xenopus laevis)
FAM76B	family with sequence similarity 76, member B
SEC31A	SEC31 homolog A (S. cerevisiae)
CTSE	cathepsin E
PLIN2	adipose differentiation-related protein
MCF2L	MCF.2 cell line derived transforming sequence-like
PORCN	porcupine homolog (Drosophila)
OVOL3	ovo-like 3 (Drosophila)
UBQLN4	ubiquilin 4
PFDN4	prefoldin subunit 4
GAB2	GRB2-associated binding protein 2
LOC286109	hypothetical protein LOC286109
SH2B1	SH2B adaptor protein 1
GOLGA6L4	hypothetical protein LOC161527
CLEC18B	C-type lectin domain family 18, member B
SNAR-B1	small ILF3/NF90-associated RNA B1
SLC6A4	solute carrier family 6 (neurotransmitter transporter, serotonin), member 4
ADRBK1	adrenergic, beta, receptor kinase 1
SPIRE2	spire homolog 2 (Drosophila)
HPR	haptoglobin-related protein; haptoglobin
HP	haptoglobin
LOC441426	hypothetical gene supported by AK126863

JUP	junction plakoglobin
STARD4	StAR-related lipid transfer (START) domain containing 4
SNORD45A	small nucleolar RNA, C/D box 45A
SNORD45C	small nucleolar RNA, C/D box 45C
SNORD45B	small nucleolar RNA, C/D box 45B
STK17A	serine/threonine kinase 17a
EMP1	epithelial membrane protein 1
KIAA1731	KIAA1731
ZNF721	zinc finger protein 721
POLA2	polymerase (DNA directed), alpha 2 (70kD subunit)
CYP2S1	cytochrome P450, family 2, subfamily S, polypeptide 1
PSMB9	proteasome (prosome, macropain) subunit, beta type, 9
TGFB1I1	transforming growth factor beta 1 induced transcript 1
MAN1B1	mannosidase, alpha, class 1B, member 1
DUSP6	dual specificity phosphatase 6
ID1	inhibitor of DNA binding 1, dominant negative helix-loop-helix protein
TRBV6-9	T cell receptor beta variable 6-9
UHRF1	ubiquitin-like with PHD and ring finger domains 1
MIR939	microRNA 939
MMP23B	matrix metallopeptidase 23A (pseudogene); matrix metallopeptidase 23B
AHSA2	AHA1, activator of heat shock 90kDa protein ATPase homolog 2 (yeast)
C1orf131	chromosome 1 open reading frame 131
ENO1	enolase 1, (alpha)
SNAR-B2	small ILF3/NF90-associated RNA B2
ARRB2	arrestin, beta 2
VCL	vinculin
SLC2A2	solute carrier family 2 (facilitated glucose transporter), member 2
ANXA3	annexin A3
MCM9	minichromosome maintenance complex component 9
LOC100128668	hypothetical protein LOC100128668
ICT1	immature colon carcinoma transcript 1
CCNE2	cyclin E2
ADAP1	ArfGAP with dual PH domains 1
KCNK7	potassium channel, subfamily K, member 7
ARHGEF10L	Rho guanine nucleotide exchange factor (GEF) 10-like
PYCRL	pyrroline-5-carboxylate reductase-like
HIPK3	homeodomain interacting protein kinase 3
SQLE	squalene epoxidase
LOC100287497	similar to Transmembrane protein FLJ23183

IFT81	intraflagellar transport 81 homolog (Chlamydomonas)
EFR3B	EFR3 homolog B (S. cerevisiae)
LOC642236	similar to FRG1 protein (FSHD region gene 1 protein)
RPF2	brix domain containing 1 pseudogene; brix domain containing 1
ARHGAP21	Rho GTPase activating protein 21
STK17B	serine/threonine kinase 17b
WEE1	WEE1 homolog (S. pombe)
TBC1D25	TBC1 domain family, member 25
C10orf112	chromosome 10 open reading frame 112
WRB	tryptophan rich basic protein
VRK3	vaccinia related kinase 3
CXorf24	chromosome X open reading frame 24
SNORD13P2	RNA, U13 small nuclear pseudogene 2
STARD9	StAR-related lipid transfer (START) domain containing 9
ZNF248	zinc finger protein 248
WHAMMP1	WAS protein homolog associated with actin, golgi membranes and microtubules pseudogene 1
ANKRD20A4	ankyrin repeat domain 20 family, member A4
NAP1L1	nucleosome assembly protein 1-like 1
SLC16A13	solute carrier family 16, member 13 (monocarboxylic acid transporter 13)
CHMP2B	chromatin modifying protein 2B
HTR3A	5-hydroxytryptamine (serotonin) receptor 3A
PMS2	PMS2 postmeiotic segregation increased 2 (S. cerevisiae)
TLE1	transducin-like enhancer of split 1 (E(sp1) homolog, Drosophila)
CCDC150	coiled-coil domain containing 150
FAM197Y8	similar to CYorf16 protein
SEPT7P2	septin 13
RBM18	RNA binding motif protein 18
DFNA5	deafness, autosomal dominant 5
PAN2	PAN2 poly(A) specific ribonuclease subunit homolog (S. cerevisiae)
ZNF581	zinc finger protein 581
BAIAP2L1	BAI1-associated protein 2-like 1
SLC39A5	solute carrier family 39 (metal ion transporter), member 5
SIRT1	sirtuin (silent mating type information regulation 2 homolog) 1 (S. cerevisiae)
LONP2	lon peptidase 2, peroxisomal
CDC42EP4	CDC42 effector protein (Rho GTPase binding) 4
GTF2H2B	general transcription factor IIH, polypeptide 2B

GTF2H2C	general transcription factor IIH, polypeptide 2C
GTF2H2	general transcription factor IIH, polypeptide 2, 44kDa
GTF2H2D	general transcription factor IIH, polypeptide 2D
C11orf93	Uncharacterized protein LOC120376
ATP5O	ATP synthase, H+ transporting, mitochondrial F1 complex, O subunit
SLC23A1	solute carrier family 23 (nucleobase transporters), member 1
LOC100289637	hypothetical protein LOC100289637
KCTD9P2	potassium channel tetramerisation domain containing 9 pseudogene 2
ECHDC1	enoyl Coenzyme A hydratase domain containing 1
ILKAP	integrin-linked kinase-associated serine/threonine phosphatase 2C
PLK1S1	non-protein coding RNA 153
HGC6.3	similar to HGC6.3
IMMP2L	IMP2 inner mitochondrial membrane peptidase-like (S. cerevisiae)
OR4F2P	olfactory receptor, family 4, subfamily F, member 2 pseudogene
DNM1P24	DNM1 pseudogene 24
TIGD2	tigger transposable element derived 2
SNRPN	small nuclear ribonucleoprotein polypeptide N
SNURF	SNRPN upstream reading frame
BTF3L4	basic transcription factor 3-like 4; similar to hCG2008008
HMGCS1	3-hydroxy-3-methylglutaryl-Coenzyme A synthase 1 (soluble)
SNORD12C	small nucleolar RNA, C/D box 12C
YAF2	YY1 associated factor 2
CNN2	calponin 2
ARRDC3	arrestin domain containing 3
DHRS2	dehydrogenase/reductase (SDR family) member 2
PILRB	paired immunoglobin-like type 2 receptor beta
C16orf93	chromosome 16 open reading frame 93
HNMT	histamine N-methyltransferase
ROR1	receptor tyrosine kinase-like orphan receptor 1
ETNK1	ethanolamine kinase 1
SLC8A2	solute carrier family 8 (sodium/calcium exchanger), member 2
COL1A1	collagen, type I, alpha 1
ABR	active BCR-related gene
ZKSCAN3	zinc finger with KRAB and SCAN domains 3
LEAP2	liver expressed antimicrobial peptide 2
CENPM	centromere protein M
EGFR	epidermal growth factor receptor

	(erythroblastic leukemia viral (v-erb-b) oncogene homolog, avian)
TRAV12-1	T cell receptor alpha variable 12-1
TCTN1	tectonic family member 1
TMC6	transmembrane channel-like 6
TMEM183B	transmembrane protein 183A; transmembrane protein 183B
PPM1L	protein phosphatase 1 (formerly 2C)-like
DHRS4L1	dehydrogenase/reductase (SDR family) member 4 like 1
EPS8	epidermal growth factor receptor pathway substrate 8
IGFBP1	insulin-like growth factor binding protein 1
KDM1B	amine oxidase (flavin containing) domain 1
GK	glycerol kinase
DNMBP	dynamin binding protein
SCARNA21	small Cajal body-specific RNA 21
CSRP2BP	CSRP2 binding protein
RASD1	RAS, dexamethasone-induced 1
CLEC2D	C-type lectin domain family 2, member D
MIR941-4	microRNA 941-4
GK5	glycerol kinase 5 (putative)
EPM2AIP1	EPM2A (laforin) interacting protein 1
PBX1	pre-B-cell leukemia homeobox 1
TRIM66	tripartite motif-containing 66
SFXN2	sideroflexin 2
TRIM61	tripartite motif-containing 61
LOC284009	hypothetical protein LOC284009
ZNF567	zinc finger protein 567
LOC100130357	similar to hCG2038897
LRCH4	leucine-rich repeats and calponin homology (CH) domain containing 4
C21orf33	chromosome 21 open reading frame 33
RNPC3	RNA-binding region (RNP1, RRM) containing 3
ZNF841	zinc finger protein 841
RFC4	replication factor C (activator 1) 4, 37kDa
PCMTD1	protein-L-isoaspartate (D-aspartate) O-methyltransferase domain containing 1
LOC100133299	GALI1870
PRINS	psoriasis associated RNA induced by stress (non-protein coding)
PKIA	protein kinase (cAMP-dependent, catalytic) inhibitor alpha
PARP11	poly (ADP-ribose) polymerase family, member 11
LOC220729	succinate dehydrogenase complex, subunit A, flavoprotein pseudogene
SNORD31	small nucleolar RNA, C/D box 31
HELLS	helicase, lymphoid-specific

CPSF1	cleavage and polyadenylation specific factor 1, 160kDa
ERAS	ES cell expressed Ras
FBXO22	FBXO22 opposite strand (non-protein coding); F-box protein 22
SEPP1	selenoprotein P, plasma, 1
ASB3	ankyrin repeat and SOCS box-containing 3
FOSL2	FOS-like antigen 2
ALOX12P2	arachidonate 12-lipoxygenase pseudogene 2
POU5F1P3	POU class 5 homeobox 1 pseudogene 3
ZNF620	zinc finger protein 620
RFX5	regulatory factor X, 5 (influences HLA class II expression)
C10orf118	chromosome 10 open reading frame 118
DDIT4	DNA-damage-inducible transcript 4
TMEFF1	transmembrane protein with EGF-like and two follistatin-like domains 1
MSH6	mutS homolog 6 (E. coli)
HERC2P4	hect domain and RLD 2 pseudogene 4
LACTB2	lactamase, beta 2
VAT1	vesicle amine transport protein 1 homolog (T. californica)
RMI1	RMI1, RecQ mediated genome instability 1, homolog (S. cerevisiae)
STX7	syntaxin 7
FOXD4L1	forkhead box D4-like 1
MTMR10	myotubularin related protein 10
CYP4F8	cytochrome P450, family 4, subfamily F, polypeptide 8
OR4F29	olfactory receptor, family 4, subfamily F, member 29
OR4F16	olfactory receptor, family 4, subfamily F, member 16
OR4F3	olfactory receptor, family 4, subfamily F, member 3
SNAR-C1	small ILF3/NF90-associated RNA C1
MIR1234	microRNA 1234
DDX11L5	similar to DEAD/H box polypeptide 11 like 9
NKTR	natural killer-tumour recognition sequence
NAPB	N-ethylmaleimide-sensitive factor attachment protein, beta
CHST15	carbohydrate (N-acetylgalactosamine 4-sulfate 6-O) sulfotransferase 15
LOC100128131	hypothetical LOC100128131
GPRC5C	G protein-coupled receptor, family C, group 5, member C
SLC7A5P1	solute carrier family 7 (cationic amino acid transporter, y+ system), member 5 pseudogene 1
CXorf57	chromosome X open reading frame 57

RER1	RER1 retention in endoplasmic reticulum 1 homolog (S. cerevisiae)
SPATA2	spermatogenesis associated 2
PEG3	PEG3 antisense RNA (non-protein coding)
ZIM2	zinc finger, imprinted 2
MIR98	microRNA 98
SNORA33	small nucleolar RNA, H/ACA box 33
OTUB2	OTU domain, ubiquitin aldehyde binding 2
SPTLC3	serine palmitoyltransferase, long chain base subunit 3
CCDC142	coiled-coil domain containing 142
ALAS1	aminolevulinate, delta-, synthase 1
CCDC68	coiled-coil domain containing 68
BTBD11	BTB (POZ) domain containing 11
KCNQ1OT1	KCNQ1 overlapping transcript 1 (non-protein coding)
GPRIN2	G protein regulated inducer of neurite outgrowth 2
IRF9	interferon regulatory factor 9
PPP1R3C	protein phosphatase 1, regulatory (inhibitor) subunit 3C
JPH4	junctophilin 4
SMAD4	SMAD family member 4
HEPACAM	hepatocyte cell adhesion molecule
HEPN1	HEPACAM opposite strand 1
ANKLE2	ankyrin repeat and LEM domain containing 2
PHLDA2	pleckstrin homology-like domain, family A, member 2
ATP9B	ATPase, class II, type 9B
ITFG2	integrin alpha FG-GAP repeat containing 2
SERPINE1	serpin peptidase inhibitor, clade E (nexin, plasminogen activator inhibitor type 1), member 1
KRT81	keratin 81
PFKFB3	6-phosphofructo-2-kinase/fructose-2,6-biphosphatase 3
C2orf80	chromosome 2 open reading frame 80
ZNF461	zinc finger protein 461
HIST1H2AE	histone cluster 1, H2ae
HIST1H2AB	histone cluster 1, H2ab
NEDD4L	neural precursor cell expressed, developmentally down-regulated 4-like
ZNF544	zinc finger protein 544
SFXN1	sideroflexin 1
S100A3	S100 calcium binding protein A3
ZSWIM5	zinc finger, SWIM-type containing 5
H2AFY	H2A histone family, member Y
MCCD1	mitochondrial coiled-coil domain 1

FANCM	Fanconi anemia, complementation group M
LOC100289574	hypothetical protein LOC100289574
PAGE2	P antigen family, member 2 (prostate associated)
OR2T12	olfactory receptor, family 2, subfamily T, member 12
POTEF	POTE ankyrin domain family, member F
ASB9	ankyrin repeat and SOCS box-containing 9
BRIP1	BRCA1 interacting protein C-terminal helicase 1
ZNF761	zinc finger protein 761
CTGF	connective tissue growth factor
LOC100288637	similar to hCG1982161
HNRNPH1	heterogeneous nuclear ribonucleoprotein H1 (H)
BMP2K	BMP2 inducible kinase
NAB2	NGFI-A binding protein 2 (EGR1 binding protein 2)
ATF7IP2	activating transcription factor 7 interacting protein 2
SMURF2	SMAD specific E3 ubiquitin protein ligase 2
LOC100233156	hypothetical protein LOC100233156
LOC100130027	hypothetical protein LOC100130027
AKAP12	A kinase (PRKA) anchor protein 12
KRT8	keratin 8 pseudogene 9; similar to keratin 8; keratin 8
CDA	cytidine deaminase
ANKRD27	ankyrin repeat domain 27 (VPS9 domain)
SNORD101	small nucleolar RNA, C/D box 101
MIR573	microRNA 573
NEK6	NIMA (never in mitosis gene a)-related kinase 6
LRP4	low density lipoprotein receptor-related protein 4
RPSA	ribosomal protein SA
LOC374890	hypothetical gene supported by BC030765
MIR636	microRNA 636
CPVL	carboxypeptidase, vitellogenic-like
RPLP0	ribosomal protein, large, P0
SLC7A4	solute carrier family 7 (cationic amino acid transporter, y+ system), member 4
IGHV4-61	immunoglobulin heavy variable 4-61
FST	follistatin
LOC100271836	SMG1 homolog, phosphatidylinositol 3-kinase-related kinase pseudogene
PSMD3	proteasome (prosome, macropain) 26S subunit, non-ATPase, 3
ATOX1	ATX1 antioxidant protein 1 homolog (yeast)
RECQL5	RecQ protein-like 5
ZNF417	zinc finger protein 417
UROS	uroporphyrinogen III synthase
SLC19A2	solute carrier family 19 (thiamine transporter), member 2
ZNF613	zinc finger protein 613
SLC22A3	solute carrier family 22 (extraneuronal monoamine transporter), member 3
CRYAA	crystallin, alpha A

HMGCR	3-hydroxy-3-methylglutaryl-Coenzyme A reductase
ACAD8	acyl-Coenzyme A dehydrogenase family, member 8
NUDT13	nudix (nucleoside diphosphate linked moiety X)-type motif 13
ANGPTL4	angiopoietin-like 4
SLC5A9	solute carrier family 5 (sodium/glucose cotransporter), member 9
PSPN	persephin
RETSAT	retinol saturase (all-trans-retinol 13,14-reductase)
SNORD108	small nucleolar RNA, C/D box 108
STARD5	StAR-related lipid transfer (START) domain containing 5
ABHD15	abhydrolase domain containing 15
METTL7A	methyltransferase like 7A
DSN1	DSN1, MIND kinetochore complex component, homolog (S. cerevisiae)
NR2C1	nuclear receptor subfamily 2, group C, member 1
ZNF550	zinc finger protein 550
LGR4	leucine-rich repeat-containing G protein-coupled receptor 4
AGAP6	ArfGAP with GTPase domain, ankyrin repeat and PH domain 6
AGAP4	ArfGAP with GTPase domain, ankyrin repeat and PH domain 4
C10orf12	chromosome 10 open reading frame 12
C9orf147	chromosome 9 open reading frame 147
ATRIP	ATR interacting protein
SASH1	SAM and SH3 domain containing 1
PDE11A	phosphodiesterase 11A
JMY	junction mediating and regulatory protein, p53 cofactor
MOSPD1	motile sperm domain containing 1
MRRF	mitochondrial ribosome recycling factor
KIAA0754	hypothetical LOC643314
SNORD18C	small nucleolar RNA, C/D box 18C
SNORD18A	small nucleolar RNA, C/D box 18A
SNORD18B	small nucleolar RNA, C/D box 18B, C/D box 18C
FAM157C	family with sequence similarity 157, member C
SAMD5	sterile alpha motif domain containing 5
SDCCAG8	serologically defined colon cancer antigen 8
LOC730268	similar to anaphase promoting complex subunit 1
MIR922	microRNA 922
SLC7A6OS	solute carrier family 7, member 6 opposite strand
UTRN	utrophin
KRBA2	KRAB-A domain containing 2
KIAA1841	KIAA1841
JAG1	jagged 1 (Alagille syndrome)
GAS2	growth arrest-specific 2

LOC100128002	hypothetical LOC100128002
MYSM1	Myb-like, SWIRM and MPN domains 1
DLEU1	deleted in lymphocytic leukemia 1 (non-protein coding)
CNTNAP1	contactin associated protein 1
MIR1204	microRNA 1204
SNORD36B	small nucleolar RNA, C/D box 36B
SNORD36A	small nucleolar RNA, C/D box 36A
LOC400548	hypothetical gene supported by BC040918
RNF41	ring finger protein 41
TAF13	TAF13 RNA polymerase II, TATA box binding protein (TBP)-associated factor, 18kDa
ALG5	asparagine-linked glycosylation 5
PLEKHM2	pleckstrin homology domain containing, family M (with RUN domain) member 2
METTL2B	methyltransferase like 2B
LOC401010	nucleolar complex associated 2 homolog (S. cerevisiae) pseudogene
RPPH1	ribonuclease P RNA component H1
FANCL	Fanconi anemia, complementation group L
GREB1	GREB1 protein
RPS4X	ribosomal protein S4, X-linked
METTL6	methyltransferase like 6
HMGB1	high-mobility group box 1; high-mobility group box 1-like 10
DNHD1	dynein heavy chain domain 1
SNORA40	small nucleolar RNA, H/ACA box 40
LOC643401	hypothetical protein LOC643401
LRRC37A	leucine rich repeat containing 37A
SMYD3	SET and MYND domain containing 3
LTB4R2	leukotriene B4 receptor 2
MRPS25	mitochondrial ribosomal protein S25
CHIC2	cysteine-rich hydrophobic domain 2
CALM2	calmodulin 2 (phosphorylase kinase, delta)
CALM1	calmodulin 1 (phosphorylase kinase, delta)
CALM3	calmodulin 3 (phosphorylase kinase, delta)
ARID3B	AT rich interactive domain 3B (BRIGHT-like)
RRP7B	ribosomal RNA processing 7 homolog B (S. cerevisiae)
ZC3H12A	zinc finger CCCH-type containing 12A
LOC100128340	hypothetical protein LOC100128340
LOC541471	hypothetical LOC541471; non-protein coding RNA 152
DNA2	DNA replication helicase 2 homolog (yeast)
VLDLR	very low density lipoprotein receptor
TPM4	tropomyosin 4
COX10	COX10 homolog, cytochrome c oxidase assembly protein, heme A:

	farnesyltransferase (yeast)
IMPA1	inositol(myo)-1(or 4)-monophosphatase 1
FLJ14186	hypothetical LOC401149
FAM185A	family with sequence similarity 185, member A
LOC389602	hypothetical LOC389602
RAP1GAP	RAP1 GTPase activating protein
ENY2	enhancer of yellow 2 homolog (Drosophila)
CCDC14	coiled-coil domain containing 14
MLXIPL	MLX interacting protein-like
CBL	Cas-Br-M (murine) ecotropic retroviral transforming sequence
CTGLF12P	centaurin, gamma-like family, member 12 pseudogene
SRGAP2	SLIT-ROBO Rho GTPase activating protein 2
LOC400464	similar to FLJ43276 protein
POTEG	POTE ankyrin domain family, member G
ZXDB	zinc finger, X-linked, duplicated B
LOC440416	hypothetical gene supported by BC072410
CSAG3	CSAG family, member 3
CSAG2	CSAG family, member 2
E2F2	E2F transcription factor 2
CRYGS	crystallin, gamma S
FOXO3	forkhead box O3
LOC100133616	hypothetical LOC100133616
SMG1	SMG1 homolog, phosphatidylinositol 3-kinase-related kinase (C. elegans)
CCDC134	coiled-coil domain containing 134
ATM	ataxia telangiectasia mutated
CPEB4	cytoplasmic polyadenylation element binding protein 4
ADCK2	aarF domain containing kinase 2
CHMP5	chromatin modifying protein 5
HIST2H2BA	histone cluster 2, H2ba
C14orf37	chromosome 14 open reading frame 37
OGDHL	oxoglutarate dehydrogenase-like
ATAD3B	ATPase family, AAA domain containing 3B
CYP3A5	cytochrome P450, family 3, subfamily A, polypeptide 5
ZADH2	zinc binding alcohol dehydrogenase domain containing 2
ZNF44	zinc finger protein 44
LOC389906	hypothetical protein LOC441528
FMO5	flavin containing monooxygenase 5
LOC285505	hypothetical protein LOC285505
ZNF20	zinc finger protein 20
PLK3	polo-like kinase 3 (Drosophila)
LNP1	leukemia NUP98 fusion partner 1
PRIM1	primase, DNA, polypeptide 1 (49kDa)

S100A16	S100 calcium binding protein A16
CRNN	cornulin
RNF43	ring finger protein 43
RIOK3	RIO kinase 3 (yeast)
SERPINB10	serpin peptidase inhibitor, clade B (ovalbumin), member 10
RPS27L	ribosomal protein S27-like
C4orf21	chromosome 4 open reading frame 21
C2orf44	chromosome 2 open reading frame 44
PDZK1P1	PDZ domain containing 1 pseudogene 1
PDZK1P2	PDZ domain containing 1 pseudogene 2
LOC595101	PI-3-kinase-related kinase SMG-1 pseudogene
LOC440354	PI-3-kinase-related kinase SMG-1 pseudogene
FAM82B	family with sequence similarity 82, member B
TFF3	trefoil factor 3 (intestinal)
VEZF1	vascular endothelial zinc finger 1
LOC100133612	similar to hCG1815312
MYOF	myoferlin
PPARGC1A	peroxisome proliferator-activated receptor gamma, coactivator 1 alpha
LRLE1	liver-related low express protein 1
ARHGEF9	Cdc42 guanine nucleotide exchange factor (GEF) 9
NOTCH2NL	Notch homolog 2 (Drosophila) N-terminal like
LOC100134822	similar to hCG1739109
DET1	de-etiolated homolog 1 (Arabidopsis)
CLCF1	cardiotrophin-like cytokine factor 1
ANKRD36	ankyrin repeat domain 36; similar to ankyrin repeat domain 36
TLCD1	TLC domain containing 1
LOC221272	hypothetical LOC221272
DEDD2	death effector domain containing 2
LOC100129473	hypothetical LOC100129473
SNORD59B	small nucleolar RNA, C/D box 59B
SNORD59A	small nucleolar RNA, C/D box 59A
SLC46A1	solute carrier family 46 (folate transporter), member 1
CTGLF8P	centaurin, gamma-like family, member 8 pseudogene
C11orf48	chromosome 11 open reading frame 48
SLC7A6	solute carrier family 7 (cationic amino acid transporter, y+ system), member 6
RSRC2	arginine/serine-rich coiled-coil 2
TMEM165	transmembrane protein 165
LOC644249	hypothetical LOC644249
LOC100129917	hypothetical protein LOC100129917
HSF4	heat shock transcription factor 4
RABGGTB	Rab geranylgeranyltransferase, beta subunit
CRYZL1	crystallin, zeta (quinone reductase)-like 1
ENGASE	endo-beta-N-acetylglucosaminidase

VAMP7	vesicle-associated membrane protein 7
LOC731275	hypothetical LOC731275
MSH5	mutS homolog 5 (E. coli)
MT1CP	metallothionein 1C (pseudogene)
C4orf32	chromosome 4 open reading frame 32
SNORD28	small nucleolar RNA, C/D box 28
CDC6	cell division cycle 6 homolog (S. cerevisiae)
WASH3P	WAS protein family homolog 3 pseudogene; WAS protein family homolog 2 pseudogene; WAS protein family homolog 1; WAS protein family homolog 5 pseudogene
WASH5P	WAS protein family homolog 3 pseudogene; WAS protein family homolog 2 pseudogene; WAS protein family homolog 1; WAS protein family homolog 5 pseudogene
CCBP2	chemokine binding protein 2
UGT2B11	UDP glucuronosyltransferase 2 family, polypeptide B11
S100A6	S100 calcium binding protein A6
RCN3	reticulocalbin 3, EF-hand calcium binding domain
ZNF286B	zinc finger protein 286B
IER5L	immediate early response 5-like
FAM109B	family with sequence similarity 109, member B
LOC284926	hypothetical protein LOC284926
IGHV3-30	immunoglobulin heavy variable 3-30; similar to Ig heavy chain V-III region VH26 precursor
PPP1R3E	protein phosphatase 1, regulatory (inhibitor) subunit 3E
MPP6	membrane protein, palmitoylated 6 (MAGUK p55 subfamily member 6)
NAP1L4	nucleosome assembly protein 1-like 4
KIF3C	kinesin family member 3C
GDF15	growth differentiation factor 15
CLEC18A	C-type lectin domain family 18, member A
FTX	Thrombocytosis, familial X-linked
NPHP3	nephronophthisis 3 (adolescent)
ACAD11	acyl-Coenzyme A dehydrogenase family, member 11
FDFT1	farnesyl-diphosphate farnesyltransferase 1
ABCB4	ATP-binding cassette, sub-family B (MDR/TAP), member 4
RABL2A	RAB, member of RAS oncogene family-like 2A
PPP1R15A	protein phosphatase 1, regulatory (inhibitor) subunit 15A
CBWD3	COBW domain containing 3
CBWD7	COBW domain containing 7
CBWD5	COBW domain containing 5
MTUS1	mitochondrial tumour suppressor 1
KCNMB3	potassium large conductance calcium-activated channel, subfamily M beta member 3

CTGLF10P	centaurin, gamma-like family, member 10 pseudogene
FOXD4L4	forkhead box D4-like 2; forkhead box D4-like 4
FOXD4L2	forkhead box D4-like 2; forkhead box D4-like 4
SIAH1	seven in absentia homolog 1 (Drosophila)
ABCC6	ATP-binding cassette, sub-family C (CFTR/MRP), member 6
ABCC6P2	ATP-binding cassette, sub-family C, member 6 pseudogene 2
TSKU	tsukushin
FAM160B1	family with sequence similarity 160, member B1
CYP1A1	cytochrome P450, family 1, subfamily A, polypeptide 1
LOC645513	hypothetical LOC645513
HPCAL1	hippocalcin-like 1
LCAT	lecithin-cholesterol acyltransferase
EPHA2	EPH receptor A2
PRICKLE4	prickle homolog 4 (Drosophila)
FTCD	formiminotransferase cyclodeaminase
COQ4	coenzyme Q4 homolog (S. cerevisiae)
TRNAU1AP	tRNA selenocysteine 1 associated protein 1
EML6	echinoderm microtubule associated protein like 6
PDE3B	phosphodiesterase 3B, cGMP-inhibited
WDR76	WD repeat domain 76
ORM1	orosomucoid 1
C11orf58	chromosome 11 open reading frame 58
PMS2L2	similar to postmeiotic segregation increased 2-like 2
LRG1	leucine-rich alpha-2-glycoprotein 1
DMBX1	diencephalon/mesencephalon homeobox 1
EPB41L1	erythrocyte membrane protein band 4.1-like 1
KRTAP9-4	keratin associated protein 9-4
SERTAD2	SERTA domain containing 2
PITPNM1	phosphatidylinositol transfer protein, membrane-associated 1
FAM161A	family with sequence similarity 161, member A
SPSB1	splA/ryanodine receptor domain and SOCS box containing 1
GSTA4	glutathione S-transferase alpha 4
TUBA4A	tubulin, alpha 4a
P2RY2	purinergic receptor P2Y, G-protein coupled, 2
LSS	lanosterol synthase (2,3-oxidosqualene-lanosterol cyclase)
CNNM3	cyclin M3
CDHR2	protocadherin 24
RPL23AP82	ribosomal protein L23a pseudogene 82
AXL	AXL receptor tyrosine kinase
MPZL3	myelin protein zero-like 3
DDX5	DEAD (Asp-Glu-Ala-Asp) box polypeptide 5

CCDC18	coiled-coil domain containing 18
LOC100130193	hypothetical protein LOC100130193
BPHL	biphenyl hydrolase-like (serine hydrolase)
PLCXD1	phosphatidylinositol-specific phospholipase C, X domain containing 1
SNORD56B	small nucleolar RNA, C/D box 56B
SNORD26	small nucleolar RNA, C/D box 26
DDX11L16	DEAD/H (Asp-Glu-Ala-Asp/His) box polypeptide 11 pseudogene
TAS2R14	taste receptor, type 2, member 14
ZFP36L2	zinc finger protein 36, C3H type-like 2
RPLP2	ribosomal protein, large, P2
SPDYE7P	speedy homolog E7 (Xenopus laevis), pseudogene
RAB3B	RAB3B, member RAS oncogene family
LOC100129596	hypothetical protein LOC100129596
GTF2IRD2B	GTF2I repeat domain containing 2B
STAM	signal transducing adaptor molecule (SH3 domain and ITAM motif) 1
ZNF839	zinc finger protein 839
ZNF708	zinc finger protein 708
SPRY2	sprouty homolog 2 (Drosophila)
RBMS2	RNA binding motif, single stranded interacting protein 2
PRPF4B	PRP4 pre-mRNA processing factor 4 homolog B (yeast)
PAR5	Prader-Willi/Angelman syndrome-5
SNAR-H	small ILF3/NF90-associated RNA H
UQCRQ	ubiquinol-cytochrome c reductase, complex III subunit VII, 9.5kDa
CDC7	cell division cycle 7 homolog (S. cerevisiae)
SLC13A3	solute carrier family 13 (sodium-dependent dicarboxylate transporter), member 3
LRRN4	leucine rich repeat neuronal 4
RBM39	RNA binding motif protein 39
RNU7-45P	RNA, U7 small nuclear 45 pseudogene
TMEM44	transmembrane protein 44
CDKN1A	cyclin-dependent kinase inhibitor 1A (p21, Cip1)
SDR42E1	short chain dehydrogenase/reductase family 42E, member 1
USP12	ubiquitin specific peptidase 12
PDZK1	PDZ domain containing 1
GATC	glutamyl-tRNA(Gln) amidotransferase, subunit C homolog (bacterial)
RUSC2	RUN and SH3 domain containing 2
KRTAP10-1	keratin associated protein 10-1
ZNF518A	zinc finger protein 518A
LOC100133315	similar to hCG1640299
TMEM168	transmembrane protein 168

MIR941-2	microRNA 941-2
MIR941-3	microRNA 941-3
MIR941-1	microRNA 941-1
LRRC8D	leucine rich repeat containing 8 family, member D
POLR1A	polymerase (RNA) I polypeptide A, 194kDa
IER3	immediate early response 3
MIR149	microRNA 149
FAM13B	family with sequence similarity 13, member B
LOC374443	CLR pseudogene
POLR2J4	polymerase (RNA) II (DNA directed) polypeptide J4, pseudogene
HEY1	hairy/enhancer-of-split related with YRPW motif 1
SNORA55	small nucleolar RNA, H/ACA box 55
CRYBA2	crystallin, beta A2
KRTAP17-1	keratin associated protein 17-1
USP32	ubiquitin specific peptidase 32
ENOSF1	enolase superfamily member 1
LOC284373	hypothetical protein LOC284373
RNF207	ring finger protein 207
IL1RAP	interleukin 1 receptor accessory protein
KLHL15	kelch-like 15 (Drosophila)
DAAM1	dishevelled associated activator of morphogenesis 1
DUSP18	dual specificity phosphatase 18
PASK	PAS domain containing serine/threonine kinase
ELMOD3	ELMO/CED-12 domain containing 3
ZYX	zyxin
ANKAR	ankyrin and armadillo repeat containing
TRIB3	tribbles homolog 3 (Drosophila)
C9orf9	chromosome 9 open reading frame 9
LOC100130557	hypothetical LOC100130557
ZNF780B	zinc finger protein 780B
LOC730102	hypothetical protein LOC730102
ARV1	ARV1 homolog (S. cerevisiae)
HSPA1A	heat shock 70kDa protein 1A
HSPA1B	heat shock 70kDa protein 1B
HKDC1	hexokinase domain containing 1
DDX46	DEAD (Asp-Glu-Ala-Asp) box polypeptide 46
ZNF250	zinc finger protein 250
RAB9A	RAB9A, member RAS oncogene family
ERRFI1	ERBB receptor feedback inhibitor 1
MIR604	microRNA 604
KRT78	keratin 78
SPRR2F	small proline-rich protein 2F
TRAPPC2P1	trafficking protein particle complex 2 pseudogene 1
TRAPPC2	trafficking protein particle complex 2
SLC25A24	solute carrier family 25 (mitochondrial carrier; phosphate carrier), member 24
ANKRD10	ankyrin repeat domain 10

SDHAP3	succinate dehydrogenase complex, subunit A, flavoprotein pseudogene 3
APOL1	apolipoprotein L, 1
GRHL1	grainyhead-like 1 (Drosophila)
NDUFS7	NADH dehydrogenase (ubiquinone) Fe-S protein 7, 20kDa (NADH-coenzyme Q reductase)
SGK2	serum/glucocorticoid regulated kinase 2
TAX1BP1	Tax1 (human T-cell leukemia virus type I) binding protein 1
ZNF682	zinc finger protein 682
SHPRH	SNF2 histone linker PHD RING helicase
MFSD8	major facilitator superfamily domain containing 8
ELK3	ELK3, ETS-domain protein (SRF accessory protein 2)
IGKC	immunoglobulin kappa constant
MST4	serine/threonine protein kinase MST4
CSTF3	cleavage stimulation factor, 3' pre-RNA, subunit 3, 77kDa
BMS1P5	BMS1 pseudogene 5
TAS2R30	taste receptor, type 2, member 30
LOC100288807	similar to Putative WBSCR19-like protein 7
PCBD2	pterin-4 alpha-carbinolamine dehydratase2
RASA4B	RAS p21 protein activator 4B
DCAF8	WD repeat domain 42A
HCG8	HLA complex group 8
RNF11	ring finger protein 11
AP1M2	adaptor-related protein complex 1, mu 2 subunit
KCTD18	potassium channel tetramerisation domain containing 18
RHBDD3	rhomboid domain containing 3
AGAP10	ArfGAP with GTPase domain, ankyrin repeat and PH domain 10
CTGLF11P	centaurin, gamma-like family, member 11 pseudogene
AGAP9	ArfGAP with GTPase domain, ankyrin repeat and PH domain 9
AGAP5	ArfGAP with GTPase domain, ankyrin repeat and PH domain 5
COL4A5	collagen, type IV, alpha 5
PIM1	pim-1 oncogene
TMEM42	transmembrane protein 42
C1orf112	chromosome 1 open reading frame 112
RFX2	regulatory factor X, 2 (influences HLA class II expression)
PIGL	phosphatidylinositol glycan anchor biosynthesis, class L
VNN1	vanin 1
KHK	ketohexokinase (fructokinase)
RTTN	rotatin

IGLC1	immunoglobulin lambda constant 1 (Mcg marker)
IGLC2	immunoglobulin lambda constant 2 (Kern-Oz-marker)
IGLV2-11	immunoglobulin lambda variable 2-11
IGHV2-70	immunoglobulin heavy variable 2-70; similar to hCG1742309
FOXD4	forkhead box D4
TYSND1	trypsin domain containing 1
KRTAP9-7	keratin-associated protein 9-2-like 1-like; keratin associated protein 9-7
POM121C	POM121 membrane glycoprotein C
RRAGC	Ras-related GTP binding C
DUXAP10	double homeobox A pseudogene 10
CST4	cystatin S
ZNF638	zinc finger protein 638
SPRY4	sprouty homolog 4 (Drosophila)
TRIM52	tripartite motif-containing 52
GAS8	growth arrest-specific 8
LOC644794	hypothetical LOC644794
SHPK	sedoheptulokinase
SNORD24	small nucleolar RNA, C/D box 24
SNORD76	small nucleolar RNA, C/D box 76
RASAL2	RAS protein activator like 2
FARP1	FERM, RhoGEF (ARHGEF) and pleckstrin domain protein 1 (chondrocyte-derived)
TMC7	transmembrane channel-like 7
GINS2	GINS complex subunit 2 (Psf2 homolog)
CYP2D6	cytochrome P450, family 2, subfamily D, polypeptide 6
ZNF678	zinc finger protein 678
WARS2	tryptophanyl tRNA synthetase 2, mitochondrial
SNX33	sorting nexin 33
LOC285540	hypothetical protein LOC285540
PNPLA3	patatin-like phospholipase domain containing 3
MAGOH2	mago-nashi homolog 2, proliferation-associated (Drosophila)
SNX9	sorting nexin 9
ANO8	anoctamin 8
MGST2	microsomal glutathione S-transferase 2
METTL3	methyltransferase like 3
GOLGA8B	golgi autoantigen, golgin subfamily a, 8B
GOLGA8A	golgi autoantigen, golgin subfamily a, 8A
CHMP4C	chromatin modifying protein 4C
CYP2W1	cytochrome P450, family 2, subfamily W, polypeptide 1
FAM78B	family with sequence similarity 78, member B
FARP2	FERM, RhoGEF and pleckstrin domain protein 2
SNORD22	small nucleolar RNA, C/D box 22

RNF121	ring finger protein 121
SNORD29	small nucleolar RNA, C/D box 29
MESDC2	mesoderm development candidate 2
NPAT	nuclear protein, ataxia-telangiectasia locus
MERTK	c-mer proto-oncogene tyrosine kinase
SLC26A6	solute carrier family 26, member 6
SEPW1	selenoprotein W, 1